UV radiation as a new tool to control microalgal bio-product yield and quality

A thesis presented in partial fulfilment of the requirements for the degree of

Doctor of Philosophy

in

Industrial Biotechnology

at

Massey University, Palmerston North, New Zealand

Roland Schaap

2018

Abstract

While ultraviolet (UV) radiation is most commonly known as an abiotic stress, various studies have shown targeted UV exposure increases bioproduct and biomass yields in microalgae. Microalgal cultivation processes face significant limitations in achievable bioproduct and biomass yields and thus improvements offered by targeted UV treatments during large-scale microalgae cultivation provide an opportunity for development of a novel UV treatment tool. Growing demand in microalgae (bio)products indicate there may be a substantial market for such UV treatment tools. No initiatives that explore the development of targeted UV treatments during large-scale microalgae cultivation have been found in the literature or in the industry. In collaboration with industrial partner BioLumic, a company specializing in applying targeted UV treatments in plants as a tool in agriculture, this PhD research examined if specific treatments of UV radiation (i.e. specific in UV waveband, irradiance and exposure duration) can reliably increase carotenoid accumulation in the microalga *Dunaliella salina* and if this new understanding can be feasibly used to develop an industrial system for UV treatment of microalgae.

The PhD research was conducted utilizing *D. salina* after evaluation in four commercially relevant microalgae species: *Arthrospira platensis, Chlorella vulgaris, Haematococcus pluvialis* and *D. salina*. A UV-A induced carotenoid accumulation response was identified in *D. salina* (strain UTEX 1644). Targeted UV-A treatments reliably induced carotenoid accumulation in this species, and the magnitude of the response depended on the UV-A wavelength, UV irradiance, UV exposure duration, and UV dose. The UV-A carotenoid accumulation response was induced within 6 hours and was largely complete in 96 hours (24 $h \cdot d^{-1}$ UV exposure). The highest UV-A dose tested induced the highest carotenoid accumulation rates and the highest total carotenoid concentrations after continuous UV exposure (24 $h \cdot d^{-1}$) at the highest UV-A irradiance tested (30 $W \cdot m^{-2}$). Total carotenoid concentration increases of up to 162% were thus observed after 72 hr of UV-A exposure. UV-A exposure was associated with slowed or stopped cell proliferation as well as increased *D. salina* cell size (up to 15%) and altered intracellular structural organization. Carotenoid accumulation ceased and cell proliferation increased when UV-A exposure was stopped, leading to a subsequent resumption of cell proliferation. UV-A induced carotenoid accumulation was improved 51% during UV-A exposure concomitant with non-UV carotenogenic stimuli (high PAR intensity and salinity) compared to UV-A exposure alone.

The observations from experiments carried out in the thesis served as inputs in a techno-economic analysis (TEA) model developed to assess feasibility of large-scale UV treatment. The TEA model was developed to allow assessment of the most critical areas for improving profitability of large-

scale UV treatment technology, rather than provide absolute economical outputs for revenue and profit. The TEA was based on two reference cultivation systems currently used for commercial *D. salina* cultivation. The TEA analysis considered four locations for the UV treatment system applied along the cultivation process: pre-cultivation stage (i.e. inoculum), main cultivation stage, post-cultivation stage (i.e. immediately prior to harvest) and during fluid transfer between stages. A dedicated post-cultivation UV treatment stage was shown to have a number of advantages over other treatment options.

A model cultivation system for the case-study of *D. salina* was developed assuming an annual β-carotene production of 1,000 kg. The developed TEA model cultivation system and TEA UV treatment system were able to identify a potential increase in profitability generated from the application targeted UV treatment during large-scale *D. salina* cultivation. The maximum increase in profitability was achieved using a broad wavelength UV treatment system (irradiance = 30 $W \cdot m^{-2}$, exposure duration = 24 $h \cdot d^{-1}$, surface area coverage = 100%) applied during an intensive cultivation post-cultivation system. A relatively small contribution of the UV treatment system to CAPEX and OPEX to overall β-carotene production cost (i.e. < 10%) combined with the large increase in β-carotene production (711 $kg \cdot y^{-1}$ and 895 $kg \cdot y^{-1}$ for fluorescent UV tube and UV LED systems, respectively) leads to potentially large increases in profitability. The TEA analysis identified the magnitude of the UV-A induced carotenoid accumulation response to be the most important factor to influence the potential profitability. Moreover, the TEA indicated the increases in profitability are strongly influenced by optical efficiency, electrical efficiency and maximum optical power. The profitability estimates from the current TEA indicate that UV treatment during commercial microalgae cultivation has potential and justifies further research.

To our knowledge the exploration of the fundamental UV photobiology in microalgae required to develop UV treatment regimes from discrete UV wavebands, complemented with a commercial microalgal-engineering insight, to produce UV treatment regimes and UV treatment technology for application during large-scale microalgae cultivation, has never been attempted. The multidisciplinary approach employed during this PhD research explored for the first time the development of a UV treatment system from laboratory observations to commercial cultivation. The current research described for the first time the UV response behaviour of *D. salina* (strain UTEX 1644) to varying UV waveband, UV irradiance, UV exposure durations as well as UV response interactions with PAR and salinity. The case-study of UV treatment during large-scale *D. salina* cultivation in this PhD research allowed recommendations to be made to the industrial partner BioLumic on potential areas of focus for continued research and development.

Acknowledgments

First and foremost, I would like to thank my supervisors Professor Benoit Guieysse, Associate Professor Jason Wargent and Professor Julian Heyes for their support and encouragement throughout this project. My time as a PhD student got off to a rocky start but I am thankful to my supervisors for their understanding and efforts during the unplanned end of one PhD project and the seamless transition into another. I am grateful to have had the opportunity to develop myself academically and professionally under their tutelage.

Thank you to BioLumic for offering me the opportunity to work on this project. Thank you to all the staff at BioLumic and in particular Warren Bebb and Hangfeng Ji at BioLumic for all their help. Also, I would like to thank Callaghan Innovation for providing the funding that made this research possible by awarding the R&D Fellowship Grant on not one, but two occasions.

My PhD would not have been the same had I not been surrounded by great people at Massey. Thank you first and foremost to all my colleagues in the office, in the lab and all around Massey with whom I have gotten to share my PhD journey. I'd like to thank everyone for the help they provided during my research in between the endless hours of banter, lunches, activities and beers we got to enjoy together. I'm glad I got to share so many good times with so many great people.

I would like to extend my gratitude to all the staff at the Riddet Institute for making my time at Massey a good one. Special thanks go out to all the staff at the Microlab for all their technical support and for always providing laughter and chatter during the endless hours in the lab. Thank you to Ann-Marie Jackson, Kylie Evans, John Edwards, John Sykes, Julia Good and Nereda Corbett for making the lab such an enjoyable place to be and tolerating me poking my nose in everywhere. Thank you to Glenda for all her work and for letting us stay in our office despite 'the state of it'.

As our three-year trip turned in to four (and counting) there has been a lot that we have had to miss out on back home. I would like to thank my family and friends in the Netherlands for all the support we have received and all the effort everyone has made to stay in frequent contact all these years. I am very grateful I got to share some of our life here in New Zealand with those who were able to make the time and effort to come and visit us on the other side of the world.

And last but definitely not least, I would like to thank my partner Mirjam de Oude who agreed to join me on a journey to the other side of the world, into the unknown, just so I could do my PhD research. She has been my support through thick and thin and I am proud of everything we have achieved here in New Zealand.

Table of contents

List of Figures

List of Tables

Abbreviations and terms

BWF	Biological weighing function
CAPEX	Capital expense
Car:Chl	Ratio 'total carotenoid concentration to total chlorophyll *(a+b)* concentration'
Cellular carotenoid/ chlorophyll *(a+b)* content	µg pigment·10^6 cells^{-1}
CPD	Cyclobutane-type pyrimidine dimer
DW	Dry weight
Extensive cultivation	Commercial microalgae cultivation process using open ponds
Carboxy-H_2DFFDA	5-(and-6)-carboxy-2',7'-difluorodihydrofluorescein diacetate
HRT	Hydraulic retention time (days)
Intensive cultivation	Commercial microalgae cultivation process using raceway ponds
MAA	Mycosporine-like amino acid
OD_{687}	Optical density at λ = 687 nm
ΔOD_{687}	Change in OD_{687} over time
OPEX	Operational expense
PAR	Photosynthetically Active Radiation (λ = 400 - 700 nm)
PAR-Only	Cultures exposed to PAR radiation only during experimental treatments
PFD	Photon Flux Density (µmol·m^{-2}·s^{-1})
PSII	Photosystem II
ROS	Reactive oxygen species
TEA	Techno-economic analysis
Total carotenoid/ chlorophyll *(a+b)* concentration	µg pigment·mL culture^{-1}
UV	Ultraviolet radiation (λ = 100 - 400 nm)
UV-A	Part of UV waveband with λ = 315 - 400 nm
UV-B	Part of UV waveband with λ = 280 - 315 nm

UV-C	Part of UV waveband with λ = 100 - 280 nm
λ_{max}	Emission peak

1 Introduction

The production of natural and sustainable bioproducts is a fast-growing market. Microorganisms such as bacteria, yeast, fungi and algae are all known to produce various bioproducts of commercial interest. Many microorganisms are now grown on large-scale to capitalize on these bioproducts. In recent years, microalgae have received attention as a source of high-value bioproducts such as carotenoids, (poly unsaturated) fatty acids, and raw biomass used as food or food ingredients (Borowitzka, 2013b). Microalgae are particularly well suited to the production of these high-value bioproducts as numerous microalgae species are known to possess some of the highest contents per unit dry weight of any organism - e.g. β-carotene in *Dunaliella salina* or astaxanthin in *Haematococcus pluvialis*. Furthermore, new high-value bioproducts from algae with a wide range of applications are being identified through ongoing research (Plaza et al., 2009).

Sustainable tools to improve bioproduct and biomass productivity or yield are desirable to any industry and microalgal biotechnology is no exception. Microalgal biotechnology in particular faces significant limitations in the achievable yields of microalgal bioproducts (Tredici, 2010). Additionally, a limited ability to control which bioproducts are expressed impairs down-stream processing (Molina Grima et al., 2004). In recent years various studies in microalgae describe examples of increases in bioproduct and biomass yields resulting from targeted ultraviolet (UV) radiation exposure. Examples include increased growth rate (Balan & Suraishkumar, 2014), increased high-value bioproduct formation such as carotenoids (Jahnke, 1999; Wu et al., 2010) and fatty acids (Forján et al., 2011). While the biotechnological application of targeted UV radiation treatment during commercial microalgae cultivation has been suggested by some (e.g. Salguero, et al., 2005), the development of such an application has not yet been reported in any literature reviewed. Growing demand in microalgae (bio)products indicate there may be a substantial market for such a UV treatment tool.

The industrial partner BioLumic has been developing targeted UV treatment regimes and UV treatment technology in plants since 2013 based on over 10 years of scientific research (see Box 1). BioLumics' UV treatment systems have been shown to grant plants beneficial effects over their lifetime leading to hardier, more productive crops. The often non-linear nature of UV responses means that maximizing the desired UV response is complex and requires an understanding of the intricate dependence of the UV response on UV composition and dose (i.e. UV wavelength, UV irradiance and UV exposure duration). Therefore, in order for BioLumic to develop UV treatment

regimes and UV treatment technologies, a fundamental understanding is required of a target species' UV photobiology and the desired UV response. Funded by Callaghan Innovation and BioLumic, in collaboration with the Massey School of Engineering, the current PhD research takes a multi-disciplinary approach towards assessing whether BioLumics' knowledge of large-scale UV treatment technology can be used to develop a targeted UV treatment process for commercial microalgae cultivation processes.

Box 1 - BioLumic

BioLumic is a New Zealand based start-up company specialised in developing targeted UV delivery regimes and UV treatment technology in plants for use as a tool in agriculture. BioLumic develops targeted UV delivery regimes and UV treatment technology by applying fundamental knowledge of plant UV photobiology to stimulate and control plant metabolic pathways to maximize a desired UV response. The company expands on UV photobiology research conducted by founder Dr. Jason Wargent (industry PhD supervisor). In plants, BioLumic's targeted UV delivery regimes have been shown to grant plants, and by extension entire crops, beneficial effects over their lifetime including: hardier, more productive crops, increased produce quality and increased insect and disease resistance.

To our knowledge the exploration of the fundamental UV photobiology in microalgae required to develop UV treatment regimes from discrete UV wavebands, complemented with a commercial microalgal-engineering insight, to produce UV treatment regimes and UV treatment technology for application during large-scale microalgae cultivation, has never been attempted. To this end the PhD research will focus on the case-study of the microalga *D. salina*.

The primary hypotheses of this PhD research are:

That specific treatments of UV radiation (i.e. specific in UV waveband, irradiance and exposure duration) can reliably increase bioproduct accumulation in *D. salina* and that a new understanding of *D. salina* UV response characteristics can be feasibly used to develop an industrial system for UV treatment of microalgae.

The first of the hypotheses focusses on improving understanding of the *D. salina* UV photobiology and determining if *D. salina* bioproduct metabolic pathways can be stimulated and controlled using targeted UV exposure. The current state of the scientific knowledge of *D. salina*

photobiology and UV response is insufficient for the development of targeted UV treatments and therefore a better understanding is required. The second hypothesis then aims to build on this new understanding of the *D. salina* UV photobiology and UV response to develop targeted UV treatment regimes for *D. salina* complemented with a commercial microalgal-engineering insight. To provide recommendations for BioLumic, a techno-economic analysis (TEA) is developed to provide indications on the industrial and economic feasibility of UV treatment technology during commercial *D. salina* cultivation. However, due to the limitations of the methodology employed during the current research and the available large-scale cultivation data, the TEA is unable incorporate the level of detail required to provide accurate economical outputs for revenue and profit as for example a business-study would. In the absence of relevant knowledge and data in the field, the scope of the TEA developed is such that it allows assessment of the most critical areas for improving profitability of large-scale UV treatment technology based on novel PhD research findings. Based on assessment of various scenarios using the TEA model, recommendations are made to BioLumic whether further research and development is warranted. The PhD thesis will emphasise discussing results more broadly and qualitatively in the context of developing UV treatment regimes and UV treatment technology. Less emphasis will be given to the costing of the production system in order to focus instead on the added value of the UV treatment regime and technology.

The thesis objectives resulting from the hypotheses are as follows:

- Quantify the impact of UV radiation (i.e. UV waveband, irradiance and exposure duration) on *D. salina* photosynthetic pigment content and growth (i.e. carotenoid and cholorophyll*(a+b)*), cell growth and cell morphology).
- Quantify the interaction of the UV carotenoid accumulation response in *D. salina* with stimuli known to be involved in non-UV-A induced carotenoid accumulation (PAR intensity and salinity).
- Develop a techno-economic model for targeted UV treatment during commercial *D. salina* cultivation based on research findings.
- Employ the developed TEA to provide indications on the economic feasibility of UV treatment technology during commercial *D. salina* cultivation and the most critical areas for improving profitability.
- Provide recommendations to the industrial partner BioLumic for continued development of UV treatment regimes and UV treatment technology during commercial microalgae cultivation.

The outline of the thesis is as follows: First, relevant scientific literature is reviewed in Chapter 2. Chapter 3 describes the scope of the research and methods and materials employed. Chapter 4 then presents the UV response characteristics in *D. salina* under different UV wavebands and UV exposure regimes with regards to photosynthetic pigment content (i.e. carotenoid and cholorophyll*(a+b)*), cell growth and cell morphology. In Chapter 5 the impact of manipulations of UV dose composition (irradiance and exposure duration) and a limited number of non-UV carotenogenesis stimuli (PAR intensity and salinity) in *D. salina* is presented. In Chapter 6 assessment of targeted UV treatments regimes developed based on the understanding of the *D. salina* UV response. The knowledge obtained from the experimental work is then used to develop a TEA model to provide indications of the economic feasibility of different UV treatment approaches during commercial microalgae cultivation. Finally, recommendations to the industrial partner BioLumic for continued development of UV treatment regimes and UV treatment technology during commercial microalgae cultivation are discussed.

2 Literature Review

2.1 Introduction

Products from microalgae range from high-value bioproducts such as carotenoids and (poly unsaturated) fatty acids to bulk human and animal feed produce. The microalgal biotechnology industry has grown to a multibillion dollar industry in recent decades (Borowitzka, 2013b). For instance, the total market for carotenoids alone is thought to be worth $1.4 billion USD[1] (data from 2011). Producing low value, bulk products from microalgae at competitive prices is a great challenge: 'algal biofuels' is an example where, despite widespread research and investment, the state of the art has yet to prove economic viability (Borowitzka, 2013b). In contrast, the production of fatty acids, carotenoids, cosmetics ingredients, nutrition and pharmaceutical applications from microalgae is proven to be economically viable (Dufossé et al., 2005).

The commercial production of microalgae is not without pitfalls; it is complicated by significant limitations in the achievable yields of microalgal biomass and bioproducts (Grobbelaar, 2010; Tredici, 2010). Approaches such as bioprocess engineering (e.g. improving reactor design, media composition and process optimisation), strain selection and use of selective pressures can help overcome some limitations but not all. Research has shown UV exposure can lead to increased microalgal biomass growth or metabolite production (Jahnke, 1999; Forján et al., 2011; Balan et al., 2014). The often-non-linear nature of UV responses means that maximizing the desired UV response through UV treatment regimes and UV treatment technology is complex and requires an understanding of the dependence of the UV response on UV composition and dose (i.e. UV wavelength, UV irradiance and UV exposure duration).

The literature review aims to illustrate the importance of UV wavelength and UV dose on the resulting photobiology. The aim of the literature review is to review the current understanding of the fundamental UV photobiology of the projects' target microalgae, *D. salina*. In the industrial context of the current project, the literature review will first briefly discuss the physical nature of UV radiation and the current state-of-the-art of UV treatment technology. Prior to the discussing *D. salina* UV photobiology, metabolic pathways involved in response to UV exposure and UV damage are reviewed broadly across all microalgae. Subsequently the review will focus on the *Dunaliella* genus and the target species *D. salina*. First, the biotechnological application of the *Dunaliella* genus is reviewed with a focus on the carotenoid accumulation response (induced by

[1] BCC Research. 2011. *The global market for carotenoids* [Report no: FOD025D]. BCC Research LLC. Wellesley, USA.

both UV and other stimuli). This is followed by a detailed review of the current understanding of the fundamental UV photobiology of the *Dunaliella* genus is presented (i.e. illustrating the intricate dependence of the UV response on UV wavelength, UV irradiance and UV exposure duration).

2.2 Ultraviolet radiation

2.2.1 UV radiation and UV damage

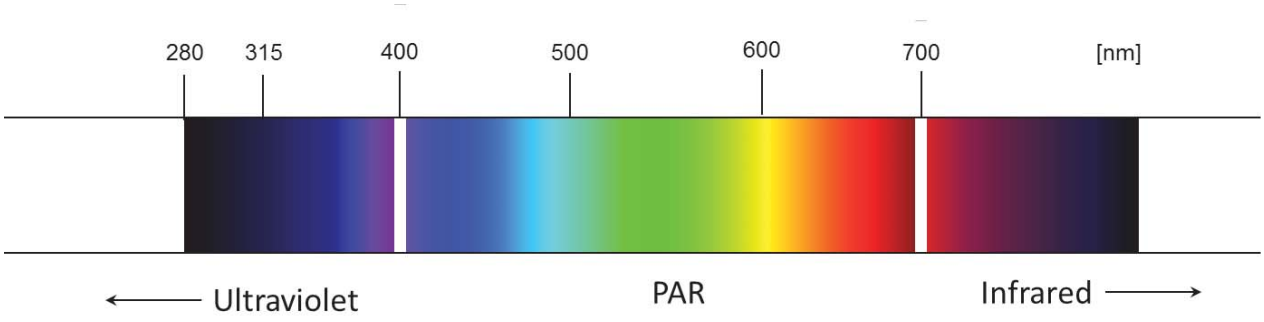

Figure 2-1 Schematic representation of the solar spectrum

Ultraviolet (UV) radiation is defined as the region of the electromagnetic spectrum with wavelengths between λ = 100 - 400 nm (Figure 2-1). There are three arbitrary classes, namely; UV-A (λ = 315 – 400 nm), UV-B (λ = 280 – 315 nm) and UV-C (λ = 100 - 280 nm). Around 7% of total incoming solar radiation consists of UV radiation (λ < 400 nm), 38% consists of photosynthetically active radiation (PAR) and the rest is infrared (λ > 700 nm) (Aphalo et al., 2012). The Earth's atmosphere plays an important role in preventing UV radiation from reaching Earth's surface. Oxygen, nitrogen (both atomic and diatomic) and ozone are the main absorbers in the λ = 200 - 300 nm range, preventing the penetration of UV-C and blocking part of the UV-B (Ghetti et al., 2006). While numerous other factors impact UV penetration through the atmosphere, UV-A passes the atmosphere largely unhindered. In 1985 a report was published indicating decreasing stratospheric ozone levels over Antarctica (Farman et al., 1985). Decreasing atmospheric ozone column thickness has been shown to lead to increased levels of UV-B that reach the Earth's surface in particular (Madronich et al., 1995).

Reports of decreasing stratospheric ozone levels have sparked research aimed at understanding the effect of increasing UV-B levels on terrestrial life. Equation 1 defines the relationship of the energy per photon (E) per wavelength (λ):

$$E = \frac{hc}{\lambda} \quad \text{(Eq. 1)}$$

where h represents Planck's constant and c the speed of light in vacuum. Decreasing wavelengths lead to increased energy per photons.

2.2.2 UV radiation as a tool

A novel application employing UV treatment technology as a tool has been developed by the projects' industrial partner Biolumic. Scientific research improved the understanding of UV radiation as a signalling component in higher plants (Jenkins, 2009). The research has identified a number of non-damaging metabolic responses attributed to UV radiation exposure (UV-B specifically) which include (Holmes, 2006; and Wargent & Jordan, 2013; and references therein):

- Physical changes in e.g. leaf thickness and leaf area
- Increased growth rate and photosynthetic rates
- Induction of anti-oxidants and pathogenesis-related products
- Induction of photoprotective compounds
- Resistance to fungal and viral disease
- Resistance to insect herbivory

For a number of years BioLumic has worked on applying the knowledge of these non-damaging and signalling components of UV radiation into a tool for agriculture. BioLumic's first commercial product is a UV seedling treatment system, where a moving UV LED array exposes young plant seedlings to proprietary treatments of UV light. Such seedlings are typically transplant crops, where after a period of days or weeks in a nursery or glasshouse, seedlings are transplanted into the field for onward growth to harvest. The aim of BioLumic's treatment is to increase the performance of those plants during the field phase. BioLumic's approach aims to be very distinct from the supplementary crop lighting (or 'grow-lighting') commercial space, due to the focus on a treatment to induce biological outcomes, as opposed to simple enhancement of growth rate via photosynthetic stimulation alone, which is often the target of supplementary grow-lighting products (pers. comm. Dr. J. Wargent).

UV radiation has been employed as a tool during UV-C disinfection during large-scale applications for many years. UV-C radiation (λ = 100 – 280 nm) is typically employed as a chemical free method

to reduce pathogen levels on surfaces and in liquids and air (e.g. laboratories, drinking water sanitation, food and beverage disinfection processes). The goal of UV-C disinfection is to supply a minimum lethal UV radiation dose to any pathogen present on a surface or liquid to achieve targeted removal. Required UV-C doses to remove pathogens are well established industry standards[2]. For liquids, UV-C disinfection usually consists of a 'brute force' approach where a high irradiance UV-C source is enclosed in (or surrounds) a narrow vessel through which the liquid flows and adequate delivery of the minimum required dose can be guaranteed all the way to the walls of the vessel (Metcalf & Eddy, 2003). The minimum lethal UV-C doses determine the required irradiance and contact time which in turn determine the delivery vessel dimensions, the flow rate and the UV source specifications. Incidentally, while microalgae can be killed by UV-C, in waste water treatment UV-C is not typically used as the sole source for reducing microalgae levels as the lethal doses required are often very high compared to other microorganisms (Masschelein, 2002). Other widespread applications of UV radiation technology include UV-A lamps for curing adhesives, coatings, inks, varnishes, decorative glazes and lacquers and the use of UV-A and UV-B in skin treatments and tanning beds[3]. While these applications are often widespread, their application does not typically occur at large-scales.

The use of UV in a microalgal biotechnology application to induce desirable responses has been suggested by Salguero et al. (2005) and Wu et al. (2005) but an actual application has not yet been reported in the literature reviewed. While literature in the UV research field in microalgae is valuable in its contribution to our understanding, the impact of UV wavelength and UV dose is often considered in a narrow range (i.e. employing a single UV light source). The targeted UV treatment regimes and UV treatment technology, employed to maximize a desired UV response such as those developed by BioLumic require a detailed understanding of the optimal UV wavelengths and UV dose (i.e. UV irradiance and exposure duration). Sunlight or fluorescent UV tubes are commonly employed in UV research and cover broad wavelength UV in the UV-A (λ = 320 - 400 nm) or UV-B (λ = 280 - 320 nm) parts of the UV spectrum (often in combination with UV filters). While UV irradiance or UV photon flux density (PFD) are commonly reported, the spectral composition of UV emitted by the source is not. Furthermore, the delivered UV dose and its biological effectivity is commonly not considered (i.e. interdependence of UV irradiance and exposure duration). The current understanding generated by the literature is therefore not

[2] Ministry of Health. 2013. *Guidelines for Drinking-water Quality Management for New Zealand 2013*. Third edition. Wellington: Ministry of Health.

[3] Analytik Jena (www.uvp.com)

sufficient to provide a starting point for UV exposure regime development by BioLumic. The literature aims to illustrate the importance of UV wavelength and UV dose by reviewing the metabolic pathways involved in response to UV exposure and UV damage broadly across all microalgae and subsequently in more detail in *D. salina*.

To our knowledge the exploration of the fundamental UV photobiology in microalgae required to develop UV treatment regimes from discrete UV wavebands, complemented with a commercial microalgal-engineering insight, to produce UV treatment regimes and UV treatment technology for application during large-scale microalgae cultivation, has never been attempted. The following sub-sections of the literature review will briefly review UV damage, UV protection and means of UV perception found in microalgae.

2.2.3 UV damage

UV radiation is most commonly known as an abiotic stress. Absorption by UV radiation photons in the cell can be damaging, especially at shorter wavelengths (Hollósy, 2002). Figure 2-2 and Table 2-1 represent an overview of the damaging effects of UV radiation, focussing on photosynthetic organisms. The impact of UV damage as well as UV damage repair mechanisms are discussed in more detail for the microalgae genus *Dunaliella* in sub-chapter 2.3. Please consult work from other authors for exhaustive reviews on UV damage and cellular UV repair mechanisms in other microalgae (Häder, 1997; Roy, 2000; Hollósy, 2002; Sinha & Häder, 2002; Lesser, 2006; Fernanda Pessoa, 2012).

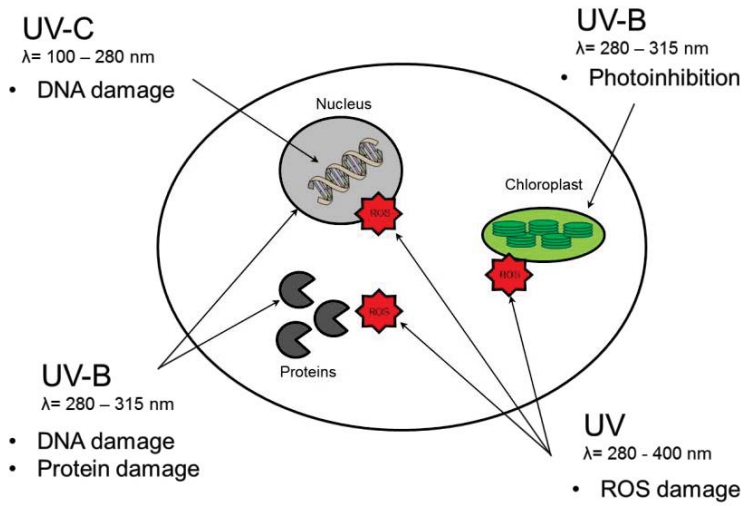

Figure 2-2 Schematic representation of points of UV damage at a cellular level. The figure depicts a photosynthetic eukaryotic cell but is equally applicable to non-photosynthetic and prokaryotic cells.

Table 2-1 General overview of UV damage commonly experienced by photosynthetic organisms.

Type of UV	Target	Damage
UV-C λ = 100 – 280 nm	Direct absorption by nucleotides in the DNA.	Direct absorption by nucleotides causes breakages to the DNA strand, deletion and insertion of nucleotides and inactivation of DNA repair proteins (Sinha et al., 2002). Direct absorption by nucleotides also causes dimerization of adjacent pyrimidines in the same DNA strand leading to cyclobutane-type pyrimidine dimers (CPDs) and the pyrimidine (6-4) pyrimidinone photoproduct ([6-4]PD)) (Sinha et al., 2002).
UV-B λ = 280 – 315 nm	Direct absorption by nucleotides in the DNA.	CPD formation, see above.
	Damage to photosynthetic machinery	UV-B photodamage causes inactivation of PSII through D1 protein destruction resulting in photoinhibition (Hollósy, 2002). Photoinhibition creates redox imbalances in the thylakoid membrane, leading to the accumulation of ROS in the thylakoid membrane which goes on to cause further photodamage. Furthermore, UV-B interferes with the activity of ribulose 1,5-bisphosphate carboxylase/oxygenase (RuBisCo) (Xue et al., 2005).
	Direct absorption by amino acids and proteins.	The aromatic amino acids phenylalanine, tryptophan, tyrosine, histidine, cysteine and cysteine absorb strongly in the UV-B region. Photooxidation, photolysis and chemical changes can alter the functionality of the amino acid (Hollósy, 2002). All proteins in a photosynthetic organism are targets with the potential to disturb vital metabolic functions such as photosynthesis, transcription, DNA replication, and translation (Hollósy, 2002).
	Photosensitization	UV-B generates ROS such as superoxide (O_2^-), hydroxyl radical ($OH^\bullet$) or hydrogen peroxide (H_2O_2) through direct photosensitization (Lesser, 2006). ROS subsequently react with cell components leading to e.g. degradation of proteins, DNA strand breaks, DNA cross- links and lipid peroxidation.

UV-A λ = 315 – 400 nm	Damage to photosynthetic machinery	UV-A has a number of targets in the photosynthetic apparatus: the catalytic Mn-cluster of the water-oxidizing complex (Vass et al., 2002), D1 and D2 proteins and plastoquinone (Q_A and Q_B) binding sites (Verdaguer et al., 2016). UV-A damages these targets through photosensitization of photodegradation, primarily affecting electron transport.
	Photosensitization	Photosensitization generates ROS which subsequently reacts with cell components (see UV-B) (Lesser, 2006).

2.2.4 Defence against UV in aquatic environments

Besides the repair of direct and indirect UV damage (discussed in sub-chapter 2.3), UV avoidance and UV screening are the main strategies utilized by microalgae to protect against UV-radiation (Roy, 2000). Research has shown a UV sensitivity is based on habitat (e.g. Dring et al., 1996) and species specific (Xiong & Komenda, 1997; Holzinger & Lütz, 2006) – e.g. free floating phytoplankton in the open ocean often have different defence mechanisms than motile microalgae found in lakes and different again from benthic microalgae or macroalgae in intertidal habitats. Common UV avoidance and UV screening strategies in aquatic environments will be briefly reviewed in the following sub-sections. The perception of UV in microalgae is discussed in the final sub-section.

The habitat of the microalgae dictates to a large extent the level of UV radiation a microalga is exposed to and what UV avoidance strategies are available to it. Phototaxis and physical screening are two important UV avoidance strategies commonly used by microalgae. UV irradiation can penetrate down to depths of 10-15 meters in lakes, 20-30 m in marine environments and up to 70 m in clear Antarctic Ocean (Fernanda Pessoa, 2012) depending on factors such as incidence of solar radiation, suspended solids in the water and possible wind effects disrupting surface penetrability. Vertical migration in the water column is used by microalgae as a way to modulate the optimal PAR/UV conditions for photosynthesis. Migration through the water column to prevent PAR or UV photodamage mediated by photoreceptors is one of the main physical defence strategies that microalgae have at their disposal (Jiménez, et al., 1996; Moon, et al., 2012; Richter, et al., 2007). Examples of physical UV screening include: mutual shading offered by high microalgae density exposed to solar UV, protecting the microalgae underneath (Roy, 2000), formation of colonies by those microalgae living in intertidal or shallow waters, moving in and out of the sediment layers for photoprotection and intentional formation of layers of elemental sulfur or salt crystals (Sinha, et al., 2001).

Besides UV avoidance, UV screening is the most common strategy employed by a large diversity of organisms. There are many classes of photoprotective compounds spread across the various kingdoms. UV screening pigments are thought to originate from simple UV screening molecules aiding survival of the first (aquatic) photosynthetic organisms in a high intensity UV environment of a pre-ozone layer world. The complex polyphenol compounds found in many higher plants today are assumed to have evolved from simple phenols. Evolution of complex polyphenols as UV screening pigments is thought to have facilitated colonisation of the land in the pre-ozone layer

world (Rozema et al., 2002). These compounds all rely on the use of double bonds and aromatic ring structure to absorb and dissipate UV radiation.

Mycosporine like amino-acids (MAAs, bottom left, Figure 2-3), are photostable UV screening pigments common in cyanobacteria, microalgae and animals. These photoprotective compounds have maximum UV absorption between λ = 310 - 362 nm and can dissipate absorbed radiation efficiently as heat without producing ROS. Scytonemin (top left, Figure 2-3) is the predominant UV-A-photoprotective compound in sheath of some cyanobacteria sheath reducing UV-A penetration into the cell by 90% (Gao & Garcia-Pichel, 2011). The purified form of scytonemin also absorbs significantly at λ = 252, λ = 278 and λ = 300 nm, thus protecting cyanobacteria against both UV-B and UV-C radiation (Rastogi et al., 2010).

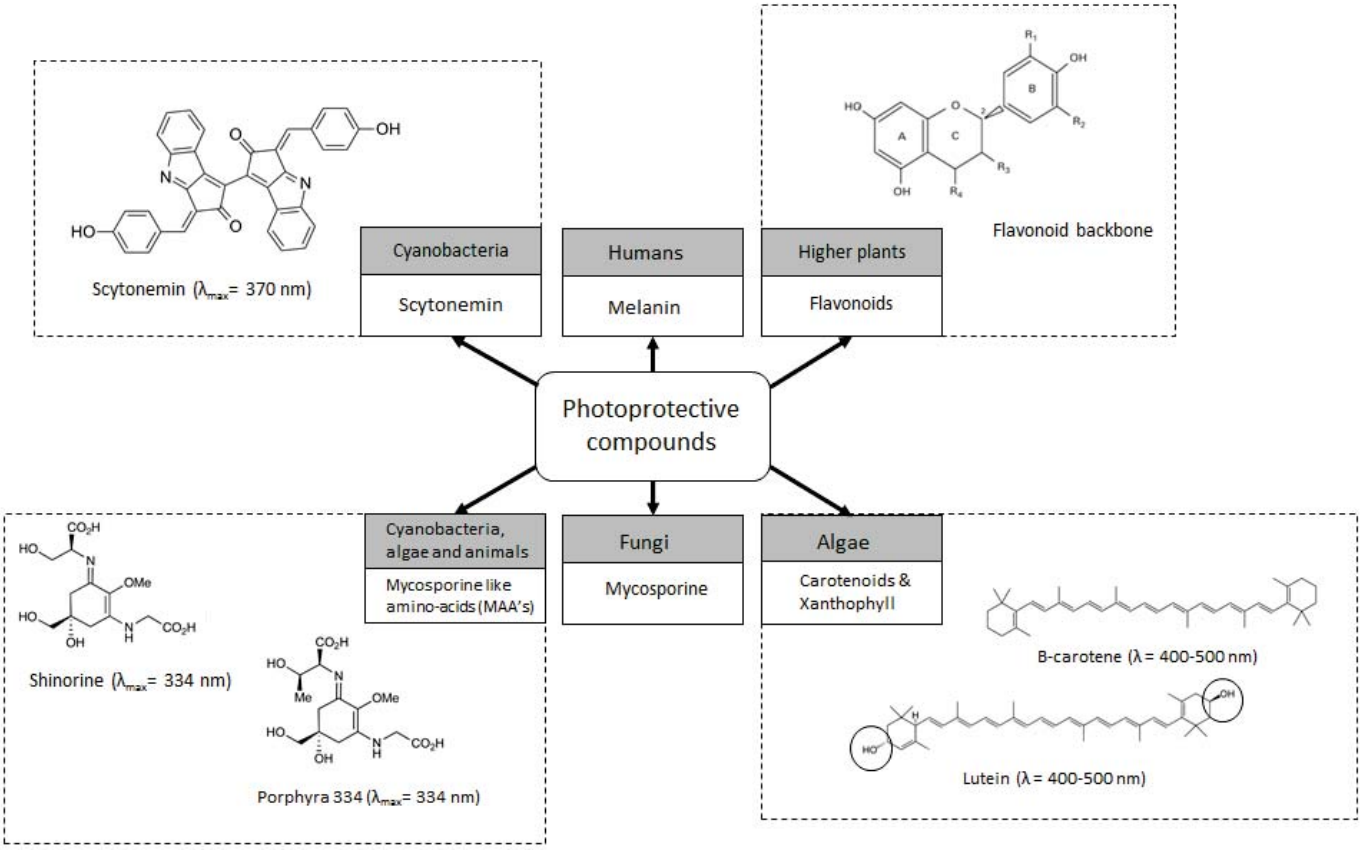

Figure 2-3 A selection of photoprotective compounds found in nature. The absorption maximum (λ_{max}) or absorption region is shown in brackets below the compound. The circles around the –OH groups on lutein indicate the difference between carotenoids (non-oxygenated) and xantophylls (oxygenated).

Carotenoids and xanthophylls (bottom right, Figure 2-3) are important components of the photosynthetic apparatus and are thus found in all photosynthetic organisms (Lichtenthaler,

2012). The carotenoids closely associated with the photosynthetic apparatus are referred to as primary carotenoids. Secondary carotenoids are found in various cell compartment membranes and extraplastidial globules, and are often directly involved with stress response (Lemoine & Schoefs, 2010). The mode of UV protection by carotenoids differs from that of MAAs (and flavonoids) in that carotenoids typically do not absorb in the UV region (absorbing between λ = 400-550 nm) (Gao et al., 2011). Rather, carotenoids are thought to neutralize ROS and quench photosensitization products (non-photochemical quenching) resulting from UV exposure, similar to their functions under high PAR light stress (Demmig-Adams & Adams, 1992). One example, called xanthophyll cycling, involves the reversible de-epoxidation of violaxanthin to its active, heat-dissipating forms antheraxanthin and zeaxanthin resulting from chlorophyll over-excitation (Niyogi et al., 1997). Additionally, carotenoid accumulation in cell membranes and in globules has been recorded for a number of microalgae species and is thought to provide a form of intracellular shading (Ben-Amotz & Avron, 1989b; Lemoine et al., 2010).

The final class of photoprotective pigments discussed here are the flavonoids (top right, Figure 2-3). Flavonoids are a group of polyphenols which include flavones, flavonols, anthocyanins, aurones, and isoflavonoids. Flavonoids are the main UV photoprotective pigments in higher plants, thought to have replaced MAAs during the establishment of terrestrial plants (Rozema et al., 2002). Flavonoids were historically thought to serve as protection against UV solely through screening and antioxidant activity, being found only in tissue close to the external parts of the plant. Flavonoids have since been shown to play a wider role in regulatory and signalling pathways in response to UV exposure (Agati et al., 2013). Over 6,400 flavonoid compounds have been identified thus far in higher plants (Winkel, 2006), typically falling in absorption wavebands λ = 310 - 350 nm (Band I) and λ = 250 - 280 nm (Band II) offering protection against UV-A and UV-B. It has long been assumed microalgae and cyanobacteria do not have biosynthetic pathways to produce flavonoids. Recent research has called this assumption into question with numerous flavonoids found in different microalgae phyla (Goiris et al., 2014).

2.2.5 UV perception

In order to appropriately respond UV radiation and initiate the UV defence mechanisms described above, microalgae need to be able to sense incoming UV radiation. Six major types of sensory photoreceptors (BLUF-proteins, cryptochromes, phototropins, phytochromes, rhodopsins and xanthopsins) are used in nature to regulate developmental processes, photosynthesis, photoorientation, and control the circadian clock (Möglich et al., 2010). Photoreceptor chromophore domains absorb in specific waveband regions. Once excited, conformational

changes of the chromophore domains translate the light signals into changes in biological activity through effector domains (e.g. photoreceptor DNA-binding or kinase domains) or interactions with other proteins (Ziegler & Möglich, 2015). The increasing availability of sequenced genomes and genetic data has led to the identification of a number of homologous DNA sequences encoding photoreceptors in higher plants and microalgae (Kianianmomeni & Hallmann, 2014). Unfortunately, the characterisation of photoreceptors in microalgae is still in its infancy (Hegemann, 2008).

To date the general regulation of the UV-A response by photoreceptors has been poorly investigated in both plants and microalgae (Hegemann, 2008; Verdaguer et al., 2016). The UV-B photoreceptor response on the other hand has been (comparatively) well characterized since the discovery of the UV Resistance Locus 8 (UVR8) specific UV-B photoreceptor (Kliebenstein et al., 2002). This sub-section will discuss microalgal UV-A and UV-B photoreceptors and known responses. An overview of microalgal (prokaryotic and eukaryotic) photoreceptors capable of responding to UV-A (λ = 315 - 400 nm) and UV-B (λ = 320 - 400 nm) is presented in Figure 2-4. Table 2-2 provides a brief summary of microalgal photoreceptor UV-A responses, UV-B photoreceptors are discussed below Table 2-2.

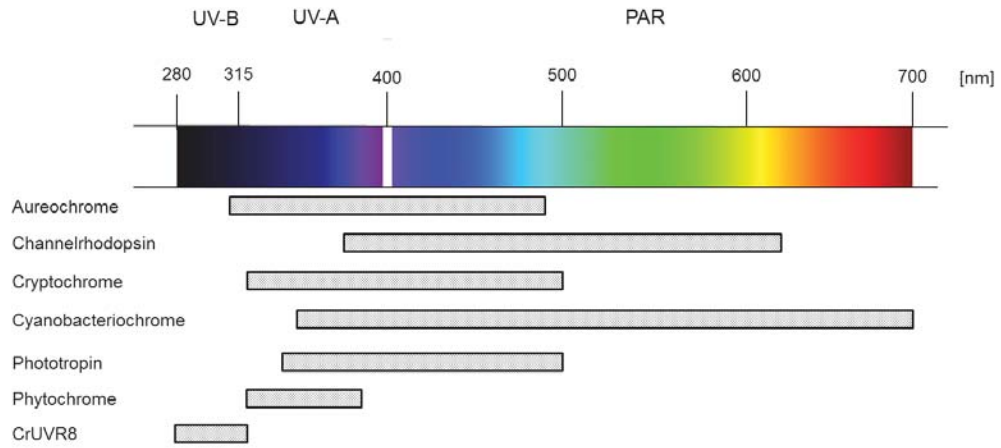

Figure 2-4 Microalgae photoreceptors potentially involved in sensing and responding to UV radiation. The bars beneath the spectrum represent the wavelengths at which the photoreceptor absorbs PAR/UV radiation.

Table 2-2 Overview of microalgal photoreceptors focussed on UV-A absorbance and response. The number below the photoreceptor name represents the active response wavelength region.

Photoreceptor	UV responses in microalgae
Aureochrome (λ = 310 – 480 nm) (Takahashi et al., 2007).	Aureochromes are a recently discovered class of microalgae photoreceptors that shows absorption at 390 nm (absorption λ = 310 – 480 nm) (Takahashi et al., 2007). Besides absorption in the UV-A region, nothing is known about UV-A response.
Channelrhodopsin (λ = 370-600 nm) (Nagel, 2002; Nagel et al., 2003)	A number of rhodopsin-like photoreceptors have been found in microalgae. There appears to be no recorded cellular responses to UV-A from the rhodopsin or rhodopsin-like receptors (Deininger et al., 1995; Ebnet et al., 1999). A rhodopsin found in *C. reinhardtii* was recently shown to be switched between a blue-light and UV-A absorbing state (Luck et al., 2012). This switching behaviour has not yet been coupled to a UV-A signalling response.
Cryptochrome (λ = 320 – 500 nm) (Yu et al., 2010)	A number of cryptochromes are found in cyanobacteria and microalgae and strong absorption peaks in the blue and long wavelength UV-A regions (λ = 360 - 390 nm) (Kianianmomeni et al., 2014). No records of UV-A responses mediated by cryptochromes were found. Cryptochromes are closely related to photolyases and have been reported to repair various types of DNA damage in the diatom *P. tricornutum* (Coesel et al., 2009).
Cyanobacteriochrome (CBRC) (λ = 350 – 700 nm) (Song et al., 2011)	The cyanobacteriochrome UirS-GAF, part of the GAF (cGMP- phosphodiesterase, adenylate cyclase, FhlA) protein family, has been shown to be involved in negative phototaxis responses to high fluence UV-A in *Synechocystis* sp. (Song et al., 2011). The exact pathways have not yet been elucidated but due to conformational similarities to certain plant domains (ethylene-binding domain of the *Arabidopsis* ethylene receptor, ETR1), it is thought that CBRCs may also respond to the ROS generated during (high fluence) UV-A (Song et al., 2011).

Phototropin (λ = 340 – 500 nm) (Briggs & Christie, 2002)	Phototropins, part of the Light-Oxygen-Voltage (LOV) protein family, have been shown to induce a negative phototaxis response in *C. reinhardtii* exposed to near UV-A (LED, λ_{max} = 405 nm) (Trippens et al., 2012). Phototropins have been shown to be involved in carotenoid accumulation in *C. reinhardtii* under PAR conditions (UV not specifically tested) (Im et al., 2006). Apart from these reports, very little is known about the role of the phototropin photoreceptors with regards to UV-A signalling and response in microalgae.
Phytochrome (λ = 300 – 380 nm) (Moon et al., 2011)	Cyanobacterial phytochrome 2 (Cph2) has been shown to be involved in inhibiting positive phototaxis toward low fluence UV-A in *Synechocystis* sp. (Moon et al., 2011). Phytochrome Cph1 undergoes classic red/far-red reversibility *in vitro*.

The action spectrum for the expression of MAA shinorine in the cyanobacteria *Chlorogloeopsis* sp. (PCC 6912) was shown to have an peak at λ = 310 nm, suggesting the presence of a putative photoreceptor in the UV-B region but this was not confirmed (Portwich & Garcia-Pichel, 2000) (action spectra are discussed in Box 3). UV Resistance Locus 8 (UVR8) is the only UV-B photoreceptor characterized in microalgae thus far. (Tilbrook et al., 2016). UVR8 was first identified in *Arabidopsis thaliana* (Kliebenstein et al., 2002) and an orthologue of UVR8 was recently confirmed in *Chlamydomonas reinhardtii* (Tilbrook et al., 2016). The orthologue, Cr-UVR8, was shown to interact with proteins and compliment mutants in *A. thaliana* confirming that it is indeed a full UV-B photoreceptor and closely related to UVR8 found in *A. thaliana* (Tilbrook et al., 2016). Tryptophan amino acid residues act as a light sensing system in UVR8, absorbing between UV-B wavelengths λ = 280 - 300 nm (Rizzini et al., 2011). UVR8 monomerization upon UV-B absorption mediates the formation of photoprotective compounds like flavonoids, antioxidant responses and DNA damage repair leading to UV-B acclimation (Tilbrook et al., 2013). In *A. thaliana,* UVR8 has been shown to play an important role in higher plant photomorphogenesis[4] (Jenkins, 2009; Wargent et al., 2013). Transcriptome analysis identified a set of approximately 70 genes under the control of UVR8 stimulated by UV-B in *A. thaliana* (Brown et al., 2005) meaning more functions are likely to be unravelled in the future.

In *C. reinhardtii*, Cr-UVR8 was shown to aid in UV-B acclimation through increased re-synthesis of the D1 and D2 proteins in PSII under normally photoinhibitory levels of UV-B (Tilbrook et al., 2016). Furthermore, UV-B was found to induce increased accumulation of violaxanthin and energy-dependent non-photochemical quenching related proteins in the Light Harvesting Complex Stress Related protein family and Photosystem II Subunit S (LHCSR1 and PSBS, respectively). CrUVR8 was also shown to induce nuclear gene expression of photosynthesis regulatory proteins targeted for the chloroplast (Allorent et al., 2016). Due to the recent nature of its discovery, the extent of the UV-B signalling pathway and the acclimation response in *C. reinhardtii* are not yet clear however.

[4] Development of plant morphology mediated by light.

2.2.5.1 UV damage as a signalling component

The indirect perception of UV exposure could also occur through general cellular damage (Table 2-2). While not necessarily specific to UV perception, the following components are thought to play a role in activation of UV defence strategies. UV-A and UV-B generate ROS in microalgae such as superoxide (O_2^-), hydroxyl radical ($OH^\bullet$) or hydrogen peroxide (H_2O_2) through direct photosensitization (Lesser, 2006). The chemistry of the different ROS species allows for high target selectivity by ROS detecting molecules (D'Autréaux & Toledano, 2007). Numerous ROS signalling pathways have been identified in both prokaryotes and eukaryotes involved in homeostasis[5] (D'Autréaux et al., 2007). Although ROS is implicated in a large number of UV research studies, no research investigating ROS signalling in UV in microalgae has yet been reported. The mechanisms for ROS sensing in higher plants are also still not fully understood (Tripathy & Oelmüller, 2012).

Additionally, UV-A and UV-B have been shown to damage numerous components of the photosynthetic apparatus, resulting in redox imbalances in the thylakoid membrane (amongst other things). UV-A for example has been shown to damage the catalytic Mn-cluster of the water-oxidizing complex (Vass et al., 2002), D1 and D2 proteins and plastoquinone (Q_A and Q_B) binding sites (Verdaguer et al., 2016), all of which alter the redox state. The redox state of components of the photosynthetic process has been shown to be involved in expression of both chloroplast and nuclear genes to allow adaptation to changing photosynthetic environmental conditions (Pfannschmidt, 2003). The mechanisms by which the redox imbalances are detected and how this is translated into a signal to the cell are still largely unclear however.

[5] Homeostasis refers to the maintenance of a constant internal environment.

2.3 *Dunaliella* UV response

The microalga *D. salina* was chosen as the focus for the current PhD research. Species of the *Dunaliella* genus have been cultivated commercially since the 1980s, with an estimated annual production higher than of 1200 tons algal DW·y^{-1} (as per 2006, Spolaore, et al., 2006). Furthermore *Dunaliella* species have also been used as a model system for studying microalgae cellular responses to visible light and UV radiation stress due to their high UV tolerance (Ghetti et al., 1998). In recent years, several *Dunaliella* species have been shown to have a large UV-A induced carotenoid accumulation response (Jahnke, 1999; Salguero et al., 2005; Mogedas et al., 2007). The UV-A induced carotenoid accumulation response was confirmed for the experimental species *D. salina* (strain UTEX 1644) during the proof-of-principle stages of the project (see Chapter 3 and Appendix 9.2).

The known impacts of UV exposure on species of the *Dunaliella* species will be discussed in more detail. This part of the literature review aims to identify those factors that are likely to impact the development of UV delivery regimes and UV treatment technology during large-scale *D. salina* cultivation. First the biology and biotechnology of *Dunaliella* will be briefly reviewed. The next sub-section will then review the UV-A induced carotenoid accumulation response as well as non-UV-A induced carotenoid accumulation in *Dunaliella*. The function and regulatory mechanisms for the carotenoid accumulation will be discussed in detail. Finally, the impact of UV exposure on species of the *Dunaliella* genus other than the UV-A induced carotenogenic response are reviewed.

2.3.1 *Dunaliella* biotechnology

2.3.1.1 *Dunaliella*

The morphology of the halotolerant *Dunaliella* genus was reviewed extensively in Borowitzka & Siva (2007). An overview is summarized here. Cells of *Dunaliella* are unicellular and typically ovoid or ellipsoid in shape (Figure 2-5). Cells can be motile with flagella located at the anterior part of the cell. There is a single large posterior chloroplast occupying most of the cell volume which is either cup-, dish- or bell-shaped and contains a pyrenoid (Figure 2-5). Cells of *Dunaliella* lack a rigid cell wall meaning that cells change shape, particularly as a result of changing environmental conditions. Extreme conditions such as following osmotic shock, increased salinity and changing temperatures can cause cells to become spherical temporarily before returning to their normal shape.

Most species of *D. salina* (inc. *D. salina*) reproduce by means of both vegatative and sexual reproduction. Vegetative cell division in *D. salina* involves nuclear division followed by infurrowing of the cell (Borowitzka & Siva, 2007). Sexual reproduction, the fusion of two gametes to form a zygote, has been shown to be inducible in *Dunaliella* species by reducing culture media salinity (Borowitzka & Siva, 2007). Lerche (1937) showed that 5 out of 6 *Dunaliella* species tested could be induced to reproduce sexually in this manner. The zygote has a thick outer layer and can withstand exposure to freshwater prolonged periods of dryness (Oren, 2005). Zygotes of *Dunaliella* species can germinate to release up to 32 haploid daughter cells (Lerche, 1937).

Species of the *Dunaliella* genus have two defining traits. The first is that all species can accumulate high levels of the intracellular osmolyte glycerol to survive the extreme saline conditions of the species' habitat (Ginzburg & Ginzburg, 1985). The second defining trait is the ability of some Dunaliella species (*D. bardawil, D. salina, D. parva, D. pseudosalina*) to accumulate high levels of intracellular carotenoids, most commonly β-carotene (up to 10% algal DW) (Ben-Amotz et al., 1982). The β-carotene biosynthesized in *Dunaliella* accumulates in β-carotene rich globules (Figure 2-5), largely consisting of the 9-cis and all-trans stereoisomers (40% and 50% of the total respectively). This ratio is characteristic for PAR light induced carotenogenesis (Ben-Amotz et al., 1988).

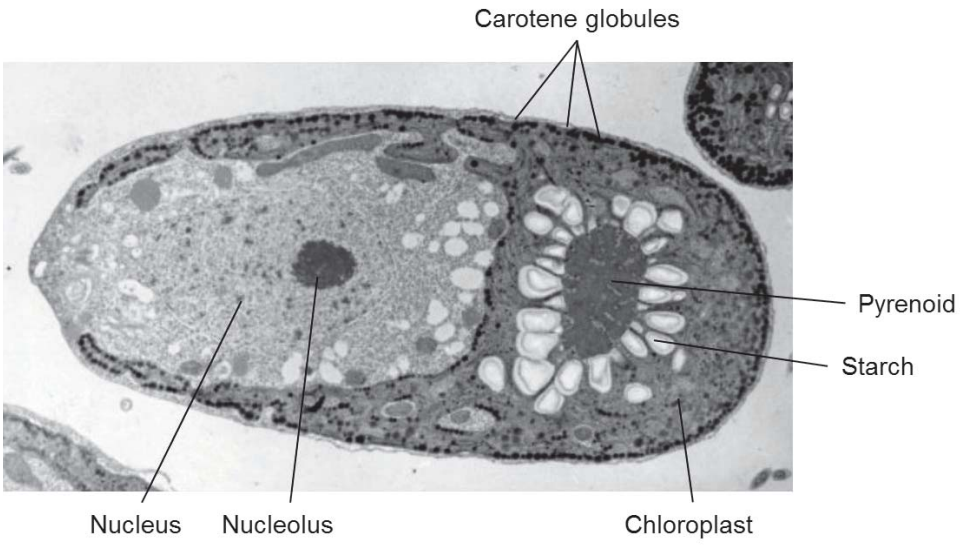

Figure 2-5 Electron micrograph of D. bardawil *cell with intermediate carotenoid content. Note the dark carotenoid-containing lipid droplets in the chloroplasts. Adapted from Borowitkza (2013a) with publisher permission.*

2.3.1.2 *Dunaliella* carotenoid accumulation under non-UV carotenogenic conditions

The main factors known to positively influence the β-carotene content of *Dunaliella* are: PAR intensity (Loeblich, 1982), salinity (Borowitzka et al., 1984), nitrogen deficiency, phosphorus deficiency, temperature and CO_2 supply (Ben-Amotz et al., 1982). An overview of factors is shown in Table 2-3.

Table 2-3 Summary of the influence of various environmental factors on the biomass and β-carotene content in D. salina. + = stimulating effect; - = inhibitory effect; 0 = no effect. Source: Borowitzka & Borowitzka (1989)

Factor	Biomass	β-carotene
Increase in salinity	-	+++
Decrease in salinity	+	-
N deficiency	-	+
P deficiency	-	+
Increase in CO_2 supply	+	0
Increase in PAR intensity	0	++++
Decrease in PAR intensity	0	-
Increase in temperature	0	+
Decrease in temperature	-	-
Increase in $[O_2]$	0	-

High levels of PAR intensity (> 500 $\mu mol \cdot m^{-2} \cdot s^{-1}$ PAR) and high salinity (up to saturation) are the two largest contributors to the massive β-carotene accumulation in *Dunaliella* species, with the combination of both being most effective (Ben-Amotz & Avron, 1983). Conversely, an inverse relationship exists between β-carotene and biomass growth rate meaning factors that improve accumulation (except high PAR intensity) typically slow growth (Borowitzka et al., 1984). Despite the above knowledge being applied to the commercial cultivation process for decades, the exact function and signalling involved in massive β-carotene accumulation remain unclear (Lamers et al., 2008; Ye et al., 2008). The main hypotheses are discussed in sub-section 2.3.2.

2.3.1.3 Commercial *Dunaliella* cultivation

Commercial cultivation of *Dunaliella* was started in the 1980s, making the β-carotene sourced from these microalgae the first high-value bioproduct produced by means of commercial microalgae cultivation (Borowitzka, 2013b). Synthetically produced β-carotene is entirely of the all-trans β-carotene, while the 9-cis isomer found in *Dunaliella* offers significant market differentiation. The origin of the β-carotene often leads to the product being referred to as 'natural β-carotene'. β-carotene is most commonly used as a food additive for its pigmentation

properties as well as its nutritional properties (primarily as pro-vitamin A). Markets include aquaculture and pet feed industries as well as human consumption (Dufossé et al., 2005). High-value applications include colourant and anti-oxidant in cosmetic and pharmaceutical industries (Dufossé et al., 2005). The market for natural β-carotene is estimated to about US$ 55 - 80 million, making up 20 – 30% of the total β-carotene market share (Borowitzka, 2013b). A global annual production of 1200 t algal dry weight *Dunaliella* biomass was reported in 2006 (Spolaore et al., 2006).

The cultivation of *Dunaliella* lends itself particularly well to biotechnological applications due to the species' tolerance to high salinity. While e.g. *D. bardawil* grows optimally at 1 – 2 M NaCl, it can survive in concentrations exceeding 2 M NaCl up to saturated brine (Moulton et al., 1987b). High salinity (> 2M NaCl) is employed as a means of predator control as well as a means of inducing β-carotene accumulation (in combination with high PAR levels). Additionally, large-scale cultivation commonly employs media N-deficiency to control β-carotene accumulation (Ben-Amotz, 2004).

Commercial *Dunaliella* cultivation takes place in two main cultivation systems termed 'extensive' – large, unmixed, shallow open ponds – and 'intensive' – mixed, open raceway ponds (Figure 2-6) (Borowitzka, 2013a). While the culture of *Dunaliella* has been attempted in closed photobioreactors, attempts at commercialisation have been called a 'spectacular failure' (Borowitzka, 2013a). Fundamental principles involved in large-scale microalgae cultivation are presented in Box 2.

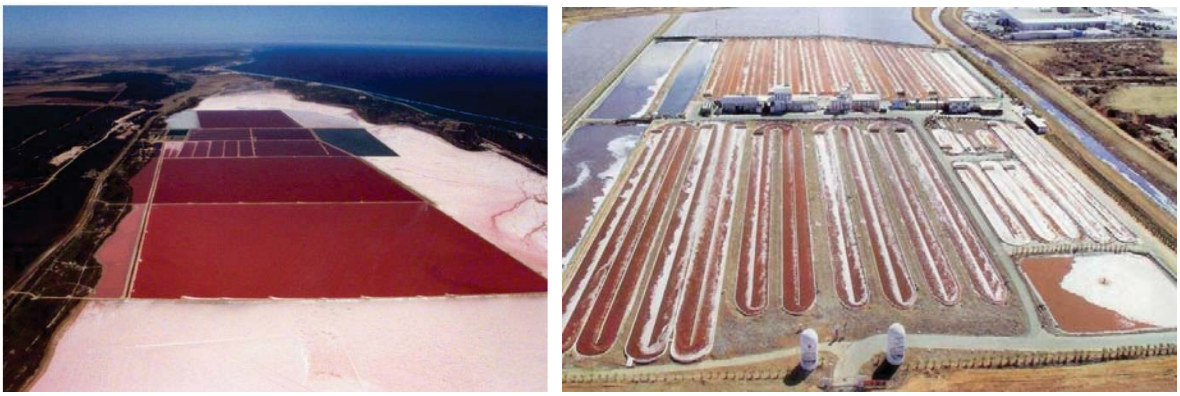

Figure 2-6 Examples of the two most common cultivation methods employed during commercial Dunaliella *cultivation. (Left) Extensive cultivation, Cognis plant at Hutt Lagoon, Western Australia. (Right) Intensive cultivation, NBT Ltd. at Eilat, Israel. Left image taken from Borowitkza (2013a) with publisher permission. Image to the right was provided by, and used with permission, by Dr. Ami Ben-Amotz (National Institute of Oceanography, Israel).*

The two cultivations system differ significantly in their modes of operation and aerial productivities. An overview literature values for key cultivation parameters are shown in Table 2-4. The design principles for large-scale cultivation system are discussed in more detail in Box 2.

Table 2-4 Key cultivation parameters as found in literature describing commercial D. salina cultivation. Values represent averaged (annual) values. Literature sources are given below table.

	Unit	Extensive	Intensive
Surface area pond	m^2	6,000 - 2,000,000[f]	3,000-4,000[b]
Pond depth	m	0.3[d]	0.2-0.3[d]
Active mixing	N/A	No[b,d]	Yes[b,d]
Cellular β-carotene content	% w/w algal DW	5%[d]	5%[a]
β-carotene conc.	g β-carotene·m^{-3}	0.1[b,e]	5-15[b,e]
$P_{\beta\text{-carotene}}$	g β-carotene·m^{-2}·d^{-1}	0.01[e]	0.2-0.25[a,b]
Biomass conc.	g algal DW·L^{-1}	0.1[c,d]	0.5[a]
$P_{Biomass}$	g algal DW·m^{-2}·d^{-1}	0.05 – 0.1[e]	5[a]

Sources:
[a] (Ben-Amotz & Avron, 1989a), [b] (Ben-Amotz, 2004), [c] (Borowitzka & Borowitzka, 1990), [d] (Borowitzka, 2013a) [e] (Hosseini Tafreshi & Shariati, 2009), [f] (Moulton & Borowitzka, 1987a)

Box 2 – Engineering aspects of large-scale *Dunaliella* cultivation

The extensive and intensive cultivation methods differ significantly in their mode of operation as illustrated in Figure 2-6 and Table 2-4. This box provides a general overview of underlying engineering considerations per mode of operation. This box will focus on engineering aspects which will be considered throughout the thesis and in the TEA in chater 6. Please refer to other literature sources for detailed analysis of large-scale microalgae cultivation (Richmond, 2004; Andersen, 2005; Barsanti & Gualtieri, 2006).

- **Photosynthetic efficiency**

Photosynthetic organisms rely on energy provided by solar radiation for carbon fixation and thus growth and bioproduct formation. The maximum efficiency of photosynthesis under sola radiation can be calculated. The chemical energy required to fix CO_2 into 1 mole of biomass is estimated equivalent to that of 10 to 12 PAR photons (Tredici, 2010). Considering only around 45% of solar radiation is PAR and that not all the absorbed photons are of the correct wavelengths to drive photosynthesis efficiently , a maximum theoretical photosynthetic efficiency of 10 % has been calculated for photosynthetic organisms (Tredici, 2010). In the field, photosynthetic efficiency decreases from the theoretical maximum as a result of various factors including reflection of light

off the waterbody, transmission of PAR into the culture vessel, (dark) respiration and photorespiration and also photosaturation and photoinhibition (Tredici, 2010).

- **Mixing: Photosynthetic rate and the impact of cell density**

There is a distinct relationship between photosynthetic rate (P) and PAR light intensity (I) shown in Figure Box 2-1 has a profound impact on microalgae productivity.

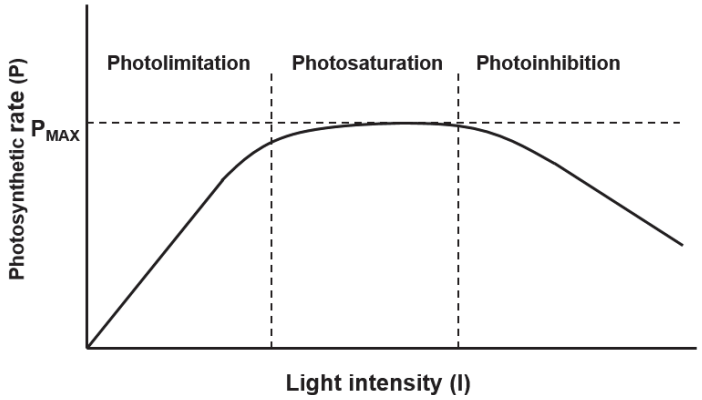

Figure Box 2-1 Impact of light intensity on photosynthetic rate.

The curve has three general regions. At low light intensity, photolimitation occurs where the rate of electron turn-over in PS II exceeds photon absorption meaning carbon fixation is limited by the photon flux. At increased light intensity, a point is reached where the rate of photon absorption matches the rate of electron transfer in PSI II, also known as photosaturation, and the maximum photosynthetic rate is achieved (P_{MAX}). As light intensity increases further, the photon absorption exceeds rate of electron turnover in PS II and eventually this leads to a light-induced depression of photosynthesis, commonly referred to as photoinhibition (Richmond, 2004).

During large scale microalgae cultivation, cells are exposed to a light intensity gradient as the

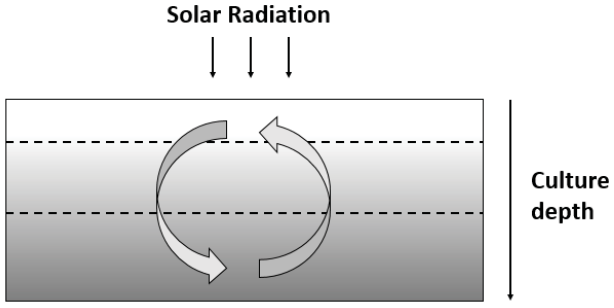

Figure Box 2-2 Light intensity gradient as a function of culture depth. Large arrows represent microalgae cell movement.

cells move vertically through the culture vessel (Figure Box 2-2). Depending on the cell density, the light intensity at a given depth in the culture vessel leads to regions where cells experience photoinhibition (top), photosaturation (middle) and photolimitation (bottom). Hence, the most efficient growth occurs in the region of photosaturation (middle), with decreased growth rate occurring in the photoinhibited (top) and photolimited (bottom) regions. The depth at which the photosynthetic rates are experienced by the cells depends on the light transmission into the culture media which decreases exponentially as a function of cell density (Tredici, 2010, see also sub-chapter 5.3). Therefore, the amount of time cells spend in each region has a large impact on photosynthetic rates and thus the achievable biomass productivity of a large-scale cultivation system – i.e. the degree of vertical mixing. In the case of the two large-scale *Dunaliella* cultivation systems this is reflected by significant differences in biomass productivity and concentration resulting from the mode of mixing - i.e. no mixing vs active mixing in extensive and intensive cultivation respectively. Mixing also aids in preventing cell settling, avoiding thermal stratification, distributing nutrients and promoting gas exchange (i.e. diffusion of CO_2 and removal of photosynthetically generated oxygen from the culture media) (Tredici, 2004).

- **Cultivation vessel sizing**

The size of a large-scale microalgae cultivation system is determined by the required annual production. The production per unit time of the desired product, be it biomass or bioproduct, is commonly calculated as areal productivity with units 'product (g) · unit area $(m^2)^{-1}$ · unit time $(d)^{-1}$'. In the case of large scale *Dunaliella* cultivation these are expressed as areal productivity of biomass $P_{Biomass}$, or bioproduct $P_{\beta\text{-}carotene}$, in units 'g algal DW·$m^{-2}$·$d^{-1}$' and 'g β-carotene·$m^{-2}$·$d^{-1}$' respectively. Based on the maximum photosynthetic efficiency assumptions and limitations, a theoretical maximum $P_{Biomass}$ averaged throughout the year for large-scale algae cultivation has been calculated as 14.31 g algal DW·m^{-2}·d^{-1} (Grobbelaar, 2010).

Due to the harsh cultivation conditions (i.e. high PAR and high salinity) the $P_{Biomass}$ during large-scale *Dunaliella* cultivation is considerably lower than the theoretical maximum. Furthermore, the $P_{Biomass}$, and thus $P_{\beta\text{-}carotene}$, is 25 – 100 times higher in the intensive cultivation system compared to extensive cultivation (Table 2-4). The difference results primarily from active mixing employed in the intensive system as well as other forms process control (see below). It follows that, in order to achieve the same annual production, the culture vessel surface area of the extensive systems has to be 25 – 100 times larger than that of the intensive system.

- **Mode of operation and process control**

This sub-section will focus only on the process control considerations for the extensive and intensive cultivation systems. Grobbelaar (2010) states the parameters that can be controlled in large-scale microalgae cultivation as follows: the culture operation (being either semi-continuous, continuous or batch), culture depth, mixing (and resultant turbulence), supply of nutrients and CO_2 (and resultant pH control), and biomass concentration. Large-scale cultivation of *Dunaliella* also requires salinity levels to be maintained.

The reference extensive cultivation process is described by Borowitzka (2013a) (referenced unless stated otherwise). Process control during the large-scale extensive cultivation is minimal which contributes to the low operating cost of this type of cultivation system. To control salinity and replenish evaporated water, seawater augmented with salt and nutrients is pumped into the system. Nutrients that are added include nitrogen (as nitrate), phosphorus (as phosphate), iron (as iron (III) chloride in chelated form with EDTA) and micronutrients (Ben-Amotz et al., 1989a). Sulphate, magnesium and potassium content are commonly high in seawater and are not supplied. The ponds are continuously harvested and with continuous supplementation of seawater or recycled media this results in effectively continuous operation. The flow generated by media supplementation and harvest, combined with natural convection, also contributes to mixing in the extensive cultivation system. No further process control is reported in the literature.

More process control is included in intensive cultivation which adds to operational expenses. The reference intensive cultivation process is described by Ben-Amotz & Avron(1989a) (referenced unless stated otherwise). Intensive cultivation systems operated as batch or semi-continuous systems which recycle more media than the due to the increased nutrient content (required for increased productivity). Fresh media is supplied with the same salt and nutrients as described above. Due to the fragile nature of *Dunaliella* cells mixing is achieved by means of a single paddle wheel and turbulence is increased by baffles. The motile nature and positive phototactic behaviour allow low linear liquid velocities of at least 10 $cm \cdot s^{-1}$ for optimal growth. The pH usually is maintained at 7.5 ± 0.2 by both CO_2 gas and HCl. The CO_2 is regularly bubbled into the culture whereas HCl is added occasionally as upper threshold control. Supplementation of CO_2 gas is also used as an inorganic carbon supply.

- **PhD research scope**

The incorporation of the above engineering aspects and parameters in the experimental research design is discussed in sub-chapter 3.2.

2.3.2 *Dunaliella* carotenogenesis

As mentioned in the first part of this subcsub-section, the main factors known to positively influence the β-carotene content of *Dunaliella* are; PAR intensity, salinity, N-deficiency, P-deficiency, temperature and CO_2 supply (Table 2-3). Research has shown UV-A exposure as another parameter that positively influences the β-carotene content of *Dunaliella* (Jahnke, 1999). This sub-chapter will review the UV induced carotenogenic response in *Dunaliella* and subsequently discuss the main hypotheses on the function and regulation of β-carotene accumulation in *Dunaliella*. The effects of direct and indirect UV damage in *Dunaliella* other than the UV induced carotenogenic response are reviewed in the next sub-chapter.

2.3.2.1 *Dunaliella* UV induced carotenogenesis

The current sub-section focusses on UV-A induced carotenoid accumulation in *Dunaliella*; the function of the accumulated carotenoids and the hypotheses on the signalling involved in their induction is discussed below. The first record of UV-A induced carotenoid accumulation in *Dunaliella* species was reported by Jahnke (1999). The author found that under UV-A exposure conditions tested (UV-A = λ = 345 – 400 nm, UV-A = 20 - 116 µmol m^{-2} s^{-1}, 24 h·d^{-1} exposure) the carotenoid to chlorophyll ratio (Car:Chl) was increased in *D. bardawil* UTEX[6] 2538 and *D. salina* strain UTEX 1644 but not *D. salina* UTEX 200, *D. parva* or *D. tertiolecta*. Furthermore, the author found an increased Car:Chl under all growth conditions without impacting growth (PAR = 95 – 1,500 µmol m^{-2} s^{-1}, salinity = 0.5 – 3 M NaCl). The Car:Chl increases resulted primarily from increased cellular carotenoid content, rather than decreased chlorophyll content. Exposure to 6% UV-A (UV-A = 81 µmol m^{-2} s^{-1}, PAR = 1,500 µmol m^{-2} s^{-1}) yielded a cellular carotenoid increase upwards of 100% with little impact on chlorophyll content. In comparison, increasing PAR intensity 4-fold and 15-fold resulted in a maximum 50% cellular carotenoid increase (PAR = 95 - 1,500 µmol m^{-2} s^{-1}). Salguero et al. (2005) and Mogedas et al. (2009) found β-carotene to be the main carotenoid accumulated during UV-A exposure in *D. bardawil*. Furthermore, Salguero et al. (2005) found changes in xanthophyll contents with 180% increase in lutein, 234% increase in violaxanthin and 407% increase in zeaxanthin contents, concomitant with β-carotene accumulation.

Jahnke (1999) found the UV-A induced carotenoid accumulation in *D. bardawil* to be proportional to UV-A photon flux density (PFD). The author found maximum carotenoid accumulation in *D. bardawil* was observed at the highest UV-A PFD tested (116 µmol m^{-2} s^{-1}) although other authors

[6] UTEX = Culture Collection of Algae at the University of Texas at Austin identifier

reported a decrease in carotenoid accumulation above 70 µmol m^{-2} s^{-1} in *D. bardawil* (Salguero et al., 2005). Studies employing similar UV exposure regimes (24 h·d^{-1}, UV-A PFD = 70 – 90 µmol m^{-2} s^{-1}) found carotenoid accumulation induction in *D. bardawil* to occur anywhere from 1-2 days (Jahnke, 1999) up to 12 days (Mogedas et al., 2009). The studies utilized different reactor volumes of 150 mL (Jahnke, 1999) and 3.2 L (Mogedas et al., 2009) (both well mixed), which may explain an increased induction time. The impact of non-UV carotenogenic stimuli was investigated by Mogedas et al. who found combining UV-A exposure with N-depletion increased cellular carotenoid content (as pg·$cell^{-1}$) 6.4-fold over exposure with UV-A only. Despite the increase in cellular carotenoid content, the authors found the concomitant decreased growth resulting from N-depletion led the final total carotenoid concentration (as mg·mL^{-1}) being lower in the N-depleted cultures (Mogedas et al., 2009). Applying other stress conditions (PAR intensity up to 1,500 µmol m^{-2} s^{-1} and salinity up to 3 M) was found to enhance the UV induced Car:Chl (Jahnke, 1999).

While the authors speculate on the mechanisms behind the UV-A induced carotenoid accumulation, to date no clear mechanism has been found (Lamers et al., 2008). The function and regulation of the hyper accumulated carotenoids is discussed below.

2.3.2.2 Function and signalling of hyper accumulated β-carotene

In *Dunaliella* species the hyper accumulated β-carotene collects in lipid globules in the interthylakoid spaces, primarily at the chloroplast periphery, contrary to the primary β-carotene located in the thylakoid membrane (Borowitzka et al., 1990). The widely accepted hypothesis for the role of the β-carotene in *Dunaliella* is that the globules aid in photoprotection by screening excess light (Ben-Amotz et al., 1989c). Due to the absorbance characteristics of β-carotene, the screening capacity of β-carotene in *Dunaliella* is restricted to the UV-A/blue region of the spectrum (λ < 496 nm) (Ben-Amotz et al., 1989c). In *D. bardawil* the photoprotective function of β-carotene was evidenced through a significant reduction in photoinhibition under high PAR light conditions as well as improved recovery (Ben-Amotz et al., 1987). The β-carotene biosynthesis in *D. bardawil* was dependent on PAR irradiance but independent of light quality within the PAR radiation region; light sources with peak emissions of λ = 546 nm, λ = 578 nm or longer than λ = 645 nm as well as white light all induced β-carotene accumulation equally well (Ben-Amotz et al., 1989b). The observation that red light longer than λ = 645 nm was as effective as white light at inducing β-carotene accumulation lead the authors to suggest that light absorption by chlorophyll is sufficient as a first step to inducing carotenogenesis rather than involving a PAR-photoreceptor.

In the PSII reaction centre, especially under high PAR irradiance, $^1O_2$ is quenched by β-carotene (Tripathy et al., 2012). The physical distance between the hyper accumulated β-carotene and the photosynthetic machinery has been suggested to prevent efficient quenching of ROS. The selective photoprotection offered by β-carotene (below λ = 578) has been suggested as further evidence that β-carotene acts as a screen rather than an anti-oxidant (ROS are assumed to be generated at all wavelengths at photoinhibitory levels) (Ben-Amotz et al., 1989c). However, Shaish et al. (1993) have shown that ROS plays an integral part in the induction of β-carotene accumulation. Induction of carotenogenesis is achieved using both non-light and light dependent ROS generators (Rose-Bengal, Acifluorfen, cumene hydroperoxide and t-butyl-hyperoxide) as well as anti-oxidant enzyme inhibitors (azide, inhibits SOD and catalase). All ROS generators induced accumulation of β-carotene in *D. bardawil* under non-inducing, low PAR light conditions without interference to growth. Similar levels of β-carotene accumulation were found under these conditions as those typically observed by high PAR light induction. The ROS generated during photooxidation processes has therefore been suggested to function as a primary or secondary messenger for the induction of β-carotene accumulation, although a 'ROS receptor' has not yet been identified (Lamers et al., 2008).

Despite the clear UV-A induced carotenoid accumulation response in *Dunaliella* species, there have been no studies into the cellular mechanisms involved. A putative UV-A photoreceptor has been suggested but has not been investigated to date. Rather, the suggested reason for the UV-A induced carotenoid accumulation response by most authors is the overlap of non-UV carotenogenesis signals and the forms of UV damage resulting from UV-A exposure (PSII photodamage, electron transfer interference and ROS generation through direct photosensitization or damage to PSII). The consensus in literature therefore appears to be that UV-A indirectly induces carotenoid accumulation through UV-A damage (Lamers et al., 2008). Imbalances in the photosynthetic apparatus redox state, in particular that of the plastoquinone pool, resulting from high PAR intensity have been suggested as signal for β-carotene induction (Lamers et al., 2008; Borowitzka, 2013a). While no conclusive research has been carried out in *Dunaliella*, the plastoquinone redox state was indicated as leading to the expression of carotenoid biosynthesis genes in *H.pluvialis* (Steinbrenner & Linden, 2003).

2.3.3 *Dunaliella* UV responses

In order to better understand the feasibility of using targeted UV treatment for the control of biomass and bioproduct formation in commercial *D. salina* cultivation, it is important to understand the range of UV responses reported in *Dunaliella* literature, other than UV-A induced carotenoid accumulation. A better understanding of the wider range of UV responses may help identify constraints and added benefits important for application of UV treatment during commercial cultivation. For the purpose of this sub-chapter, various aspects of the UV response will be discussed per topic. It should be noted that direct comparison of data between published articles is troublesome due to the large variation of UV waveband compositions and irradiances used. This is further complicated by conflicting reports under similar conditions.

2.3.3.1 Cell morphology

Exposure to all UV wavebands has been found to alter cell morphology in *Dunaliella* species. Segovia et al. (2015) found that exposure to broad wavelength UV-A (λ = 320 - 400 nm) left cell size unchanged while and broad wavelength UV-A + UV-B (λ = 300 – 400 nm) increased cell volume. Cell proliferation was found to continue, albeit at a decreased rate compared to PAR-Only exposure. A study by Masi & Melis (1997) in *D. salina* found an 108% increase in cell volume during UV-B exposure (λ = 280 – 320 nm). Interestingly the total biomass content remained similar to PAR-Only ($n_{control} \cdot Vol_{control} \approx n_{UV\text{-}B} \cdot Vol_{UV\text{-}B}$) during this experiment. The authors of the two respective reports suggest two different reasons for the increase in cell size. Segovia et al. (2015) suggest the increases in cell size are a protection mechanism against UV damage by increasing internal self-shading (as discussed by Garcia-Pichel, 1994). Masi & Melis (1997) on the other hand propose cells of *D. salina* exposed to UV-B may be halted in G2 cell cycle stage due to DNA damage, while still being able to continue growing in size.

Transmission electron micrographs (TEM) of *D. tertiolecta* exposed to combinations of broad wavelength UV-A (λ = 320 - 400 nm) and UV-A + UV-B (λ = 300 – 400 nm), either in the presence and absence of PAR, showed numerous detrimental effects. Exposure to broad wavelength UV-A for 48 h led to an accumulation of starch and an aggregation of chromatin. Thylakoids appeared organised, and none of the organelles showed evidence of damage (Segovia et al., 2015). Exposure to UV-A + UV-B in the absence of PAR showed a considerable margination of chromatin and accumulation of lipid drops in otherwise intact cells (Segovia et al., 2015). Another study found exposure to UV-A + UV-B in the presence of PAR led to chromatin disaggregation, albeit only in the first hours of exposure, with starch accumulation and the start of chloroplast disintegration

after 48 hours exposure (García-Gómez et al., 2012). Zhang et al. (2015) and Tian & Yu (2009) found chloroplast, pyrenoid, vacuole and mitochondrial structures in *D. salina* were swollen or irregular in size during increased UV-B exposure (i.e. above solar UV-B levels). These observations indicate UV-B exposure interferes with biological processes in these organelles. White & Jahnke (2002) report photobleaching in *D. bardawil* and *D. salina* as a result of UV-B exposure (λ = 290 – 340 nm) at UV PFDs higher than 1.9 $\mu mol \cdot m^{-2} \cdot s^{-1}$.

2.3.3.2 Cell proliferation (growth)

Reports of growth rate changes are varied across *Dunaliella* species and UV wavebands. Studies investigating growth rate changes resulting from long wavelength UV-A (λ = 340 -400 nm) exposure either found no changes in cell proliferation for *D. bardawil* and *D. tertiolecta* (Hannach & Sigleo, 1998; Jahnke, 1999), or increases in cell proliferation exposure in *D. bardawil* (Salguero et al., 2005; Mogedas et al., 2007, 2009). The growth rate of *D. bardawil* was found not to be affected even when UV-A comprised 46% of the total radiation (i.e. 81 $\mu mol \cdot m^{-2} \cdot s^{-1}$ UV-A and 95 $\mu mol \cdot m^{-2} \cdot s^{-1}$ PAR) (Jahnke, 1999). Mogedas et al report that increased growth rate appeared to be of limited duration, as cell proliferation was decreased after more than 100 h of continuous UV-A exposure (Mogedas et al., 2007, 2009). Exposure to broad wavelength UV-A (λ = 320 - 400 nm) showed decreases in growth rate in *D. tertiolecta* (Segovia et al., 2015). Growth rates in *D. tertiolecta* have been reported to decrease during exposure to broad wavelength UV-A + UV-B (λ = 300 – 400 nm) (Hannach et al., 1998; García-Gómez et al., 2012, 2016; Bouchard et al., 2013; Segovia et al., 2015). While growth rates are decreased below those of PAR-Only in all cases, cell proliferation continued. Bouchard et al. (2013) found 'around 20%' cell death after 48 h UV-A + UV-B exposure after which cell numbers remained stable. Conversely, García-Gómez et al (2012, 2016) and Segovia et al (2015) found that 97% and 99% of cells remained viable at the end of the experiments using the same UV-A + UV-B irradiance (144 h UV exposure).

The impact of UV-B (λ = 280 – 320 nm) on growth rates has not been well reported. Andreasson & Wängberg (2007) constructed a biological weighting function (BWF) for *D. tertiolecta* growth rate by which they clearly showed that growth is inhibited at decreasing UV wavelength (starting at λ < 320 nm) (see Box 3 for action spectra and BWF explanation). Masi & Melis (1997) found a similar decrease in cell proliferation in *D. salina* as a result of UV-B exposure (0.75 $\mu mol \cdot m^{-2} \cdot s^{-1}$) in *D. salina*.

Box 3 – Action spectrum and Biological Weighting Function

Photosynthetic organisms do not respond to all wavebands in the visible and UV spectrum equally. The simplest approach for quantifying the impact of different wavebands on a single monitored biological phenomenon (e.g. DNA damage, photosynthesis) is a response spectrum, which quantifies the response to a fixed irradiance across narrow waveband regions (Aphalo et al., 2012). However, because irradiance is rarely fixed in natural environments, it is difficult to estimate the effectiveness of a given waveband at inducing the response. An action spectrum therefore incorporates measurement of the monitored response at different irradiances in each narrow waveband region. The slope of the response curve (per narrow waveband waveband) is termed the spectral weighting coefficient, ε(λ), and represents the effectiveness of a narrow waveband region at inducing the observed response.

A distinction is made between monochromatic and polychromatic action spectra. Monochromatic action spectra observe responses in isolated narrow wavebands (Neale, 2000) (referenced below unless stated otherwise). Polychromatic action spectra utilize cut-off filters, i.e. filters that pass longer wavelength light starting at shorter cut-off wavelengths and generating successively larger wavebands. Polychromatic action spectra aim to incorporate interactions of different wavebands to more closely simulate natural conditions, at the expense of specificity. Polychromatic action spectra are commonly referred to as biological weighting functions (BWF). The spectral weighting in a BWF is often represented as a mathematical function best describing spectral weighting across a wider range of wavebands as, for example for the UV range, $E^* = \sum_{\lambda=280\ nm}^{400\ nm} \varepsilon(\lambda) E\ (\lambda) \Delta\lambda$, where E^* represents effectiveness, ε(λ) represents the spectral weighting coefficient, E(λ) represents the spectral exposure and Δλ represents the waveband range covered.

2.3.3.3 Photosynthesis

Species of *Dunaliella* have been shown to be particularly resistant to photoinhibition compared to dinoflagelates (Bouchard et al., 2013) and to other marine microalgae (Montero et al., 2002). Furthermore, intraspecies differences were found in photoinhibition sensitivity between different members of the *Dunaliella* genus, thought to be a function of cell size (Jahnke et al., 2009). Research into the impact of UV-A exposure on photosynthesis has received little interest compared to UV-B exposure however (Verdaguer et al., 2016). The relatively low number of

studies that have assessed the impact of UV-A exposure on photosynthesis in *Dunaliella*, have led to some contradictory findings.

Action spectra and BWFs have been used in *Dunaliella* species to determine the photoinhibitory effects of different spectral regions. Experiments by Herrmann, et al. (1997, 1996), and Ghetti, et al. (1998, 1999) in *D. salina* have led to the construction of a BWF based on both chlorophyll fluorescence (F_v/F_m ratio) and oxygen evolution studies using sun simulators and natural daylight, the result of which is shown in Figure 2-7.

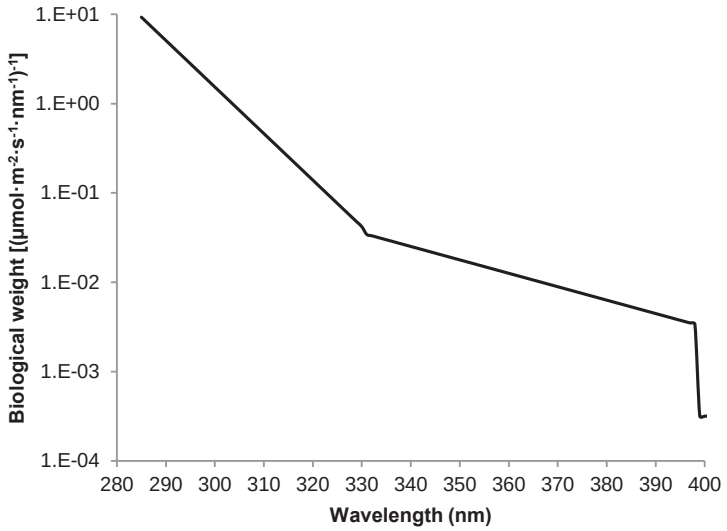

Figure 2-7 The biological weighting function for photoinhibition in D. salina *(measured as chlorophyll fluorescence parameter F_v/F_m). Replotted based on data in Ghetti et al. (1999).*

Most studies have found that, while there is a photoinhibitory effect of UV-A in *Dunaliella* species, it is comparatively small to that of UV-B as exemplified by the BWF in Figure 2-7 (Herrmann et al., 1996, 1997, Ghetti et al., 1998, 1999; Heraud & Beardall, 2000; White & Jahnke, 2004). As reported by the authors, the effectiveness of UV-B at inhibiting photosynethesis is around two orders of magnitude higher than that of UV-A, which in turn is about two orders of magnitude higher than that of PAR.

Several studies have found that short term (30 min) exposure to UV-A + UV-B and UV-B exposure in *D. tertiolecta* led to a drop of the F_v/F_m ratio from the normal value of F_v/F_m = 0.6 - 0.65 to around F_v/F_m = 0.1 - 0.2, indicating severe photoinhibition (Herrmann et al., 1997; Ghetti et al., 1999; García-Gómez et al., 2012). Some studies have reported slight increases in F_v/F_m up to 0.2 - 0.4 during prolonged UV-A + UV-B and UV-B exposure (24 - 72 h) depending on the treatment, suggested by the authors of several studies to indicate a form of acclimation (Hannach et al., 1998; García-Gómez et al., 2012, 2014, 2016; Bouchard et al., 2013). While typically severely inhibited

by UV-A + UV-B and UV-B exposure, recovery has been shown to occur rapidly (24-48 h) after UV is removed, although not always completely (Herrmann et al., 1997; García-Gómez et al., 2012, 2016).

However, some authors have reported contradictory results, indicating UV-A may play an equal or larger role in photoinhibition (contradictory to the BWF in Figure 2-7). White & Jahnke (2002) showed decreased F_v/F_m ratios in *D. bardawil* and *D. salina* resulting from UV-A exposure (λ = 320 – 400 nm) while F_v/F_m ratios under UV-B exposure (λ = 290 – 340 nm) remained unchanged. Experiments by Segovia et al. (2015) showed severe decreases in F_v/F_m ratios in *D. tertiolecta* as a result of both UV-A, UV-B and UV-A+UV-B exposure. Decreases in F_v/F_m ratio for both UV-A and UV-B exposure were found to be similar. In both studies UV-A PFD was 10 – 100 times larger than the UV-B PFD. Due to the different waveband compositions and irradiances used, the studies proved difficult to compare directly.

Studies in *Dunaliella* species have focussed much on PSII and particularly photodamage to the D1 protein as one of the main sources of photoinhibition (Melis et al., 1992). Studies into the molecular pathways in natural phytoplankton communities have shown that damage to the D1 protein of PSII by UV-B exposure plays an important role in photoinhibition (Bouchard et al., 2005). A similar trend in degradation of D1 protein (and D2 protein) resulting in photoinhibition has been reported in cultures of *D. salina* exposed to UV-B (Masi et al., 1997). The UV-B repair response has been modelled as a first-order kinetic response based on fluorescence and carbon fixation experiments (Lesser et al., 1994; Heraud et al., 2000). The model describing the change in photosynthetic efficiency in *D. tertiolecta* suggested by Heraud & Beardall (2000) is represented by equation 2:

$$\frac{P}{P_{initial}} = \frac{r}{k+r} + \frac{k}{k+r} e^{-(k+r)t} \qquad \text{(Eq. 2)}$$

where P represents photosynthetic rate at time exposure time t, $P_{initial}$ represents the initial photosynthetic rate, k represents the rate constant related to inhibition of photosynthesis and r represents the rate of photosynthesis recovery. The model describes a first-order kinetic response and is consistent with repair rate being proportional to the pool size of inactivated D1 protein. The model implies that an equilibrium is reached at large t, where the final photosynthetic rate is dependent on the ratio between damage and repair. The factors r and k scale non-linearly with UV-B irradiance ($W \cdot m^{-2}$), with k increasing faster than r, leading to the observation that photoinhibition is increasingly suppressed at higher UV-B irradiance.

Experiments by Heraud & Beardall (2000) and by Bouchard et al., (2005) showed that the turn-over of the D1 protein is likely to be the main repair process at play (making use of the chloroplast encoded D1 protein synthesis inhibitor lincomycin). The *psbA* gene, coding for D1 protein synthesis was found to be highly upregulated during UV-A+UV-B exposure in *D. tertiolecta* by Garcia-Gómez et al. (2016). Interestingly, Bouchard et al. (2005), found little change in D1 pool size on increased UV-B irradiance although photoinhibition was worsened. The authors therefore suggested that the inactivation of *de novo* D1 synthesis rather than the increased degradation of the D1 protein may be causing accelerated rates of D1 disappearance. Contrary to authors' expectations, the repair rate as described in the model was found to be significantly higher during N-depletion in *D. tertiolecta*, (Shelly et al., 2002).

More recent studies have indicated that, despite the detrimental effects of UV-B exposure, radiation in the UV-B waveband plays an important role in activating repair mechanisms. As mentioned earlier, photoinhibition was found to be similar in *D. tertiolecta* exposed to UV-A and UV-A + UV-B (Segovia et al., 2015). However, only cultures where the UV-B component was included were found to upregulate the transcription of the *psbA* gene leading to the subsequent expression of D1 protein. A rapid increase in ROS was found in UV-A + UV-B exposed cultures which was reversed after 48 h exposure, suggesting an anti-oxidant response (discussed below). Cultures exposed to UV where the UV-B component was included were found to recover F_v/F_m levels rapidly (24 h) while those exposed to UV-A did not (<72 h). Although purely speculative at this stage, combined these data suggest the UV-B component plays an important role in photoprotection which is suggestive of the involvement of a UV-B photoreceptor (such as e.g. UVR8) in *D. tertiolecta*.

2.3.3.4 DNA damage

UV radiation interacts with DNA either through direct absorption of reactive (oxygen) species. The formation of CPDs is one of the most common mutagenic DNA lesions (Sinha et al., 2002) while oxidation of the sugar and base moieties of DNA are the most common interaction with ROS (Lesser, 2006). The formation of CPDs has been shown to be common in *Dunaliella* species, particularly under the influence of UV-B. Research by García-Gómez et al. (2012, 2014, 2016) has shown up to a 7-fold increase in CPDs in *D. tertiolecta* as a result of exposure to broad wavelength UV-A + UV-B (λ = 300 – 400 nm). A continuous exposure regime (24 $h \cdot d^{-1}$) as opposed to a photoperiod exposure was shown to significantly increase the levels of CPDs observed in *D. tertiolecta* (Bouchard et al., 2013). The high survivability of *Dunaliella* species under UV exposure has been suggested to stem from the various DNA repair and anti-oxidant mechanisms that are

activated once DNA damage is detected. A CPD photolyase was first identified in *D. salina* (Cheng et al., 2007) and shown to be highly upregulated in *D. tertiolecta* (up to 450-fold) under exposure to broad wavelength UV-A + UV-B (λ = 300 – 400 nm). Levels of the DNA repair proteins Cell Proliferation Nuclear Antigen (PCNA) and Repressor of Transcriptional Gene Silencing (ROS1), known to be involved in base- and nucleotide excision repair, increased 3 to 6-fold during 72 h of UV exposure (García-Gómez et al., 2012, 2014). Evidence of these DNA repair mechanisms has been suggested as playing a major part in *Dunaliella* survivability under UV exposure. The role of anti-oxidant molecules and enzymes reducing DNA damage are discussed below.

2.3.3.5 Oxidative stress

Due to the short lifetimes of ROS combined with a lack of fluorescent probes that are photostable under UV radiation treatment (Lesser, 2006; García-Gómez et al., 2014) researchers have made use of the non-specific fluorescent ROS probe carboxy-H_2DFFDA. The probe serves to quantify the accumulated ROS at the time of measurement and has been used in numerous *Dunaliella* studies. No changes in the number of ROS-positive cells were found in *D. tertiolecta* under continuous UV-A exposure (λ = 320 – 400 nm) (Segovia et al., 2015). Several studies have reported an increase in ROS-positive cells within the first 24 h of exposure under continuous exposure to broad wavelength UV-A + UV-B (λ = 300 – 400 nm). Experiments in *D. tertiolecta* by Segovia et al. (2015) and García-Gómez et al. (2016) showed a rapid decline in ROS upon 48 h exposure while Bouchard et al. (2013) report a sustained level of ROS-positive cells throughout the exposure.

More informative perhaps is the inference of oxidative stress from the presence of anti-oxidant metabolites and enzymes. Exposure of *D. bardawil* and *D. salina* to UV-A (λ = 320 – 400 nm) showed significant increases in ascorbate peroxidase (APX) activity and ascorbate pool size but no significant changes in either parameter when exposed to UV-B (λ = 290 – 340 nm) (White et al., 2002). Bouchard et al. (2013) showed a steady increase in superoxide dismutase (SOD) content (10-fold by 144 h exposure) in *D. tertiolecta* exposed to broad wavelength UV-A + UV-B (λ = 300 – 400 nm). At the same time a dramatic increase in the catalase (CAT) content (30-40 fold by 48 h exposure) was found. Interestingly the exposure regime (semi-continuous, 12 $h \cdot d^{-1}$ vs. continuous, 24 $h \cdot d^{-1}$) played a large part in the persistence of the CAT levels. While the initial response was similar for both regimes, the CAT levels during continuous exposure decreased after 96 h exposure back to pre-UV levels. The authors suggest continuous exposure may lead to damage of CAT enzymes leading to decreased protection from ROS (observed as increased ROS-positive cells and increased CPD accumulation).

2.3.3.6 UV induced photoprotective pigments

As mentioned in the introduction, the *Dunaliella* genus has a defining trait in that some of its species are able to hyper accumulate carotenoids in the cells' interthylakoid space (Figure 2-5). It has been found that the carotenoid hyper accumulation can be induced in *D. bardawil* by UV-A exposure (λ = 340 – 400 nm) (Jahnke, 1999; Salguero et al., 2005; Mogedas et al., 2007, 2009). No changes in carotenoid content were found as a result of enhanced UV-B exposure (in cultures pre-acclimated to UV-B) in another species of *D. salina* (Tian et al., 2009). This specific response will be discussed in more detail below as it represents the reason for choosing *Dunaliella* as a model species for this study.

Reports of changes in xanthophyll cycle de-epoxidation state are contradictory (Buma et al., 2009). Salguero et al. (2005) report changes in xanthophyll content with 180% increase in lutein, 234% increase in violaxanthin and 407% increase in zeaxanthin contents, concomitant with β-carotene hyper accumulation. These increases point towards the potential involvement of the xanthophyll cycle to aid in preventing photooxidative damage. Similar patterns were found by Dohler et al. (1998) in *D. tertiolecta*. Under nearly identical experimental conditions Mogedas et al. (2009) found no significant changes in violaxanthin or zeaxanthin levels however. Sogevia et al. (2015) show an apparent delayed onset of increased de-epoxidation state in *D. tertiolecta* with initial increases in violaxanthin (after 24-48 h exposure) and subsequent transitions to anteraxanthin (after 72 h exposure) and finally increased levels of zeaxanthin (144 h). Inclusion of UV-B in the exposure regime increased initial levels of violaxanthin but no significant differences were observed in the other two xanthophylls.

The BWF in Figure 2-8 shows a wavelength dependence of the de-epoxidation state with three distinct phases (Buma et al., 2009). De-epoxidation increased at lower wavelengths as shown by Buma et al. (2009). Under natural solar radiation (inc. UV-A and UV-B) the effects of the xanthophyll de-epoxidation in *D. tertiolecta* were found to be modest however, suggesting to the authors the increased epoxidated xanthophyll pools may serve a more direct anti-oxidant role rather than xanthophyll-cycling (van de Poll et al., 2010).

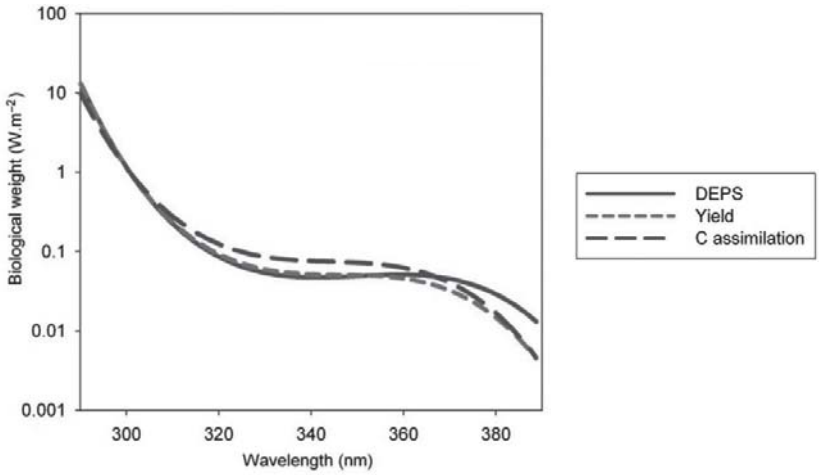

Figure 2-8 BWF of xanthophyll cycle de-epoxidation state (DEPS), biomass yield and carbon assimilation (C assimilation) in D. tertiolecta. *Taken with publisher permission from Buma, et al. (2009).*

There are two reports of *Dunaliella* species producing photoprotective pigments specifically in the UV-B region. The MAAs shinorine (λ_{max} = 334 nm), porphyra-334 (λ_{max} = 334 nm) and palythinol (λ_{max} = 332 nm) were found resulting from enhanced UV-B exposure (in cultures pre-acclimated to UV-B) in *D. salina* (Tian et al., 2009). All increased rapidly and reached peaks at different time points. The MAA mycosporine-glycine (λ_{max} = 310 nm) was identified as a result of UV-B exposure in *D. tertiolecta* (Hannach et al., 1998). *D. tertiolecta* was found to exhibit shoulders around the mycosporine-glycine peak in the HPLC chromatogram indicating to the author a larger range of photoprotective pigments may be present but these could not be adequately identified.

2.4 Conclusions – Using UV as a tool in the culture of *D. salina*

The goal of this thesis is to examine if specific treatments of UV radiation (i.e. specific in UV waveband, irradiance and exposure duration) can reliably increase carotenoid accumulation in the microalga *D. salina* and if this new understanding can be feasibly used to develop an industrial system for UV treatment of microalgae. The purpose of this conclusion is to highlight the extent of current research and point out the new knowledge needed to answer the hypotheses.

The literature review has focussed primarily on UV screening responses, both in *Dunaliella* and microalgae in general, as a potential target for development of UV as a tool during commercial cultivation processes. The target UV response central to the current research, the UV-A induced carotenoid accumulation response in *Dunaliella*, falls into an interesting 'middle ground' from a research perspective. The impact of the UV-A wavelength range on photosynthetic organisms has not received as much research attention as the impact of UV-B (thus UV-A is aptly termed 'the known unknown' by Verdaguer et al., 2016). The cellular mechanisms involved in UV-A perception and signalling are not nearly as well understood as those involved in UV-B exposure, if at all. Furthermore, the perception and signalling involved in carotenogenesis response in *Dunaliella* have not been elucidated and the role of UV-A in this process has received very little attention since its discovery. Due to the limited number of dedicated studies in *Dunaliella*, the UV-A induced carotenoid accumulation response therefore appears to be in a 'research middle ground' between the UV research field and the carotenogenesis research field.

As mentioned, the cellular mechanisms that govern the non-UV induced carotenogenic response in *Dunaliella* have not been fully elucidated. Despite a lack of in-depth understanding of the cellular mechanism, there is a wealth of knowledge on how to manipulate culture conditions to maximize non-UV induced carotenogenesis that has facilitated the commercialisation of β-carotene production from *D. salina*. Similarly, no studies were found in the literature that have investigated the cellular mechanisms that govern the UV-A induced carotenoid accumulation. The studies that are available show that the UV-A induced carotenoid accumulation in *Dunaliella* may be controlled through manipulation of UV irradiance, UV exposure duration and non-UV carotenogenic stimuli. Although suggested by some (Salguero et al., 2005), no examples have been found in literature or in industry that explore development of targeted UV treatments during large-scale *D. salina* cultivation. This PhD research therefore aims to determine the *D. salina* UV response characteristics by examining if specific treatments of UV radiation (i.e. specific in UV

waveband, irradiance and exposure duration) can reliably increase carotenoid accumulation towards assessing the feasibility of UV treatment as a tool in commercial *D. salina* cultivation.

Because the commercial *D. salina* cultivation process relies on both biomass growth and bioproduct formation, the photosynthetic pigment content (i.e. carotenoid and cholorophyll*(a+b)*), cell growth and cell morphology will be studied during experiments. The large variety and complexity of UV responses reported in *Dunaliella* show that UV-A induced carotenoid accumulation is not the only response to occur during UV-A exposure. The range of photodamage repair, DNA-damage repair and anti-oxidant responses show that UV exposure is clearly stressful for the cells. Elucidation of the cellular mechanisms behind the UV-A induced carotenoid accumulation response would require a more fundamental approach outside the scope of the current research. The increased availability of powerful tools for generating genetic, proteomic and photosynthetic health data as well as the generation of *Dunaliella* mutants specifically for the investigation of UV response would likely expand the fundamental understanding of the UV-A induced carotenoid accumulation response. Furthermore, review of both the UV literature and non-UV induced carotenogenesis literature indicates that there is an overlap of stimuli inducing carotenogenesis in *Dunaliella* (PSII photodamage, electron transfer interference and ROS generation through direct photosensitization or damage to PSII). Further investigation of the UV-A induced carotenoid accumulation response may benefit both fields.

3 Experimental design

Based on the conclusions from the literature review chapter, the chapter below discusses the research strategy and the methodology used. A brief summary is given of the research strategy followed by the project constraints. The project constraints discuss the boundaries within which the research strategy was conducted and the limits of their applicability. The subsequent sub-sections describe the methodology and data analysis.

3.1 Research strategy

The experimental research strategy was carried out as follows:

1. An experimental setup was designed, constructed and validated to be suitable for the study of UV response under precisely quantifiable and controllable conditions.
2. A microalgal species was selected based on proof-of-principle experiments. Commercially relevant strains *A. platensis, C. vulgaris*, *D. salina* and *H. pluvialis* were tested. *D. salina* was selected for further testing.

   Note: Proof-of-principle results are not discussed in main body of thesis. Please refer to Appendix 9.2
3. The impact of UV-A on *D. salina* photosynthetic pigment content (i.e. carotenoid and cholorophyll *(a+b)*), cell growth and cell morphology was characterized in various wavebands in the UV-A region.
4. The effect of individual constituents of long wavelength UV-A treatment (λ = 360-400 nm) on the UV response were systematically examined to create a better understanding of controlling the beneficial UV response in *D. salina*.
5. Understanding of the beneficial UV response in *D. salina* from the previous point was combined to engineer two UV treatments thought to optimize beneficial UV response.
6. Experimental data was used is input data for a techno-economic analysis model to estimate the technical and economic feasibility of UV as a tool.

3.2 Research scope

The scope of the current research was determined in part by project constraints as summarized in Table 3-1. The analytical parameters measured are shown in Table 3-2.

Table 3-1 Project constraints

Condition	Constraint	Rationale
Experimental design	No commercial or large-scale experiments possible	In the absence of relevant fundamental knowledge and data a decision was made to perform experiments under controlled laboratory conditions (see sub-section 3.3.3). No experiments were scaled-up or performed outdoors due to material and time restrictions. While valuable for developing a fundamental understanding, findings from small scale laboratory experiments inevitably suffer from limited applicability to large(r) scale conditions. Furthermore, the laboratory experimental setup was designed with UV photobiology research as a primary focus. The experimental setup was not designed to be as representative of a full scale process as practically possible. Data obtained from the current research should therefore not be used as direct inputs for large-scale cultivation system engineering calculations. However, to be able to comment on the technological and economic potential for the technology, the current work will attempt to discuss the trends observed from the current research in a large-scale microalgae cultivation context while being mindful of the limitations.
	Techno-economic analysis	Results from controlled laboratory experiments are unable to account for a large number of variables that impact the performance of large-scale outdoor cultivation system e.g. cultivation system design, weather effects such as temperature and rainfall, impact of solar UV radiation, impact of solar PAR variations throughout the day and diurnal light:dark cycles. The TEA was developed unable to incorporate these variables but is mindful of the resulting shortcomings of the obtained outputs. The TEA can therefore not claim to provide absolute economic outputs for e.g. revenue and profit. However, a lack of relevant data in the field, means that the novel findings of the PhD research serve as valuable inputs towards a high-level TEA used assessment of the most critical areas for improving profitability of large-scale UV treatment technology.

Experimental setup	Culture vessel	Method development on the experimental setup was carried out during preliminary experiments at the start of the PhD research. Microalgal UV photobiology literature describes many different culture vessels used during experiments without a clear consensus on the appropriateness of each. During method development, a flat plate photobioreactor was identified as the optimal vessel for experiments due to the following features: - Flat, defined illuminated surface area made of material of choice - Defined optical path length - Rapid mixing using bubbling - Active CO_2 control - Temperature control - Large volume (>2 L), allowing repeated sampling without significant impact on culture conditions Attempts to cultivate *D. salina* (strain UTEX 1644) in a flat plate reactor were unsuccessful (data not shown). After extended experimentation, Pyrex flasks were chosen as culture vessel. The choice of culture vessel is discussed sub-section 3.3.3. The focus of the current project is on the UV-A region and the use of vessels with higher UV transmission (e.g. quartz) was not deemed necessary (see sub-section 3.3.3).
	PAR intensity	PAR intensity is highly variable during the day and weather dependent. For controlled laboratory experiments the PAR intensity was fixed. Furthermore, low PAR used intensity of 30 $\mu mol \cdot m^{-2} \cdot s^{-1}$ was applied during experiments to ensure non-inductive PAR conditions for carotenoid accumulation – i.e. eliminating PAR as a potential source of carotenoid accumulation during experiments. Carotenoid accumulation rate was confirmed to be constant under low PAR conditions (Figure 3-4). Research also shows that microalga cells exposed to the (fluctuating) light regimes observed during large-scale cultivation, become low-light acclimated as a result of spending more time in the low-

		light zones of the culture (Havelková-Doušová et al., 2004). The PAR intensity was shown to be sufficient for microalgal growth, albeit under light limited conditions (see Appendix 9.3).
	No active CO_2 supply	Forms of dissolved CO_2 serve as primary carbon source for microalgae. During large-scale cultivation CO_2-control plays a large role in optimizing productivity (Grobbelaar, 2010). Furthermore, gas phase CO_2-concentration has been shown to impact the UV damage response in *D. tetriolecta* (García-Gómez et al., 2016). Due experimental limitations the impact of CO_2 could not be accounted for during laboratory scale experiments. None of the CO_2-controlled incubators in the laboratory were suitable to fit the experimental setup. Gas phase CO_2-concentration could therefore not be controlled and CO_2 could not be actively supplied. Dissolved carbon levels resulting from ambient CO_2 concentrations were shown to be growth limiting for all experiments (see Appendix 9.3).
	Mixing	Mixing was incorporated to improve gas exchange. Due to the fragile nature of *D. salina* cells, mixing was achieved through orbital mixing (rather than stirring or bubbling). Orbital mixing was the most applicable method for laboratory experiments but only has limited comparability to mixing conditions during large-scale *D. salina* cultivation (i.e. no mixing or paddle wheel mixing).
	Action Spectrum	The construction of action spectra and BWFs is a commonly employed tool in UV photobiological research (Aphalo et al., 2012). However, determination of an action spectrum is a demanding exercise (Neale, 2000) as it involves repeated irradiance experiments at ≥ 5 narrow wavebands. In the interest of exploring a wider range of parameters other than waveband specificity, a very limited action spectrum was constructed using three UV-A wavebands (sub-section 3.3.3). An absence of action spectra for UV induced carotenogenesis in the reviewed literature for *D. salina* means the limited action spectrum provides novel insights into UV-A waveband dependency of the UV induced carotenogenesis response.

Analytical techniques	Key parameters	Key parameters used to assess the performance of *D. salina* during large-scale cultivation include (as per Table 2-4): biomass concentration (g biomass·m^{-3}), cell numbers (cells·mL^{-1}), β-carotene concentration (g·m^{-3}), cellular β-carotene content (% w/w algal DW) and aerial productivity $P_{biomass}$ and $P_{\beta\text{-carotene}}$ (g·m^{-2}·d^{-1}). Analytical techniques were chosen to allow rapid and daily assessment of key parameters deemed important for the feasibility assessment during large-scale cultivation. The analytical parameters measured are shown in Table 3-2.
	Biomass proxy	Microalgal dry weight (DW, determined as ash free DW) and Total organic carbon (TOC) analyses were trialled as biomass proxy. Both were found to be unreliable due to high salt concentration in the culture media. Variable levels of salt accumulate on filter membranes during DW measurement, resulting in high variability between repeat samples (data not shown). Washing cell pellets of *D. salina* with dH_2O or buffered solutions (e.g. 0.5 M ammonium bicarbonate, Zhu & Lee, 1997) causes cell disruption through osmotic shock meaning filtration can no longer be applied. Manufacturer supplied documentation for TOC (Shimadzu, Model TOC-$L_{CPH/CPN}$) outlines a maximum salt concentration of 1000 mg·mL^{-1} to prevent excessive salt accumulation in the combustion tube and catalyst. Washed cell pellets with dH_2O were found to result in high variability in repeat samples (data not shown). Cell counting is unaffected by salt concentration and commonly used in microalgae photobiology and was therefore chose as a biomass proxy. Cell counting does not allow for quantification of biomass (in g·L^{-1}) directly.
	Photosynthetic pigment quantification	Photosynthetic pigments were analysed quantitatively by spectrophotometry (Lichtenthaler, 1987). The employed method does not allow qualification of the photosynthetic pigments (i.e. identification of individual carotenoids) Quantitative and qualitative analysis of photosynthetic pigments by HPLC was trialled (Wright et al., 1991). This approach was deemed too time consuming for daily monitoring. Furthermore, no reference photosynthetic pigment standards were available and were deemed too costly and time consuming to generate.

Table 3-2 Analytical parameters measured during experiments.

Parameter	Unit
Cell number	cells·mL culture^{-1}
Cell settling	ΔOD_{687}
Microscopy: Cell area (from 2D images)	μm^2
Microscopy: Morphology	N/A
pH	N/A
Pigment: Total carotenoid or chlorophyll *(a+b)* concentration	µg pigment·mL culture^{-1}
Pigment: Cellular carotenoid or chlorophyll *(a+b)* content	µg pigment·10^6 cells^{-1}

3.3 Materials and Methods

3.3.1 Microalgae

Preliminary experiments, carried out at the start of the PhD research, screened four major industrial species for beneficial UV responses (based on literature review, see Appendix 9.1). Species that are used only for bulk biomass production (e.g. those common in aquaculture industry [7]) were excluded in the choice of potential microalgae species. The preliminary experiments led to the continued use of only *D. salina* (strain UTEX 1644) as the focus for the current project. The results of the preliminary experiments are discussed in detail in Appendix 9.2 and will be briefly summarized here.

The four commercially relevant microalgae species were obtained from University of Texas Culture Collection (UTEX). The microalgae species were imported after ensuring appropriate import licences were obtained from Ministry of Primary Industries (MPI, permit No. 2014053186). *D. bardawil*, the most commonly used *Dunaliella* species in the literature, could not be shown to be 'Not New' to New Zealand and would therefore require exhaustive procedures to obtain permits from the Environmental Protection Agency (EPA) to allow its import to New Zealand.

- *Athrospira (Spirulina) platensis* UTEX LB 1926
- *Chlorella vulgaris* UTEX 259
- *Dunaliella salina* UTEX LB 1644
- *Haematococcus pluvialis* UTEX 2505

[7] *Thalassiosira pseudonana, Skeletonema sp., Chaetoceros spp., Chlorella minutissima, Isochrysis galbana, Pavlova spp., Phaeodactylum tricornutum, Nitzschia sp., Gomphonema sp.,* and *Tetraselmis subcordiformis* (Duerr et al., 1998).

The prefix 'LB' denotes a xenic culture (i.e. not axenic, with unknown contaminant). Attempts were made to remove the contaminations from the xenic cultures but efforts proved time consuming and ultimately unsuccessful (data not shown). Contaminations were not detected during regular culture maintenance and only occasionally detected during late stages of experiments. Due to its occurrence during late stages of experiments, the contamination was assumed not to interfere with normal microalgae growth.

Preliminary experiments employed UV treatment technology provided by BioLumic (i.e. prototype UV LED technology) as well as custom-built fluorescent UV tube setups. Different UV wavebands, UV irradiances and UV exposure durations were employed to screen the UV responses in the selected microalgae species. Where literature sources were available UV treatment conditions were based on those used by other researchers (Jahnke, 1999; Balan et al., 2014). When no literature sources were available, the maximum UV irradiance of the BioLumic UV LED technology was employed (maximum UV irradiance = 0.35 – 0.38 $W \cdot m^{-2}$).

The magnitude of the UV response was found to be highest in the microalgae *D. salina*, showing a 52% increase in Car:Chl ratio when exposed to broad wavelength UV-A (λ = 320 – 400 nm, 10.7 $W \cdot m^{-2}$, 24 $h \cdot d^{-1}$). *D. salina* was therefore chosen as focus for the PhD research. In *A. platensis* pigment levels of phycocyanin and chlorophyll a were found to increase as a result of short wavelength UV-A exposure (λ = 320 – 350 nm, 0.38 $W \cdot m^{-2}$, 12 $h \cdot d^{-1}$). Experimentation with *A. platensis* was discontinued due to contamination of stock culture however. The microalgae *C. vulgaris* showed either no significant change or a decreased growth rate under the influence of short wavelength UV-A (provided by BioLumic UV LED technology). The microalgae *H.pluvialis* showed reddening of the cells coupled with decreased cell numbers. For a more detailed overview of results please refer to Appendix 9.2.

3.3.2 *D. salina* culture conditions

Cultures of *D. salina* (strain UTEX 1644) were grown in Modified Johnson Media (MJM) (Borowitzka et al., 1990) at a salinity of 1.9 M NaCl (11.25%) supplemented with a 50 mM Tris buffer at pH 8 (based on Harrison & Berges)(2005). See Table 3-3 for media recipe.

Table 3-3 Chemical composition of Modified Johnson media

Chemical element	Final concentration in media ($gr \cdot L^{-1}$)
NaCl	112.5
Tris HCl	5.32
Tris Base	1.97
$MgCl_2 \cdot 6\ H_2O$	1.5
$MgSO_4 \cdot 7\ H_2O$	0.5
KCl	0.2
$NaHCO_3$	0.043
KH_2PO_4	0.035
KNO_3	1.0
$CaCl_2 \cdot 2\ H_2O$	0.2
Na_2EDTA	$1.89 \cdot 10^{-4}$
$FeCl_3 \cdot 6H_2O$	$2.44 \cdot 10^{-4}$
H_3BO_3	$6.1 \cdot 10^{-4}$
$(NH_4)6Mo_7O_{24} \cdot 4H_2O$	$3.8 \cdot 10^{-4}$
$CuSO_4 \cdot 5H_2O$	$0.6 \cdot 10^{-4}$
$CoCl_2 \cdot 6H_2O$	$0.51 \cdot 10^{-4}$
$ZnCl_2$	$0.41 \cdot 10^{-4}$
$MnCl_2 \cdot 4H_2O$	$0.41 \cdot 10^{-4}$

Cultures were maintained at $25^{o} \pm 1\ ^{o}C$ in an incubator shaker (Environ shaker 3597, Lab line Instruments, Melrose Park, IL) at 100 rpm supplied with 2% CO_2 under 24 $h \cdot d^{-1}$ PAR exposure (30 – 45 $\mu mol \cdot m^{-2} \cdot s^{-1}$, Lifemax TLD18W, Philips). Backup cultures were maintained at $20\ ^{o} \pm 1\ ^{o}C$ in sterile, transparent 50 mL containers under a 12h:12h light:dark cycle (20 $\mu mol \cdot m^{-2} \cdot s^{-1}$, based on Lorenz, et al., 2005). Cultures of *D. salina* were successfully cryopreserved (based on Day & Brand)(2005).

3.3.3 Culture vessel

No clear consensus was found in literature as to the 'standardized' experimental procedure for microalgae UV photobiology research. Therefore, method development on the culture vessel choice and experimental setup was carried out during preliminary experiments at the start of the PhD research. The following desired traits for the experimental setup were used as guidelines during method development:

- Growth of microalgae.
- Precisely quantifiable and controllable temperature and CO_2-levels
- Homogeneous mixing without damaging the microalgae.
- Long term axenic culture of microalgae.
- Adjustable and homogeneous levels of PAR and UV irradiation
- Unhindered penetration of UV through the wall of the culture vessel
- Adequate volume size to allow repeated sampling

Numerous cultivation vessels were tested during preliminary experiments: liquid and agar based Petridish cultivation, 6 and 24 well plates, beaker, Erlenmeyer flask, bubbled 1 L Schott bottle cultivation and flat-plate photobioreactor. All cultivation vessels were assessed in their ability to satisfy the desired traits listed above. Finally, Pyrex Erlenmeyer flasks were chosen as cultivation vessels for the experimental setup due to the following features:

- Long-term (≥ 7 days) microalgae cultivation in the Pyrex flask culture vessels was confirmed. Despite aseptic handling of flasks during preparation and sampling, contamination could not be prevented due the xenic nature of the origin strain.
- Cultivation in the experimental setup using the Pyrex flasks was reproducible, based on n = 48 PAR-Only control experiments (see sub-section 3.4.2).
- Experiments were carried out in a temperature controlled room at 25 ^{o}C ± 1 ^{o}C at ambient CO_2-concentrations.
- During experiments cultures were mixed by orbital shaking at 200 rpm (KS 260 basic, IKA®, Staufen, Germany). Cell damage because of mixing was negligible as confirmed by microscopy (data not shown).
- PAR and UV transmission through the vessel wall was confirmed by both spectrophotometer readings (UV-1800, Shimadzu, Kyoto, Japan) as well as spectroradiometer readings (OL-756, Gooch and Housego, Ilminster, UK) (see Appendix 9.4). UV transmission in the UV-A region was between 73% and 90% between λ = 320 –

350 nm and 90% between λ = 350 – 400 nm. UV transmission through the Pyrex flask wall dropped rapidly below λ = 320 nm and reached 0% at λ = 270 nm (see Appendix 9.4).

Two downsides to using the flasks as culture vessel were identified. The first is the potential impact of the flask shape – i.e. a lack of flat surfaces. To reduce distortion of incoming PAR and UV by the flask neck's slanted surface exposure to PAR and UV from the side rather than the top (see Figure 3-1) was employed. PAR and UV exposure from the side of the flask was also required for adjustment of PAR and UV intensity independently. Exposure from the side leads to a smaller irradiated surface area and longer optical pathlength which is likely to reduce the amount of UV experienced by individual cells.

The second downside is the limited cultivation volume (300 mL) and the relatively large impact of sampling. Volumes removed by sampling led to a 120 mL, or 40 %, decrease in culture volume over the standard 5-day experimental period (cultures were harvested on 5th experimental day). The sampled volumes were not replaced with fresh media as cell density changes as a function of growth were prioritized over maintaining a constant cultivation volume (i.e. UV penetration is determined by cell density, see Appendix 9.11 for transmittance data). However, the reduction in culture volume resulted in a further reduction in both illuminated surface area and optical pathlength which potentially leads to changes in UV irradiance per cell. The impact of the reduction in sample volume on the UV treatment was not measured as part of the experimental procedure and the impact was assumed negligible for the purpose of observing the global UV treatment trends.

The impact of sampling volume on culture volume and subsequently the UV treatment is rarely discussed in UV photobiology literature. The changing experimental conditions over time mean the obtained experimental results may be compared only to data obtained in a similar experimental setup (i.e. with significantly reducing culture volume over time). Furthermore, besides the impact of scale, the variable culture volume combined with the batch cultivation means results cannot be extrapolated to reflect effects that may be observed during large-scale cultivation. However, in the absence of relevant knowledge and data, the results obtained are used as input for the TEA regardless, in order to be able to provide recommendations to BioLumic whether further research and development is warranted.

3.3.4 Experimental setup

The final experimental setup design is shown in Figure 3-1 and could satisfy most of the desired traits within the time and financial constraints of the project. The experimental was used throughout the PhD research described in the thesis.

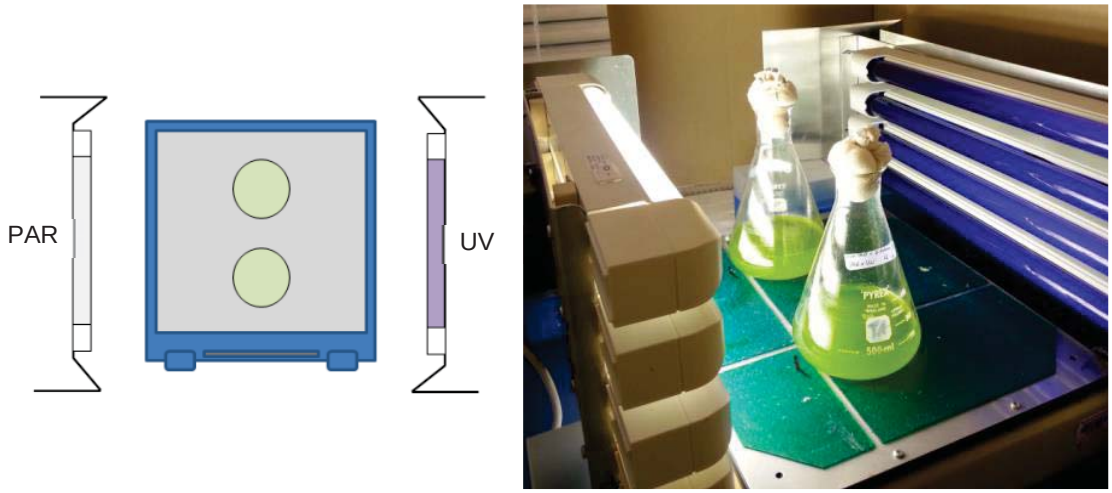

Figure 3-1 (Left) Schematic representation of the setup as seen from above (Right) Image of experimental setup. The fluorescent UV tubes are shown on the far right of the image.

Experiment was started by aseptically diluting dense microalgae cultures of optical density $OD_{687} \approx 1.0$ (absorbance measured at λ = 687 nm, OD_{687}) to a starting optical density of OD_{687} = 0.100 ± 0.050 Abs. This was the highest OD_{687} which allowed UV transmittance through the entire flask culture at the start of the experiment (flask diameter = 10 cm, see Appendix 9.11 for transmittance data). Per experiment, six 500 mL Pyrex conical flasks (Kimble Chase, Vineland, NJ) were filled with 300 mL of diluted culture. Two of the six flasks were designated as PAR-Only controls for every experiment. A 30 mL sample was taken from each flask every 24 h during the experiment.

Experiments were carried out in a temperature controlled room at 25 ^{o}C ± 1 ^{o}C at ambient CO_2-concentrations. Incubators with CO_2 control were not available during the PhD research. Ambient temperature was recorded throughout the experiments using Thermochron iButton temperature data loggers (Maxim Integrated, San Jose, CA). The experimental setup was surrounded by cardboard panels to prevent interference from outside light sources and protect the user from UV radiation. Computer fans were installed in the cardboard panels to provide lateral airflow to maintain a constant temperature in the experimental setup (UV lights were found to contribute to an increase in temperature in early experiments).

PAR illumination was provided from the side of the flask by four Cool White fluorescent tubes (Lifemax TL-D-10W, Philips Amsterdam, Netherlands). PAR intensity was measured using a light-meter (Licor LI-250A, LI-COR Biosciences, Licoln, NE). For high PAR intensity experiments (1000 µmol m^{-2} s^{-1} and up), prototype PAR LED panels with blue/red LEDs developed by BioLumic were used (see Appendix 9.2 for spectrum). Emission spectra from the PAR light sources were confirmed not to contain UV radiation using a UV-VIS spectroradiometer (OL-756, Gooch and Housego, Ilminster, UK). (data not shown).

UV radiation was delivered from the side using fluorescent UV tubes, namely; generic UV-A blacklight fluorescent tubes (unbranded), UV-A blacklight fluorescent tubes (TL-D-18W BLB, Philips, Amsterdam, Netherlands) and Q-panel UV-A-340 fluorescent tubes (Q-Lab, Cleveland, OH). Emission spectra of the fluorescent UV tubes were recorded with a spectroradiometer (OL-756, Gooch and Housego, Ilminster, UK). The emission spectra are shown in Figure 3-2. UV penetration into the culture vessel was confirmed prior to experiments (see Appendix 9.4 for UV

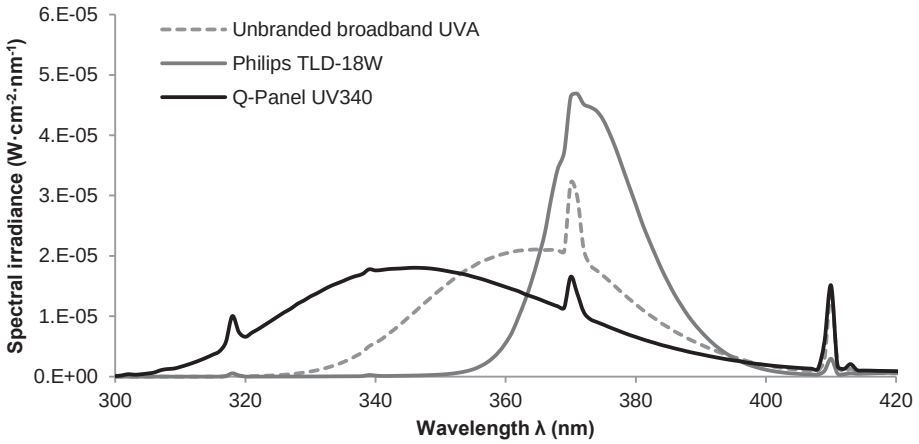

Figure 3-2 Emission spectra of fluorescent UV tubes used during the experiments.

transmission)

UV irradiance was controlled by changing distance to the light source based on spectroradiometer readings. Irradiance was measured over a range of three distances from the light source and the data plotted. A trendline was fit to the plotted data which was used to determine the distance required from the lights for each desired irradiance (up to 15 cm from the light source). Quality measurements of the fluorescent UV tubes were carried out at least after every 3 experiments. Fluorescent UV tubes were replaced when performance decreased.

Various short wavelength UV-A wavebands were created using Q-panel UV-A-340 fluorescent tubes (Q-Lab, Cleveland, OH) and a combination of a custom sized 350 nm shortpass filter (Filter

ZHS0350, Asahi Spectra USA Inc., Torrance, CA) and UV-B screening mylar plastic film (130 clear, LEE Filters, Hampshire, UK). Effects of the filters on Q-panel UVA-340 fluorescent tube emission spectrum is shown in Appendix 9.5.

3.3.5 Analytical techniques

- Pigment extraction for spectroscopy

All manipulations were carried out in low light conditions at all times (i.e. majority of lab lights off). Measurements were carried out as quickly as possible after extraction to prevent pigment degradation. For pigment extraction, 10 mL of mircoalgal culture was centrifuged in 15 mL centrifuge tubes (Falcon, Corning, Corning, NY) at 10,000 rpm for 5 minutes (Centrifuge 5702, Eppendorf, Hamburg, Germany). Media supernatant was discarded and the pellet re-suspended in 10 mL 100% analytical grade methanol (Labserv AR ACS, Thermo Fisher, Waltham, MA). Extraction was carried out by placing the centrifugation tubes horizontally on an orbital shaker at 50 rpm (KS 260 basic, IKA®, Staufen, Germany) for 15 min at 4^{o}C in the dark. Centrifugation tubes were covered in aluminium foil to ensure dark conditions. An extraction time of 15 minutes ensured a completely white pellet after centrifugation (10,000 rpm, 3 min). Total chlorophyll and carotenoids in the supernatant were calculated from UV-VIS spectrophotometer readings (UV-1800, Shimadzu, Kyoto, Japan) using the equations in Lichtenthaler (1987).

Methanol, 100% (pure solvent): (Eq. 3)

$$C_a = 16.72 \cdot Abs_{665.2} - 9.16 \cdot Abs_{652.4}$$

$$C_b = 34.09 \cdot Abs_{652.4} - 15.28 \cdot Abs_{665.2}$$

$$C_{a+b} = 1.44 \cdot Abs_{665.2} + 24.93 \cdot Abs_{652.4}$$

$$C_{x+c} = \frac{1000 \cdot Abs_{470} - 1.63 \cdot C_a - 104.96 \cdot C_b}{221}$$

where C_a represents the chlorophyll a content, C_b represents the chlorophyll b content, C_{a+b} represents the sum of the chlorophyll a and b and C_{x+c} represents the total carotenoid content. The resolution of the spectrophotometer was lower than that required as input for the formulas. Absorption data from the nearest whole wavelength are used as the closest approximation.

- Cell counting

Algal dry weight was trialled as a biomass proxy but proved unreliable due to high salt content of the culture media (see Table 3-1). Cell counting was therefore used. *D. salina* is flagellated meaning cells were still actively moving after sampling. For cell counting purposes, cells were

immobilized immediately after sampling by adding Lugol's iodine staining solution[8] up to a final concentration of 0.5% (commonly referred to as "a light tea colour" in literature). Lugol's was added to a 1 mL well-mixed cell suspension. Cells were counted using a Neubauer hemocytometer (Cat. No. BS.748, Hawksley, Sussex, UK) loaded with 10 µL immobilized cell suspension (as per Lund, et al., 1958). Cells were initially counted manually by examining the slide using a benchtop light microscope (CH-2, Olympus, Tokyo, Japan) at 4x magnification. Cell counting was later automated by using digital images in combination with the ImageJ image processing software (www.imagej.nih.gov/ij) (see Appendix 9.6 for protocol). Digital microscopy images were taken using a light microscope equipped with a (BX-53, Olympus, Tokyo, Japan) at 4x magnification. Compared to manual image counts the automated counts overestimated the cell number by on average 1% (Appendix 9.6).

3.4 Data analysis

3.4.1 PAR and UV distribution experimental setup

Each experiment was started by diluting dense microalgae cultures of $OD_{687} \approx 1.0$ (λ = 687 nm, OD_{687}) to the desired starting optical density of $OD_{687} = 0.100 \pm 0.050$ Abs. Per experiment, six 500 mL Pyrex conical flasks (Kimble Chase, Vineland, NJ) were filled with 300 mL of diluted culture with 2 flasks serving as PAR-Only control. The light distribution of the fluorescent PAR and UV tubes

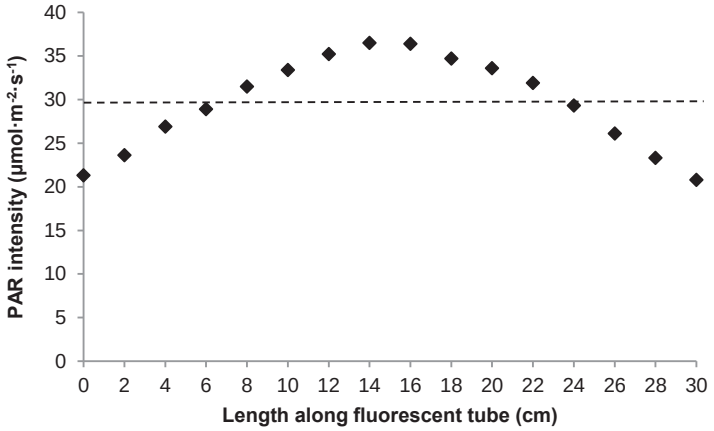

Figure 3-3 PAR light intensity distribution across the PAR light source used during experiments. Measurements were taken at a fixed distance from the light source of 18 cm by moving the light meter along the length of the fluorescent tube (Lifemax TL-D-10W, length = 30 cm). The dotted line represents the target PAR intensity for the majority of experiments (30 µmol·m^{-2}·s^{-1}).

[8] Recipe provided by Cawthron Institute (Nelson, New Zealand). Lugols iodine solution is a solution in milliQ water of 100 g·L^{-1} KI, 50 g·L^{-1} I_2 and 100 mL g·L^{-1} glacial acetic acid.

(Figure 3-3) meant that only two fixed positions on each orbital shaker could be occupied that shared the same PAR and UV intensities (equidistant from the centre of the fluorescent PAR and UV tubes).

Great effort was taken to ensure similar PAR and UV intensity for each flask through repeated light meter and spectroradiometer readings prior to the start of experiments. Despite careful placement at the start of the experiment, (re)placement after each sampling led to inevitable minor changes in PAR and UV intensities between flasks. Due to the different PAR and UV microclimate experienced by each flask, all flasks cannot be said to be identical between sampling points and each flask is therefore considered an experimental replicate (rather than simply a technical replicate). The sub-sections below show the impact on the mean and variability of the key parameters measured during the thesis.

3.4.2 Photosynthetic pigment content

Every experiment included two PAR-Only (PAR = 30 µmol·m^{-2}·s^{-1}, 24 h·d^{-1}) replicates, resulting in a total of PAR-Only 48 replicates. Per replicate, photosynthetic pigment analyses were carried out in duplicate for each sample (initial pigment analyses were carried out in triplicate but variability was shown to be low, data not shown). The averaged total carotenoid concentration and total chlorophyll *(a+b)* concentration are shown in Figure 3-4 and Table 3-4.

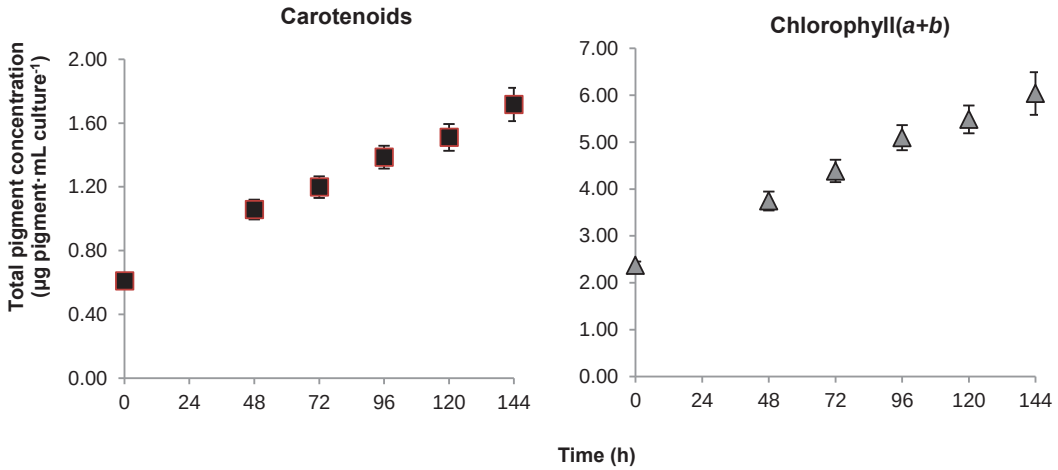

*Figure 3-4 Mean total carotenoid concentration (left) and total chlorophyll (*a+b*) concentration (right) of all PAR-Only controls. Error bars represent standard error (n=48).*

Table 3-4 Mean total carotenoid concentration and total chlorophyll (a+b) concentration of all PAR-Only controls with standard error (n = 48).

Time (h)	0	48	72	96	120	144
Total carotenoid concentration (µg Car·mL culture^{-1})	0.61 ± 0.03	1.06 ± 0.06	1.20 ± 0.07	1.39 ± 0.07	1.51 ± 0.08	1.72 ± 0.10
Total chlorophyll *(a+b)* concentration (µg Chl·mL culture^{-1})	2.37 ± 0.08	3.74 ± 0.20	4.38 ± 0.24	5.09 ± 0.27	5.48 ± 0.30	6.04 ± 0.46

3.4.3 Cell count

Every experiment included two PAR-Only (PAR = 30 µmol·m^{-2}·s^{-1}, 24 h·d^{-1}) replicates, resulting in a total of 48 replicates. Per replicate, cell counts were carried out in triplicate ensuring a total of 400 cells or more were counted per sample (Lund et al., 1958). The mean cell count with standard error is shown in Figure 3-5 (and *Table 3-5*).

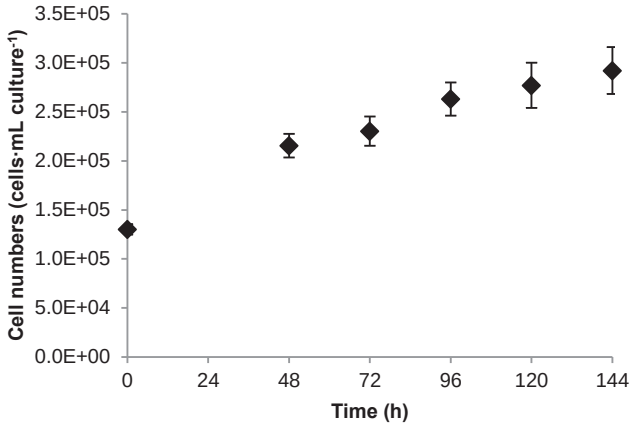

Figure 3-5 Mean cell count of all PAR-Only controls. Experimental treatments were started after 48 h acclimation. Error bars represent standard error (n=48).

Table 3-5 Mean cell count of all PAR-Only controls with standard error (n = 48).

Time (h)	0	48	72	96	120	144
Cell number (cells·mL culture^{-1})	$1.3\cdot10^5$ ± $5.4\cdot10^3$	$2.2\cdot10^5$ ± $1.2\cdot10^4$	$2.3\cdot10^5$ ± $1.5\cdot10^4$	$2.6\cdot10^5$ ± $1.7\cdot10^4$	$2.8\cdot10^5$ ± $2.3\cdot10^4$	$2.9\cdot10^5$ ± $2.4\cdot10^4$

3.4.4 Data normalization

Pigment content and cell count data for all experiments are normalized to the PAR-Only average at culture age = 48 h (i.e. start of experimental treatment). Due to slight variations in experimental conditions, experimental data points for pigment content and cell count were regularly recorded to be outside the standard error range of the averaged PAR-Only value at t = 48 h (n = 48). Relative changes observed between experimental replicates were observed in a narrow range (as indicated by standard error of plotted data throughout the thesis). Experimental data were normalized such that all plotted data would share the same origin, aiding in data visualisation and interpretation.

Normalization was performed by calculating according to equation 4 thus shifting all data points up or down equally (PAR-Only average, n = 48; measured experimental value, n = experiment dependent).

$$Normalization = Experimental\ value - \ (Experimental\ value\ (t = 48\ h) - PAR\ Only\ average\ value\ (t = 48\ h)) \quad \text{(Eq. 4)}$$

All data therefore share the same origin. Relative changes between data points resulting from UV treatment are unaffected by normalization. Therefore, the thesis will only base discussions on relative changes observed during experiments (e.g. % change) and compare relative changes between experiments rather than compare absolute values. Where absolute values are discussed the impact of data normalization will be clearly stated.

4 Experimental chapter 1 – Characterizing the UV carotenoid accumulation response in *D. salina*

The literature review and the screening experiments carried out during the start of this PhD research identified, and confirmed a UV-A induced carotenoid accumulation response in the *D. salina*. Proof-of-principle experiments during early stages of this project showed *D. salina* (strain UTEX 1644) to have the clearest industrially beneficial UV response out of the commercial algae species tested (results shown in Appendix 9.2). An increase in carotenoid to chlorophyll ratio (Car:Chl) of 52% was found in response to broad wavelength UV-A exposure (λ = 320-400 nm, 8 $W \cdot m^{-2}$, 24 $h \cdot d^{-1}$) (Appendix 9.2). Controlling and enhancing the production of this high value bioproduct was identified as a potential target for development of UV treatment regimes during large-scale *D. salina* cultivation.

In order for BioLumic to develop UV treatment regimes and UV treatment technologies, a fundamental understanding is required of a target species' desired UV response and UV photobiology. While the UV-A induced carotenoid accumulation response in *D. salina* has been reported by several authors, the understanding of the photobiology behind the UV-A induced accumulation response is limited. Furthermore, UV photobiology research in the wider *Dunaliella* genus has identified numerous other cellular responses to UV exposure other than carotenoid accumulation which can affect cell morphology, cell proliferation and the photosynthetic machinery. Therefore, the first experimental chapter of the PhD research investigates the *D. salina* UV response and photobiology by investigating the impact of targeted UV exposure (i.e. specific in UV waveband, irradiance and exposure duration) on the photosynthetic pigment content and carotenoid accumulation response. Moreover, the impact of targeted UV exposure on cell proliferation, cell morphology, cell size and cell shape are investigated. The current chapter aims to address the following thesis objective:

- Quantify the impact of UV radiation (i.e. UV waveband, irradiance and exposure duration) on *D. salina* photosynthetic pigment content (i.e. carotenoid and cholorophyll*(a+b)*), cell growth and cell morphology.

The current chapter investigates the impact of exposure different UV-A wavebands on *D. salina* photosynthetic pigment content (sub-section 4.2.1) and cell numbers (sub-section 4.2.2). The impact of a single UV waveband on cell morphology and cell size and shape (sub-section 4.2.3) is subsequently investigated. Additional observations with regards to cell settling and UV response to UV-B exposure are also discussed (sub-section 4.2.4 and 4.2.5 respectively). The impact of UV irradiance, UV exposure duration and the interaction wth non-UV carotenogenesis stimuli is discussed in Ch. 5.

4.1 Materials and methods

The UV-A induced carotenoid accumulation response for *D. salina* UTEX 1644, the species used during this project, is only briefly mentioned in one piece of literature (Jahnke, 1999). The ability of *D. salina* UTEX 1644 to exhibit a similar UV-A induced carotenoid accumulation response was confirmed by preliminary experiments (Appendix 9.2). Futhermore, the impact of different UV-A wavebands on the UV-A induced carotenoid accumulation response in any *Dunaliella* genus has not been described in literature thus far. The biological effectiveness of UV is known to change as a function of wavelength (see sub-section 2.3.3.3 and 2.3.3.6). Additionally, knowledge of the effectiveness of different UV-A wavebands at inducing carotenoid accumulation is required for design of targeted UV treatment systems by BioLumic.

The general experimental procedure used is described in the Material and Methods sub-section. All experiments discussed in this chapter are based on 24 $h \cdot d^{-1}$ UV exposure in conjunction with 24 $h \cdot d^{-1}$ PAR exposure. For the purpose of the chapter, the wavebands used have been grouped into 'Long wavelength UV-A', 'Broad wavelength UV-A' and 'Short wavelength UV-A' (Table 4-1). UV radiation was delivered using Philips TL-D18W BLB UV-A blacklight fluorescent tubes and Q-Lab Q-panel UVA-340 fluorescent tubes (emission spectra shown in Figure 3-2) with and without UV filters.

Table 4-1 Summary of wavebands and UV irradiance ($W \cdot m^{-2}$) used during experiments. The UV irradiance refers in all cases to the cumulative irradiance over all wavelengths in the waveband.

	Waveband	Filters used	UV irradiance used ($W \cdot m^{-2}$)	Replicates (n = …)
PAR	30 $\mu mol \cdot m^{-2} \cdot s^{-1}$ for 24 $h \cdot d^{-1}$, unless stated otherwise			
Long wavelength UV-A	360-400 nm	N/A	4.0	8
			8.0	4
			16.0	4
			24.0	4
			30.0	4
Broadband wavelength UV-A	300-400 nm (incl. UV-B)	N/A	12.3	2
			14.4	2
	320-400 nm (excl. UV-B)	Mylar filter only	11.6	4
Short wavelength UV-A	300-350 nm (incl. UV-B)	350 nm shortpass filter only	4.7	4
	320-350 nm (excl. UV-B)	350 nm shortpass + Mylar filter	2.8	4

The wavebands were generated using a combination of different light sources and UV filters (see Appendix 9.5 for more detail). The relative contribution of 10 nm wavelength segments to the overall irradiance in each waveband is shown Figure 4-1 (e.g. the relative contribution of wavelengths between 370-379 nm to the irradiance in the Long wavelength UV-A waveband is 49%).

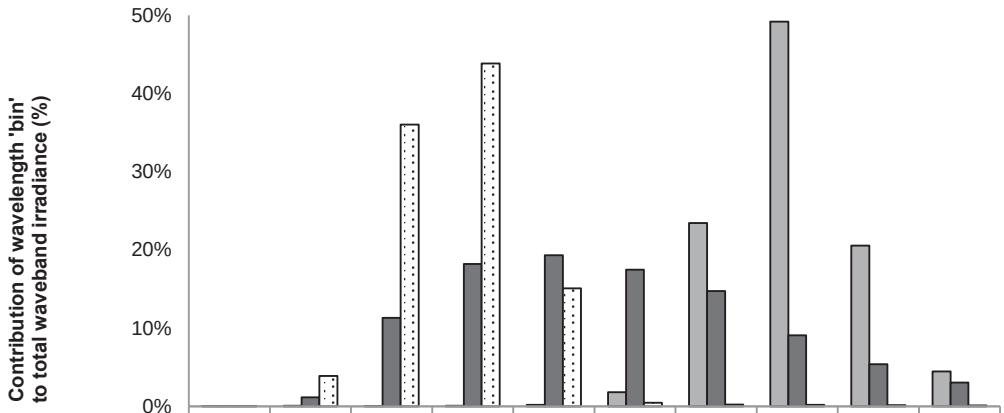

	300 - 309	310 - 319	320 - 329	330 - 339	340 - 349	350 - 359	360 - 369	370 - 379	380 - 389	390 - 399
Long wavelength UV-A	0%	0%	0%	0%	0%	2%	23%	49%	21%	4%
Broadband wavelength UV-A	0%	1%	11%	18%	19%	17%	15%	9%	5%	3%
Short wavelength UV-A	0%	4%	36%	44%	15%	0%	0%	0%	0%	0%

Figure 4-1 Relative contribution of wavelengths to total waveband irradiance for the three different wavebands described in the text. Spectral irradiance is summed per 10 nm 'bin'.

4.2 Results

4.2.1 Photosynthetic pigment content

The UV-A induced carotenoid accumulation response in *D. salina* was observed in all UV-A wavebands tested. Carotenoid accumulation was evidenced by a strong increase in absorbance of the whole cell methanol extracts between λ = 350 - 500 nm (Figure 4-2). Comparing the absorbance spectrum in Figure 4-2 with peak emissions reported by Ben-Amotz et al., indicated β-carotene was likely highly represented among the accumulated carotenoids induced by UV-A in *D. salina*. Absorbance peaks were observed at λ = 340, 443, 471 and 665. Ben-Amotz et al. (1982) showed the absorbance peaks of the isolated carotenoid globules were found to correspond with 9-cis and 15-cis isomers β-carotene (λ_1 = 443 nm and λ_2 = 471 nm). The presence of other UV screening pigments such as MAAs and flavonoids was not investigated.

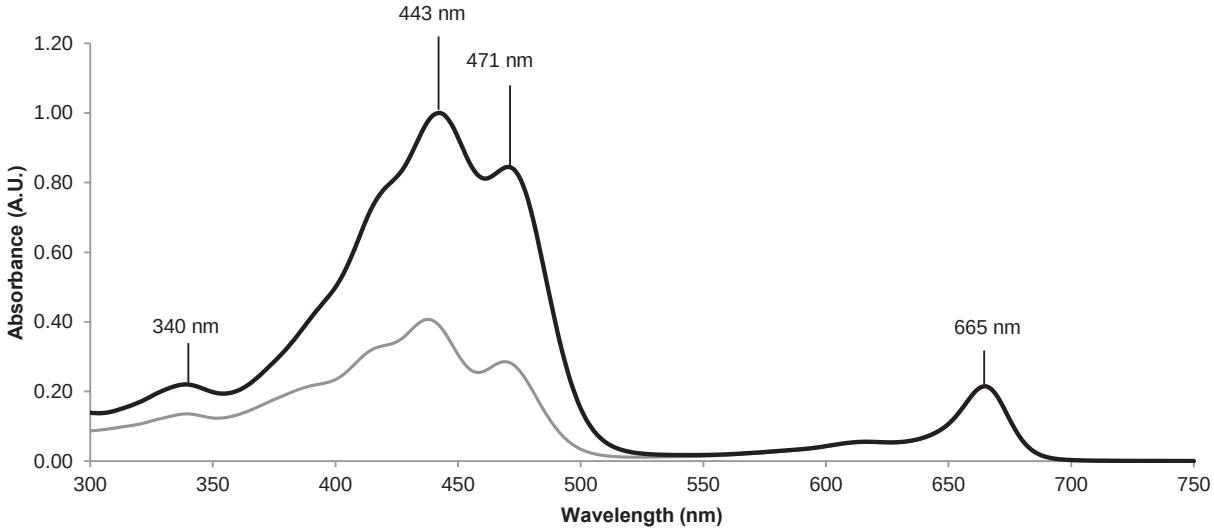

Figure 4-2 Absorption spectra of whole cell methanol extracts obtained from (grey line) a PAR-Only control and (black line) a UV-A exposed culture (UV treatment = 96 h, long wavelength UV-A = 30W·m^{-2} at 24 h·d^{-1}). Spectra are normalized to λ = 665 nm. Numeric values represent absorbance peaks.

Changes in photosynthetic pigment content were found as a result of exposure to all UV-A wavebands tested (Figure 4-3).

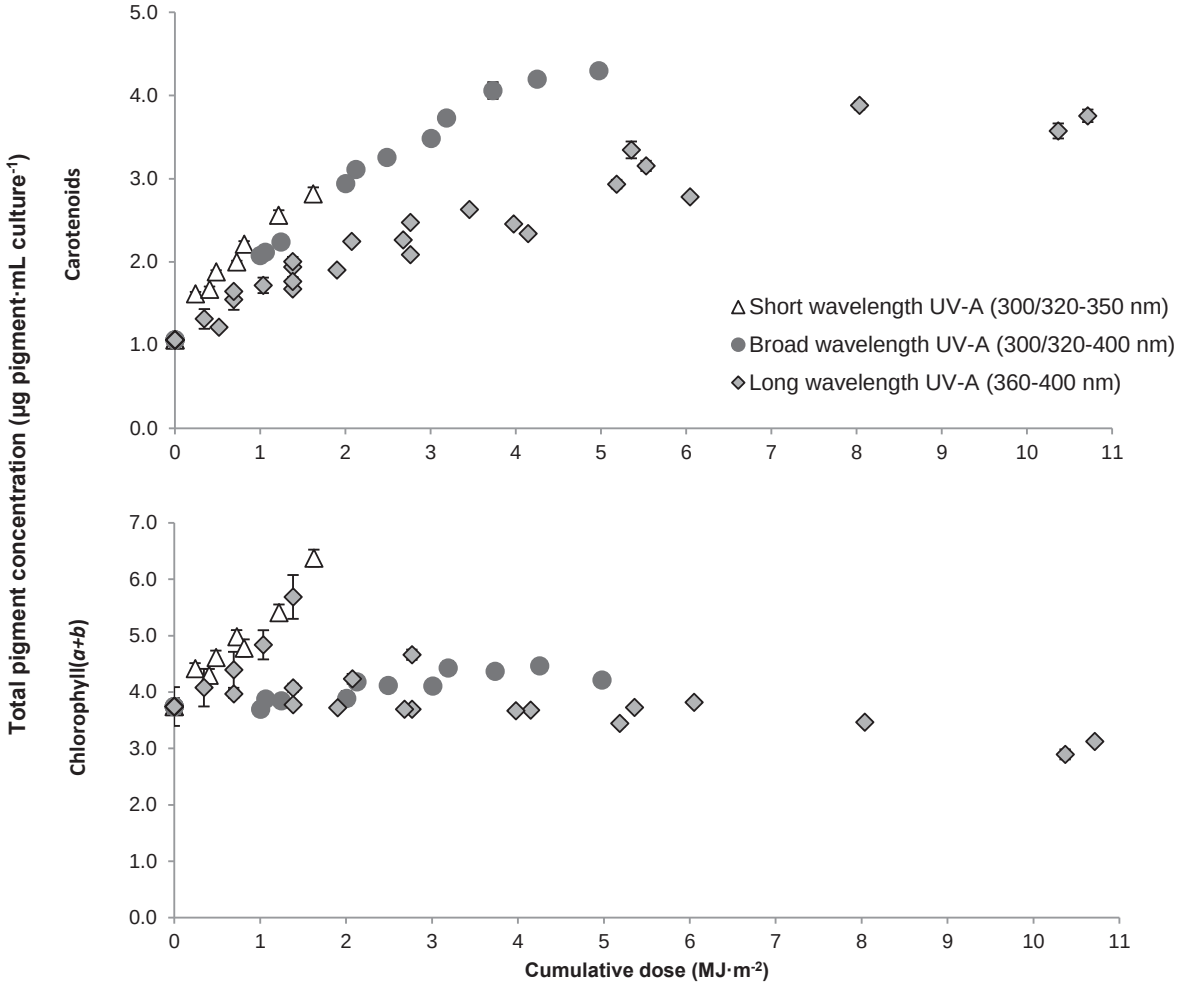

*Figure 4-3 (Top) Total carotenoid concentration under different UV-A waveband and irradiance exposure regimes (see Table 4-1) (Bottom) Total chlorophyll(*a+b*) concentration under different UV-A waveband and irradiance exposure regimes (see Table 4-1). Error bars represent standard error (n = 4 for short wavelength UV-A, n = 2 or 4 for broad wavelength UV-A and n = 4 to 8 for long wavelength UV-A).*

UV induced carotenogenesis in *D. salina* (strain UTEX 1644) (top, Figure 4-3) was most efficient during short wavelength UV-A exposure (λ=320-350 nm) and broad wavelength (λ=320-400 nm) - i.e. similar UV doses induce higher carotenoid accumulation at short and broad UV wavelengths. UV-A induced carotenogenesis is less efficient during long wavelength (λ=360-400 nm) UV-A exposure. Exposure to UV-A was found to slow or halt total chlorophyll *(a+b)* accumulation during certain UV-A exposure regimes (bottom, Figure 4-3), with the magnitude of the total chlorophyll *(a+b)* concentration change apparently dependent on UV-A irradiance rather than UV-A

wavelength (Figure 4-3 and Table 4-2). Table 4-2 lists changes in total pigment concentration (µg pigment·mL culture^{-1}) and intracellular pigment content (µg pigment·10^6 cells^{-1}) at UV treatment = 72 h when maximum carotenoid accumulation was achieved in most treatments. The UV dose efficiency is shown in Figure 4-4 below.

Table 4-2 Total pigment concentration and cellular pigment content calculated from whole cell methanol extracts of cultures treated with PAR-Only or different UV-A waveband and irradiance exposure regimes. Cultures were UV exposed for 72 hours (24 h·d^{-1},). (n =4 for short wavelength UV-A, n = 2 or 4 for broad wavelength UV-A and n = 4 to 8 for long wavelength UV-A). All data in this table are normalized.

Light source	Cumulative UV dose (MJ·m^{-2})	UV irradiance used (W·m^{-2})	Total carotenoid conc. (µg·mL culture^{-1})	Total chlorophyll *(a+b)* conc. (µg·mL culture^{-1})	Cellular carotenoids conc. (µg·10^6 cells^{-1})	Cellular chlorophyll *(a+b)* conc. (µg·10^6 cells^{-1})
PAR-Only	N/A	N/A	1.51 ± 0.08	5.48 ± 0.30	5.68 ± 0.33	21.13 ± 1.45
Short wavelength UVA	1.22	4.7 (300-350 nm)	2.56 ± 0.08	5.42 ± 0.15	10.24 ± 0.87	21.13 ± 0.96
	0.72	2.8 (320-350 nm)	2.11 ± 0.02	4.98 ± 0.13	7.95 ± 0.25	19.98 ± 1.30
Broadband wavelength UV-A	3.19	12.3 (300-400 nm)	3.73 ± 0.03	4.48 ± 0.05	16.62 ± 0.87	18.95 ± 1.09
	3.73	14.4 (300-400 nm)	4.06 ± 0.04	4.37 ± 0.03	20.48 ± 1.17	22.37 ± 1.27
	3.01	11.6 (320-400 nm)	3.57 ± 0.03	4.10 ± 0.09	16.09 ± 0.48	19.20 ± 0.64
Long wavelength UV-A (360-400 nm)	1.03	4.0	1.71 ± 0.09	4.84 ± 0.26	7.38 ± 0.68	19.16 ± 1.89
	2.07	8.0	2.24 ± 0.03	4.23 ± 0.09	9.11 ± 0.26	17.48 ± 0.61
	4.14	16.0	2.22 ± 0.02	3.70 ± 0.03	8.63 ± 0.25	15.28 ± 0.44
	6.05*	24.0	2.78 ± 0.06	3.82 ± 0.02	13.62 ±0.47	17.30 ± 0.56
	8.04	30.0	3.88 ± 0.05	3.47 ± 0.02	22.74 ± 1.33	19.94 ± 0.93

* 70 h UV exposure instead of 72 h.

Trends observed from the data presented in Table 4-2:

- The magnitude of total carotenoid accumulation is higher at shorter UV-A wavelengths when similar cumulative doses (MJ·m^{-2}) are applied – e.g. broad wavelength UV-A at irradiance 14.4 W·m^{-2} to long wavelength UV-A at irradiance 16 W·m^{-2} receive a similar cumulative dose but

total carotenoid content is nearly doubled when broad wavelength UV-A is used. Figure 4-4 elaborates further on UV dose efficiency.

- Total carotenoid content was increased as the cumulative dose increased. Higher irradiance aided in delivering the UV dose more rapidly and thus led to higher carotenoid accumulation. The carotenoid accumulation originated from an increase in cellular carotenoid concentration.
- Total chlorophyll *(a+b)* accumulation is slowed or halted upon UV-A exposure at all wavelengths. The decrease in total chlorophyll *(a+b)* content was smallest at UV irradiance < 5 $W \cdot m^{-2}$ (i.e. the points in bottom of Figure 4-3 that show a steady increase in chlorophyll *(a+b)*). At UV irradiances > 5 $W \cdot m^{-2}$ the total chlorophyll *(a+b)* accumulation was severely slowed or halted (i.e. the points in bottom of Figure 4-3 that increase slightly or stay similar to the starting value at 0 $MJ \cdot m^{-2}$).

The final observation thought to be the result of slowed or ceased cell proliferation (discussed in the next sub-section). However, It may also may be a result of photodestruction or decrease in light harvest complex size (Smith et al., 1990) but does not appear to be exacerbated at shorter wavelength UV-A. Increased effectivity of short wavelengths UV-A at PSII inactivation (Vass et al., 2002) and photoinhibition (Ghetti, et al., 1999) does not appear to affect total chlorophyll *(a+b)* concentration.

Figure 4-4 illustrates the observation that the UV dose efficiency [Δ(µg Car·mL culture^{-1})·Δ(MJ·m^2)$^{-1}$] of total carotenoid accumulation is higher at shorter UV-A wavelengths. The UV dose efficiency was similar within wavebands but differed significantly between wavebands (i.e. short, broad and long wavelength UV-A) (Figure 4-4). The data in Figure 4-4 indicate UV dose efficiency is both UV-A wavelength and UV-A irradiance dependent. The observation that short wavelength UV-A is most efficient at inducing carotenoid accumulation is novel and has not been reported in literature.

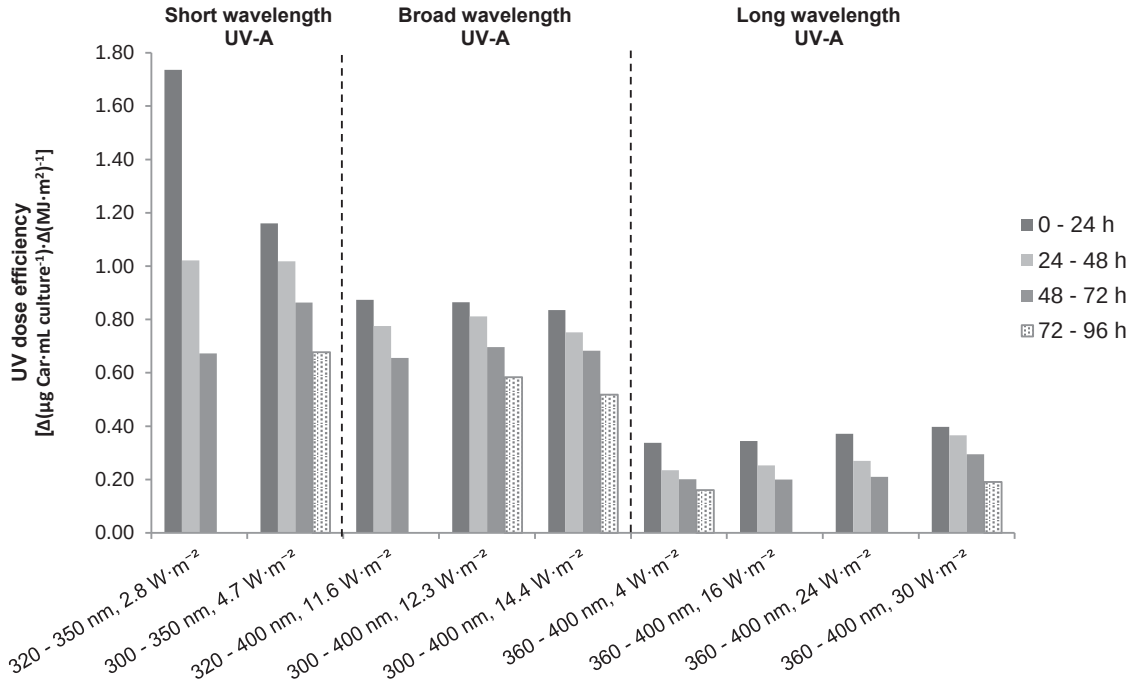

Figure 4-4 Dose efficiency of UV-A induced carotenoid accumulation under different UV-A waveband and irradiance exposure regimes. Series represents dose efficiency per UV-A irradiance between successive time points (separated by 24 h UV exposure) in Figure 4-3. Values are calculated by subtracting total carotenoid concentration between successive time points shown in the legend. Data points for UV exposure = 96 h were not collected during all experiments.

The increased UV biological effectivity in the shorter waveband regions indicates increased effectivity of short wavelength UV-A at inducing carotenoid accumulation. This concurs with the BWFs for photoinhibition and de-epoxidation state discussed in the literature review, which both show increased biological effectivity of decreasing wavelengths in *D. tertiolecta*, with a sharp rise in biological effectivity around λ ≈ 330 nm (Figure 2-7 and Figure 2-8). A number of hypotheses for the increased UV dose efficiency of UV-A induced carotenoid accumulation are proposed based on the proposed function of accumulated carotenoids – i.e. UV shielding and antioxidant – and

the signalling involved in carotenoid accumulation – i.e. ROS, plastoquinone imbalance and photoreceptor.

The hyperaccumulation of β-carotene in *Dunaliella* species under non-UV carotenogenesis conditions is thought to provide a screening function aimed at reducing photodamage (Ben-Amotz et al., 1989c). The induction of carotenoid accumulation by both long- and short wavelength UV-A suggests a shared signalling pathway across the UV-A wavelength range. However, the accumulated carotenoids resulting from UV-A exposure in the current work show the highest absorbance between λ = 360 – 500 nm (Figure 4-2). While the accumulated carotenoids may thus offer UV shielding in the long wavelength UV-A region, UV shielding in the short wavelength UV-A range (λ < 360 nm) is expected to be limited. However, it may be that *D. salina* cannot synthesize other pigments that could offer protection in the short wavelength UV-A region meaning these carotenoids have to be accumulated in high concentrations to provide protection.

As discussed in the literature review both photooxidative stress and imbalances in plastoquinone redox state resulting in PSII photoinhibition have been suggested as triggers for carotenoid accumulation in *Dunaliella* (Lamers et al., 2008). Long wavelength UV-A exposure in *D. bardawil* and *D. salina* led to significant increases in ascorbate peroxidase (APX) activity and ascorbate pool size (White et al., 2002) while short wavelength UV-A has been shown to increase anti-oxidant enzyme activity (SOD and CAT) in *D. tertiolecta* (Bouchard et al., 2013). The UV-A induced carotenoid accumulation may therefore be related to ROS generation (leading to photodamage) and fulfil an antioxidant role rather than a shielding role. Lamers, et al. (2008) discuss the role of a putative 'singlet-oxygen sensor' involved in carotenoid accumulation signalling although no such sensor has been identified in microalgae.

Plastoquinone redox signalling through redox state imbalances resulting from photodamage have also been suggested as a signal for carotenoid accumulation but this has not been studied in *Dunaliella* (Pfannschmidt, 2003; Lamers et al., 2008). Due to the limited understanding of microalgae photoreceptors, the involvement of an unknown algal UV-A photoreceptor inducing carotenoid accumulation cannot be ruled out. Phototropin, rhodopsin and cryptochrome photoreceptors all absorb in the UV-A region and could potentially act as UV-A photoreceptors involved in carotenoid accumulation (Moon et al., 2012; Kianianmomeni et al., 2014). The construction of an action spectrum for UV-A induced carotenoid accumulation would be required to demonstrate this conclusively.

Interestingly UV dose efficiency levels are similar within each waveband for successive time points (particularly evident in broad and long wavelength UV-A). The UV dose efficiency reduction over time suggests the activation of other cellular processes to assist in combating UV damage (e.g. PSII photodamage repair, DNA damage repair and anti-oxidant responses). At the highest UV-A irradiance in the long wavelength UV-A region (30 $W \cdot m^{-2}$), the decrease in UV dose efficiency is less than at lower long wavelength UV-A irradiances. The delayed decrease in dose efficiency at the highest UV-A irradiance (30 $W \cdot m^{-2}$) may indicate the UV-A induced carotenoid accumulation response remains upregulated until the trigger for carotenoid accumulation has been sufficiently reduced.

4.2.2 UV-B inclusion

Although no literature studies of UV-B induced carotenoid accumulation were found, UV-B has been shown to have increased biological effectivity of UV-B wavelength region compared to UV-A (Ghetti et al., 1999). However, Zhang et al. (2015) report increases in carotenoid content as a result of enhanced UV-B exposure in UV-B acclimated cells of *D. salina*. Therefore, efforts were made to investigate the impact of UV-B exposure on UV-A induced carotenoid accumulation using the available equipment. The UV-B radiation present in the broad wavelength UV-A fluorescent tubes (λ = 300-400 nm, Q-Panel UV340) was included or excluded during experiments by covering the fluorescent tubes with Mylar UV-B filter[9]. Broadband UV-A irradiance during experiments was 11.3 $W \cdot m^{-2}$. Broad wavelength UV-A + UV-B irradiance during experiments was 12.4 $W \cdot m^{-2}$ (a UV-B contribution of 1.1 $W \cdot m^{-2}$). Please see Appendix 9.7 for results.

No differences in photosynthetic pigment content (i.e. carotenoid and cholorophyll *(a+b)*), cell growth and cell morphology were found between broad wavelength UV-A and broad wavelength UV-A+UV-B exposure. While the current observations suggest that UV-B does not aid in UV-A induced carotenoid accumulation in *D. salina*, this does not mean to say there is no cellular response to the inclusion of UV-B radiation. UV-B impacts a large number of cellular responses (Ghetti et al., 1999; García-Gómez et al., 2014; Segovia et al., 2015). Furthermore, *Dunaliella* species including *D. salina* have been shown to produces MAAs as a response to enhanced UV-B irradiation (Hannach et al., 1998; Tian et al., 2009).

[9] Mylar blocks UV-B but also reduces UV-A irradiance. The experimental setup was adjusted accordingly to ensure the same UV-A irradiance in all experiments.

4.2.3 Cell numbers

Cell numbers, together with cellular pigment content (µg pigment·10^6 cells^{-1}), determine total pigment concentrations (µg pigment·mL culture^{-1}). UV-A exposure led to slowed cell proliferation compared to PAR-Only controls in all UV-A wavebands tested (and to decreased cell numbers during broad wavelength UV-A exposure) (Figure 4-5).

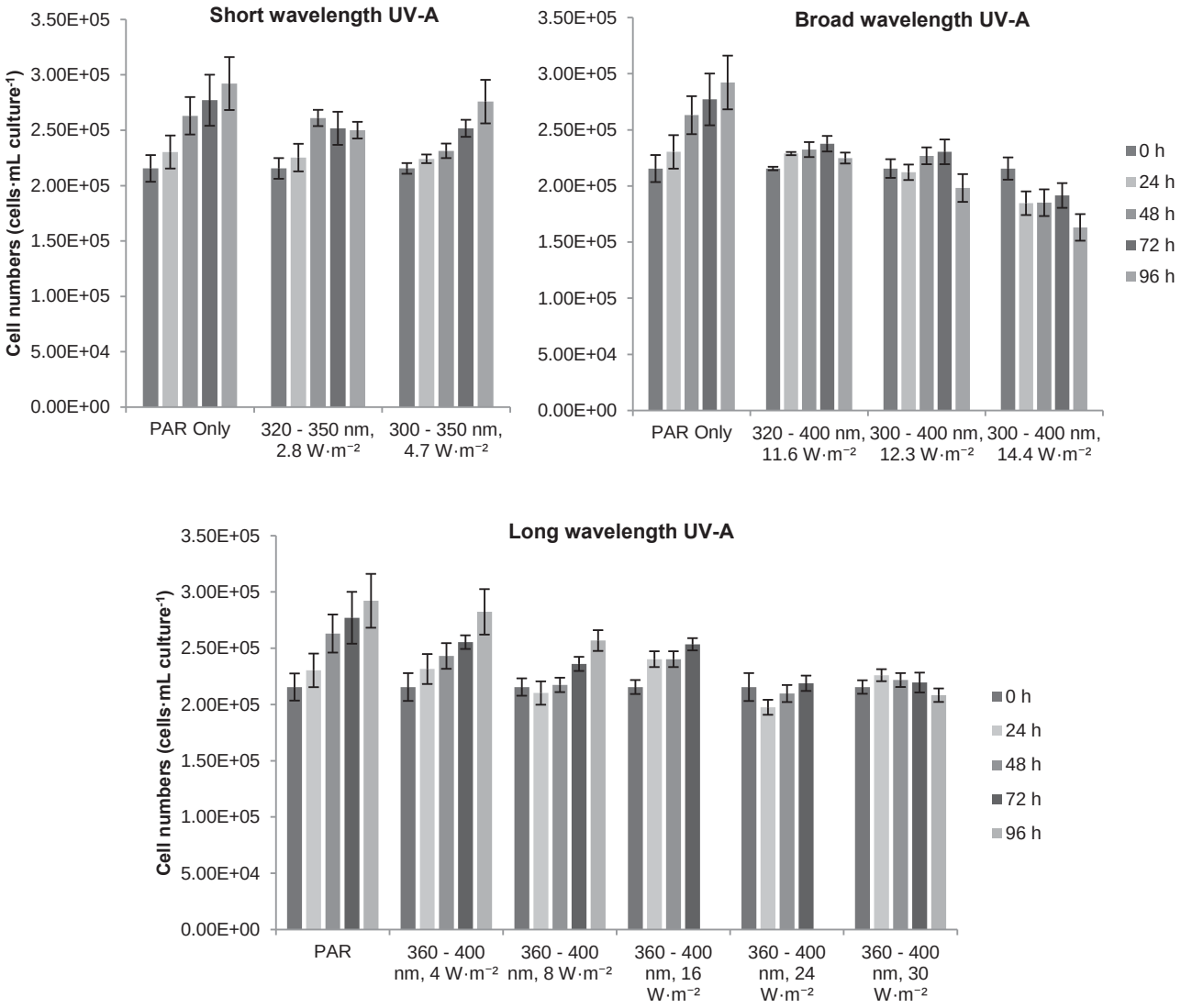

Figure 4-5 Cell proliferation in D. salina under different UV-A waveband and irradiance exposure regimes (see Table 4-1). Error bars represent standard error (n = 4 for short wavelength UV-A, n = 2 or 4 for broad wavelength UV-A and n = 4 to 8 for long wavelength UV-A). It should be noted that experiments for long wavelength UV-A values for 8 W·m^{-2} and 30 W·m^{-2} suffered from low starting cell numbers and cell numbers displayed here are increased due to normalization to PAR-Only values. The observed trend remains valid.

The cause of slowed or ceased cell proliferation in *Dunaliella* species during broad wavelength UV-A exposure has two leading hypotheses: diversion of metabolic fluxes to repair processes (Segovia et al., 2015) and cell cycle arrest resulting from UV radiation induced DNA-damage and photoinhibition (Masi et al., 1997; García-Gómez et al., 2012). Both hyotheses indicate UV exposure as a stressor by the cell. Cultures exposed to low UV-A irradiance (< 5 $W \cdot m^{-2}$) showed the smallest impact on cell proliferation in all UV-A wavebands tested (Figure 4-5) indicating that UV irradiance plays a large role in the slowing or halting of cell proliferation.

Cell death resulting from UV-A exposure was not investigated during the experiments and therefore cannot be ruled out. Cell numbers appear to be relatively stay stable during broad- and long wavelength UV-A exposure (i.e. cell numbers are the same or lower than UV exposure day = 0 d) suggesting that the rate of cell death resulting from UV-A exposure is low. This observation is consistent with observations by other authors in *D. tertiolecta* where cell death was minimal (< 3%) during UV-A exposure (Segovia et al., 2015). Contradictory to the current results (Figure 4-5), several authors report no change in growth rate, or increased growth rates, in *D. bardawil* during long wavelength UV-A exposure (Jahnke, 1999; Salguero et al., 2005; Mogedas et al., 2009). Other authors report decreased growth rates in *D. tertiolecta* during short wavelength UV-A exposure (Andreasson & Wängberg, 2007; Segovia et al., 2015).

4.2.4 Cell morphology

Changes in cell morphology, size and shape in response to UV exposure have been reported in species of the *Dunaliella* genus by numerous authors (see sub-section 2.3.3.1). No records of cell morphology, size and shape changes during UV-A induced carotenoid accumulation were found in the literature and were thus investigated here. Cells grown under PAR-Only conditions remained green throughout all experiments (UV exposure = 0 h, Figure 4-6). A number of morphological changes were observed in cells during UV-A exposure: yellowing, 'disorganized' chloroplast structure, cell size changes and cell roundness changes (UV exposure = 48 h and 96 h, Figure 4-6).

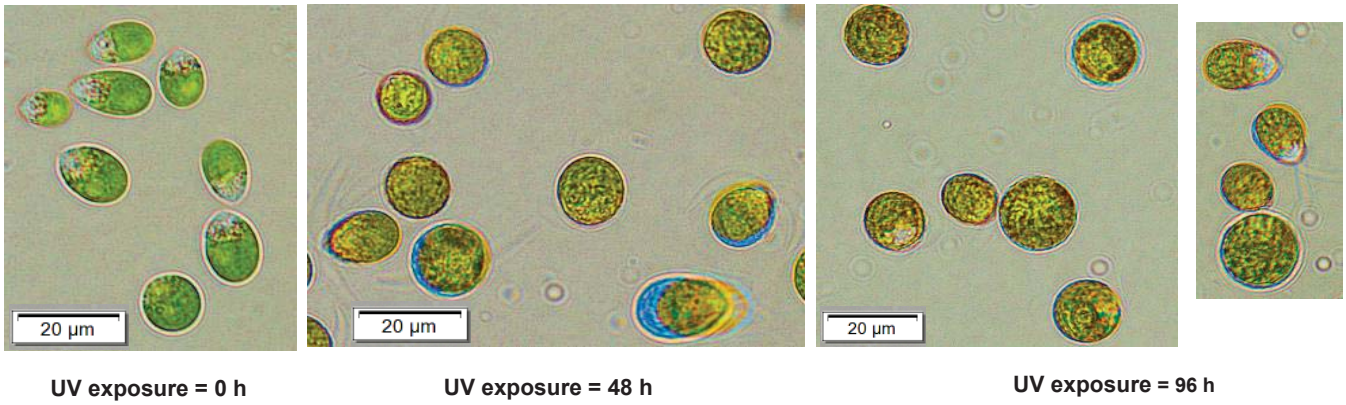

Figure 4-6 Time course of morphological changes observed during UV-A exposure after UV exposure = 0 h (left), 48 h (middle) and 96 h (right). The images represent a selection illustrating the variety of cell morphologies observed. Images were taken in cultures exposed to long wavelength UV-A (30 W·m^{-2}, 24 h·d^{-1}). Images were taken of live cells with an Olympus BX53 microscope at 400x magnification.

The most notable change as a result of UV-A exposure is yellowing of the cells, thought to result from carotenoid accumulation. Orange or red cells, commonly found during commercial *Dunaliella* cultivation as a result of carotenoid hyperaccumulation, were not observed (Borowitzka & Siva, 2007). The yellowing of the cells is thought to be related to the observed changes in chloroplast internal organization (UV exposure = 48 h and 96 h, Figure 4-6). While the shape of the chloroplast is seemingly maintained, it has a noticeably 'disorganized' structure compared to the PAR-Only control. Image quality was best at 400x magnification but the images do not allow for detailed analysis of the chloroplast structure (in-focus images at 1000x magnification proved difficult due to cell movement). Visual assessment of *Dunaliella* morphology during carotenoid accumulation is not commonly reported in literature. A recent study by Fachet et al. (2016) showed an increase in granularity during *D. salina* stress responses utilizing dynamic tracking flow cytometry. The authors propose increased granularity is due to accumulation of storage

molecules, such as starch, neutral lipids and β-carotene. This concurs with results from other studies: in *D. bardawil* carotenoid accumulation leads to the formation of oily droplets in the interthylakoid space, initially forming at the chloroplast periphery and then spreading throughout the chloroplast (Ben-Amotz et al., 1982) and broad wavelength UV-A exposure in *D. tertiolecta* has been reported to induce starch accumulation and the start of chloroplast disintegration after 48 hours UV exposure (García-Gómez et al., 2012). Based on the above it is deemed likely the 'disorganized' structure is a sign of UV-A stress response in *D. salina*.

Changes in cell size[10] and cell shape (as roundness)[11] were quantified using digital image analysis. Cells exposed to PAR-Only increased in size and became increasingly spherical during the experimental cultivation period (Figure 4-7). Cells exposed to long wavelength UV-A were found to increase in size 15% ± 2% compared to those exposed to PAR-Only (left, Figure 4-7). Cells in both PAR-Only and UV-A exposed became more spherical as a function of time (increased median and skewness of distribution, right, Figure 4-7). UV-A exposed cells appeared to be on average less spherical than the PAR-Only exposed cultures. A larger range of cell shapes was found in UV-A exposed cultures compared to PAR-Only cultures.

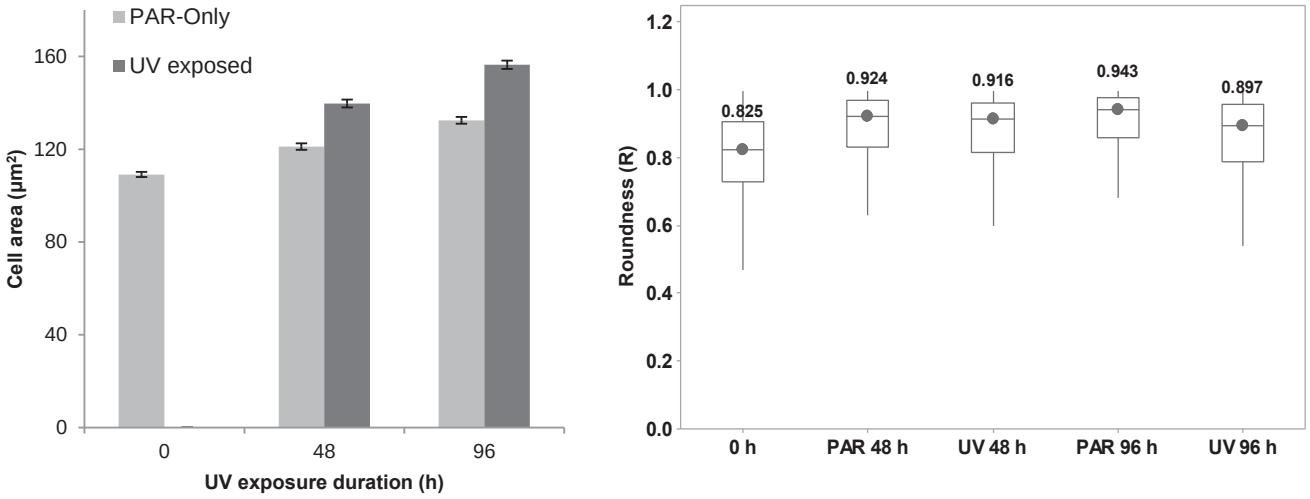

Figure 4-7 Time course of cell area (left) and cell roundness (right) based on digital image analysis. Images were taken during repeat experiments of long wavelength UV-A exposure (30 W·m^{-2}, 24 h·d^{-1}). Data analysis was carried out using a minimum of 400 counts. Error bars represent standard error (left) (n = 4). Values in boxplot represent median values with 95% confidence interval.

[10] Because cells are radially symmetrical (Borowitzka et al., 2007), changes in cell area are assumed to correspond to changes in cell volume. Cell area data sets exhibited normal distribution (p=0.05 or lower).

[11] The "roundness" in ImageJ is defined as R = 4 x $\frac{[Area]}{\pi \times [Major\ axis]^2}$. This compares the area of an ellipse to that of a circle based on the length of the major axis, where Roundness = 1 donates a perfect circle.

Cell size increase in *D. salina* during long wavelength UV-A exposure as shown here has not been reported in the literature. Segovia et al. (2015) report no cell size change in *D. tertiolecta* during broad wavelength UV-A exposure. A study by Masi & Melis (1997) in *D. salina* found a 108% increase in cell volume during UV-B exposure (λ = 280 – 320 nm). Segovia et al suggest the increase in cell size is a protection mechanism against UV damage by increasing internal self-shading (referencing o work by Garcia-Pichel, 1994). Masi & Melis (1997) on the other hand propose cells of *D. salina* exposed to UV-B may be halted in G2 cell cycle stage due to DNA damage, while still being able to continue growing in size.

Cells were mostly ellipsoid and typically motile at the beginning of the experiment at UV exposure = 0 h (Figure 4-6 and Figure 4-7). The observed cell size increase and increased roundness have been observed as a common signs of aging in *Dunaliella* cultures (Borowitzka & Siva, 2007). Cell size increase and increased roundness are observed in the PAR-Only controls suggesting culture aging may contribute to the change. However, cells of *Dunaliella* lack a cell wall and are thus able to change shape and size with relative ease. Under extreme, non-UV conditions cells of *Dunaliella* are known to become spherical temporarily before returning to their normal shape (Borowitzka & Siva, 2007). Extreme conditions include nutrient limiting conditions (e.g. nitrogen in Uriarte, et al., 1993), osmotic shock (Ginzburg et al., 1985) and high PAR light (Shaish et al., 1993). The accumulation of carotenoids which often accompanies growth in these extreme conditions has also been correlated to cell size (Massyuk, 1973; referenced in Borowitzka & Siva, 2007). Based on the above literature reports, the observed cell size increase may result from UV-A exposure as an extreme condition. Ultimately, from the current data it remains unclear whether cell size increases due to interference with cell cycle, a targeted means of UV-A defence, extreme conditions or carotenoid accumulation. Furthermore, it is unclear what causes the differences in cell shape distribution between PAR-Only and UV-A exposed cultures.

4.2.5 Settling

Harvest has been highlighted as the most important area of process improvement in commercial *D. salina* cultivation (Moulton et al., 1987a). Settling of microalgae cells aids in concentrating the cells prior to, or as a means of harvesting. Cells of *D. salina* exposed to all UV-A wavebands were observed to settle to the bottom of the culture vessel at a faster rate than those exposed to PAR-Only . Rapid experiments were carried out to quantify the observation. The data from all rapid experiments were grouped and plotted in Figure 4-8 (i.e. all PAR-Only and all UV exposure data). Limited experiments mean data can only exemplify the observed trends during experiments.

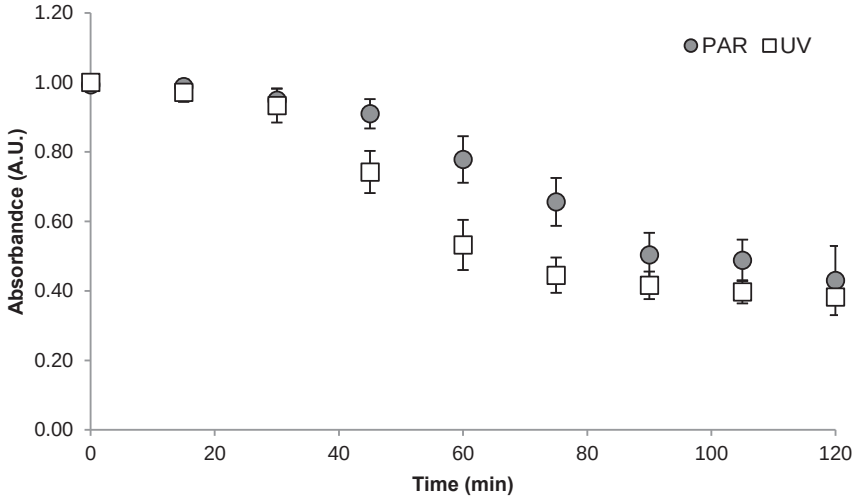

Figure 4-8 Timecourse of cell settling after UV exposure. Settling is measured as a change in OD_{687}. Sample was considered settled when OD_{687} stays constant for 3 consecutive timepoints. Settling was carried out in the dark to remove phototaxis effects. Error bars represent standard deviation (n=16).

Changes in cell size and shape as described in the previous sub-section may offer an explanation for the observed increased degree of settleability. Jiménez et al have shown that cells lose all ability for phototaxis after 10 h UV-A or UV-B exposure, with normal behaviour recovered after 24 h exposure (Jiménez et al., 1996). The phototactic response in *D. salina* in response to UV-A exposure was not examined further in the current experiments. Settleability experiments were carried out in the dark however, meaning it is unlikely phototaxis would have influenced the settleability. Alternatively, cells of *D. salina* have been reported to form aplanospores (vegetative cysts) under extreme conditions (Borowitzka & Huisman, 1993), with cell contents appearing 'granular'. The formation of aplanospores as a result of UV-A exposure may offer an alternative explanation. However, the formation of aplanospores under current conditions is deemed unlikely as analysed images indicated no clear signs of aplanospore formation (thick, rough cell walls).

4.3 Conclusions

Controlling and enhancing the production of high value carotenoids was identified as a potential target for development of UV treatment regimes during large-scale *D. salina* cultivation. In order for BioLumic to develop targeted UV treatment regimes and UV treatment technologies, a fundamental understanding is required of the target species' desired UV response and UV photobiology. The experiments carried out in current chapter have led to a number of important UV photobiology and UV response observations with regards to the UV treatment system design.

While UV-A induced carotenoid accumulation is observed in *D. salina* exposed to all UV-A wavebands tested here, the process is most efficient during short wavelength (λ=320-350 nm) UV-A exposure, followed by broad wavelength (λ=320-400 nm) (Figure 4-4). UV-A induced carotenoid accumulation is least efficient during long wavelength (λ=360-400 nm) UV-A exposure. The apparent increased biological effectivity of short wavelength UV-A at inducing carotenoid accumulation concurs with observations of the impact UV on other biological processes. No reports have been found in the literature that indicate UV-B induces carotenoids and carotenoid accumulation was not improved when UV-B wavelengths were included during broad wavelength UV-A exposure. These novel findings aid BioLumic in choosing the correct UV-A (LED) light source. The TEA in sub-chapter 6-4 will discuss the impact of UV light source on the UV treatment technology design in more detail.

However, as the results clearly show, there are a multitude of other responses that cannot be uncoupled from the carotenoid accumulation response. Decrease or stagnation of total chlorophyll *(a+b)* concentration and cell numbers as well as changes in cell morphology all suggest a stress response resulting from UV-A exposure. These stress responses are likely to impact targeted UV treatment during commercial *D. salina* cultivation if UV is applied as a tool. Total chlorophyll *(a+b)* concentration is stagnated or decreased by UV-A exposure as a result of both cellular chlorophyll *(a+b)* content changes and cell number changes (Figure 4-3). Cell proliferation is slowed or halted as a result of UV-A exposure (Figure 4-5). There are numerous morphological changes resulting from UV-A exposure, the most notable of which are the yellowing of the cells, disorganized appearance of the chloroplast and the increase in cell size and roundness (Figure 4-6 and Figure 4-7). UV-B added to UV-A exposure regimes showed no significant changes to the observed parameters. These novel observations for *D. salina* strain UTEX 1644 indicate the need for further investigation.

The continued focus of the current work will be on furthering the understanding of how the total carotenoid concentration (µg pigment·mL culture^{-1}) can be maximized as a resultant of all the responses observed in the current chapter.

5 Experimental chapter 2 – Manipulating the UV-A response

In chapter 4, the UV-A induced carotenoid accumulation response in *D. salina* was identified as the target for manipulation by UV radiation as a tool. The UV-A induced carotenoid accumulation response was also shown to effect changes in total chlorophyll *(a+b)* concentration, cell numbers and cell morphology suggesting a stress response resulting from UV-A exposure. The results of these changes are likely to impact targeted UV treatment during commercial *D. salina* cultivation. The thesis will continue expanding on these observations by investigating how the *D. salina* UV-A induced carotenoid accumulation response can be manipulated to maximize total carotenoid concentration (μg Car·mL culture^{-1}). Sufficient understanding of target UV response is required to allow for the development of commercial scale UV treatment system by BioLumic. The manipulation of the parameters outlined in Table 5-1 will be quantified with focus on maximizing total carotenoid concentrations.

Table 5-1 UV control parameters

Parameter	Description
UV-A waveband (nm)	The impact of UV-A waveband was explored in the previous chapter and is therefore not considered further. Long wavelength UV-A exposure was used for all experiments discussed below. The higher efficiency of short wavelength UV-A at inducing carotenoid accumulation was not determined until later in the PhD project.
Irradiance (W·m^{-2})	The UV-A irradiance was shown in Chapter 4 to impact the magnitude of *D. salina* UV-A induced carotenoid accumulation response (Table 4-2). Furthermore, the UV-A irradiance required to maximize the total carotenoid concentration is directly related to the capital and operational expense of a large-scale UV treatment system.
Exposure duration (hours or days)	It is not clear from Chapter 4 how the UV-A induced carotenoid accumulation response is maintained upon reducing UV exposure duration. Reducing the UV exposure duration (to 6 and 12 h·d^{-1} rather than 24 h·d^{-1}) is thought to be related to reducing the capital and operational expense of a large-scale UV treatment.
UV transmission into culture	Cell density and mixing are thought to play a large role in UV transmission into dense microalgae culture. Changes in cell density and mixing may therefore impact the UV-A induced carotenoid accumulation response.
Non-UV carotenogenesis stimuli	Increased PAR irradiance and salinity are the most important stimuli involved in non-UV-A induced carotenoid accumulation in *D. salina* (Loeblich, 1982). There is limited understanding of how these stimuli interact with the UV-A induced carotenoid accumulation response.

5.1 UV-A Irradiance

The UV-A irradiance ($W \cdot m^{-2}$) was shown in Chapter 4 to impact the magnitude of the *D. salina* UV-A induced carotenoid accumulation response (Table 4-2), with higher UV-A irradiance yielding higher total carotenoid concentration (µg Car·mL culture^{-1}). It is hypothesised that an increase in UV-A irradiance is likely to upregulate metabolic pathways controlling carotenoid accumulation. However, results from Chapter 4 also indicate negative impacts of increased UV-A irradiance in the form of total chlorophyll *(a+b)* content and slowed cell proliferation.

From an industrial perspective, the UV-A irradiance required to maximize the total carotenoid concentration is directly related to the capital and operational expense of a large-scale UV treatment system through e.g. cost of UV radiation source, required UV source density and UV source electricity usage. The impact of the UV irradiance on the UV-A induced carotenoid accumulation was investigated. Experiments were carried out in which the UV irradiance was varied while UV exposure duration was kept constant at 24 $h \cdot d^{-1}$. Parameters that were impacted by the level of irradiance will be discussed below.

5.1.1 Experimental procedure

The general experimental procedure used is described in the Material and Methods. In summary:

PAR — 30 µmol m^{-2} s^{-1} for 24 $h \cdot d^{-1}$ for the duration of the experiment

UV — Long wavelength UV-A was used for UV-A exposure (λ = 360 – 400 nm, 24 $h \cdot d^{-1}$)
Irradiances used: 4, 16, 24 or 30 $W \cdot m^{-2}$.
Cultures were acclimatized for 2 days (PAR-Only, no UV).
At the start of culture day 3, UV was turned on (UV exposure = 0 h)
At the start of culture day 7, UV was turned off (UV exposure = 96 h)

5.1.2 Results

The results presented below expand on data presented previously in Table 4-2 and focus on long wavelength UV-A only. As previously discussed carotenoid accumulation was induced at all UV-A irradiances as shown in Figure 5-1. Other experiments carried out using different UV light sources yielded similar observations as those discussed below. Data is not shown here due to limited datasets. See Appendix 9.8 for details.

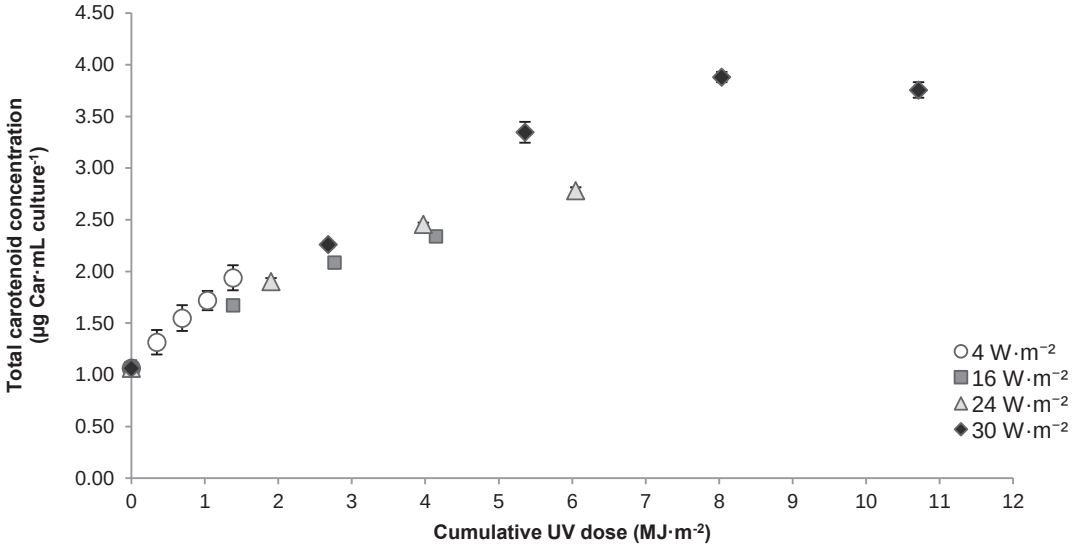

Figure 5-1 Total carotenoid concentration changes under different UV-A irradiance exposure regimes based on spectrophotometric analysis of whole cell methanol extracts. Cultures were exposed to UV-A at the specified irradiance (24 hr·d^{-1}). Where larger than icons, error bars represent standard error (n = 8 for 4 W·m^{-2}, n = 4 for all others)

For different UV-A irradiances the UV dose efficiency [Δ(µg carotenoids·mL culture^{-1})·Δ(MJ·m^{-2})$^{-1}$] was found to be similar within the same UV-A waveband (i.e. Long wavelength UV-A in this case) (Figure 5-2). UV dose efficiency was highest during the first exposure (i.e. between the first sampling points) after which the dose efficiency dropped over time, resulting in slowed carotenoid accumulation. In the case of 30 W·m^{-2} irradiance, long-term exposure (96 h) led to a drop in total carotenoid concentration (Figure 5-1). The data suggest that total carotenoid concentration may no longer continue to increase on sustained UV-A exposure. The observations above are expanded on below.

The dose efficiency [Δ(µg carotenoids·mL culture^{-1})·Δ(MJ·m^{-2})$^{-1}$] for UV-A induced carotenoid accumulation was similar for all UV-A irradiances and was decreased over time similarly for all irradiances (Figure 5-2). The UV dose efficiency decrease observed at UV-A exposure at 30 W·m^{-2} is an exception as the decrease is less rapid in this case.

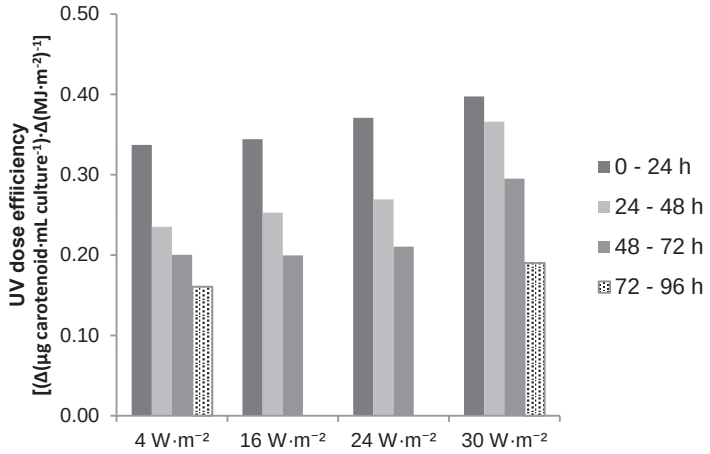

Figure 5-2 *Dose efficiency of UV-A induced carotenoid accumulation under different UV-A irradiance exposure regimes. Series represents dose efficiency per UV-A irradiance between successive data points in Figure 5-1 (separated by 24 h UV exposure). Data points were not collected for UV exposure = 96 h at UV exposures 16 W·m^{-2} and 24 W·m^{-2}.*

The high UV dose efficiency observed between 0 – 24 h exposure indicates that the metabolic pathways that lead to carotenoid accumulation are rapidly initiated regardless of UV irradiance. Furthermore, the UV dose efficiency decreases over time, regardless of the administered dose (i.e. the cumulative dose at 24 W·m^{-2} after each day UV exposure is 6 times higher than at 4 W·m^{-2}). Drawing the analogy with photosynthetic efficiency, the similarity in UV dose efficiency for all UV-A irradiances tested (4, 16, 24 and 30 W·m^{-2}) suggests that a UV-A 'receptor' - i.e. cellular mechanism controlling UV-A induced carotenoid accumulation – is activated at UV-A irradiance as low as 4 W·m^{-2} but has not reached a UV radiation saturation point at 30 W·m^{-2}. This suggests higher UV-A irradiances than those tested here may be possible before the response is saturated.

The subsequent decrease in UV dose efficiency cannot be readily explained based on the current limited data. Two hypotheses are put forward. The first is that the signal triggering the UV-A 'receptor' is sufficiently reduced due to accumulation of carotenoids (i.e. through UV shielding). The alternative hypothesis is that other cellular UV defence mechanisms (e.g. DNA repair, antioxidant and photosynthetic machinery repair) are activated more slowly or only after sustained UV exposure. The other UV defence mechanisms may then fulfil a supporting function

and reduce the need for high intracellular carotenoid contents. Upregulation of oxidative stress defence protein expression in *H.pluvialis* can range anywhere from 12 - 48 h under oxidative stress conditions (conditions that also induce astaxanthin accumulation) (Wang et al., 2004).

The magnitude of the total carotenoid accumulation rate (µg carotenoid·mL culture^{-1}·d^{-1}) was determined by UV-A irradiance (Figure 5-1). The total carotenoid accumulation rate was highest during initial delivery and subsided within 48 – 96 h depending on the irradiance (Figure 5-3). The same trend was observed in experiments using different UV-A light sources (see Appendix 9.8).

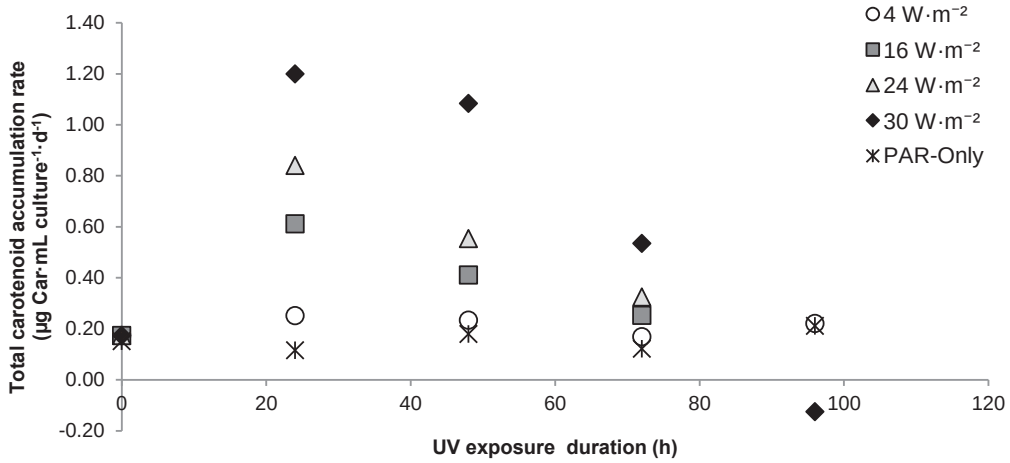

Figure 5-3 UV-A induced carotenoid accumulation rates under different UV-A irradiance exposure regimes. Data point on UV exposure = 0 h represents the carotenoid accumularion rate measured during the acclimation phase (no UV exposure). Cultures were exposed UV-A at the specified irradiance (24 h·d^{-1}).

Figure 5-3 indicates the magnitude of the total carotenoid accumulation rate (µg carotenoid·mL culture^{-1}·d^{-1}) is determined by the UV-A irradiance. The highest rates were found during initial delivery. When the accumulation rate subsides (i.e. 96 h+) it remains unclear whether the total carotenoid concentration is maintained by carotenoids being continually degraded and re-accumulated or by carotenoids being stored. A similar, exposure duration dependent response curve is observed in the model for UV-B photoinhibition in *D. tertiolecta* by Herraud and Beardall (2000), which shows a rapid increase in photoinhibition followed by equilibrium. In the model, the equilibrium that is reached is dependent on the ratio of UV damage and repair. Similarities observed with the current work (i.e. decrease in accumulation rate back to base levels in Figure 5-3) suggest a similar ratio between a signalling trigger ('damage', i.e. any of the potential carotenoid accumulation triggers discussed thus far) and carotenoid accumulation ('repair'). A carotenoid accumulation equilibrium is also observed in *D. bardawil* although the timescales over which these occur vary from 3 to 24 days exposure (Jahnke, 1999; Mogedas et al., 2009).

In the context of *Dunaliella* UV responses, numerous authors have discussed the concept of 'reciprocity'– the assumption that the total cumulative dose ($MJ \cdot m^{-2}$) as opposed to the rate at which it is administered (irradiance) is the dominant factor in determining the extent of an observed UV response (Jahnke et al., 2009). The varying UV dose efficiencies and total carotenoid accumulation rates in the current work indicate that the UV-A induced carotenoid accumulation response may go through phases (e.g. rapid accumulation, a transition phase and equilibrium) suggesting reciprocity likely does not hold (reciprocity was not tested).

The impact of UV-A exposure on cell numbers was discussed Chapter 4. UV-A induced carotenoid accumulation led to a decrease or cessation of cell proliferation (please see Figure 4-5 for cell proliferation changes for 4, 16, 24 and 30 $W \cdot m^{-2}$). Figure 5-4 indicates a relationship between the magnitude of the UV-A induced carotenoid accumulation (as cellular carotenoids, µg carotenoid$\cdot 10^6$ $cells^{-1}$) and cell proliferation ($cells \cdot mL\ culture^{-1}$). Cellular carotenoid content increased (dependent on UV irradiance) to a point beyond which cell proliferation stopped[12]. Experiments carried out using different UV light sources yielded similar observations as those

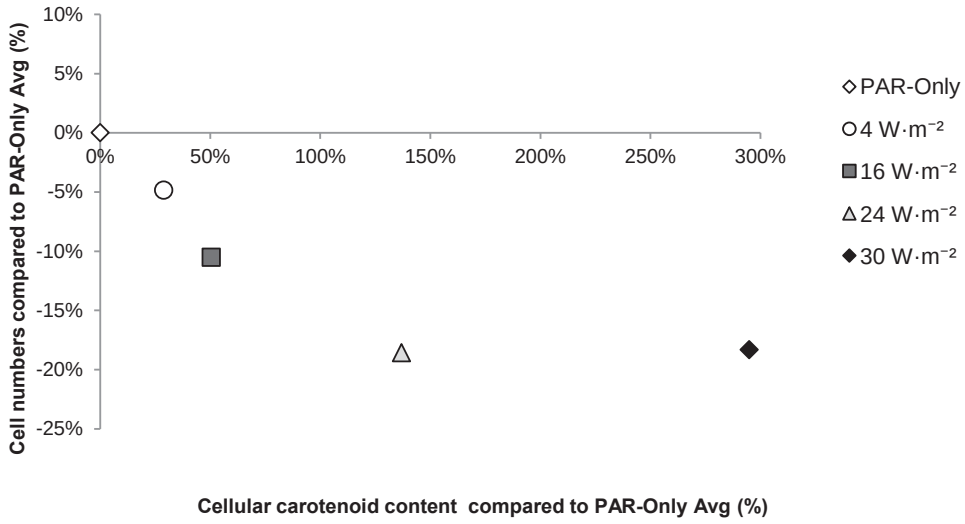

Figure 5-4 Impact of the magnitude of the UV-A induced carotenoid accumulation (x-axis) on cell proliferation (y-axis) under different UV-A irradiance exposure regimes. Cultures were exposed UV-A at the specified irradiance (24 $h \cdot d^{-1}$) for UV treatment = 72 h.

shown below (see Appendix 9.8).

[12] Please note that the maximum decrease in cell numbers (-19% relative to PAR at irradiances 24 $W \cdot m^{-2}$ and up) means that cell numbers are unchanged after UV irradiance is started while the PAR-Only culture continue to proliferate.

The cause of slowed or ceased cell proliferation in *Dunaliella* species during broad wavelength UV-A exposure has two leading hypotheses: diversion of metabolic fluxes to repair processes (Segovia et al., 2015) and cell cycle arrest resulting from UV radiation induced DNA-damage and photoinhibition (Masi et al., 1997; García-Gómez et al., 2012). Results in Ch. 4 show that UV-A exposure leads to slowed or stopped cell proliferation rather than cell death (Figure 4-5). The data in Figure 5-4 suggest that the magnitude of the UV-A induced carotenoid accumulation response impacts cell proliferation capacity (i.e. slowing or stopping proliferation), potentially through diversion of metabolic fluxes away from cell proliferation. The data in Figure 5-4 suggests that there is an 'optimal' irradiance range (i.e. from 4 and 16 $W \cdot m^{-2}$) allowing for both increased carotenoid accumulation and continued cell proliferation, albeit at a slower rate. While it appears that UV induced cellular carotenoid content (µg $Car \cdot 10^6$ $cells^{-1}$) and cell proliferation are connected, further research is required to confirm a correlation. Interestingly, research by Jahnke (1999) in *D. bardawil* shows no significant change in specific growth rate with PFD of 81 $\mu mol \cdot m^{-2} \cdot s^{-1}$ (≈ 28 $W \cdot m^{-2}$) UV-A. Salguero et al. (2005) report an increase in specific growth rate in *D. bardawil* under 40 $\mu mol \cdot m^{-2} \cdot s^{-1}$ (≈ 14 $W \cdot m^{-2}$) and 80 $\mu mol \cdot m^{-2} \cdot s^{-1}$ (≈ 24.3 $W \cdot m^{-2}$) UV-A exposure while 90 $\mu mol \cdot m^{-2} \cdot s^{-1}$ (≈ 31.4 $W \cdot m^{-2}$) led to a decrease in specific growth rate. In Mogedas (2009) growth rates are variable under 8.7 $W \cdot m^{-2}$ UV-A exposure.

Ultimately, UV-A exposure at different UV-A irradiances for extended periods of time lead to significantly different increases of total carotenoid concentration of PAR-Only as shown in Figure 5-5. Despite decreases in cell growth, total carotenoid accumulation was highest at a UV-A irradiance of 30 $W \cdot m^{-2}$.

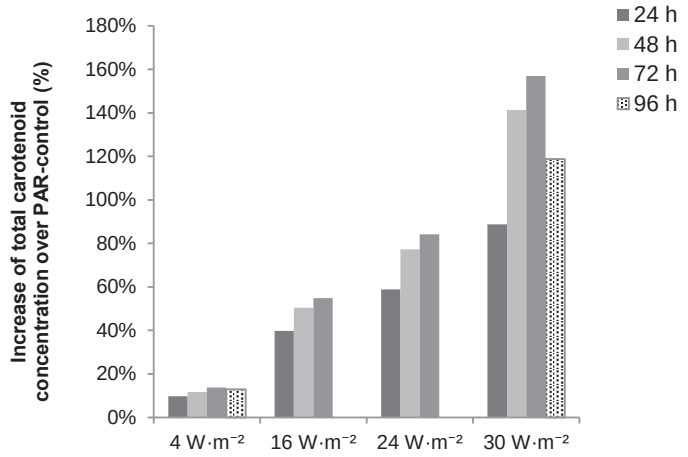

Figure 5-5 Time course of total carotenoid concentration over the PAR-Only control (%) under different UV-A irradiance exposure regimes. Values represent total carotenoid increase in hours after experiment was started (h, see legend) over cultures exposed to PAR only, no UV (%). Cultures were exposed to UV-A at the specified irradiance (24 $h \cdot d^{-1}$). Data points for UV exposure = 96 h were not collected for 16 $W \cdot m^{-2}$ and 24 $W \cdot m^{-2}$.

5.2 Exposure duration

The PhD research described up to this point has employed continuous, 24 $h \cdot d^{-1}$ UV exposure only. From an industrial perspective, reducing the UV treatment system electricity consumption by employing a semi-continuous UV exposure regime (6 and 12 $h \cdot d^{-1}$ rather than 24 $h \cdot d^{-1}$) could offer several advantages. Reducing UV exposure duration, while maintaining carotenoid accumulation, would reduce operational expense. Furthermore, it may allow a single UV treatment system to be used on multiple culture systems (shared between e.g. 2, 4 or 8 systems depending on the required UV exposure duration) reducing capital expenses compared to continuous UV exposure. However, the impact of a UV exposure duration reduction on the UV-A induced carotenoid accumulation response is unclear. It is unclear how metabolic pathways are impacted and whether the UV accumulation response can be maintained upon reducing UV exposure duration. This sub-chapter therefore investigates the impact of semi-continuous UV exposure regimes on UV-A induced carotenoid accumulation. This is done by first investigating what happens to UV-A induced carotenoid accumulation after UV-A exposure is stopped and subsequently investigation whether the UV-A induced carotenoid accumulation response can be maintained by semi-continuous UV-A exposure.

5.2.1 Response longevity after removal of UV-A signal

The industrial partner BioLumic uses an approach where plants are irradiated with targeted UV treatments during the seedling stages [pers. comm. JJ Wargent]. Targeted UV treatment provides the seedlings with lasting benefits after UV exposure is stopped. While this does not imply the UV response itself remains active, it shows that the changes induced by the UV response lead to long-lasting beneficial effects. To gain a better understanding of the timescales involved in the UV-A induced carotenoid accumulation response in *D. salina*, the current sub-section investigates the longevity of the UV response in *D. salina* after UV exposure is stopped.

5.2.1.1 Experimental procedure

The general experimental procedure used is described in the Material and Methods. In summary:

PAR 30 $\mu mol\ m^{-2}\ s^{-1}$ for 24 $h \cdot d^{-1}$ for the duration of the experiment

UV Long wavelength UV-A was used for UV-A exposure (λ = 360 – 400 nm at 16 $W \cdot m^{-2}$, 24 $h \cdot d^{-1}$)

Cultures were acclimatized for 2 days (PAR-Only, no UV).

At the start of culture day 3, UV was turned on (UV-A = 0 h)

At the start of culture day 5, UV was turned off (UV-A = 48 h)

Note: Due to issues with cell proliferation during these experiments, the results are referenced to the PAR-Only control data obtained during those experiments rather than the averaged PAR-Only control from all experiments.

5.2.1.2 Results

After UV-A exposure was stopped, total carotenoid concentration (µg carotenoids·mL culture^{-1}) was maintained at similar levels until the end of the experiments[13] (83 h, Figure 5-6).

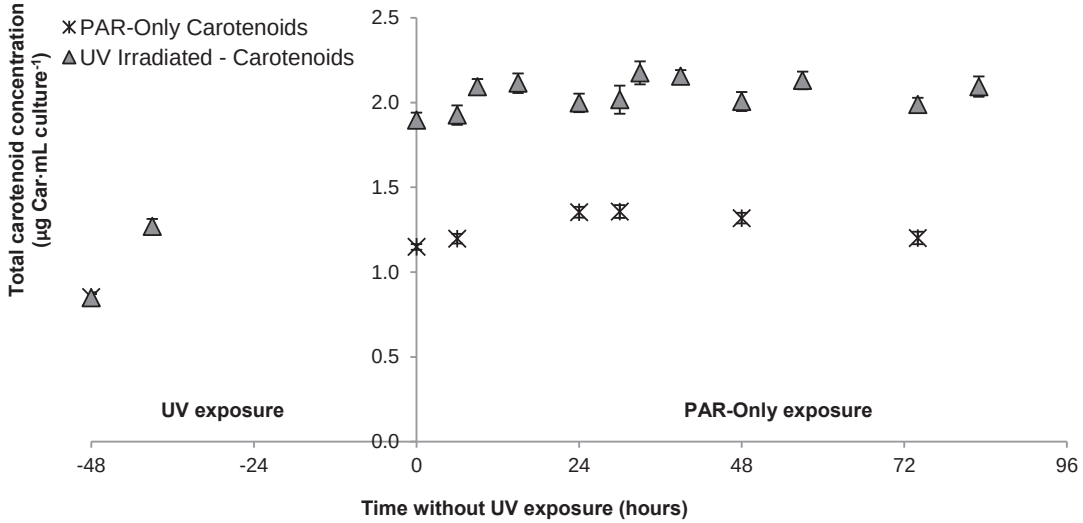

Figure 5-6 Total carotenoid concentration changes during 48 h UV-A exposure and 83 h PAR-Only, based on spectrophotometric analysis of whole cell methanol extracts. Left part of the graph represents the hours of UV exposure (represented as '-' hours). Right side of the graph represents the subsequent hours of PAR-Only. Cultures were exposed to UV-A for the first 48 h after acclimation (24 h·d^{-1}). Where larger than the icons, error bars represent standard error (n = 4).

[13] Both PAR-Only and UV exposed cultures show no change in total carotenoid concentration (µg Car·mL culture^{-1}). Due to experimental issues, no cell proliferation was observed in both PAR-Only and UV exposed cultures although cells remained viable (assessed through microscopy) and carotenoid accumulation could still be induced. A lack of cell proliferation may be an alternative explanation for the lack of total carotenoid change.

While total carotenoid concentration was maintained at a similar level, UV-A induced cellular carotenoid accumulation (µg carotenoid·10^6 $cells^{-1}$) was reversed in 12-24 hours after UV-A exposure was stopped (Figure 5-7). Cell proliferation (cell·mL $culture^{-1}$) was increased in 24-36 hours after UV-A exposure is stopped (Figure 5-8)[14]. The results may provide an explanation why the total carotenoid concentration is maintained rather than reversed for at least 83 h.

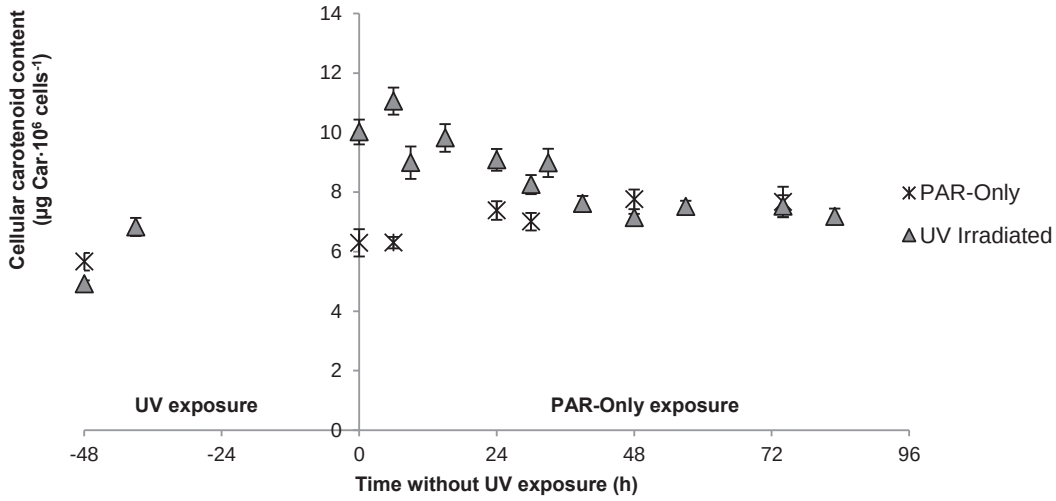

Figure 5-7 Cellular carotenoid content changes during 48 h UV-A exposure and 83 h PAR-Only. Left part of the graph represents the hours of UV exposure (represented as '-' hours). Right side of the graph represents the subsequent hours of PAR-Only. Where larger than the icons, error bars represent standard error (n = 4).

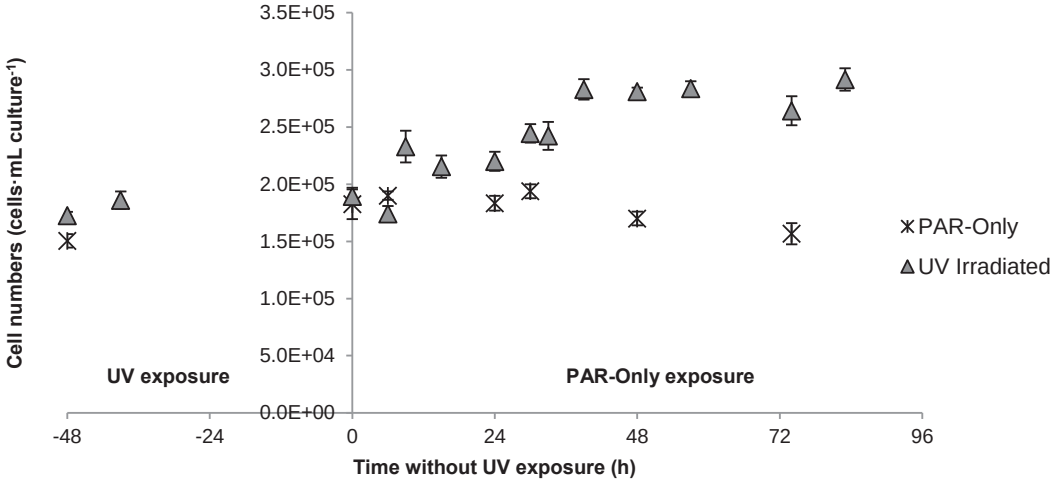

Figure 5-8 Cell numbers changes during 48 h UV-A exposure and 83 h PAR-Only. Left part of the graph represents the hours of UV exposure (represented as '-' hours). Right side of the graph represents the subsequent hours of PAR-Only. Where larger than the icons, error bars represent standard error (n = 4).

[14] PAR-Only cultures continued to show no cell proliferation during this period.

The observations in Figure 5-7 concur with results by Jahnke (1999) showing that the UV-A response in *D. bardawil* is reversed in 24-48 hours after UV-A irradiation is stopped. In the case of UV induced photoinhibition, cultures of *D. tertiolecta* have been shown to fully recover from 6 days UV exposure within 24 hours (Segovia et al., 2015). Cultures of *D. salina* were shown to partially recover from photoinhibition and fully recover photosynthetic O_2 production in 3 hours, after 3 hours of UV exposure (Herrmann et al., 1997). Reports from the literature and current results indicate species of *Dunaliella* rapidly recover from UV radiation effects, including the need for carotenoid accumulation.

Interestingly, UV-A exposure has enabled a proportion of the UV-A exposed cells, previously prevented from proliferating, to resume cell proliferation (no cell proliferation is observed during UV treatment or in the PAR-Only control, Figure 5-8). The decreased cellular carotenoid content (Figure 5-7) and increased cell proliferation (Figure 5-8) suggest redirection of the metabolic fluxes from UV protection (inc. UV-A induced carotenoid accumulation) to cell proliferation (i.e. the opposite of what is suggested by Figure 5-4). Intracellular carotenoid accumulation have been suggested as a carbon source storage in microalgae. *Haematococcus lucastris* hyperaccumulates astaxanthin and uses this to survive and recover after stress (Hagen, et al., 1993). However, *D. bardawil* has been found not to utilize accumulated β-carotene as a carbon source on transfer to darkness or to a CO_2-free medium in the light (Ben-Amotz et al., 1982). Parent cells may also maintain high cellular carotenoid content while newer generations (i.e. not exposed to UV-A) do not produce increased cellular carotenoid levels (termed transgenerational plasticity, Salinas, et al., 2013). It remains unclear however how the prior UV-A treatment has enabled cells previously unable to proliferate, to continue proliferating. The subject is discussed further in Ch. 6.2.

From an industrial perspective, the above results would suggest carotenoid production in a commercial cultivation process is essentially stopped for 83 h. Furthermore, numerous changes indicating the reversal of the UV-A induced carotenoid accumulation are observed, suggesting there is no long-lasting UV-A induced carotenoid accumulation effect. This assertion will be tested during novel UV treatment regime experiments described in Chapter 6.2.

5.2.2 UV exposure duration

From an industrial perspective, using a semi-continuous UV exposure regime (6 and 12 $h \cdot d^{-1}$ rather than 24 $h \cdot d^{-1}$) could offer several advantages. The previous sub-section showed that the UV-A induced carotenoid accumulation response is starting to be reversed in 12-24 h when UV-A exposure is stopped however. It is therefore unclear whether the repeated use of semi-continuous UV exposure (6 and 12 $h \cdot d^{-1}$) could be sufficient to maintain a UV-A induced carotenoid accumulation response. The current sub-section investigates whether repeated UV exposure within this 12-24 h reversal timeframe could be sufficient to maintain the UV carotenoid accumulation response.

5.2.2.1 Experimental procedure

The general experimental procedure used is described in the Material and Methods sub-section. In summary:

PAR — 30 µmol m^{-2} s^{-1} for 24 $h \cdot d^{-1}$ for the duration of the experiment

UV — Long wavelength UV-A (λ = 360 – 400 nm at 16 $W \cdot m^{-2}$) during or 6 and 24 $h \cdot d^{-1}$ UV-A exposure

Cultures were acclimatized for 2 days (PAR-Only, no UV).

At the start of culture day 3, UV was turned on (UV day = 0)

At the start of culture day 7, UV was turned off (UV day = 4)

Note: Due to issues with cell proliferation during these experiments, the results are referenced to the PAR-Only control data obtained during those experiments rather than the averaged PAR-Only control from all experiments.

Note: An additional experiment was carried out to investigate additional semi-continuous UV regimes (6, 12 and 24 $h \cdot d^{-1}$). Due to the different experimental conditions (UV-A light source and irradiance), results are not shown here. Please see Appendix 9.9.

5.2.2.2 Results – Exposure duration

While total carotenoid content was increased over PAR-Only during semi-continuous UV-A exposure (6 h·d^{-1}), carotenoid accumulation was lower than during continuous exposure (24 h·d^{-1}, Figure 5-9).

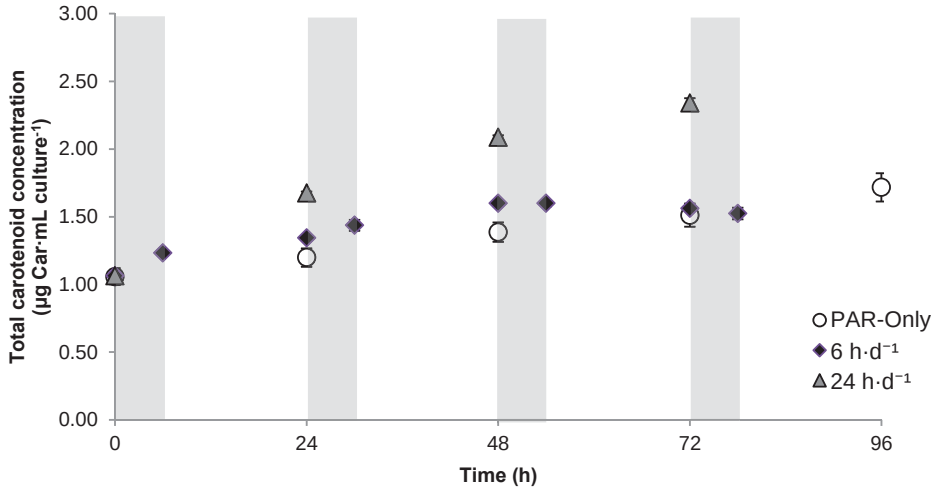

Figure 5-9 Total carotenoid concentration during semi-continuous (6 h·d^{-1}) and continuous UV exposure regimes. Grey bars represent the periods during which UV-A was applied. Sampling was carried out immediately prior and after UV-A exposure. Continuous cultures (24 h·d^{-1}) were sampled every 24 h. Where larger than the icons, error bars represent standard error (n = 8).

The dose efficiency for UV-A induced carotenoid accumulation [Δ(µg carotenoids·mL culture^{-1})·Δ(MJ·m^{-2})$^{-1}$] was higher in semi-continuous exposure during the first two UV-A exposures but then dropped significantly (Figure 5-10).

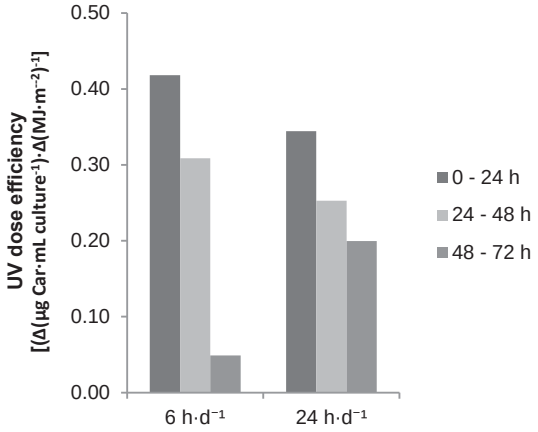

Figure 5-10 Dose efficiency of UV-A induced carotenoid accumulation under semi-continuous (6 h·d^{-1}) and continuous UV exposure regimes. Series represents dose efficiency per UV-A irradiance between successive data points in Figure 5-9 (separated by 24 h UV exposure).

The results in Figure 5-10 indicate that carotenoid accumulation during semi-continuous is efficient during initial 48 h of the exposure regime (i.e. two rounds of 6 hour UV-A exposure), despite the observed low total carotenoid accumulation. The semi-continuous UV-A exposure regime does not appear to allow for continued accumulation however. This suggests the low cumulative dose used in the current experiment is sufficient to induce a carotenoid accumulation response but not to maintain it. Furthermore the UV dose efficiency is comparable to that observed during experiments discussed in the previous sub-chapter (Figure 5-2). It is thought that the effectiveness stems from the fact that the continuous exposure interferes with cell proliferation while semi-continuous exposure does not (see Appendix 9.10). In the literature a difference in the magnitude of the UV stress response has been reported for *D. tertiolecta* during semi-continuous UV exposure (Bouchard et al., 2013). Higher cell proliferation was observed by the authors in the semi-continuous exposed cultures (12 h·d^{-1}, broad wavelength UV-A+UV-B) compared to continuous exposure (24 h·d^{-1}). Conversely, levels of ROS content, CPD formation and SOD and CAT activity were higher in continuously exposed cultures (24 h·d^{-1}) compared to semi-continuous exposure (12 h·d^{-1}). The authors suggest the semi-continuous exposure may allow cells to recover from UV stress and possibly repair themselves. In the current experiment this means basal levels of carotenoid accumulation (i.e. the increase through cell proliferation) continue during as in cultures exposed to PAR-Only.

The total carotenoid accumulation rate (µg carotenoid·mL culture^{-1}·day^{-1}) was increased during periods of UV exposure and decreased between periods of when UV-A exposure (i.e. PAR exposure only) (line in Figure 5-11).

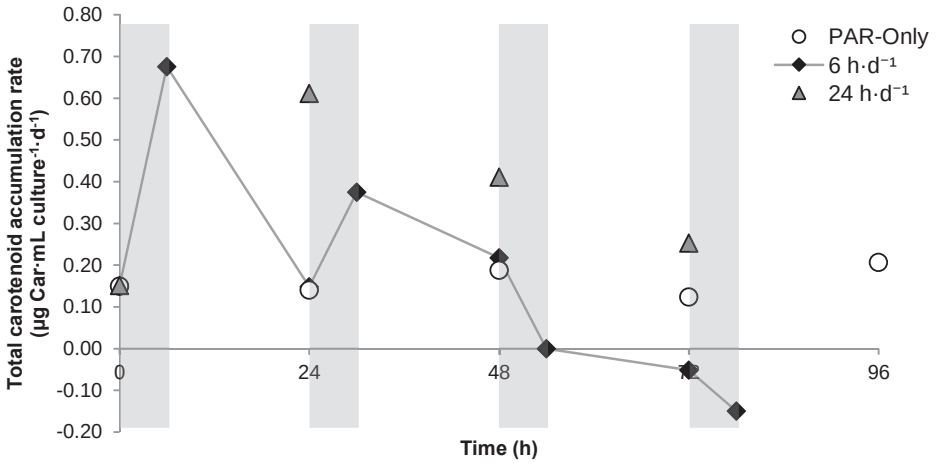

Figure 5-11 Carotenoid accumulation rates under semi-continuous (6 h·d^{-1}) and continuous UV exposure regimes. Sampling was carried out immediately prior and after UV-A exposure. Continuous cultures (24 h·d^{-1}) were sampled every 24 h.

Based on the current observations, carotenoid accumulation rates appear to be increased only during UV-A exposure (although arguably the resolution of the current data would need to be improved to confirm this). The data in Figure 5-11 show a reversal of UV-A induced carotenoid accumulation rate within 18 h after UV-A exposure is stopped. This leads to an averaged semi-continuous carotenoid accumulation rate which is only slightly higher than the PAR-Only control (i.e. averaged over a 24 hour period , 6 h PAR+UV + 18 h PAR, the highest value is 0.28 µg carotenoid·mL culture^{-1}·d^{-1}, with the average PAR-Only carotenoid accumulation rate being 0.17 ± 0.05 µg carotenoid·mL culture^{-1}·d^{-1}). The low average carotenoid accumulation rate resulting from semi-continuous UV-A exposure therefore resulted in a small total carotenoid concentration increase, smaller than would be expected based on the UV-A irradiance used.

All studies found in the literature of UV-A induced carotenoid accumulation in *Dunaliella* employ a continuous PAR and UV exposure regime (24 h·d^{-1}). No reports have been found comparing the impact of semi-continuous and continuous exposure on UV-A induced carotenoid accumulation in *Dunaliella*. The current experimental results indicate repeated UV exposure within the 12-24 h 'carotenoid accumulation reversal timeframe' (see previous sub-section 5.2.1) is not sufficient to maintain the UV carotenoid accumulation response comparable to the level of continuous exposure. Results in the previous sub-section show that the decrease in cellular carotenoid content (µg carotenoid·10^6 cells^{-1}) can take up to 48 hours. Together these data suggest that the

remaining levels of carotenoid may affect the carotenoid accumulation rate upon subsequent UV-A exposures, resulting in a smaller carotenoid accumulation response per semi-continuous UV-A exposure. Results do suggest accumulated carotenoid may not fully dissipate so further research investigating a 12 $h \cdot d^{-1}$ UV treatment regime is recommended (e.g. experiments in Appendix 9.9, not included due to different experimental conditions).

Ultimately, from an industrial perspective, even if the response can be maintained using semi-continuous UV exposure, it is unlikely to result in similar total carotenoid concentrations as continuous exposure. As discussed in the introduction to the sub-chapter, employing a semi-continuous UV exposure regime (6 and 12 $h \cdot d^{-1}$ rather than 24 $h \cdot d^{-1}$) could offer reductions in capital and operational expense. However, the carotenoid accumulation levels observed during experiments presented in this sub-chapter suggest that, despite the reductions in expense, it is unlikely that a semi-continuous UV exposure regime would result in significantly increased profitability if employed as a UV treatment system.

5.3 Determining the effect of environmental conditions: UV transmission

This sub-chapter investigates the impact of UV transmission into a microalgal culture. As discussed in Box 2-2 in Ch. 2.3.1, PAR transmission into the culture vessel has a large impact on areal productivity. Similarly cell density and mixing are thought to play a large role in UV transmission into dense microalgae culture, similar to their impact on PAR transmission into dense microalgae culture (Grobbelaar, 2010). Both PAR and UV transmission into a microalgal suspension are theoretically modelled by Lambert-Beer's law (equation 5):

$$I_z = I_0 \cdot e^{-zK} \qquad \text{(Eq. 5)}$$

where I_0 represents the PAR/UV intensity at the surface of the liquid, K represents the liquids' extinction coefficient and I_z represents the PAR/UV intensity at optical path length z. Moving away from the surface – i.e. increasing the optical path length z - therefore means that PAR and/orUV intensity is reduced, up to a point where levels are close to zero. The extinction coefficient K for UV has been shown to be a function of the microalgae cell density (Navarro, et al., 2014) meaning a similar UV gradient exists in high cell density cultures. To improve PAR exposure during large-scale microalgae cultivation, mixing is commonly employed to move microalgal cells through the PAR light gradient resulting from high cell density. Changes in cell density and mixing are therefore thought to impact the UV-A induced carotenoid accumulation response. Furthermore, understanding how UV transmission impacts the UV-A response is needed to design a large-scale UV treatment system, impacting both reactor design (e.g. culture depth, geometry, mixing regime) and reactor operation (e.g. cell density and mixing frequency).

5.3.1 Experimental procedure

UV transmittance ($T = I_z \cdot I_0^{-1}$, with z = 0.01 m) was first measured as a function of cell density measured as OD_{687}. The UV carotenoid accumulation response was subsequently investigated at different starting culture cell densities. The experimental procedure used is described in the Material and Methods sub-section. Optical density ($Abs_{\lambda= 687nm}$, OD_{687}) measurements were used as indicator of cell density with culture starting cell densities show in

Table *5-2*. Experiment in summary:

PAR	30 µmol m^{-2} s^{-1} for 24 h·d^{-1} for the duration of the experiment

UV Long waveband UV-A was used for UV-A exposure (λ = 360 – 400 nm at 8 $W \cdot m^{-2}$, 24 $h \cdot d^{-1}$)

Cultures were acclimatized for 2 days (PAR-Only, no UV).

At the start of culture day 3, UV was turned on (UV treatment = 0 h)

At the start of culture day 7, UV was turned off (UV treatment = 96 h)

Table 5-2 Starting optical densities used during the experiment. Experiments were normally started at an OD_{687} = 0.100 ± 0.050. One UV control at this density was included (UV culture 2).

Culture	Starting OD_{687}
PAR culture 1	0.175
PAR culture 2	0.300
UV culture 1	0.050
UV culture 2	0.100 (control)
UV culture 3	0.175
UV culture 4	0.300

5.3.2 Results

UV transmittance ($T = I_z \cdot I_0^{-1}$, with z = 0.01 m) was first measured as a function of cell density measured as OD_{687}. The OD_{687} was found to scale linearly with cell density under PAR-Only growth conditions (data not shown) with OD_{687} = 0.100 Abs corresponding to cell density of $1.3 \cdot 10^5$

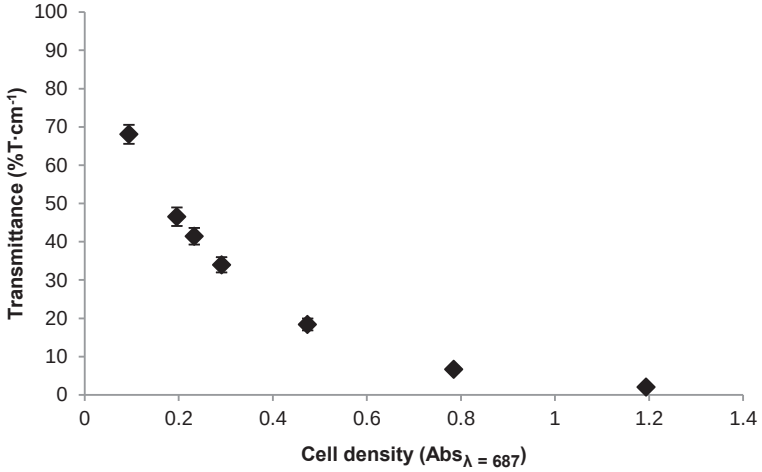

Figure 5-12 UV transmittance as a function of cell density. Data points in the figure represent the average of the transmission in this UV waveband. Transmittance was measured in disposable cuvettes between λ = 300 - 400 nm. Error bars represent the total transmittance range measured for any given data point.

cells·mL^{-1} (Ch. 3.4). UV transmittance was found to decrease rapidly at increasing cell density. These observations concur with reports by Navarro et al. (2014).

In cultures of cell density OD_{687} = 0.100 Abs, UV radiation is attenuated 98% within 10 cm (diameter of 500 mL culture flask) (see Appendix 9.11). Due to the orbital motion of the mixing during experiments, microalgal cells are therefore likely to experience only limited levels of UV radiation when furthest removed from the UV-A source. In cultures of cell density OD_{687}= 0.300 Abs, UV is completely attenuated within 5 cm of entering the microalgal culture (i.e. halfway through the culture flask) meaning half the culture volume is unlikely to experience UV radiation (see Appendix 9.11).

While UV transmittance was rapidly reduced as cell density increased (Figure 5-12), starting culture cell densities between OD_{687} = 0.050 – 0.300 Abs did not appear to impact the UV-A induced carotenoid accumulation response (Figure 5-13)[15]. Based on the results in Figure 5-13, cultures at all cell densities show a similar UV-A induced carotenoid accumulation response.

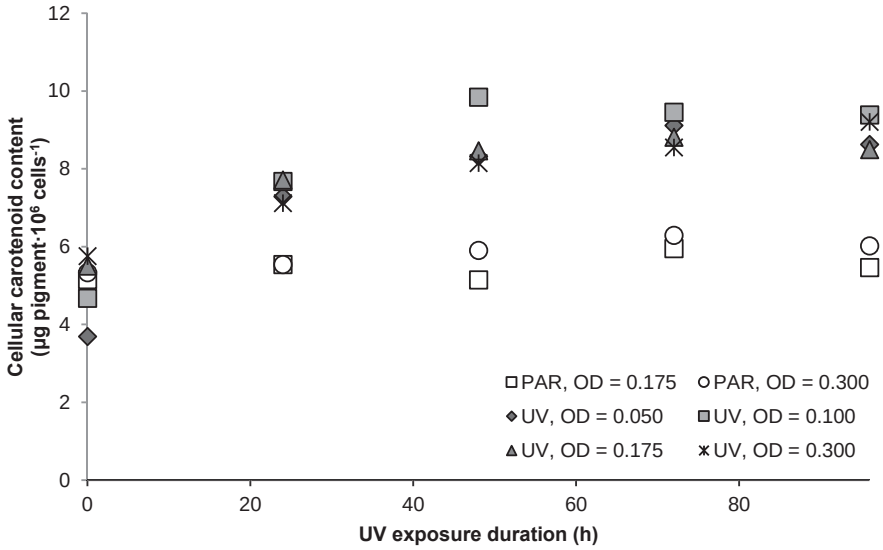

Figure 5-13 Cellular carotenoid content resulting from UV-A exposure at different cell densities (n=1). Legend values represent the OD_{687} values prior to acclimation (i.e. 2 days prior to UV treatment = 0 h).

[15] The UV-A induced carotenoid accumulation response is expressed as cellular carotenoid accumulation (µg carotenoid·10^6 cells^{-1}) rather than total carotenoid concentration (µg carotenoid·mL culture^{-1}) as in previous figures. Different cell densities exhibit substantially different total carotenoid concentrations due to cell numbers.

While UV-A transmittance at the tested cell densities varies between 35-70% cm^{-1}, the impact on the UV-A induced carotenoid accumulation appears negligible. It may that the UV-A induced carotenoid accumulation response is not affected until UV transmittance is decreased further. Alternatively, the rapid orbital mixing used during the experiment (200 rpm), resulting in millisecond to second UV exposure timescales, may enable contact with the UV-A signal frequently enough to induce a consistent UV-A induced carotenoid accumulation response. The applicability of the observed results on the impact of cell density on the UV response are therefore likely to be limited however, as the rapid mixing used during the experiment is unlikely to be encountered under large scale cultivation conditions (as discussed below).

The mixing timescales achieved in large-scale cultivation system used for *D. salina* cultivation (see sub-chapter 2.3.1) - i.e. unmixed open ponds (extensive mode) or mixed raceway ponds (intensive mode) – are unlikely to be achievable. Unfortunately, modelling the effect of PAR and UV on microalgae culture vessels or natural environments is complex and literature values are commonly highly situation specific (Neale et al., 2003; Béchet et al., 2013). In a turbid shallow lake (photoactive layer < 50 cm), used here as an analogue for extensive cultivation, vertical mixing times of < 5 minutes over the upper 50 cm were estimated during windy periods (Macintyre, 1993). However, this observation was made in a body of water where interactions with water layers below the photoactive layer were also shown to impact vertical mixing, something which is not the case in extensive large-scale cultivation systems. In raceway ponds the culture media is actively mixed by a paddlewheel with the linear liquid velocity determining the degree of turbulence in the linear sub-sections of the pond. In raceway ponds with low linear liquid velocity, such as the case of large-scale *Dunaliella* cultivation (velocities of 10 - 20 $cm \cdot s^{-1}$ are commonly employed; Ben-Amotz & Avron, 1989a), movement of microalgae between the surface layers and deeper layers is typically modest in the linear sub-sections of the pond with most vertical mixing occurring at the paddle wheel and in the bends (Grobbelaar, 2012; Prussi et al., 2014; Chisti, 2016). A conclusive value for vertical mixing time could not be found in the literature but is expected to be in the order of minutes rather than seconds. Under natural conditions vertical mixing times have been shown to vary from minutes to hundreds of hours depending on the body of water (Neale et al., 2003).

To ensure adequate UV exposure, large-scale UV-C water disinfection is carried out almost exclusively using submerged systems with a high density of UV-C sources, often in a confined space (Metcalf et al., 2003). This ensures homogenous UV-C distribution, in part to eliminate the reliance on adequate mixing. When an external UV source is used however (e.g. solar radiation

or UV treatment system suspended over a cultivation area), the increased attenuation caused by cell shading is thought to have a larger impact on the UV-A induced carotenoid accumulation unless adequate mixing times can be achieved. Microalgae cells are more likely to spend time in regions with low UV radiation intensity or no UV at all. Results from the previous sub-chapter showed that the UV-A induced carotenoid accumulation response was less efficient when UV-A exposure was not continuous. Chapter 6.3 will investigate the impact of shorter UV exposure duration in more detail.

5.4 Determining the effect of environmental conditions: Non-UV carotenogenesis stimuli - PAR intensity and salinity

Increased PAR irradiance and salinity are the most important stimuli involved in non-UV-A induced carotenoid accumulation in *D. salina* (Loeblich, 1982). The impact of PAR and salinity on non-UV induced β-carotene accumulation and the implications on β-carotene production cost have been extensively characterised in commercial *D. salina* cultivation (Moulton et al., 1987a). While growth conditions commonly employed during commercial *D. salina* cultivation (e.g. salinity above 3.4 M NaCl) are suboptimal for growth, they are used to induce carotenogenesis and to minimize issues with predation in the open photobioreactors (Borowitzka et al., 1984). The interaction of high PAR and high PAR + high salinity with the UV-A induced carotenogenesis response has not been reported in literature for *D. salina* (strain UTEX 1644). The experiments discussed in this sub-chapter investigate the effectiveness of UV exposure in combination with the non-UV inducing stimuli PAR intensity and salinity.

5.4.1 Experimental procedure –PAR intensity and salinity

The modified version of the experimental procedure described in Material and Methods was used. Combinations of PAR intensity and salinity that were tested are shown in Table 5-3. In summary:

PAR — 30 µmol m^{-2} s^{-1} ('Low') or 100 µmol m^{-2} s^{-1} ('High') for 24 h·d^{-1} for the duration of the experiment.

Salinity — Salinities of 11.25% (1.9 M NaCl, 'Low') or 20% (3.4 M NaCl, 'High') salinity were used. Cultures grown in 20% salinity were pre-adapted in 20% MJM culture media for several weeks prior to the experiment.

UV — Broad wavelength UV-A was used for UV-A exposure (λ = 320 – 400 nm, 8 W·m^{-2}, 24 h·d^{-1})

Cultures were acclimatized for 2 days (PAR-Only, no UV).

Increased PAR intensity was started on culture day 3.

At the start of culture day 3, UV was turned on (UV hours = 0 h) and PAR intensity increased.

At the start of culture day 7, UV was turned off (UV hours = 96 h)

Table 5-3 Increased PAR and increased PAR+salinity exposure regimes tested. PAR and salinity were applied to both PAR-Only and PAR+UV cultures.

	PAR PFD ($\mu mol\ m^{-2}\ s^{-1}$)	Salinity (%)
'Low' PAR + 'Low' salinity	30	11.25%
'High' PAR	100	11.25%
'High' PAR + 'High' salinity	100	20%

5.4.2 Results – Increased PAR and salinity

Carotenoid accumulation was increased during UV-A exposure with concomitant high PAR and high PAR + high salinity over the control (low PAR + low salinity + UV) (Figure 5-14).

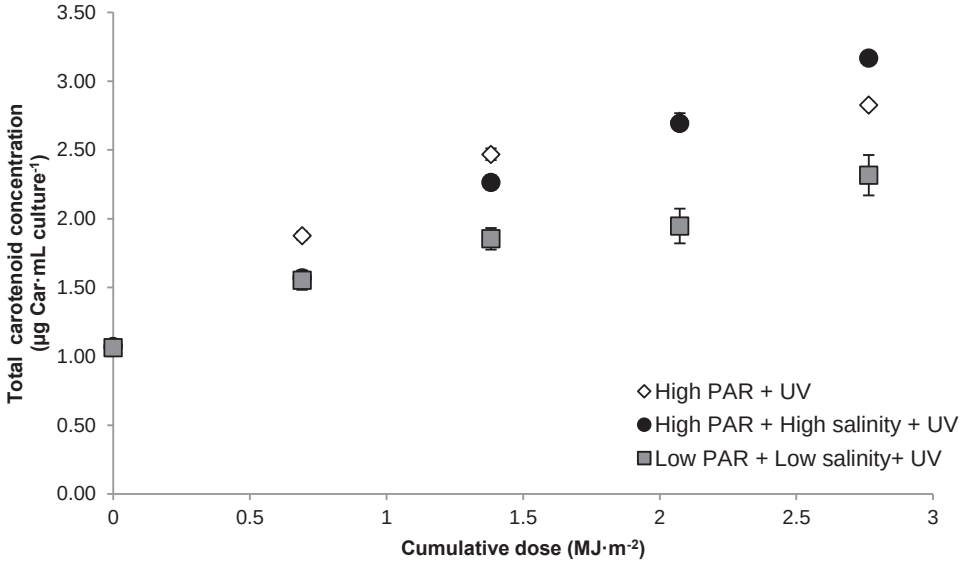

Figure 5-14 UV-A induced carotenoid accumulation during UV-A exposure with and without non-UV carotenogenesis stimuli high PAR and high PAR + high salinity. Where larger than icons, error bars represent standard error (n = 4 for High PAR experiments, n = 8 for Low PAR)

Furthermore, UV-A exposure concomitant with high PAR and high PAR + high salinity improved UV dose efficiency [$\Delta(\mu g\ carotenoids \cdot mL\ culture^{-1}) \cdot \Delta(MJ \cdot m^{-2})^{-1}$] (Figure 5-15). Concomitant exposure with high PAR doubled the dose efficiency and followed the same decrease trend over time, while high PAR + high salinity yielded increased but consistent UV dose efficiency.

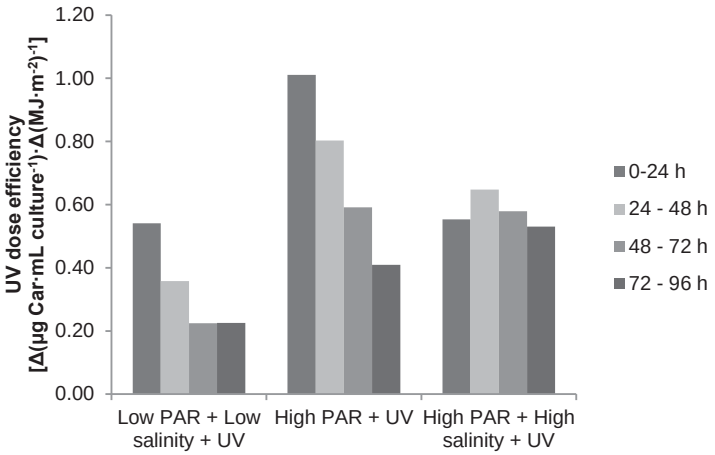

Figure 5-15 *Dose efficiency of UV-A induced carotenoid accumulation during UV-A exposure with and without non-UV carotenogenesis stimuli high PAR and high PAR + high salinity. Series represents dose efficiency per UV-A irradiance between successive data points (separated by 24 h UV exposure) in Figure 5-14.*

The UV dose efficiency for high PAR + low salinity (i.e. 'High PAR+UV' in Figure 5-15) and high PAR + high salinity differs from UV dose efficiencies recorded thus far. The high PAR + low salinity cultures have a UV dose efficiency which is consistently doubled over the low PAR + low salinity control. The high PAR + high salinity has levels increased over the low PAR + salinity control and that consistently remain high. It is thought that the impact of non-UV carotenogenic stimuli have an impact on UV dose efficiency as both stimuli lead to increased carotenoid accumulation without UV exposure (see Figure 5-17). Unfortunately, the signalling and metabolic pathways involved in non-UV carotenogenesis stimuli are poorly understood (Lamers et al., 2008), which makes it difficult to comment on their interaction with UV-A induced carotenoid accumulation.

Contrary to findings in chapter 4 and 5.1, cell proliferation was improved by UV-A exposure in combination with high PAR (Figure 5-16). High PAR + high salinity had a negative impact on cell proliferation. High salinity cultures showed lower cell proliferation during the acclimation period of cultures to low PAR + high salinity (i.e. prior to high PAR/UV-A exposure) being lower than the low PAR + low salinity control (data not shown). High salinity cell proliferation remained slowed compared to low PAR + low salinity cultures, regardless of whether cultures were UV-A exposed (Figure 5-16).

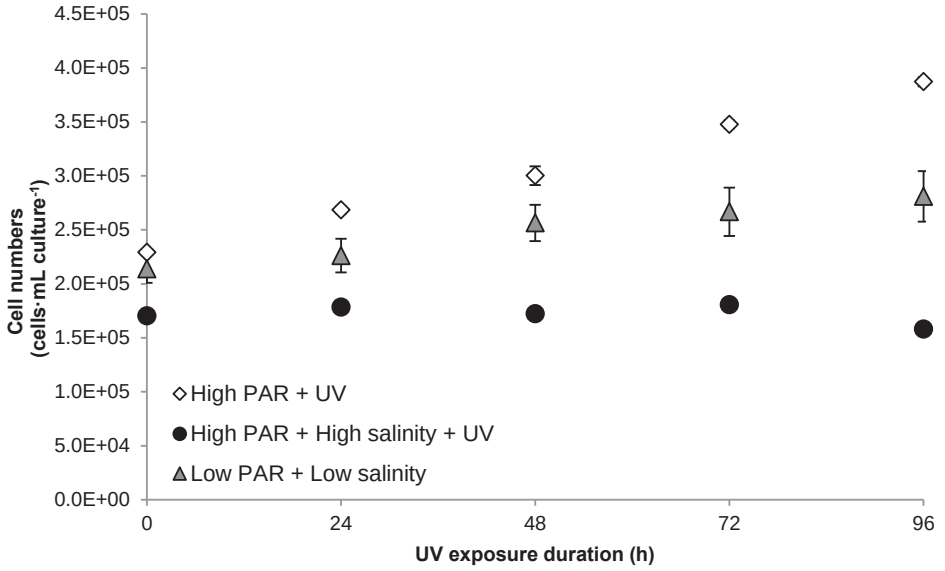

Figure 5-16 Cell proliferation during UV-A exposure with and without non-UV carotenogenesis stimuli high PAR and high PAR + high salinity. 'Low PAR + Low Salinity' represents the PAR-Only control (n = 48). *Where larger than icons, error bars represent standard error (n = 4 for High PAR experiments)*

Most other authors investigating UV-A carotenogenesis response in *D. bardawil* have reported a sustained or increased cell growth rate (Jahnke, 1999; Salguero et al., 2005; Mogedas et al., 2009). During these studies higher PAR intensities than those employed here were used (140-1500 $\mu mol \cdot m^{-2} \cdot s^{-1}$). In the current experiments, increasing PAR intensity from 30 $\mu mol \cdot m^{-2} \cdot s^{-1}$ to 100 $\mu mol \cdot m^{-2} \cdot s^{-1}$ (in the absence of UV) lead to increased cell proliferation (data not shown), indicating a positive impact of increased PAR intensity compared to those used in other experiments in the PhD thesis (30 $\mu mol \cdot m^{-2} \cdot s^{-1}$). This positive impact of high PAR may aid *D. salina* in sustaining cell proliferation during UV-A exposure. The cultivation of *D. salina* in high salinity media appears to have the opposite effect, where cell proliferation is drastically slowed or halted. Increasing PAR intensity does not improve cell proliferation in high salinity cultures (data not shown).

The UV-A induced carotenoid accumulation was improved by a UV-A exposure concomitant with high PAR intensity and high PAR + high salinity (Figure 5-17). A maximum improvement of 51% over low PAR intensity and low salinity conditions was observed.

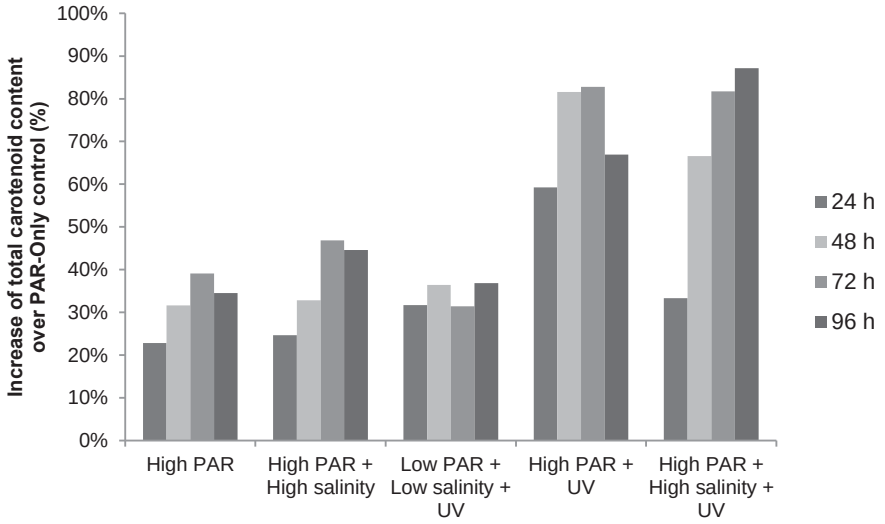

Figure 5-17 Time course of total carotenoid concentration over the 'Low PAR+Low salinity' PAR-Only control (%) during UV-A exposure with and without non-UV carotenogenesis stimuli high PAR and high PAR + high salinity. Values represent total carotenoid increase in hours after experiment was started (h, see legend) over cultures exposed to PAR only, no UV (%).

High PAR intensity and salinity were shown to be as effective, at inducing carotenoid accumulation than UV-A exposure under low PAR intensity and salinity conditions (Figure 5-17). Combined exposure to high PAR+UV and high PAR+high salinity+UV at 8 $W \cdot m^{-2}$ during the current experiment, led to carotenoid increases similar to those observed during long wavelength UV-A exposure at 24 $W \cdot m^{-2}$ and 30 $W \cdot m^{-2}$ under low PAR intensity and low salinity conditions (Figure 5-5). Along with UV-A exposed cultures, all non-UV carotenogenesis stimuli tested, induced carotenogenesis in the absence of UV-A (Figure 5-17, 'High PAR' and 'High PAR + High salinity'). These results indicate that the carotenoid accumulation by high PAR and high PAR + high salinity is additive to the UV-A induced carotenoid accumulation.

From an industrial perspective, concomitant exposure with non-UV carotenogenic stimuli improves the magnitude of the UV-A induced carotenoid accumulation, potentially leading to an additive effect. UV dose efficiency is doubled when combined with high PAR and increased consistently when high salinity is included leading to a lower UV irradiance being required to achieve similar results as higher UV irradiances. Cultures in large-scale *D. salina* cultivation will be exposed to varying degrees of both non-UV carotenogenic stimuli. The PAR intensity used during the current experiment is significantly lower than outdoor conditions which means it is unclear

how the relative improvement caused by UV-A exposure would scale with levels of PAR and salinity experienced under outdoor cultivation conditions. At higher PAR intensities (420-1500 $\mu mol \cdot m^{-2} \cdot s^{-1}$), UV-A exposure in *D. bardawil* was found to improve UV-A induced carotenoid accumulation proportional to the PAR intensity used (Jahnke, 1999). 'High' salinity levels used during the above experiments are expected to be at or even below levels expected during large-scale cultivation. It is therefore important to investigate more closely the benefits of targeted UV-A treatment under conditions of high PAR and salinity. Furthermore, due to the non-UV carotenogenic capacity of PAR and salinity, future research should investigate PAR and salinity levels at which UV supplementation may be most beneficial – e.g. UV-A supplementation during high PAR may have a relatively small impact whereas the impact may comparatively much higher with UV-A supplementation during low PAR.

5.5 Conclusions

The current PhD research has shown that UV treatment can be used to reliably induce bioproduct accumulation in *D. salina*. The goal of the current chapter was two-fold: expanding on these observations by investigating how the *D. salina* UV-A induced carotenoid accumulation response can be manipulated to maximize total carotenoid concentration (µg Car·mL culture^{-1}) and to generate an understanding of how this may impact the capital and operational expense of a large-scale UV treatment system. It has been shown that UV treatments specific in UV waveband, UV irradiance and UV exposure duration have differential impact on the magnitude of the UV induced carotenogenesis response. Furthermore, the importance of UV transmission and the impact of non-UV carotenogenic stimuli has been illustrated. The following items are the key findings from chapter 5:

1. The magnitude of the *D. salina* UV induced carotenogenesis is highest during exposure with the highest UV-A irradiance tested (30 W·m^{-2}) during continuous UV exposure (24 h·d^{-1}) (as opposed to semi-continuous exposure, 6 or 12 h·d^{-1}).
2. For all except one tested treatment, initial UV dose efficiency is the highest for all UV exposure regimes and decreases as a function of exposure duration. Depending on the irradiance used, the UV carotenoid accumulation response induced within 6 hours and is largely complete in 96 hours (24 h·d^{-1} UV exposure).
3. When UV-A exposure is stopped, carotenoid accumulation ceases and cell proliferation is increased. No long-lasting UV response leading to improved total carotenoid concentrations was found in *D. salina*.
4. The magnitude UV-A induced carotenoid accumulation response is positively influenced by the inclusion of non-UV carotenogenic stimuli (high PAR and high salinity). The UV dose efficiency is significantly improved by non-UV carotenogenic stimuli exposure (high PAR intensity and salinity) leading to a lower UV irradiance being required to achieve similar results as higher UV irradiances.
5. While UV transmission was rapidly decreased by increasing cell density, no impact on the UV-A induced carotenoid accumulation response could be observed under current experimental conditions.

The understanding generated in chapters 4 and 5 will be used to test novel UV treatment regimes, developed specifically for large-scale *D. salina* cultivation (Treat-and-release and Intermittent exposure). The UV treatment regimes will be designed aimed at reducing UV treatment system capital and operational expense.

6 Rational design of a targeted UV treatment system – technical and economic feasibility

As stated in the thesis introduction, the first part of this thesis investigated if UV treatment could be used to reliably induce and control specific UV responses in microalgae. Using *D. salina* as a model strain, Chapters 4 and 5 provide evidence that UV-A treatment can indeed reliably induce carotenoid accumulation in this species, and that the response depends on the UV-A waveband, irradiance ($W \cdot m^{-2}$), UV exposure duration, and UV dose ($MJ \cdot m^{-2}$). UV-A exposure was associated with slowed or stopped cell proliferation as well as increasing *D. salina* cell size (up to 15%) and altered intracellular structural organization. Carotenoid accumulation ceased and cell proliferation increased when UV-A exposure was stopped, leading to a subsequent resumption of cell proliferation. UV-A induced carotenoid accumulation was improved during UV-A exposure concomitant with non-UV carotenogenic stimuli (high PAR intensity and salinity) compared to UV-A exposure alone.

To our knowledge the exploration of the fundamental UV photobiology in microalgae required to develop UV treatment regimes from discrete UV wavebands, complemented with a commercial microalgal-engineering insight, to produce UV treatment regimes and UV treatment technology for application during large-scale microalgae cultivation, has never been attempted. Based on the findings reported in the PhD thesis thus far, and looking broadly across microalgae biotechnology applications, the current work will continue by exploring feasibility of developing UV treatment recipes and UV treatment technology for large scale microalgae cultivation processes. The feasibility assessment will culminate in a techno-economic analysis (TEA) model. With this objective, the first sub-chapter provides an overview of a typical microalgal biotechnology process and identifies potential placement of a UV treatment system along the cultivation process. Based on understanding of the *D. salina* UV photobiology and the placement options, the two subsequent sub-chapters describe two novel UV treatment regimes developed specifically for large-scale *D. salina* cultivation, aimed at reducing bioproduct production cost. The final sub-chapter describes the development of a TEA model to provide BioLumic with indications on the industrial and economic feasibility of UV treatment technology during commercial *D. salina* cultivation.

In the literature review, the two most well-published large-scale *Dunaliella* cultivation systems were discussed (please refer to sub-section 2.3.1 – *Dunaliella* biotechnology). The extensive cultivation operated by Cognis at Hutt Lagoon, Western Australia (as described by Borowitzka) and the intensive cultivation operated by NBT Ltd. at Eilat, Isreal (as described by Ben-Amotz) are used as reference systems throughout the chapter due to the large amount of available literature. Both cultivation systems have been shown to be economically viable and are operational at the

time of writing. However, while design and operating considerations of these systems are described in detail in the literature, the commercial nature of the operation means few details are provided on exactly how these commercial cultivation processes are operated and the costs involved. Therefore, in the absence of relevant knowledge and data, the work has developed TEA model cultivation systems, both extensive and intensive, based on available literature (discussed in more detail in sub-chapter 6.4). Due to unavoidable loss of applicability to real world cultivation processes when modelling from limited literature values, emphasis will be given to discussing results more broadly and qualitatively, and less emphasis will be given to the costing of the production system in order to focus instead on the added value of the UV treatment regime and technology. The same holds true for the applicability of the experimental data presented in Chapters 4 and 5. While the findings are instrumental in furthering our understanding of the fundamental *D. salina* UV photobiology, the applicability of the data to large scale cultivation systems is limited.

A TEA combines elements of a standard economic benefit–cost analysis with an engineering analysis by integrating scientific and economical information. TEA's are commonly employed to assess the viability of a new technology and are thus inherently high-level assessments due to a lack of knowledge and input data. Due to the nature of the data available to construct the TEA model, the scope of the TEA is such that it allows assessment of the most critical areas for improving profitability of large-scale UV treatment technology. The TEA does not aim to provide BioLumic with accurate economical outputs for revenue and profit as for example a business-study would but rather provides a tool to be able to make recommendations to BioLumic on whether further research and development is warranted.

6.1 Potential locations suitable for UV treatment during commercial algae cultivation

The PhD thesis has until this point focussed primarily on the exploration of the fundamental UV photobiology. It has thus far not considered the implications of this understanding on the design of a UV treatment system in depth. The findings in the PhD thesis have shown that UV treatment impacts various cultivation parameters, such as cell proliferation, which impact where in the large-scale cultivation process steps UV treatment is best applied. Therefore, prior to developing UV treatment regimes specifically for large scale *Dunaliella* cultivation, this sub-chapter provides an overview of the typical process steps (and parameters) involved in both extensive and intensive large-scale *Dunaliella* cultivation. The suitability of placement of the UV treatment system is assessed by the impact of UV treatment on each process step as well as the impact on the design of the UV treatment system (e.g. size). The impact of the UV treatment system placement is determined based on the findings in Chapters 4 and 5 complemented with a commercial microalgal-engineering insight; please consult reviews from other authors for exhaustive discussion on engineering principles (e.g. Richmond, 2004). The novel UV treatment regimes designed specifically for large-scale *Dunaliella* cultivation discussed in sub-chapters 6.2 and 6.3 are introduced based on the considerations discussed below.

As illustrated in Figure 6-1, commercial algae cultivation typically involves the following steps:

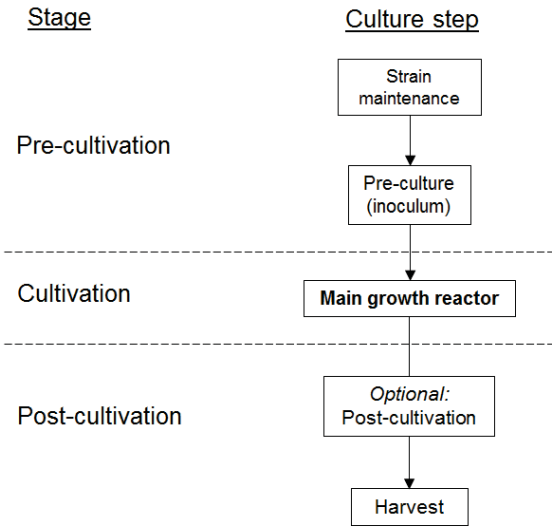

Figure 6-1 Schematic representation of the commercial microalgae cultivation process.

1. The maintenance of the strain(s) used as 'seed' at small scale, typically under well-controlled (e.g. aseptic) laboratory conditions.

2. A pre-cultivation stage aiming to generate enough seed culture for inoculating the main cultivation stage.
3. A cultivation stage where biomass is grown in large reactors (e.g. open ponds or raceway ponds). This process stage typically makes up the largest part of the large-scale cultivation system.
4. Optional (not shown in schematic): A stage after cultivation specifically designed for the induction of certain biomass properties (e.g. N-starvation and salinity to induce astaxanthin accumulation in *H.pluvialis*; Cysewski & Todd Lorenz, 2004).
5. Biomass harvesting and, depending on the application, processing (e.g. drying, extraction etc).

Based on this schematic overview, Table 6.1 discusses the feasibility of applying UV treatment prior to the cultivation stage (henceforth referred to as "pre-cultivation stage"); during the cultivation stage ("cultivation stage"); and after the cultivation stage ("post-cultivation stage"). In addition, the feasibility of applying UV during fluid transfer between any of these stages is also discussed ("transfer"). In the table and the summary below, the term 'long-lasting response' is introduced which refers to the direct or indirect effects of UV treatment, the results of which improve total carotenoid concentration (µg Car·mL culture^{-1}) at harvest.

Summarizing the potential for placement of a UV treatment system from Table 6-1:

Pre-cultivation stage: Compared to the cultivation and post-cultivation stages, only a relatively small culture area has to be treated with UV during pre-cultivation. While this reduces capital and operational expenses, the response must be long-lasting after the UV treatment has stopped (days - weeks). Furthermore, UV treatment is likely to slow cell proliferation and interfere with PAR supply through shading (i.e. UV treatment system suspended over cultivation area). There is currently no knowledge on whether a beneficial long-lasting response with regards to carotenoid accumulation can be achieved in *D. salina*. Therefore, experiments with a 'Treat-and-release' targeted UV treatment regime were conducted and are presented in sub-chapter 6.2.

Cultivation stage: The cultivation stage has the largest surface area to be irradiated. During the cultivation stage, the UV response does not necessarily need to be long-lasting (if cells are immediately harvested after cultivation) and large volumes of algae can be UV treated at once. The large UV treatment area potentially entails large capital and operational expenses. Furthermore, UV treatment is likely to slow cell proliferation and interfere with

PAR supply. To reduce potential costs and (PAR) interferences through shading (i.e. UV treatment system suspended over cultivation area), it may be preferable to reduce the daily exposure duration (reducing operational expense) or the cultivation reactor area covered by the UV treatment system (reducing capital expense and interference). Partial coverage of the reactor means microalgae cells would cycle between areas artificially exposed to UV and areas exposed only to 'normal' light[16]. As there is currently no knowledge on the impact of such a UV treatment regime, experiments with an 'Intermittent-exposure' targeted UV treatment were conducted and are presented in sub-chapter 6.3

Post-cultivation stage

A post-cultivation approach for non-UV carotenoid induction in *D. salina* cultivation has been suggested by other authors in the past (Ben-Amotz, 1995) but is currently not employed at large-scale. A UV treatment system post-cultivation stage has a number of potential advantages over other scenarios as that is no need for a long-lasting response. Furthermore, the process would be rather similar to UV treatment during cultivation with two critical differences: 1) the irradiated area may be an order of magnitude smaller than the cultivation stage (i.e. HRT of days post versus weeks during the cultivation stage); and 2) as biomass productivity is not a priority, interference of UV treatment with cell proliferation or PAR supply through shading (i.e. UV treatment system suspended over cultivation area)plays a smaller role in the UV treatment design.

Fluid transfer

UV treatment during fluid transfer could be applied anywhere in the process and technologies to apply inline UV treatment are well established (e.g. UV water steriliz. However, the rapid application of a significant UV dose into a high cell density microalgae solution has not been engineered to our knowledge, and may be challenging due to the optical properties (i.e. limited UV transmission) and short contact time typically involved. A long-lasting UV response is needed unless transfer UV treatment occurs immediately prior to biomass harvest.

[16] Depending on the light source this may include solar radiation or artificial PAR light, with or without UV radiation.

Table 6-1 Suitability of proposed locations for UV treatment during commercial algae culture.

Stage	Features	Potential and constraints for UV treatment
Pre-cultivation	The algae are photosynthetically pre-cultivated (using PAR) in relatively small reactors (e.g. illuminated area 0.1 – 100 m^2) compared to cultivation stage (see below). The algae are typically pre-cultivated for a significant period of time (days to weeks) to achieve high cell density seed cultures.	**Potential** - UV treatment can be used to promote growth properties during the cultivation stage - Small UV treatment size required to cover reactor surface area (m^2) relative to the cultivation reactor; meaning potentially low capital expenses. - Continuous UV treatment (i.e. 24 $h \cdot d^{-1}$) is possible over numerous days/weeks. **Constraints** - The UV response induced during pre-cultivation must induce a long last effect during cultivation (i.e. the response must last in the orders of days after UV treatment has been applied) - UV treatment decreases cell proliferation - UV treatment system may interfere with PAR supply by shading - Increased settleability may complicate transferring cells to next stage (if the reactor is not mixed)
Cultivation	The algae are photosynthetically cultivated (using PAR) in large reactors (e.g. illuminated area 1000 - 2.5 $\cdot 10^6$ m^2) The algae are typically cultivated for a significant period of time (weeks-months). The hydraulic	**Potential** - Large culture volumes can be treated immediately prior to harvest, meaning that a long-lasting effect is not mandatory - UV treatment can be used to complement or replace the conventional stressors inducing carotenoid accumulation.

	retention time (HRT) is commonly in the order of days-weeks. In the case of *D. salina*, stressors are introduced to induce carotenoid accumulation (salinity above 3.4 M NaCl, 20% w/v and solar PAR irradiation levels, Moulton, et al., 1987)	- Continuous UV treatment (i.e. 24 $h \cdot d^{-1}$) is possible over numerous days/weeks. **Constraints** - Entails large capital investment, especially if a large reactor area must be irradiated (see sub-section 6.3). - UV treatment decreases cell proliferation - UV treatment system may interfere with PAR supply by shading - Increased settleability may complicate transferring cells to next stage (if reactor is not mixed)
Post-cultivation	This stage is typically performed in reactors optimized for bioproduct induction (which may differ from the cultivation stage reactor design). Operation typically involves the application of a stressor to induce a specific response, leading to sub-optimal growth conditions. The HRT prior to harvest is typically in the order of days (depending on the rate of bioproduct induction).	**Potential** - A dedicated post-cultivation UV treatment reactor could be optimized solely for bioproduct induction by UV treatment system, without consideration of optimal biomass growth. - Culture volumes can be treated immediately prior harvesting, meaning that a long-lasting effect is not mandatory - Continuous UV treatment (i.e. 24 $h \cdot d^{-1}$) is possible, albeit not mandatory. - UV treatment can be used to complement or replace the conventional stressors inducing carotenoid accumulation. - Increased settleability may improve harvesting efficiency **Constraints** - The required UV exposure duration (i.e. $h \cdot d^{-1}$) determines size of the UV system as well pond infrastructure. - UV treatment system may interfere with PAR supply by shading

Fluid transfer	Short residence time relative to reactors (minutes to hours) High surface:volume ratio (assuming pipes)	**Potential** - Inline UV treatment systems are established technology - Simple to install into existing process either during transfer between reactors or as a circulation system installed in the other cultivation stages - UV treatment could be used to induce UV response during transfer between cultivation. - No interference with PAR delivery **Constraints** - Short UV contact time (i.e. 24 $h \cdot d^{-1}$ contact time is not realistic), meaning high UV irradiance is required to achieve the desired dose. - Requires the induction of long-lasting UV response effects (i.e. days) unless placed directly after (post-)cultivation stage (prior to harvest).

6.2 UV-A treatment: Pre-cultivation stage 'Treat-and-Release'

BioLumic's first commercial product is a UV seedling treatment system, where a moving UV LED array exposes young plant seedlings to proprietary treatments of UV light. Such seedlings are typically transplant crops, where after a period of days or weeks in a nursery or glasshouse, seedlings are transplanted into the field for onward growth to harvest. A similar principle was considered for large-scale *D. salina* cultivation. In an analogy, UV treatment during the pre-cultivation stage (i.e. the nursery) may lead to lasting benefits in the cultivation stage (i.e. the field) and ultimately at harvest. As identified in sub-chapter 6.1, applying a UV treatment system during the pre-cultivation stage of large-scale microalgae cultivation requires a long-lasting UV response for the beneficial impact to be noticed at harvest (days – weeks).

The current work has shown that the UV-A induced carotenoid accumulation response in *D. salina* was reversed within 24-48 hours after UV-A exposure is stopped (chapter 5.2.1). It is therefore deemed unlikely that carotenoid accumulation induced through UV-A exposure, generated during the pre-cultivation stage, can be feasibly be carried all the way to harvest (with HRTs often longer than 83 h). However, this sub-chapter investigates a targeted UV treatment regime to attempt to stimulate a long-lasting response aimed at reducing bioproduct production cost. β-carotene accumulation offers protection against photodamage at high PAR intensity (> 1000 $\mu mol \cdot m^{-2} \cdot s^{-1}$) in *Dunaliella* species (Loeblich, 1982; Ben-Amotz et al., 1989c). Hypothetically, UV-A induced carotenoids could provide similar protection against photodamage during cell cultivation at high PAR intensity. Once UV-A exposure is stopped, the UV-A induced carotenoids could therefore potentially be maintained to aid in photoprotection at high PAR. The increased photoprotection is hypothesised to lead to increased growth rate during the cultivation stage. UV-A induced carotenoid accumulation may thus lead to a lasting improvement in biomass yields.

The process of pre-treatment (i.e. a UV-A carotenoid induction phase) and release into the cultivation stage (i.e. no more UV-A exposure) will henceforth be referred to as 'Treat-and-release'. The experiment focusses on two key indicators; cellular carotenoid content ($\mu g\ Car \cdot 10^6\ cells^{-1}$) as an indicator of accumulated photoprotection (Ben-Amotz et al., 1987) and cellular chlorophyll *(a+b)* content ($\mu g\ Chl \cdot 10^6\ cells^{-1}$) as an indicator of photodamage. Unfortunately, no analytical techniques to measures of photodamage directly (e.g. PAM fluorescence, photosynthetic O_2-evolution) were available for this experiment. Therefore, for lack of a better option the cellular chlorophyll *(a+b)* content ($\mu g\ Chl \cdot 10^6\ cells^{-1}$) will be used as an indicator of photodamage. Hence, for the purposes of this experiment, changes in chlorophyll *(a+b)* content

are assumed to result from direct photodamage. Moreover, a decrease is likely to be observed resulting from the cellular process of decreasing light harvesting antenna size to protect the cell against further photodamage (Smith et al., 1990).

6.2.1 Experimental procedure

The experimental procedure used is described in the Material and Methods sub-section. In summary:

PAR 30 or 1000 µmol m^{-2} s^{-1} for 24 h·d^{-1} for the duration of the experiment. The PAR exposure regimes are shown in Table 6-2.

UV Long waveband UV-A was used for UV-A exposure (λ = 360 – 400 nm at 30 W·m^{-2}, 24 h·d^{-1})

Cultures were acclimatized for 2 days (PAR-Only, no UV).

At the start of culture day 3, UV was turned on (UV exposure = 0 h)

At the start of culture day 7, UV was turned off (UV exposure = 96 h)

Cultures were exposed to 1000 µmol m^{-2} s^{-1} PAR from culture day 7-14

Table 6-2 UV treatment regime during 'Treat-and-release' experiments. Experiment was split into three phases: Acclimation (day 0-3), Treatment (day 3-7) and high PAR exposure (day 7-14)

	Experiment phase		
Treatment	Day 0-3 Acclimation (µmol·m^{-2}·s^{-1})	Day 3-7 UV Treatment (µmol·m^{-2}·s^{-1})	Day 7-14 High PAR Only (µmol·m^{-2}·s^{-1})
Low PAR only (Control)	PAR: 30	PAR: 30	PAR: 30
Low to high PAR (Control)	PAR: 30	PAR: 30 (no UV-A exposure)	PAR LED: 1000
Low PAR + UV to high PAR	PAR: 30	PAR: 30 + UV-A: 30 W·m^{-2}	PAR LED: 1000

In summary, the experiment was carried out as follows: After acclimation, the 'Low PAR + UV' cultures were UV exposed for 96 h (culture day 3 to 7) to induce carotenoid accumulation. After UV exposure was stopped, cultures were exposed to high PAR intensity (1000 µmol·m^{-2}·s^{-1}) from culture day 7 to 14 to determine whether the induced carotenoids provide protection against high light. Two controls were included: 'Low PAR only' which was not exposed to UV or high PAR

and 'Low to high PAR' which was not exposed to UV but was exposed to high PAR from culture day 7.

6.2.2 Results - UV pre-treatment during pre-cultivation

Pre-treatment with UV-A led to UV-A induced carotenoid accumulation after 96 h UV exposure (Low PAR + UV to high PAR, black squares, Figure 6-2). Upon stopping UV exposure, subsequent exposure to high PAR lead to sustained or slightly improved cellular carotenoid content (black squares, culture day 7 to 14). High PAR exposure alone was found to induce cellular carotenoid accumulation as a form of photoprotection (Low to high PAR, grey diamonds Figure 6-2).

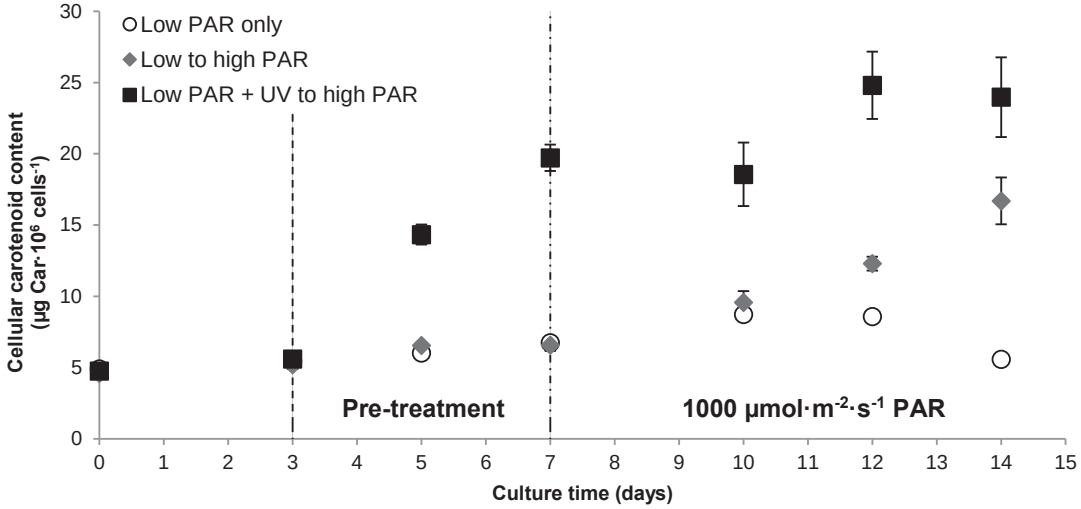

Figure 6-2 Time course of cellular carotenoid accumulation during low PAR, low to high PAR and low PAR + UV to high PAR exposure regimes. Where larger than the icons, error bars represent standard error (n = 4).

As shown in Table 6-3, total carotenoid concentrations (µg Car·mL culture^{-1}) improved equally as a result of UV pre-treatment (black squares, culture day 7, Figure 6-2) and 'Low to high PAR' exposure (grey diamonds, culture day 14, Figure 6-2). Furthermore, UV-A exposure led to faster carotenoid accumulation than high PAR exposure alone (total carotenoid conc. of ≈3.80 µg Car·mL culture^{-1} achieved in 4 days by UV-A exposure and in 7 days by high PAR exposure alone). Ultimately, UV pre-treatment did not improve the total carotenoid concentration at the end of the experiment as can be seen from culture day 14 values (right column, Table 6-3).

Table 6-3 Total carotenoid content of PAR-Only and UV pre-treated cultures exposed to 1000 µmol·m^{-2}·s^{-1}PAR exposure after 14 culture days (n=4).

	Total carotenoid concentration (µg Car·mL culture^{-1})		
	Pre UV exposure (culture day 3)	Post UV exposure (culture day 7)	Post high PAR exposure (culture day 14)
Low PAR only	1.24 ± 0.04	2.00 ± 0.03	2.46 ± 0.03
Low to high PAR	1.21 ± 0.00	1.94 ± 0.01	3.81 ± 0.24
Low PAR + UV to high PAR	1.22 ± 0.02	3.74 ± 0.09	3.42 ± 0.30

It was thought unlikely that increased cellular carotenoid content resulting from UV-A treatment prior to high PAR exposure aided in photoprotection. This was inferred from decreases in cellular chlorophyll (*a+b*) content (µg Chl·10^6 cells^{-1}) in both the UV-A exposed and PAR-Only cultures exposed to high PAR (Figure 6-3). This suggested that a long-lasting photoprotective effect of UV-A induced carotenoids was not achieved under these experimental conditions.

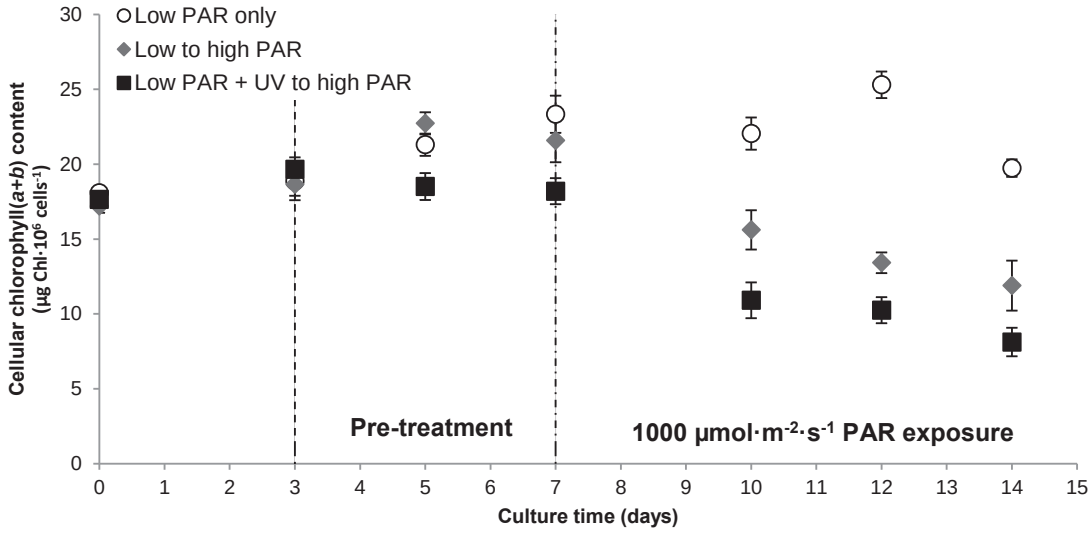

Figure 6-3 Time course of cellular chlorophyll (a+b) *content during low PAR, low to high PAR and low PAR + UV to high PAR exposure regimes. Where larger than the icons, error bars represent standard error (n = 4).*

Experiments in Ch. 5.2.1 indicated a potential for increased growth rate after a period of UV-A exposure (i.e. after UV exposure is stopped). An increase in growth rate after UV-A exposure is stopped was not observed under current experimental conditions. Contrary to previous observations, cell numbers continue to decrease after UV-A treatment is stopped (Figure 6-4). In 'Low to high PAR' no significant decreases resulting from high PAR exposure were observed, suggesting interference with cell proliferation by high PAR (1000 µmol·m^{-2}·s^{-1}) exposure may not be severe.

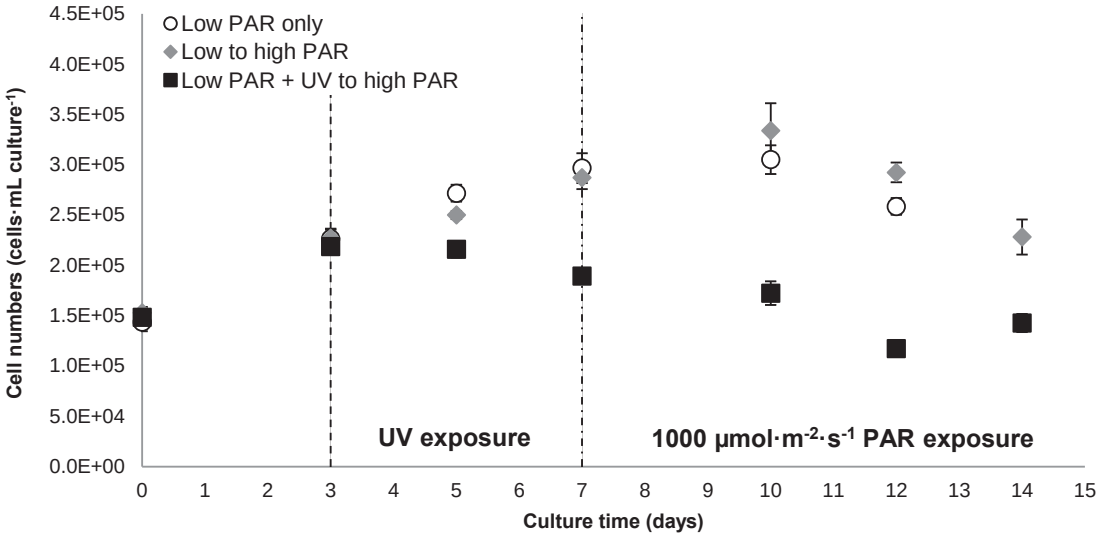

Figure 6-4 Time course of cell proliferation during low PAR, low to high PAR and low PAR + UV to high PAR exposure regimes. Where larger than the icons, error bars represent standard error (n = 4).

The notion that UV-A induced carotenoid accumulation may lead to increased photoprotection is based on the assumption that the carotenoids induced during UV-A are the same as those induced during high PAR exposure. However, because the pigment analysis 'lumps' all carotenoids it is not possible to distinguish between the specific carotenoids accumulated in response to UV-A or high PAR exposure – i.e. the carotenoids from each exposure type may offer different kinds of protection. It therefore remains unclear whether the UV-A induced carotenoids can indeed offer photoprotection to PAR. Furthermore, as discussed, the occurrence of photodamage has not been confirmed as cellular chlorophyll *(a+b)* content alone is not an adequate measure. It therefore also remains unclear whether the cells exposed to high PAR experience photodamage. The data in Figure 6-4 suggest the impact of photodamage is likely small.

The main aim of this experiment was to investigate whether a long-lasting UV-A response could be induced through photoprotection resulting from accumulated carotenoids and increased

growth after stopping UV-A exposure based on observations from previous experiments. While cellular carotenoid levels were increased due to UV-A exposure prior to high PAR exposure, there appeared to be no additional protection against high PAR photodamage based on the cellular chlorophyll *(a+b)* content (Figure 6-3). Secondly, no increase in cell growth rate was observed after stopping UV-A exposure (Figure 6-4). The current 'Treat-and-Release' UV regime therefore did not lead to any long-lasting response, with no improvement in total carotenoid concentration at the end of the experiment. From an industrial perspective, two interesting observations were made however. Cellular carotenoid concentration was shown to be maintained after UV-A exposure was stopped by high PAR exposure (Figure 6-2). Additionally, exposure to UV-A = 30 $W \cdot m^{-2}$ led to a more rapid total carotenoid concentration increase than PAR = 1000 $\mu mol \cdot m^{-2} \cdot s^{-1}$ (Table 6-3).

6.3 UV-A treatment: Cultivation stage 'Intermittent exposure'

The cultivation stage covers the largest surface area of the large scale *D. salina* cultivation process. Covering the cultivation stage with a UV treatment system would thus be most costly during this stage of the large-scale cultivation process. To reduce potential capital and operational expense and PAR supply interferences through shading (i.e. UV treatment system suspended over cultivation area), it may be preferable to reduce the daily UV exposure duration (reducing operational expense) or to cover the cultivation reactor area only partially with a UV treatment system (reducing capital expense and PAR interference). Reducing the daily exposure duration by semi-continuous UV exposure (6 and 12 $h \cdot d^{-1}$) showed a decrease in total carotenoid concentration (µg Car·mL culture^{-1}) compared to continuous exposure (see sub-chapter 5.2).

Partial coverage of the reactor means microalgae cells would cycle between regions with and without artificial UV exposure. The current sub-chapter investigates if shorter exposure cycles (i.e. shorter than semi-continuous exposure), but more rapidly applied, can achieve similar benefits to continuous exposure during full coverage. It does so by simulating this regime through timed UV exposure rather than actually covering the experimental setup (see below). Furthermore, the timescales in the experiment over which microalgae cells are UV exposed and non-UV exposed are similar to mixing timescales expected during extensive and intensive cultivation - i.e. time spent UV exposed in the top layer of the cultivation vessel and non-UV exposed in the deeper parts of the cultivation vessel. From a photobiological standpoint the results may also aid in generating an understanding on the impact of mixing timescales on the UV-A induced carotenogenesis response. Due to the nature of the experimental set-up, interpretations about mixing times will be made with great caution however.

6.3.1 Experimental procedure

The experimental procedure used is described in Material and Methods sub-section. In summary

PAR 30 µmol m^{-2} s^{-1} for 24 $h \cdot d^{-1}$ for the duration of the experiment

UV Long waveband UV-A was used for UV-A exposure (λ = 360 – 400 nm at 30 $W \cdot m^{-2}$) during intermittent exposure (see UV regime below).
Cultures were acclimatized for 2 days (PAR-Only, no UV).
At the start of culture day 3, UV was turned on (UV exposure = 0 h)
At the start of culture day 7, UV was turned off (UV exposure = 96 h)

To ensure microalgae are regularly exposed to UV during partial coverage the microalgae must be circulated so the UV treatment system is encountered regularly. Therefore, the current experiments assume the case-study of a raceway pond reactor type[17]. Treatment frequency was based on simulation of a full-scale system in raceway ponds where:

1. Illuminated area = 880 m^2 (182m x 5m, length x width)
2. Mixing velocity = 0.2 $m \cdot s^{-2}$
3. Circulation time = 30 $min \cdot circulation^{-1}$

Two treatment frequencies were chosen as illustrated in Figure 6-5.

5 min UV per 30 min circulation

('UV 5 min On – 25 min Off')

15 min UV per 30 min circulation

('UV 15 min On – 15 min Off')

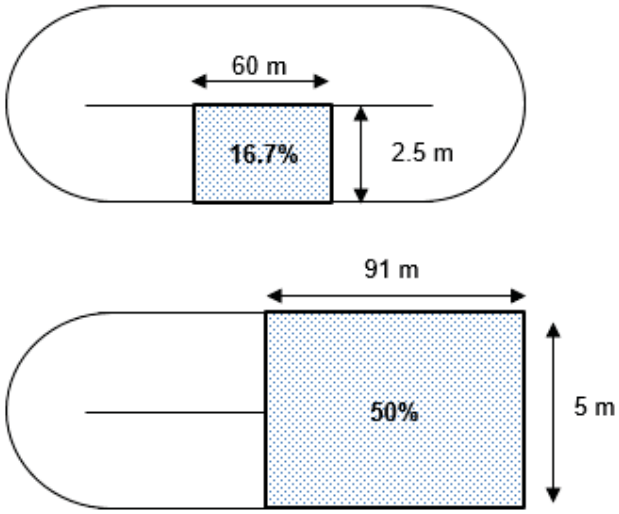

Figure 6-5 Schematic representation of open raceway pond partially covered with UV treatment system. The grey areas represent a UV treatment system placed over the reactor with the arrows representing the dimensions of the treatment system. Image is not to scale.

In a normal raceway pond the algae would be circulated around the raceway and pass underneath the treatment system. In this experiment the time passing underneath the UV treatment system is simulated by the time of UV exposure. Cultures are kept 'stationary' - i.e. fixed in place on the orbital shaker at 200 rpm. Measurements confirmed that the fluorescent UV tubes could achieve sufficient output over the chosen time periods (please see Appendix 9.12) as fluorescent tubes have a warm-up period before reaching maximum irradiance.

[17] Open ponds are typically considered unmixed. Tubular photobioreactors could also work with this principle. These are not discussed here as *D. salina* is not commercially grown in tubular photobioreactors. The intermittent exposure is also applicable when discussing UV irradiation in pipe systems e.g. transferring algae from one location to another.

6.3.2 Results – Intermittent UV exposure

UV exposure regime representing coverage of 16.7% and 50% of the cultivation reactor (henceforth referred to as 'UV 5 min On - 25 min Off' and '15 min On – 15 min Off' respectively) led to increased carotenoid accumulation (Figure 6-6 and Figure 6-7).

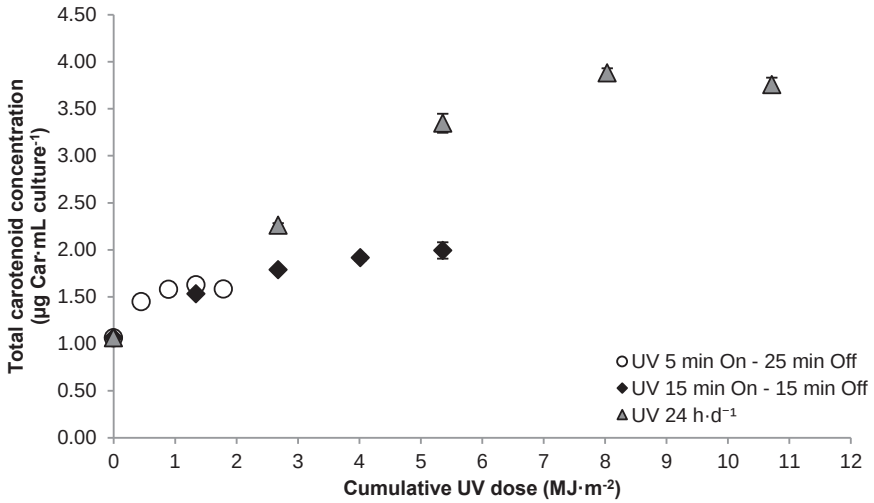

Figure 6-6 Total carotenoid concentration changes under intermittent UV-A exposure regimes. Each data point in each series represents a 24 h time period. Where larger than icons, error bars represent standard error (n = 4 for 24 h·d^{-1}, n = 8 for all others).

Dose efficiency was highest in 'UV 5 min On - 25 min Off' during the initial 24 h UV exposure period but then rapidly decreased (Figure 6-7). The '15 min On – 15 min Off' exposure regime dose efficiency followed a pattern more similar to that of continuous exposure except that UV dose efficiency was on average halved.

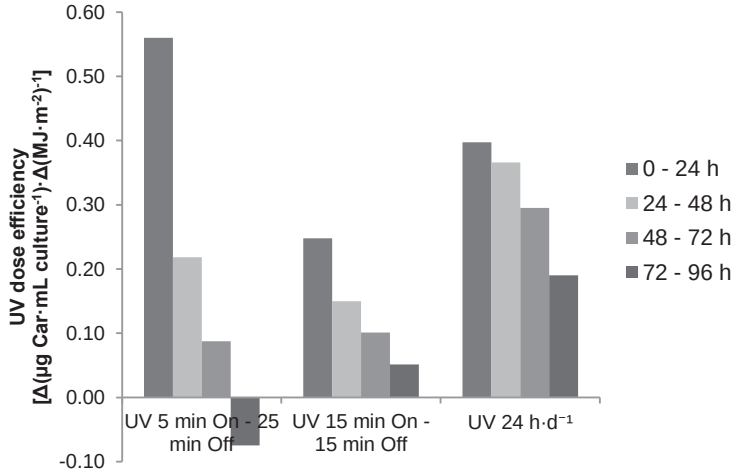

Figure 6-7 *Dose efficiency of UV-A induced carotenoid accumulation during different intermittent UV regimes. Series represents dose efficiency per regime between successive data points (separated by 24 h time period) in Figure 6-6.*

The results in Figure 6-7 suggests that initial intermittent UV exposure during the 'UV 5 min On - 25 min Off' UV regime is able to efficienctly induce an initial carotenoid accumulation response, despite the comparitively low cumulative dose. This suggests that the intial carotenoid accumulation response requires low cumulative dose to activate and concurs with observations in Ch. 5.2. The UV exposure regime induces carotenoid accumulation but appears not toallow for continued accumulation however, leading to a subsequent decrease in UV dose efficiency. A similar observation was made during semi-continuous exposure (6 $h \cdot d^{-1}$, Ch. 5.2.2). It is unclear why UV dose efficiency during the '15 min On – 15 min Off' UV regime is comparitvely low compared to the other regimes. A number of observations were made that point to biological phenomena that results from the intermittent UV-A exposure. A number of measured parameters showed similarity to the UV-A induced carotenoid accumulation response during 24 $h \cdot d^{-1}$ UV exposure: decreased cellular chlorophyll *(a+b)* content and morphological changes but a lack of the accompanying highly increased cellular carotenoid content (µg $Chl \cdot 10^6$ $cell^{-1}$). These observations suggest cells may prepare for, but not commit to, UV-A induced carotenoid accumulation while still responding to the UV-A induced stress in other ways. For more detailed description of the observations see Appendix 9.13. Allorent et al. (2016) report a similar observation in C. reainhardtii under UV-B exposure. Allorent et al suggest that UV-B acts as a proxy for high light, priming the cells for photoprotection.

Ultimately, the UV exposure regime representing partial coverage 'UV 5 min On - 25 min Off' and '15 min On – 15 min Off' respectively led to carotenoid accumulation disproportionate to the level of coverage – i.e. reducing coverage by 50% as in '15 min On – 15 min Off' does not lead to a carotenoid accumulation that is 50% lower (Figure 6-8).

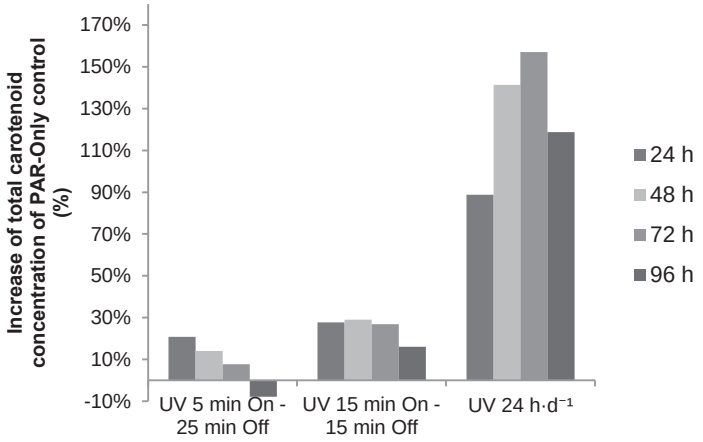

Figure 6-8 Time course of total carotenoid concentration over the PAR-Only control (%) as a function of intermittent UV exposure. Values represent total carotenoid increase in hours after experiment was started (h, see legend) over cultures exposed to PAR only, no UV (%).

While partial coverage would lead to a decrease in capital and operational expense, the partial coverage simulated in the experiment was found to lead to a decrease in total carotenoid accumulation disproportionate to the level of coverage. While the current experiments are not truly representative of real world conditions (i.e. all cells in the cultivation vessel are UV exposed at once and all cells are non-UV exposed at once), the results are thought to illustrate the impact of intermittent UV exposure on the individual cell. From an industrial perspective, it is therefore deemed unlikely that including a UV treatment system with partial coverage of the cultivation stage would lead to a scenario of decreased bioproduct production cost.

The observations of the current experiment serve a secondary purpose with regards to the impact of UV exposure frequency. As mentioned in Ch. 5.3 vertical mixing is commonly poor in raceway ponds, with most significant vertical mixing occurring at the paddle wheel and in the bends (Prussi et al., 2014). This means stratification occurs where cells may spend an entire cycle of the raceway pond at a given depth. Depending on the cell density in the culture media this may mean a cell at depth d may receive 0 to 100% incident UV radiation if the UV source is provided at the culture surface. Supposing cell spends one half-cycle at the surface and, after vertical mixing in the bend, spends one half-cycle in the lower parts of the reactor (15 min UV on, 15 min UV off), results in Figure 6-8 suggest carotenoid production could be severely reduced. These results indicate that methods to reduce time cells are receive a reduced UV signal are an important part of UV treatment system development. Strategies to improve UV exposure could include mixing regimes to ensure (rapid) vertical mixing and ensuring close proximity to the UV delivery system by submersion of the UV treatment system in the culture liquid.

6.4 Large-scale UV treatment system: *D. salina* case-study techno-economic analysis

In order for BioLumic to develop UV treatment regimes and UV treatment technologies, a fundamental understanding is required of a target species' UV photobiology and the desired UV response. Throughout the PhD thesis this novel understanding of *D. salina* UV photobiology and UV response has been developed. The current sub-chapter aims to collate the findings on *D. salina* into a techno-economic analysis (TEA) model to assess the feasibility of developing UV treatment recipes and UV treatment technology for large scale microalgae cultivation processes (Meghan Downes & Hu, 2013). A TEA combines elements of a standard economic benefit–cost analysis with an engineering analysis by integrating scientific and economical information. TEA's are commonly employed to assess the viability of a new technology and are thus inherently high-level assessments due to a lack of knowledge and input data. In the absence of relevant knowledge and data in the field, the scope of the developed model is such that it allows assessment of the most critical areas for improving profitability of large-scale UV treatment technology. The model is intended to serve as a tool to be able to make recommendations to BioLumic on whether further research and development is warranted .

The current sub-chapter assesses the economic feasibility of large-scale UV treatment in a case-study of commercial *D. salina* cultivation using a techno-economic analysis (TEA) approach (Meghan Downes et al., 2013). As discussed in the introduction, the extensive cultivation operated by Cognis at Hutt Lagoon, Western Australia (as described by Borowitzka) and the intensive cultivation operated by NBT Ltd. at Eilat, Isreal (as described by Ben-Amotz) are used as reference systems throughout the chapter due to the large amount of available literature. Closed photobioreactors represent another viable microalgae cultivation option but the commercialisation of *D. salina* production in these systems has been called 'a spectacular failure' and will therefore not be considered here (Borowitzka, 2013a). While design and operating considerations of the large-scale extensive and intensive systems are described in detail in the literature, the commercial nature of the operations means few details are provided on the operation of these commercial cultivation processes are operated and the costs involved. This includes the cost of operation of the facilities leading to a final production price of the target bioproduct β-carotene.

Due to a lack of knowledge and available data, model cultivation systems for both extensive and intensive cultivation systems were developed. Due to unavoidable loss of applicability to real world cultivation processes when modelling from limited literature values, emphasis will be given

to discussing results more broadly and qualitatively, and less emphasis will be given to the costing of the production system in order to focus instead on the added value of the UV treatment regime and technology.

The current sub-chapter will first outline development of model cultivation systems for the TEA model. The second sub-section will outline the inputs for the TEA UV treatment system and the applicability of the current work to developing a large-scale *D. salina* UV treatment system. Subsequently, the most promising application sites for UV treatment technology are revised based on experimental observations from Chapters 4, 5 and 6. Results from the TEA calculations are then discussed. Finally, suggestions for further research in the context of commercial *D. salina* cultivation and across a wider range of algae biotechnologies are discussed.

6.4.1 *D. salina* case study – Model cultivation system and TEA inputs and assumptions

First, the development of a TEA model cultivation system is discussed. Based on literature review of the extensive and intensive *Dunaliella* cultivation systems (Borowitzka et al., 1984; Borowitzka & Borowitzka, 1989a; Borowitzka et al., 1990; Moulton et al., 1987a; Ben-Amotz et al., 1989a; Borowitzka, 1992, 2013a, Ben-Amotz, 1995, 2004; Hosseini Tafreshi et al., 2009), a model *D. salina* cultivation process was developed (Figure 6-9). Due to their modes of operation, extensive and intensive cultures differ significantly in biomass- and β-carotene productivities but both have been shown to be commercially viable. This model includes all the features shared by both extensive and intensive cultivation of *D. salina* and represents the minimum elements required. The post-cultivation stage is not typically included in *D. salina* cultivation and is highlighted in grey in Figure 6-9.

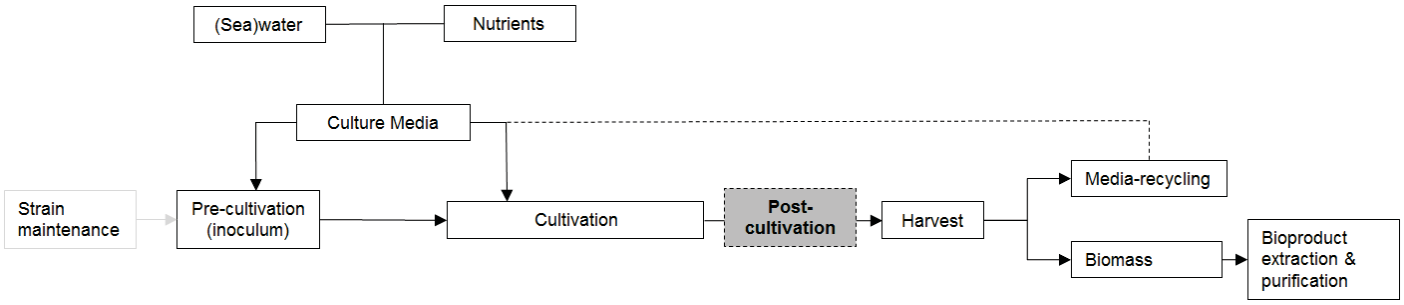

Figure 6-9 Schematic representation of the commercial D. salina *cultivation. The shaded area (Post-cultivation) is optional and is not always included in conventional microalgae cultivation processes.*

The current TEA was developed based on the model cultivation system shown in Figure 6-9. Literature values for areal biomass and β-carotene productivity ($g \cdot m^{-2} \cdot d^{-1}$), biomass concentrations ($g\ DW \cdot L^{-1}$) and cellular β-carotene contents (% w/w algal DW) were used to model the operation

and costing of the process. Data on pond depth and mixing speeds from the literature were also incorporated. Key cultivation parameter values from the literature are shown in Table 6-4. The rest of the production cost was calculated based on costing values found in literature and assumptions. A detailed discussion of all assumptions and calculations used to construct the TEA case-study is provided in Appendix 9.14. The results of the TEA for the model cultivation systems are discussed below.

Table 6-4 Key cultivation parameters as found in literature describing commercial D. salina cultivation. Values represent averaged (annual) values. Literature sources are given below table.

	Unit	Extensive	Intensive
Cellular β-carotene content	% w/w algal DW	5%[d]	5%[a]
β-carotene conc.	g β-carotene·m^{-3}	0.1[b,e]	5-15[b,e]
$P_{\beta\text{-carotene}}$	g β-carotene·m^{-2}·d^{-1}	0.01[e]	0.2-0.25[a,b]
Cell numbers	cells·mL culture $^{-1}$	0.5 – 5·10^{6}[, c]	3 – 10·10^{5}[, a]
Biomass conc.	g algal DW·L^{-1}	0.1[c,d]	0.5[a]
$P_{Biomass}$	g algal DW·m^{-2}·d^{-1}	0.05 – 0.1[e]	5[a]
Surface area pond	m^2	6,000 - 2,000,000[f]	3,000-4,000[b]
Pond depth	m	0.3[d]	0.2-0.3[d]
Active mixing	N/A	No[b,d]	Yes[b,d]

Sources:
[a] (Ben-Amotz et al., 1989a), [b] (Ben-Amotz, 2004), [c] (Borowitzka et al., 1990), [d] (Borowitzka, 2013a) [e] (Hosseini Tafreshi et al., 2009), [f] (Moulton et al., 1987a)

The TEA case-study assumes a small-scale production facility for the high value bioproduct β-carotene (as pure compound) extracted from *D. salina* biomass. The TEA case-study represents a process producing 2% of the estimated worldwide annual *D. salina* biomass production (as per data 2006, Spolaore, et al., 2006). All profitability comparisons in this sub-chapter will be made to a 'base-case' which represents a large-scale *Dunaliella* cultivation process for the production of β-carotene (as pure compound) without a UV treatment system. The base-case scenario of the TEA model cultivation is presented in Table 6-5.

Table 6-5 Overview of TEA base-case study for extensive and intensive cultivation systems. Table is continued on next page.

Base-case inputs	**Extensive**	**Intensive**
Cultivation operation lifetime (y)	20	20
Targeted annual production (kg pure β-carotene)	1,000	1,000
Target sale price ($·kg pure β-$carotene^{-1}$)	2,400	2,400
Number of operation days per annum (d)	300	300
Assumed biomass productivity (g algal DW·m^{-2}·d^{-1})	0.1	5
Assumed β-carotene content (% algal DW)	5	5

Process calculations	Extensive	Intensive
Required biomass production (kg algal DW)	25,000	25,000
Daily harvest volume ($m^3 \cdot d^{-1}$)	833	167
Size of cultivation reactor (m^2)	833,333	16,667
Cultivation reactor HRT (d)	300	30
CAPEX - Biomass production	**Extensive**	**Intensive**
Land cost	416,667	45,000
Pond construction	3,333,333	683,333
Site infrastructure	434,453	434,453
Laboratory	217,226	217,226
Pumps	25,000	5,000
Mixing and material handling equipment	28,950	48,272
Pre-cultivation (10% cultivation area)	66,667	68,333
Harvesting system	316,667	694,444
Post-harvest fluid treatment	334,250	66,850
Media recycling	931,667	932,167
Engineering cost (15% of CAPEX)	915,732	479,262
Contingency (5% of CAPEX)	305,244	159,754
Total CAPEX	7,325,854	3,834,094
Annualized CAPEX ($\$ \cdot y^{-1}$)	366,293	191,705

OPEX - Biomass production	Extensive	Intensive
Labour	375,000	500,000
Electricity use (at 0.16 $\$ \cdot kWh^{-1}$)	106,400	130,479
Pumping – Media supply +Fluid transfer	48,000	9,600
Harvest	58,400	120,000
Mixing	0	879
Harvest Consumables + Maintenance	55,000	115,000
Pump maintenance	2,500	500
Pond Maintenance	83,333	34,167
General Consumables	25000	25000
Water evaporation recovery	6250	125
Chemicals (Nutrients, CO_2, disinfection etc.)	12500	12500
OPEX ($\$ \cdot y^{-1}$)	772,383	948,249

Annualized production cost	Extensive	Intensive
Annual biomass production cost ($\$ \cdot y^{-1}$)	1,138,676	1,139,955
Annual β-carotene production cost (inc. biomass) ($\$ \cdot y^{-1}$)	2,846,690	2,849,887
Production cost per unit biomass ($\$ \cdot kg\ algal\ DW^{-1}$)	45.5	45.6
Production cost per unit β-carotene ($\$ \cdot kg\ \beta\text{-carotene}^{-1}$)	2846.7	2849.9

Product extraction and purification capital expense (CAPEX) and operational expense (OPEX) are not included explicitly in the TEA base-case overview. Rather, the annual biomass production cost

is assumed to represent 40% of the annual β-carotene production cost with product extraction and purification representing the remaining 60% (Molina Grima et al., 2003). Formulation, fill and finish of the product is not considered in this TEA.

The reported production cost per unit biomass agree with biomass production values reported in the literature, albeit at the upper end of the range presented in the literature (Borowitzka, 1992; Molina Grima et al., 2003). The assumptions made for the TEA base-case calculation have led to cultivation systems that are only economically viable if a β-carotene sale price of $2,850 · kg pure β-carotene^{-1} is assumed (i.e. not losing money). Based on literature this is at the very upper range of the β-carotene sale prices found in the literature (Borowitzka, 2013b). Production costs in the upper ranges indicate that the lack of input knowledge and data from the extensive and intensive cultivation systems has led to a model cultivation system that may be overestimating production cost compared to the real-world systems. However, values that are obtained do fall within ranges reported in the literature and the model system is therefore deemed viable for continued use within the scope of the TEA.

Sensitivity analysis on biomass production cost ($·kg algal DW^{-1}) was carried out on all costing for the CAPEX and OPEX components (Appendix 9.14). For CAPEX the media recycling and pond construction cost were identified as highest contributors of production cost. For the extensive cultivation in particular pond construction cost have a large impact on biomass production cost due to the large surface areas. For OPEX labour cost, number of staff, electricity consumption and harvesting had the largest impact on biomass production cost. Please see Figure 9-32 and Figure 9-33 for more details.

Changes in profitability resulting from addition of a UV-A treatment system during large scale *D. salina* cultivation will be referenced against the base-case biomass and β-carotene production cost as calculated in Table 6-5 throughout the continuation of the sub-chapter.

6.4.2 *D. salina* case study – Model UV treatment system

The inputs used for the TEA UV treatment system are outlined in Table 6-6. UV LEDs are employed by the industrial partner BioLumic for large scale treatment of seedlings because they emit narrower UV wavebands than UV fluorescent tubes and thus allow for more targeted UV delivery. This often comes at the cost of reduced maximum optical power of UV LEDs compared to UV fluorescent tubes due to the state-of-the-art of UV LEDs. Choices of UV LEDs for TEA modelling are based on personal communication with the industrial partner BioLumic and are compatible with the technology currently employed for their large-scale UV treatment systems. Choices of fluorescent UV tubes are based on those employed during experimental procedures.

Table 6-6 Input parameters for TEA UV treatment system. Where possible, values are based on supplier information. As not all suppliers readily provide values for all parameters values are based on the sources provided below the table.

		Waveband		
UV Source		Short waveband (λ = 320-350 nm)	Broad waveband (λ = 320-400 nm)	Long waveband (λ = 360-400 nm)
UV LED	Name	SETi UVTOP335	Nichia NCSU275-T U365	Nichia NCSU275-T U385
	Peak emission λ_{max}	335 nm	365 nm	385 nm
	Maximum optical power per LED	0.0004 W	0.148 W	0.35 W
	Lifetime	10,000 h[a]	50,000 h[b]	50,000 h[b]
	Electrical conversion efficiency*	40%[b]	40%[b]	40%[b]
	Optical efficiency**	50%	50%	50%
Fluorescent UV tube	Name	No products found. Would require use of expensive shortpass filters to achieve	QPanel UVA-340	Philips TLD BLB
	Peak emission λ_{max}		340 nm	370 nm
	Maximum optical power per tube		40 W	36 W
	Lifetime		5,000 h[a]	9,000 h[c]
	Electrical conversion efficiency*		25%[c]	25%[c]
	Optical efficiency**		50%	50%

* Electrical conversion efficiency is defined as conversion efficiency of electricity energy to the theoretical UV source optical power (W electricity·W UV optical power^{-1})

** Optical efficiency is defined as the UV irradiance loss between the UV source and culture surface as a function of distance

Sources: [a] SETi (www.s-et.com), [b] Phoseon Technology (www.phoseon.com), [c] Philips Lighting (www.philips.com)

While the PhD research was carried out within the intended scope, the laboratory research carried out in this thesis has limited applicability to large-scale cultivation systems. Only a very limited

number of cultivation parameters considered compared to those that impact large-scale cultivation. Due to a lack of knowledge or lack of input data relevant for large-scale cultivation systems, assumptions were made for the TEA model UV treatment system.

- The TEA applies all values obtained during experiments directly to the TEA modelling. Due to a lack of knowledge and data, no corrections were made to account for differences between experimental values and those found in the literature for cellular pigment contents, cell numbers, cell density or mixing.
- The interaction of UV-A induced carotenoid accumulation with key cultivation parameters pH, temperature, dissolved O_2, dissolved CO_2 and nutrient composition is not considered in the TEA model.
- The current work has not focussed on optimizing the UV treatment system design to ensure optimal UV transfer into dense microalgae cultures. The UV delivery approach employed during experiments in this thesis has assumed UV exposure external to the microalgae culture. An external UV delivery approach is therefore assumed in the TEA - i.e. top-down UV treatment technology suspended above cultivation area. Also a top-down UV treatment system is seen as the most convenient way to retrofit an existing commercial cultivation process. This UV delivery approach may not represent the optimal UV delivery system.
- The TEA model assumes outdoor cultivation under solar radiation. A top-down UV treatment system with solar radiation is likely to interfere with non-UV induced carotenogenesis in *D. salina*. Non-UV-A induced carotenoid accumulation has been shown to decrease linearly with decreasing PAR intensity (Loeblich, 1982). Furthermore, interference with solar PAR supply is assumed to interfere with photosynthetic processes required for carotenoid accumulation (e.g. carbon fixation). Therefore, in the TEA model a 'solar radiation occlusion penalty' is imposed on total accumulated β-carotene proportional to the size of the mounting infrastructure of the UV light sources. The impact on biomass productivity resulting from solar radiation occlusion is not considered in the TEA calculations as this is not a priority of the post-cultivation stage.
- Solar PAR and UV irradiances were not included in the experiments described in this thesis. There are no reports in literature on solar UV radiation on carotenoid hyperaccumulation in *D. salina*. The impact of solar PAR and UV can therefore not be accounted for in the TEA and, due to a lack of input data, the TEA therefore has to assume that the magnitude of the UV-A induced carotenoid accumulation response is the same during outdoor conditions as it was during experiments.

- The impact of a light:dark (diurnal) cycle was not considered in the experimental work in this thesis. PAR and UV exposure was continuous during experiments (24 $h \cdot d^{-1}$) unless specifically stated otherwise. Bouchard et al. (2013) have shown that photoperiod UV exposure reduces the UV stress response and may allow cells time to recover from UV damage and allow time for repair. While a diurnal cycle is likely to impact both carotenoid accumulation rates and biomass productivity (compared to 24 $h \cdot d^{-1}$ PAR and UV exposure), due to a lack of input data the TEA assumes the same UV response is achieved regardless of light:dark cycle.
- Mixing has not been explored in depth in the current study and the rapid orbital mixing used during experiments is not representative of commercial cultivation conditions. Reports by other authors on UV-A induced carotenoid accumulation are conducted only in well-mixed cultures (Jahnke, 1999; Benito Mogedas, et al., 2009; Salguero, et al., 2005). Commercial cultivation systems on the other hand employ either no active mixing (extensive cultivation) or limited vertical mixing with paddle wheels (intensive). The current research and literature provide little data on the effect of mixing on UV penetration, cycling and biomass productivity in dense microalgae cultivation systems. Because of the lack of input data, the TEA assumes UV exposure and UV response is equal in extensive cultivation and intensive cultivation. This subject will be discussed further in Ch. 6.4.2.2.
- Finally, the impact of pre-existing carotenoid levels was not explored in the current thesis. Experiments described in the thesis recorded the UV-A induced carotenoid accumulation in cells previously exposed to non-carotenogenic conditions, thus having comparatively low carotenoid content. The high salinity and high PAR intensity requirement for successful outdoor commercial cultivation of *D. salina* mean that carotenoid content of cells entering the post-cultivation stage can be variable. In *D. bardawil*, pre-existing cellular carotenoid content did not impact UV-A induced carotenoid accumulation efficiency (Jahnke, 1999). This suggests artificial UV-A treatment may remain efficient despite increased pre-existing carotenoid levels; however, this remains to be confirmed in *D. salina*. For the purpose of the TEA, an annualized average of pre-existing carotenoid levels of cells of *D. salina* entering the post-cultivation stage for UV treatment is assumed (Table 6-4). The TEA assumes pre-existing carotenoid levels do not to interfere with UV-A induction efficiency. For the purpose of the TEA, both cultivation systems are assumed to have constant cell density throughout the year.

6.4.3 *D. salina* case study – TEA Results

The current sub-section collates all of the above in order to be able to estimate the impact of incorporating a UV treatment system on the profitability of the model large-scale *D. salina* cultivation. As discussed above, the TEA model is constructed based a large number of assumptions. The profitability data resulting from the TEA therefore represent a 'best-case scenario', ignoring the impact of a large number of parameters. Rather than providing absolute economical outputs for revenue and profit, the TEA allows assessment of the most critical areas for improving profitability of large-scale UV treatment technology. The model is intended to serve as a tool to be able to make recommendations to BioLumic on whether further research and development is warranted.

The following sub-sections first discuss the proposed placement of the UV treatment system along the cultivation. Secondly, the outcomes of the TEA are first discussed with regards to the UV-A light source choice. Finally, the proposed TEA UV treatment cost and the associated increases in profitability are discussed. Recommendations to BioLumic based on the TEA are given in the next sub-section.

Tthe scope of UV treatment scenarios for TEA analysis that were considered in sub-chapter 6.1 was narrowed based on the experiments described in the thesis:

Pre-cultivation	The main constraint for the application of UV during the pre-cultivation stage is a mandatory long-lasting UV response (Table 6-1), improving total carotenoid concentration (µg Car·mL culture^{-1}) at harvest. No long-lasting UV response was found in *D. salina* (see Ch. 5.2.1 and 6.2). UV treatment during the pre-cultivation stage is therefore not considered further in this sub-chapter as a feasible UV treatment option for *D. salina*.
Cultivation	The typically large reactor surface area of the main cultivation stage mean UV treatment potentially incurs large capital and operational expense. More importantly however, continuous (24 h·d^{-1}) UV exposure was shown to slow or stop cell proliferation at most irradiances in *D. salina* (Ch. 4.2.3). Due to the interference of UV treatment with biomass growth, UV treatment during the cultivation stage is therefore not considered further in this sub-chapter as a feasible UV treatment option for *D. salina*.

Post-cultivation	As a dedicated post-cultivation carotenoid accumulation stage, the UV treatments can be specifically designed to maximize UV-A induced carotenoid accumulation. UV treatment during the post-cultivation is deemed to have fewer constraints than the previous stages. Firstly, no long-lasting UV response is required as post-cultivation is placed immediately prior to harvest. Secondly, the irradiated area may be an order of magnitude smaller than the cultivation stage requiring smaller capital and operational expenses. Lastly, as biomass productivity is not a priority, interference with cell proliferation by UV exposure or to the PAR supply by the UV treatment system play a smaller role in the UV treatment design. Post-cultivation stage UV treatment is therefore considered the UV treatment application scenario with the largest potential for feasibility in commercial *D. salina* cultivation.
Fluid transfer	The main constraints identified for UV treatment during the fluid transfer stages are limited UV exposure time and a requirement for a long-lasting UV response, unless carried out immediately prior to harvest. Although systems delivering high UV irradiance during short contact times are commonly used in waste water sanitation, the required UV exposure duration (hours to days) mean a similar approach is likely not applicable to UV induced carotenoid accumulation. While UV doses can be delivered during relatively short contact times (i.e. minutes), the lack of a sustained UV signal would cause small increases in carotenoid accumulation based on experimental observation (Ch. 5.2). UV treatment during the fluid transfer stage is therefore not considered further in this sub-chapter as a feasible UV treatment option for *D. salina*.

Based of the above, the TEA analysis will focus on the post-cultivation stage. It should be noted that the above reasoning is based on experimental results for *D. salina* and that different microalgae presenting with different UV response characteristics may benefit from and/or require application of UV treatment during other cultivation stages.

6.4.3.1 TEA Results – UV-A source

The initial assumptions for the TEA UV treatment system model (see Table 6-6) led to a UV LED-based treatment system which was not technically feasible. The UV LED treatment system

assumed in the TEA suffers from technical shortcomings that must be overcome for the treatment option to be viable:

- The TEA model currently assumes long wavelength UV-A LEDs recommended by BioLumic as those with the highest optical power (0.148 and 0.35 W·UV-A LED^{-1} for broad and long wavelength UV-A, respectively). The technical specifications for the industrial mounting infrastructure currently employed by BioLumic (based on pers. comm. BioLumic) assumed in the TEA calculations does not allow for sufficient UV LEDs to be mounted per unit area (m^2) to achieve a desired UV irradiance of 30 $W \cdot m^{-2}$ (maximum is 100 $LEDs \cdot m^{-2}$). A minimum UV LED optical power of 0.6 W·UV LED^{-1} is therefore required to achieve the desired UV irradiance assuming the UV LED density allowed by the mounting infrastructure. The technical specifications of the industrial mounting infrastructure used by BioLumic would need to be redesigned to accommodate higher power UV LEDs with a larger footprint per LED, higher current demand and cooling to compensate increased heat production. The alternative is to design a mounting infrastructure that allows higher UV LED density.
- The solar PAR supply occlusion penalty on β-carotene accumulation as currently implemented in the TEA model (see sub-chapter 6.4.2 and Appendix 9.14). The penalty has a large impact on the profitability of the UV LED treatment system. Assuming the solar PAR supply occlusion penalty is valid, mounting infrastructure cannot cover more than 41% of the reactor surface area if profitability is to be improved. To achieve this, a reduction in UV LED number and mounting infrastructure is required.

- A minimum UV LED optical power of 0.6 W·UV LED^{-1} and 1.45 W·UV LED^{-1} are required to reduce the mounting infrastructure size while still achieving desired UV irradiance = 13.8 W·m^{-2} and 30 W·m^{-2} for broad and long wavelength UV-A, respectively. Increasing maximum optical power above 0.6 W·UV LED^{-1} and 1.45 W·LED^{-1} improves profitability further, due to decreasing solar PAR occlusion and decreasing number of costly UV LEDs (Figure 6-10).

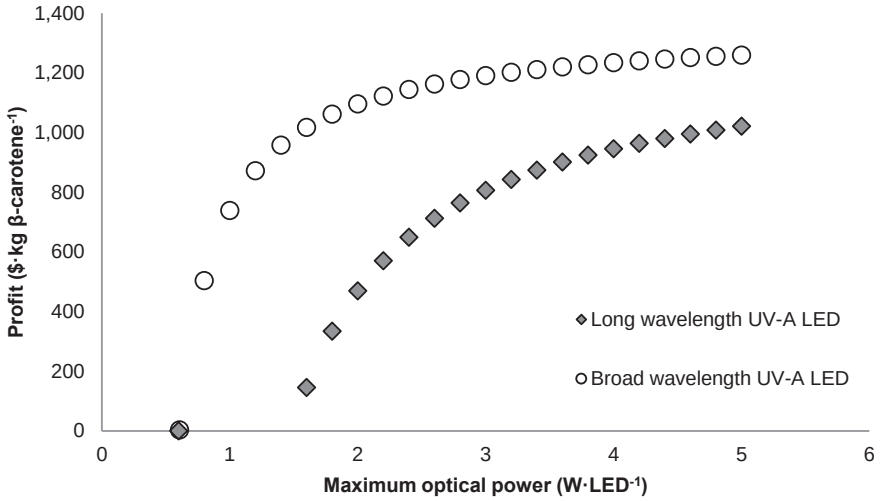

Figure 6-10 Increase in profit resulting from changes in UV LED optical power from the initial TEA assumptions in Table 6-5.

- The solar PAR supply occlusion could be removed entirely by submersing the UV treatment system in the culture media (e.g. bottom of the culture vessel).
- The coating dies currently available to manufacture UV LEDs have not yet been fully optimized for the UV region (Karlicek, 2013). As a result, maximum UV LED optical power drops rapidly at decreasing wavelengths (Karlicek, 2013). No UV-A LEDs in the short wavelength (λ = 320-350 nm) with optical power sufficient to generate a profit have been identified. From a technological standpoint it is therefore deemed preferable to use long wavelength UV-A UV LEDs until UV LED optical power at shorter UV-A wavelengths is improved.

6.4.3.2 TEA Results – UV treatment system cost

The introduction of a dedicated post-cultivation UV treatment system in the TEA base-case leads to UV treatment system options which increase profitability as shown in Table 6-7. Please refer to

Appendix 9.14 for a detailed discussion of assumptions and calculations. The data in Table 6-7 assumes the use of high power UV-A LEDs as described in sub-section 6.4.3.1 (most powerful available from supplier Nichia at 3.64 W·UV LED^{-1} and 4.64 W·UV LED^{-1} for broad and long wavelength UV-A, respectively; www.nichia co.jp/en/product/uvled.html, accessed 14/01/2018).

Table 6-7 TEA results for 'profit per unit β-carotene ($·kg β-carotene^{-1})' for all scenarios considered. (UV-A Irradiance = normalised to long waveband UV-A = 30 W·m^{-2} for all wavebands, Exposure duration = 24 h·d^{-1}, Surface area coverage = 100%).

	Profit per kg β-carotene ($·kg β-carotene^{-1})					
	Extensive cultivation			Intensive cultivation		
UV-A source	Short waveband	Broad waveband	Long waveband	Short waveband	Broad waveband	Long waveband
UV irradiance (W·m^{-2})	10.9	13.8	30	10.9	13.8	30
No UV treatment		$3			$0	
UV-A LED	N/A	$650	-$22	N/A	$1,205	$995
Fluorescent UV-A tubes	N/A	$728	$11	N/A	$1,279	$1,122

Increased profitability based on the TEA calculations indicates potential for economic feasibility of UV treatment technology during commercial *D. salina* cultivation. Broad wavelength UV-A (λ = 320-400 nm) fluorescent UV tubes and UV-A LED's show the largest profit increase.

Treatment regimes discussed elsewhere in the thesis but not shown in Table 6-7 – i.e. different UV-A irradiances, semi-continuous UV-A exposure and partial reactor coverage (intermittent exposure) – were analysed with a fast-pass analysis which confirmed the largest potential profitability is obtained with UV parameters: 30 W·m^{-2} UV-A irradiance, continuous 24 h·d^{-1} exposure and 100% reactor surface coverage (see Appendix 0).

Assuming the use of high optical power UV LEDs, cost and profit estimates were calculated using the TEA model to compare fluorescent UV tube and UV LED based UV treatment systems as shown in Table 6-8. Calculations for the two most profitable systems are shown (i.e. broadband fluorescent UV tubes or broadband UV-A LEDs in the intensive cultivation environment). Calculations include construction of a dedicated UV treatment post-cultivation pond.

Table 6-8 Overview of TEA cost estimate for fluorescent UV tube and UV LED based UV treatment systems. Calculations assume UV treatment during intensive post-cultivation using broad waveband UV-A exposure (24 h·d^{-1}, coverage = 100%). The table is continued on next page.

Inputs	**Fluorescent UV tube**	**UV LED**
UV treatment hours (h·y^{-1})	7,200	7,200
UV source	QLab QPanel UVA340	Nichia NVSU333A-U365
UV source optical power (W·UV source^{-1})	40	3.64
Price per UV source ($)	17.50	20
UV source lifetime (h)	5,000	50,000
Mounting infrastructure ($·m^{-2})	200	1,000
Electrical efficiency (%)	25%	40%
Optical efficiency (%)	50%	50%
Electricity cost ($·kWh)	0.16	0.16
Hydraulic retention time post-cultivation (h)	72	72

Process calculations	**Fluorescent UV tube**	**UV LED**
Additional β-carotene resulting from UV treatment (kg)	711	897
UV treatment system size (m^2)	1,667	1,667
Electricity consumption (kWh·y^{-1})	1,728	1,080
Time to replacement (y)	0.7	7.0
Solar PAR occlusion penalty (%)	3	8

CAPEX – UV treatment	**Fluorescent UV tube**	**UV LED**
Post cultivation pond	68,333	68,333
UV treatment system	349,196	1,919,479
Total CAPEX ($)	417,529	1,987,812
Annualized CAPEX ($·y^{-1})	20,876	99,391

OPEX - UV treatment	**Fluorescent UV tube**	**UV LED**
Running cost (electricity) ($·y^{-1})	167,073	132,514
Replacement UV source ($·y^{-1})	91,368	36,405
Pond mixing ($·y^{-1})	549	549
Pond maintenance ($·y^{-1})	1,708	1708
Total OPEX ($·y^{-1})	260,699	171,177

Annualized UV treatment cost	**Fluorescent UV tube**	**UV LED**
Annualized CAPEX ($·y^{-1})	20,876	99,391
Total OPEX ($·y^{-1})	260,699	171,177
Total annualized UV treatment cost ($·y^{-1})	281,577	270,568
Profit ($·kg β-carotene^{-1})	1,279	1,205

The CAPEX differs significantly between fluorescent UV tube and UV LED based treatment systems. This results primarily from the high mounting infrastructure cost for UV LEDs ($1000·m^{-2}) and the cost per UV LED ($20·LED^{-1}). However, the OPEX makes the largest contribution to the total annualized UV treatment cost; 93% and 63% for fluorescent UV tube and UV LED based UV treatment system respectively. The highest contribution of the OPEX results from the running cost (electricity) of the system, making up a total of 59% and 49% of total annualized cost for fluorescent UV tube and UV LED based UV treatment system, respectively. While running cost for both systems are similar, the reported long lifetime of UV LEDs leads to significant OPEX reduction compared to fluorescent UV tubes.

The individual components of the TEA model cultivation system and the TEA UV treatment to the annualized production cost for β-carotene from *D. salina* with the inclusion of UV treatment is shown in Figure 6-11.

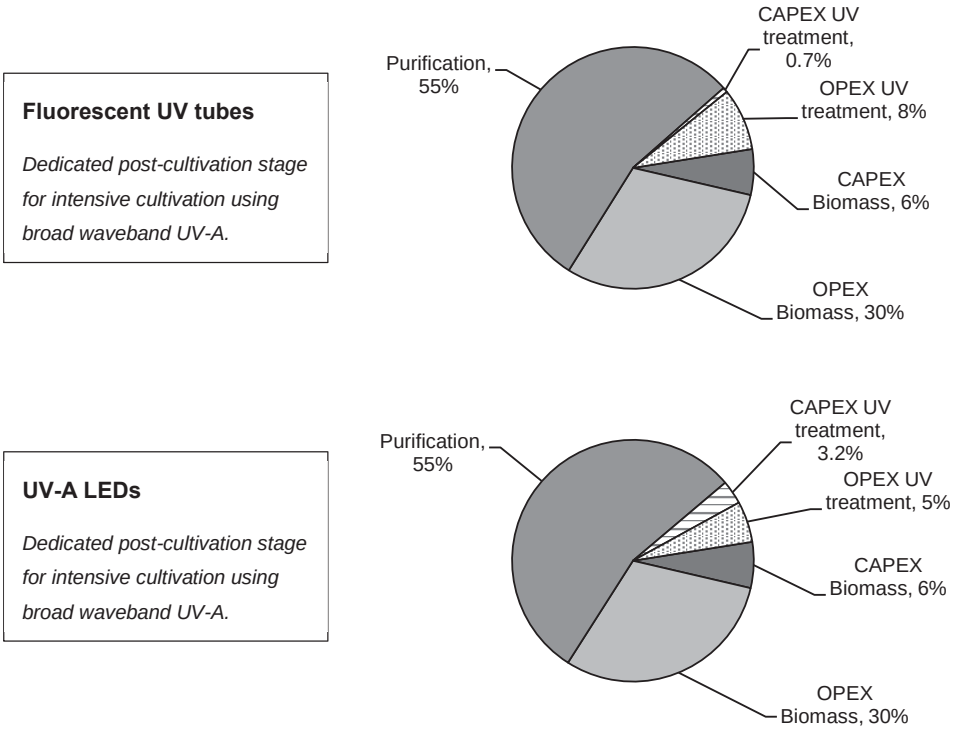

Figure 6-11 Contribution of individual components to total annualised production cost for β-carotene from D. salina*.*

A sensitivity analysis of the additional profit was performed on all CAPEX and OPEX components of the UV treatment system as well as the impact of the UV induced carotenoid accumulation. Results are shown in Figure 6-12.

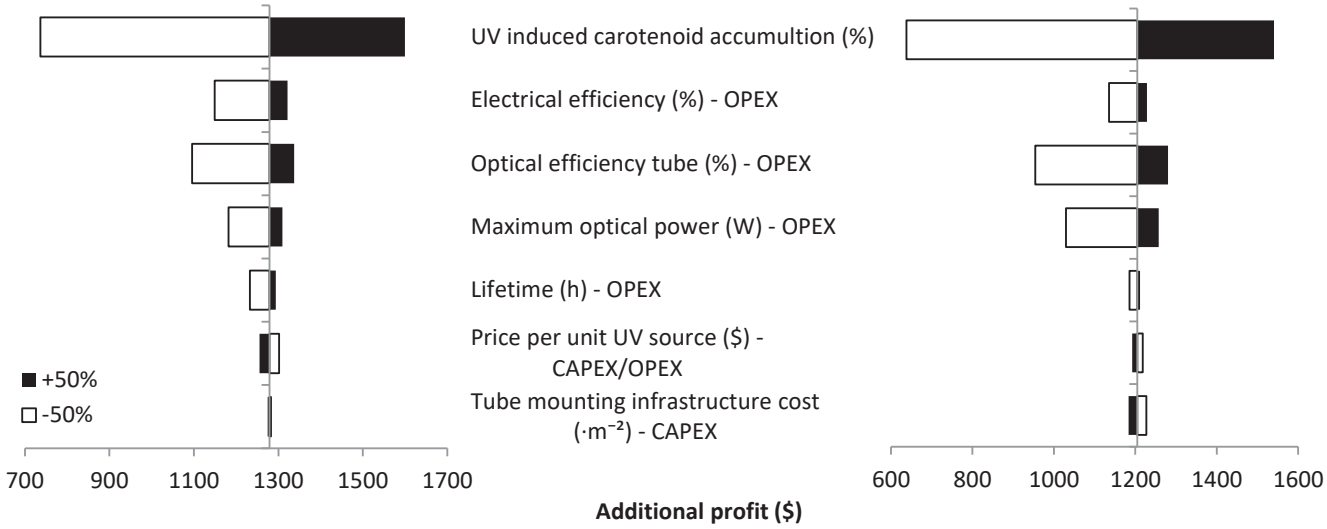

Figure 6-12 Sensitivity analysis of CAPEX and OPEX items influencing the profitability of a UV treatment system showing broad waveband fluorescent UV tubes (right) and broad waveband UV LEDs (left). Values were varied ±50%.

It is immediately clear from Figure 6-12 that the impact of the UV-A induced carotenoid accumulation response is the most significant in determining the additional profits from inclusion of a UV treatment system. This highlights the importance of the work carried out in the PhD thesis in gaining a fundamental understanding of a target species' UV photobiology and the desired UV response.

As expected from the initial calculations (Table 6-8), improvements in the OPEX processes are most likely to affect profitability of the system. The impact of optical efficiency, electrical efficiency and maximum optical power would therefore warrant further investigation as decreases from the values used in the TEA can rapidly lead to decreased profitability. A number of suggestions are discussed below.

- The optical efficiency in the TEA model is defined as the UV irradiance loss between the UV source and culture surface as a function of distance. Submersing the UV treatment system in the microalgae culture, thereby reducing the distance to the culture surface to zero is therefore seen as a means of improving profitability of the UV treatment system. Submersion is expected to significantly increase the UV source mounting infrastructure cost but does result in removal of the solar PAR occlusion penalty for both UV sources. The impact of cost

per unit and mounting infrastructure cost on UV LED treatment system is shown to be low however (Figure 6-12).

- More electrically efficient fluorescent UV tubes than those assumed in the TEA are available (current calculations are based on the fluorescent UV tubes used during experiments). Improvements in electrical efficiencies through technical improvements are deemed unlikely however, as fluorescent tube technology is already well-developed. Improvements in electrical efficiency in UV LED technology have been rapid during past years and improvements are expected to continue at a similar rate (Karlicek, 2013). It is therefore deemed likely that UV LEDs with increased electrical efficiency will become available. This is particularly important for UV LEDs with higher optical power as increased optical power reduces electrical efficiency through increased heat production (Karlicek, 2013). The impact of maximum UV LED optical power was discussed above. Maximum optical power is also expected to increase for UV LEDs in all UV wavebands as development continue (Karlicek, 2013)
- UV-A exposure at short- and broad wavelength UV-A has been shown to improve UV dose efficiency compared to long wavelength UV-A. Due to insufficient experimental data in these UV wavelength regions, only the long wavelength UV-A region has been discussed here. However, short- and broad wavelength UV-A exposure is thought to significantly reduce the electricity consumption by up to 55 – 65% (based on UV irradiances in Table 6-6) similarly high UV-A induced carotenoid accumulation is achieved.
- Increased optical power can be readily achieved with current long waveband UV-A LED technology - e.g. Nichia Corporation supplies broad wavelength UV-A LEDs up to optical power 4.6 W·UV LED^{-1} (NVSU333A-U385)[18]. It should be noted that increased optical power in UV LEDs increases cost per unit and likely also mounting infrastructure price to provide additional cooling to dissipate excess heat. The impact of cost per unit and mounting infrastructure cost on UV LED treatment system is shown to be low however (Figure 6-12).
- Other options for reducing running cost such as semi-continuous exposure or partial coverage of the cultivation reactor have been discussed in previous chapters.

[18] Nichia Corporation (www.nichia.co.jp)

6.4.4 *D. salina* case study – BioLumic recommendations and limitations

It should be reiterated that the TEA does not aim to provide BioLumic with accurate economical outputs for revenue and profit as for example a business-study would but rather provides a tool to be able to make recommendations to BioLumic on whether further research and development is warranted. TEA's are commonly employed to assess the viability of a new technology and are thus inherently high-level assessments due to a lack of knowledge and input data.

To that end, the calculations carried out in the previous sub-section using the developed TEA model cultivation system and TEA UV treatment system indicate that there is a potential for profit increases when UV treatment is applied during large-scale *D. salina* cultivation. The relatively small contribution to CAPEX and OPEX to the overall β-carotene production cost (i.e. < 10%, see Figure 6-11) combined with the large increase in β-carotene production (711 $kg \cdot y^{-1}$ and 895 $kg \cdot y^{-1}$ for fluorescent UV tube and UV LED systems, respectively, see Table 6-8) leads to potentially large increases in profitability. The current sub-section makes recommendations to BioLumic for further development of both the TEA. Moreover, the current sub-section comments on potential areas of further research and development of elements of the UV treatment system during large-scale *D. salina* cultivation but also looking broadly across microalgae biotechnology applications.

- The TEA has shown that the profitability of UV treatment during large-scale *D. salina* is impacted most profoundly by the magnitude of the UV-A induced carotenoid accumulation response. Continued research into optimization of the *D. salina* UV-A induced carotenoid accumulation is therefore recommended, particularly with regards to UV wavelength. Ultimately, the TEA model would benefit most from data collection of a UV treatment system for *D. salina* employed under real world cultivations conditions to generate input data for more accurate profitability estimates. Furthermore the impact of solar PAR and UV content, light:dark (diurnal) cycle and key variable cultivation parameters pH, temperature, dissolved O_2, dissolved CO_2 and nutrient composition (i.e. media composition and changes resulting from rain/evaporation) should be considered during future work.
- The TEA model cultivation system would benefit greatly from more detailed information from commercial large-scale *D. salina* operations (e.g. through industry contacts) to improve the TEA model cultivation system cost estimations. Ideally the model is replaced entirely with operational data of the commercial operation the UV treatment system is intended for.
- More accurate costing of the UV treatment system is required to improve the TEA UV treatment system cost estimations. The UV treatment system CAPEX plays a relatively small role (i.e. <5% of total production cost, Figure 6-11). However, raw material cost was used for

all calculations and do not consider the impact of research and development cost, manufacture, transport and installation and economies of scale.

- Future work should aim to improve the design of the UV treatment system. Firstly, the TEA UV treatment system is based on the available data from the technology utilized during experiments and that employed by BioLumic for seedling treatment. However, the scale of the UV treatment systems (e.g. 1700 m^2, see Table 6-8) and the operation thereof (i.e. continuous exposure) differ significantly from those reference conditions. This may lead to significantly different design choices. Secondly, the TEA has indicated the increases in profitability are strongly influenced by optical efficiency, electrical efficiency and maximum optical power (see Figure 6-12). As briefly mentioned in the last sub-section, submersion of the UV treatment system may be deemed preferable to increase optical efficiency and proximity of microalgae cells to the UV source. Industrial UV-C disinfection is a well-established field that employs submerged UV treatment systems at large-scale. High irradiance UV-C tubes are submerged in (or surround) a narrow vessel through which the liquid flows and adequate delivery of a minimum required dose can be guaranteed all the way to the walls of the vessel (Metcalf et al., 2003). While not directly applicable to UV treatment in dense microalgae cultures, the engineering principles employed in this field are good starting points for future development of a UV delivery design.
- Based on the assumptions used for the TEA model, a number technical shortcomings of the UV LED treatment system will need to be addressed if UV LED technology is to be successfully applied.
- Although not explicitly incorporated in the TEA, mixing is recommended to be included in future work on optimization of the UV treatment system. UV-A transmittance is below 50%·cm^{-1} at the lowest cell densities reported for commercial *D. salina* cultivation (3 - 5·10^5 cell·mL^{-1}, Table 6-4), meaning UV-A is attenuated in the first 7 cm of microalga culture. Unless the culture is mixed, the majority of cells will not receive UV exposure. Furthermore, this observation is not exclusive to *D. salina*, as UV attenuation will affect all dense microalgae cultures similarly. Limitations to the mixing system are imposed by the microalgae species used as different microalgae species have different hydrodynamic or shear stress tolerance.
- Looking more broadly across microalgal biotechnology, development of broad screening protocols to assess microalgae species-specific UV photobiology and UV response would be greatly beneficial for further species-specific UV treatment design. The UV characteristics found during the PhD research is specific to *D. salina*, leading to the outcome of the TEA UV treatment system design and operation also being specific to *D. salina*. However, due to the

varying nature of UV response between microalgae species (e.g. see preliminary PhD experiments, Appendix 9.2), the development of a commercial UV treatment system will likely be species-specific.

6.5 Conclusions

Understanding of the target species' UV photobiology and the desired UV response was found to be essential for determining the optimal placement and operation of a UV treatment system in a commercial microalgae cultivation process. UV treatment placement was determined primarily by: the required contact time for maximum carotenoid induction (timescale of days), the longevity of the UV response (no long-lasting response was found in *D. salina*) and a reduction in cell proliferation under conditions of maximum carotenoid induction. These UV characteristics limited the locations for placement of UV treatment system along the cultivation process. Due to the varying nature of UV response between microalgae species, the development of a commercial UV treatment system will likely be species-specific. Therefore, development of a rapid but broad screening protocol focused on identifying and characterizing UV responses in other species would be greatly beneficial for further development of species-specific UV treatment design.

Novel targeted UV treatments developed for *D. salina* to improve feasibility based on the observed UV characteristics proved unsuccessful. The novel 'Treat-and-release' and 'Intermittent exposure' UV treatment regimes developed specifically for large-scale *D. salina* cultivation aimed at reducing UV treatment cost did not improve total carotenoid concentration on harvest. Due to the lack of direct or indirect lasting effects a treat-and-release UV treatment regime was not deemed viable. Experiments emulating partial coverage of a cultivation reactor with UV treatment system (intermittent exposure) induced low levels of carotenoid accumulation. A linear relationship between the total carotenoid accumulation and the reactor surface area covered by a UV treatment system was not found.

Post-cultivation UV treatment was identified to have a number of advantages over other treatment options: Firstly, the required irradiated area may be an order of magnitude smaller than the area for UV treatment during the main cultivation stage, significantly reducing capital and operational expenses. Secondly, UV treatment post-cultivation stage allows for UV treatment optimization without having to account for potential loss in biomass productivity. Lastly, and contrary to UV treatment at the pre-cultivation and cultivation stages, a long-lasting UV response is not required as post-cultivation is placed immediately prior to harvest. The assumed top-down UV treatment system assumed in the TEA model led to interference with solar PAR supply, thought to play an important role in non-UV induced carotenogenesis.

The developed TEA model cultivation system and TEA UV treatment system identified a potential increase in profitability generated from the application targeted UV treatment during large-scale *D. salina* cultivation. Maximum profitability was achieved using a broad wavelength UV treatment

system (irradiance = 30 $W \cdot m^{-2}$, exposure duration = 24 $h \cdot d^{-1}$, surface area coverage = 100%) applied during an intensive cultivation post-cultivation system. A relatively small contribution to CAPEX and OPEX to the overall β-carotene production cost (i.e. < 10%, see Figure 6-11) combined with a large increase in β-carotene production (711 $kg \cdot y^{-1}$ and 895 $kg \cdot y^{-1}$ for fluorescent UV tube and UV LED systems, respectively, see Table 6-8) leads to potentially large increases in profitability. The profitability estimates from the current TEA indicate that UV treatment during commercial microalgae cultivation has potential and justifies further research.

Based on the assumptions used for the TEA model, a number technical shortcomings of the UV LED treatment system will need to be addressed if UV LED technology is to be successfully applied. Using the current TEA assumptions the use of UV-LEDs with optical power higher than 1.45 $W \cdot LED^{-1}$ is a prerequisite for the use of broad and long wavelength UV LEDs. The CAPEX and OPEX of the proposed UV treatment are comparatively small to the overall β-carotene production cost (i.e. < 10%, see Figure 6-11) with OPEX making up the majority of the cost. The TEA analysis identified the magnitude of the UV-A induced carotenoid accumulation response to be the most important factor to influence the potential profitability. Secondly, the TEA has indicated the increases in profitability are strongly influenced by optical efficiency, electrical efficiency and maximum optical power (see Figure 6-12). The case-study of UV treatment during large-scale *D. salina* cultivation led to the following recommendations for BioLumic on potential areas of focus for continued research:

- Continued research into optimization of the *D. salina* UV-A induced carotenoid accumulation is recommended, particularly with regards to UV wavelength. Ultimately, the TEA model would benefit most from a *D. salina* UV treatment system employed under real world conditions.
- It is recommended to incorporate more detailed information from real-world commercial large-scale *D. salina* operations to improve the TEA model cultivation system cost estimations.
- It is recommended to obtain more accurate costing of the UV treatment system to improve the TEA UV treatment system cost estimations.
- Future work should aim to improve the design of the UV treatment system due to the significant differences between the current state-of-the-art at BioLumic and the systems proposed in the thesis as address the key parameters identified in the TEA.
- Based on the assumptions used for the TEA model, a number technical shortcomings of the UV LED treatment system will need to be addressed if UV LED technology is to be successfully applied.
- Development of broad screening protocols to assess microalgae species-specific UV photobiology and UV response is recommended.

7 General conclusions and future prospects

7.1 Conclusions

Microalgae cultivation processes face significant limitations in achievable bioproduct and biomass yields (Tredici, 2010) and thus improvements offered by targeted UV treatments during large-scale microalgae cultivation present an opportunity for development of a novel UV treatment tool. No examples have been found in literature or in industry that explore development of targeted UV treatments during large-scale microalgae cultivation. The multidisciplinary approach employed during this PhD research explored for the first time the development of a UV treatment system for commercial microalgae cultivation based on the hypotheses: That specific treatments of UV radiation (i.e. specific in UV waveband, irradiance and exposure duration) can reliably increase bioproduct accumulation in *D. salina* and that a new understanding of UV response characteristics can be feasibly used to develop an industrial system for UV treatment of microalgae.

The development of UV treatment regimes and UV treatment technologies requires a fundamental understanding of a target species' UV photobiology and the desired UV response. While literature in the UV research field in microalgae is valuable in its contribution to our understanding, the impact of UV wavelength and UV dose is often considered in a narrow range (i.e. only one UV light source, generating a single UV waveband is employed). The current PhD research has shown for the first time that UV treatment can be used to reliably induce bioproduct accumulation in *D. salina* and that UV treatments specific in UV waveband, UV irradiance and UV exposure duration have differential impact on the magnitude of the UV induced carotenogenesis response. The novel findings from the current PhD research are that:

- UV-A induced carotenoid accumulation in *D. salina* (strain UTEX 1644) is most efficient during short wavelength (λ=320-350 nm) UV-A exposure, followed by broad wavelength (λ=320-400 nm). UV-A induced carotenoid accumulation is least efficient during long wavelength (λ=360-400 nm) UV-A exposure.
- The magnitude of the *D. salina* UV-A induced carotenoid accumulation response is highest during exposure with the highest UV-A irradiance tested (30 $W \cdot m^{-2}$) during continuous UV exposure (24 $h \cdot d^{-1}$) (as opposed to semi-continuous exposure, 6 or 12 $h \cdot d^{-1}$). Co-exposure of non-UV carotenogenic stimuli further increases the magnitude of the UV-A induced carotenoid accumulation.

Contributions to knowledge in the field of *D. salina* (strain UTEX 1644) UV-A induced carotenoid accumulation resulting from the current PhD research include:

- UV-A exposure leads to a reduction in cell proliferation under conditions of maximum carotenoid induction.
- UV-A induced carotenoid accumulation response in *D. salina* strain UTEX 1644 is induced within 6 hours and is largely complete in 96 hours (24 $h \cdot d^{-1}$ UV exposure).
- When UV-A exposure is stopped, carotenoid accumulation ceases and cell proliferation is increased. No long-lasting UV response leading to improved total carotenoid concentrations was found in *D. salina*.

Quantification of the impact of UV waveband, UV irradiance and UV exposure duration as well as non-UV-A induced carotenoid accumulation (PAR intensity and salinity) in this work has led to new knowledge essential for the development of targeted UV treatment during commercial *D. salina* cultivation. Improved knowledge of *D. salina* photobiology generated from the PhD research, complemented with a commercial microalgal-engineering insight, led to the development of UV treatment regimes and UV treatment technology for application during large-scale microalgae cultivation:

- The novel 'Treat-and-release' and 'Intermittent exposure' UV treatment regimes developed specifically for large-scale *D. salina* cultivation, based on understanding of the UV photobiology, aimed at reducing UV treatment cost did not improve total carotenoid concentration on harvest.
- Optimal placement of a UV treatment system during large-scale *D. salina* cultivation is during a dedicated post-cultivation stage in which high irradiance can be applied under continuous exposure.

The understanding of the UV response characteristics developed in this thesis were used as inputs for a techno-economic analysis (TEA) model, developed to assess feasibility of large-scale UV treatment. The absence of relevant knowledge in the field and limited input data from large-scale *D. salina* cultivation systems means the TEA model suffers from a number of limitations. The scope of the TEA is such that it allows recommendations to be made to BioLumic whether further research is warranted but does not contain the level of detail required to provide accurate economical outputs for revenue and profit as e.g. a business-study would. Predictably, not all operational parameters impacting UV-A induced carotenoid accumulation could be investigated in the current work. Specifically, the impact of variable solar radiation intensity, solar UV, diurnal

cycle and key operational parameters will need to be researched further to improve the accuracy of the TEA model.

Based on the TEA model and insights from the experimental work areas of future development for BioLumic were identified as:

- Loosely based on the UV delivery systems currently employed by BioLumic, the current top-down UV delivery system is well suited for UV treatment of plants but is not optimized for UV transmission into dense microalgae culture. Optimization of the UV delivery design for optimal UV transfer into dense microalgae cultures is recommended.
- It is recommended the impact of (rapid) vertical mixing in the UV treatment system be investigated. UV attenuation is not exclusive to *D. salina* and will affect all dense microalgae cultures similarly. The TEA analysis of the post-cultivation UV treatment system for *D. salina* indicates a relatively small contribution of mixing CAPEX and OPEX to overall UV treatment cost meaning that improvements to (rapid) vertical mixing could be readily made (e.g. baffles, more rapid mixing, bubbling).
- The PhD research has shown the UV treatment application is highly specific for *D. salina* (strain UTEX 1644). Furthermore a large diversity of photobioreactor designs and cultivation scales mean that UV delivery design is likely to be cultivation process specific. It is recommended that a broad screening protocol be developed to rapidly determine the species-specific UV characteristics and microalgae cultivation system are considered in the UV treatment technology design.

In summary, exploration of the fundamental UV photobiology in microalgae required to develop UV treatment regimes from discrete UV wavebands, complemented with a commercial microalgal-engineering insight, to produce UV treatment regimes and UV treatment technology for application during large-scale microalgae cultivation, has not been previously explored to our knowledge. It follows from this PhD thesis that the novel understanding of the UV response characteristics in *D. salina* (strain UTEX 1644) is required for developing a viable UV treatment system for commercial cultivation. The profitability estimates from the current TEA indicate that UV treatment during commercial *D. salina* cultivation has potential and justifies further research, both academically and by the industrial partner BioLumic.

Ultimately all the work carried out throughout the thesis in the case-study of UV treatment during large-scale *D. salina* led to the following recommendations for BioLumic on potential areas of focus for continued research:

- Continued research into optimization of the *D. salina* UV-A induced carotenoid accumulation is recommended, particularly with regards to UV wavelength. Ultimately, the TEA model would benefit most from a *D. salina* UV treatment system employed under real world conditions.
- It is recommended to incorporate more detailed information from real-world commercial large-scale *D. salina* operations to improve the TEA model cultivation system cost estimations.
- It is recommended to obtain more accurate costing of the UV treatment system to improve the TEA UV treatment system cost estimations.
- Future work should aim to improve the design of the UV treatment system due to the significant differences between the current state-of-the-art at BioLumic and the systems proposed in the thesis as address the key parameters identified in the TEA.
- Based on the assumptions used for the TEA model, a number technical shortcomings of the UV LED treatment system will need to be addressed if UV LED technology is to be successfully applied.
- Development of broad screening protocols to assess microalgae species-specific UV photobiology and UV response is recommended.

7.2 Recommendations for future work

The PhD research provides recommendations for both continued academic research and continued development of a commercial microalgae UV treatment protocol by the industrial partner BioLumic, both in *D. salina* and the wider microalgae biotechnology field in mind.

The literature review carried out for the current PhD research identified a knowledge gap in the understanding of UV-A photobiology of *Dunaliella* species and microalgae in a wider context (Jahnke, 1999; Verdaguer et al., 2016). In order to gain a better understanding of the fundamental UV photobiology in *D. salina*, something the current work was only able to hint at, the use of a number of analytical techniques and research methodologies is recommended. In the case of *D. salina* (strain UTEX 1644) it is recommended high pressure liquid chromatography (HPLC) be employed to qualify and quantify induvial photosynthetic pigments with a higher degree of accuracy. Analysis of the morphological changes induced by UV treatment would greatly benefit from whole cell transfer electron microscopy (TEM). TEM has been used by other researchers to

visualize the morphological changes during non-UV induced carotenogenesis (Ben-Amotz et al., 1982; Borowitzka, 2013a). The use of pulse amplitude modulated (PAM) fluorometry, commonly used in (UV) photobiology studies, is highly recommended to assess the impact of UV exposure on the photosynthetic machinery. Other avenues to explore would be the dedicated research of UV-A on PSII photooxidative damage, electron transfer and redox potential. While the aforementioned factors have been suggested as potentially involved in *Dunaliella* carotenogenesis, none of these have been accurately reported in *Dunaliella* during UV-A exposure. All of the techniques mentioned above aid in the fundamental UV photobiology which may aid in further refining UV treatment regimes.

The current work explored three wavebands in the UV-A spectrum and found a discernible difference in a UV wavebands capacity to induce carotenoid accumulation. The construction of a dedicated action spectrum for UV-A induced carotenoid accumulation would be a first step towards continued photobiological research. The action spectrum would explore a larger range of narrower wavebands to more clearly define the regions of the spectrum in which carotenogenesis is most efficiently induced by UV. From an industrial point of view, the action spectrum for UV-A induced carotenoid accumulation can be used to optimize the UV source chosen for commercial *D. salina* UV treatment. A second step would be the construction of a biological weighting function (BWF) to ascertain more clearly the relationship between UV wavelength and UV dose. Furthermore, the existence of a dedicated UV-A photoreceptor has been proposed as part of the *Dunaliella* carotenogenesis response and a dedicated action spectrum/BWF may contribute to a better understanding and may allow further targeted research into the signalling involved in *Dunaliella* carotenogenesis. A better understanding of signalling involved in (UV induced) carotenogenesis may allow for a larger degree of control in large-scale *D. salina* cultivation.

Scientific literature contains numerous examples of microalgae UV responses that would benefit commercial microalgae cultivation processes. Examples include increased growth rate (Forján et al., 2011; Balan et al., 2014) and changes in quality and composition of high-value bioproduct formation such as carotenoids (Wu et al., 2010) and lipids (Srinivas & Ochs, 2012). While three other commercially relevant microalgae were screened for a UV response during the current research, time did not allow for exploration of a sufficient number of experimental conditions to observe any significant responses. Future work should focus on identifying and characterizing UV responses in other species. It can be difficult to identify potentially beneficial UV responses, as it is often unclear what a UV response may entail and thus what to monitor. Metabolomics employing e.g. liquid chromatography – mass spectrometry (LC-MS) to monitor the impact of UV

treatment on a wider variety of metabolites could present a powerful tool in analysis of *D. salina* (strain UTEX 1644) as well as in the broader screening of other species of microalgae. The current LC-MS state-of-the-art means that many metabolites in a total cell extract can be identified with good accuracy. It may therefore become easier to monitor not only the influence of UV on a metabolite of interest but also to identify completely unknown UV responses. No literature on the use of metabolomics in UV research in microalgae has been found to date.

The current research, or any research in the laboratory, is difficult to extrapolate to commercial scale cultivation processes. For the further development of the *D. salina* UV treatment system, research into the impact of environmental conditions both in the laboratory and at large-scale would be essential to provide more accurate inputs for the TEA model. Future work should therefore initially focus on larger scale experiments (e.g. >2 L culture vessel), ideally in flat plate reactors as these provide a highly controlled cultivation environment and a flat surface of defined area for UV irradiance. In the current work, no experiments were carried out to determine the effects of CO_2 or nutrient availability under laboratory conditions and thus should be included in these larger scale laboratory experiments. As a follow up step the UV treatment would be tested in a representative outdoor cultivation systems (e.g. HRAP). The impacts of solar radiation (i.e. UV content and PAR irradiances), diurnal cycle and changing environmental parameters (e.g. temperature, salinity) on the UV-A induced carotenoid accumulation during large-scale cultivation are currently all unknown. Further knowledge on these parameters may also allow for the development of more targeted UV treatments (e.g. supplementing solar UV-A during periods of low solar UV-A instead of continuous exposure). These may lead to optimized UV treatment placement, design or operation.

Finally, While high-value bioproducts are a seemingly obvious target for potential enhancement by UV treatment, there are numerous other aspects of microalgae cultivation that could benefit from UV treatment. Overall, viability of any UV treatment is dependent on whether the induced UV response can be monetized and whether this monetization outweighs the added cost of the UV treatment system. Alternatives include, but are not limited to:

- Alterations in photosynthetic pigment composition to aid in e.g. extraction and purification efficiency (e.g. reduction of chlorophyll content)
- Non-target organism or pathogen removal – observed during own experiments with reduction in contamination during high irradiance UV-A exposure (data not shown).
- Induction of long-lasting changes – no lasting effects were measured in *D. salina* but this may be different for other species.

- Inducing cellular behaviours beneficial to specific cultivation steps (e.g. aplanospore formation prior to harvest)
- Induction of metabolites beneficial for down-stream processes – e.g. increasing specific nutritional value prior to larvae feeding in aquaculture. This would also be a way of 'locking in' the produced metabolite if the UV response is rapidly reversed, storing it in the larvae, not the microalgae.
- Small changes induced by UV treatment may be sufficient to make processes which are normally not economically viable due to high production cost viable through UV treatment.

Therefore use of UV treatment in the wider microalgae biotechnology field should therefore be explored to identify alternative aspects of microalgae cultivation that could benefit from UV treatment. Furthermore, the large variety of photobioreactor designs and cultivation scales mean that UV delivery design is likely to be microalgae cultivation process specific. The current work considers two types of cultivation reactor. Other commercial cultivation reactor designs such as polyethylene bags commonly used in aquaculture microalgae cultivation or tubular photobioreactors (for *H.pluvialis* cultivation) are also commonly used. Furthermore, tubular photobioreactors and polyethylene bags are closed systems, with wall materials may hinder UV penetration. The ability to retrofit the UV delivery system into existing cultivation processes is thought to increase the appeal of the product for existing microalgae cultivation facilities.

8 Bibliography

Agati, G., Brunetti, C., Di Ferdinando, M., Ferrini, F., Pollastri, S., & Tattini, M. (2013). Functional roles of flavonoids in photoprotection: new evidence, lessons from the past. *Plant Physiology and Biochemistry*, *72*, pp. 35–45.

Allorent, G., Lefebvre-legendre, L., Chappuis, R., Kuntz, M., & Truong, T. B. (2016). UV-B photoreceptor-mediated protection of the photosynthetic machinery in *Chlamydomonas reinhardtii*. *Proceedings of the National Academy of Sciences of the United States of America*, *113*(51), pp. 1–6.

Andersen, R. A. (2005). *Algal culturing techniques*. (R. A. Andersen, Ed.) (1st ed.). Burlington, MA: Elsevier Academic Press.

Andreasson, K. I. M., & Wängberg, S.-Å. (2007). Reduction in growth rate in *Phaeodactylum tricornutum* (Bacillariophyceae) and *Dunaliella tertiolecta* (Chlorophyceae) induced by UV-B radiation. *Journal of Photochemistry and Photobiology B: Biology*, *86*(3), pp. 227–233.

Aphalo, P. J., Albert, A., Bjorn, L. O., Mcleod, A. R., Robson, T. M., & Rosenqvist, E. (2012). *Beyond the Visible - A handbook of best practice in plant UV photobiology.* (P. J. Aphalo, A. Albert, L. O. Bjorn, A. R. Mcleod, T. M. Robson, & E. Rosenqvist, Eds.) (1st ed.). Helsinki, Finland: University of Helsinki, Department of Biosciences, Division of Plant Biology.

Balan, R., & Suraishkumar, G. K. (2014). Simultaneous increases in specific growth rate and specific lipid content of *Chlorella vulgaris* through UV-induced reactive species. *Biotechnology Progress*, *30*(2), pp. 291–299.

Barsanti, L., & Gualtieri, P. (2006). *Algae: anatomy, biochemistry, and biotechnology*. (L. Barsanti & P. Gualtieri, Eds.) (1st ed.). Boca Raton, FL: CRC Press Taylor & Francis Group.

Béchet, Q., Shilton, A., & Guieysse, B. (2013). Modeling the effects of light and temperature on algae growth: State of the art and critical assessment for productivity prediction during outdoor cultivation. *Biotechnology Advances*, *31*(8), pp. 1648–1663.

Ben-amotz, A. (2011). Algae applications for power generation and CO_2 recycling. *Presentation ISES Annual Meeting*. Tel-Aviv.

Ben-Amotz, A. (1995). New mode of Dunaliella biotechnology: two-phase growth for β-carotene production. *Journal of Applied Phycology*, *7*(1), pp. 65–68.

Ben-Amotz, A. (2004). Industrial production of microalgal cell-mass and secondary products – Major industrial species: *Dunaliella*. In A. Richmond (Ed.), *Handbook of microalgal culture* (1st ed., pp. 273–280). Oxford: Blackwell Science Ltd.

Ben-Amotz, A., & Avron, M. (1983). On the factors which determine massive β-carotene accumulation in the halotolerant alga *Dunaliella bardawil*. *Plant Physiology*, *72*(3), pp. 593–597.

Ben-Amotz, A., & Avron, M. (1989a). The biotechnology of mass culturing *Dunaliella* for products of commercial interest. In R. Cresswell, T. Rees, & N. Shah (Eds.), *Algal and cyanobacterial biotechnology* (1st ed., pp. 91–114). London, United Kingdom: Longman Scientific.

Ben-Amotz, A., & Avron, M. (1989b). The wavelength dependence of massive carotene synthesis in *Dunaliella bardawil* (Chlorophyceae). *Journal of Phycology*, *25*(1), pp. 175–178.

Ben-Amotz, A., Gressel, J., & Avron, M. (1987). Massive accumulation of phytoene induced by norflurazon in *Dunaliella bardawil* (Chlorophyceae) prevents recovery from photoinhibition. *Journal of Phycology*, *23*(2), pp. 176–181.

Ben-Amotz, A., Katz, A., & Avron, M. (1982). Accumulation of β-carotene in halotolerant alge: Purification and characterization of β-carotene rich globules from *Dunaliella Bardawil* (Chlorophyceae). *Journal of Phycology*, *18*(4), pp. 529–537.

Ben-Amotz, A., Lers, A., & Avron, M. (1988). Stereoisomers of β-carotene and phytoene in the alga *Dunaliella bardawil*. *Plant Physiology*, *86*(4), pp. 1286–1291.

Ben-Amotz, A., Shaish, A., & Avron, M. (1989c). Mode of action of the massively accumulated β-carotene of *Dunaliella bardawil* in protecting the alga against damage by excess irradiation. *Plant Physiology*, *91*(3), pp. 1040–1043.

Borowitzka, L. J., & Borowitzka, M. A. (1989a). Industrial production: methods and economics. In R. Cresswell, T. Rees, & N. Shah (Eds.), *Algal and cyanobacterial biotechnology* (pp. 294–316). London: Longman Scientific.

Borowitzka, L. J., & Borowitzka, M. A. (1989b). ß-Carotene (provitamin A) production with algae. In E. J. Van Damme (Ed.), *Biotechnology of vitamins, pigments and growth factors* (pp. 15–26). London, United Kingdom: Elsevier Applied Science.

Borowitzka, L. J., & Borowitzka, M. A. (1990). Commercial production of β-carotene by *Dunaliella salina* in open ponds. *Bulletin of Marine Science*, *47*(1), pp. 244–252.

Borowitzka, L. J., Moulton, T. P., & Borowitzka, M. A. (1984). The mass culture of *Dunaliella salina* for fine chemicals: From laboratory to pilot plant. *Hydrobiologia*, *116/117*(1), pp. 115–121.

Borowitzka, M. A. (1990). The mass culture of *Dunaliella salina*. In *Technical Resource Papers. Regional Workshop on the Culture and Utilisation of Seaweeds 2. Regional Seafarming*

Development and Demonstration Project, FAO Network of Aquaculture Centres (pp. 63–80). Bangkok, Thailand.

Borowitzka, M. A. (1992). Algal biotechnology products and processes - matching science and economics. *Journal of Applied Phycology*, *4*(3), pp. 267–279.

Borowitzka, M. A. (2013a). *Dunaliella*: Biology, production, and markets. In A. Richmond & H. Qiang (Eds.), *Handbook of Microalgal Culture: Applied Phycology and Biotechnology* (2nd ed., pp. 359–368). Oxford, United Kingdom: John Wiley & Sons Ltd.

Borowitzka, M. A. (2013b). High-value products from microalgae — their development and commercialisation. *Journal of Applied Phycology*, *25*(3), pp. 743–756.

Borowitzka, M. A., Borowitzka, L. J., & Kessly, D. (1990c). Effects of salinity increase on carotenoid accumulation in the green alga *Dunaliella salina*. *Journal of Applied Phycology*, *2*(2), pp. 111–119.

Borowitzka, M. A., & Huisman, J. M. (1993). The ecology of *Dunaliella salina* (Chlorophyceae, Volvocales) - effect of environmental conditions on aplanospore formation. *Botanica Marina*, *36*(3), pp. 233–243.

Borowitzka, M. A., & Siva, C. J. (2007). The taxonomy of the genus *Dunaliella* (Chlorophyta, Dunaliellales) with emphasis on the marine and halophilic species. *Journal of Applied Phycology*, *19*(5), pp. 567–590.

Bouchard, J. N., Campbell, D. A., & Roy, S. (2005). Effects of UV-B radiation on the D1 protein repair cycle of natural phytoplankton communities from three latitudes (Canada, Brazil, and Argentina). *Journal of Phycology*, *41*(2), pp. 273–286.

Bouchard, J. N., Garcia-Gómez, C., Rosario Lorenzo, M., & Segovia, M. (2013). Differential effect of ultraviolet exposure (UVR) in the stress response of the Dinophycea *Gymnodinium sp*. and the Chlorophyta *Dunaliella tertiolecta*: Mortality versus survival. *Marine Biology*, *160*(10), pp. 2547–2560.

Briggs, W. R., & Christie, J. M. (2002). Phototropins 1 and 2: Versatile plant blue-light receptors. *Trends in Plant Science*, *7*(5), pp. 204–210.

Brown, B. A., Cloix, C., Jiang, G. H., Kaiserli, E., Herzyk, P., Kliebenstein, D. J., & Jenkins, G. I. (2005). A UV-B-specific signaling component orchestrates plant UV protection. *Proceedings of the National Academy of Sciences of the United States of America*, *102*(50), pp. 18225–18230.

Buma, A. G. J., Visser, R. J. W., van de Poll, W. H., Villafañe, V. E., Janknegt, P. J., & Helbling, W. E.

(2009). Wavelength-dependent xanthophyll cycle activity in marine microalgae exposed to natural ultraviolet radiation. *European Journal of Phycology*, *444*(4), pp. 515–524.

Cheng, L., Qiao, D. R., Lu, X. Y., Xiong, Y., Bai, L. H., Xu, H., … Cao, Y. (2007). Identification and expression of the gene product encoding a CPD photolyase from *Dunaliella salina*. *Journal of Photochemistry and Photobiology B: Biology*, *87*(2), pp. 137–143.

Chisti, Y. (2016). Large-Scale Production of Algal Biomass: Raceway Ponds. In F. Bux & Y. Chisti (Eds.), *Algal Biotechnology* (1st ed., pp. 21–40). Switzerland: Springer International Publishing.

Coesel, S., Mangogna, M., Ishikawa, T., Heijde, M., Rogato, A., Finazzi, G., … Falciatore, A. (2009). Diatom PtCPF1 is a new cryptochrome/photolyase family member with DNA repair and transcription regulation activity. *EMBO Reports*, *10*(6), pp. 655–661.

Cysewski, G. R., & Todd Lorenz, R. (2004). Industrial production of microalgal cell-mass and secondary products – species of high potential: *Haematococcus*. In A. Richmond (Ed.), *Handbook of microalgal culture* (1st ed., pp. 281–288). Oxford, United Kingdom: Blackwell Science Ltd.

D'Autréaux, B., & Toledano, M. B. (2007). ROS as signalling molecules: Mechanisms that generate specificity in ROS homeostasis. *Nature Reviews Molecular Cell Biology*, *8*(10), pp. 813–824.

Day, J. G., & Brand, J. J. (2005). Cryopreservation methods for maintaining microalgal cultures. In R. A. Andersen (Ed.), *Algal culturing techniques* (1st ed., pp. 165–187). Burlington, MA: Elsevier Academic Press.

Deininger, W., Kröger, P., Hegemann, U., Lottspeich, F., & Hegemann, P. (1995). Chlamyrhodopsin represents a new type of sensory photoreceptor. *The EMBO Journal*, *14*(23), pp. 5849–5858.

Demmig-Adams, B., & Adams, W. W. (1992). Photoprotection and other responses of plants to high light stress. *Annual Review of Plant Physiology and Plant Molecular Biology*, *43*(1), pp. 599–626.

Dring, M. J., Wagner, A., Boeskov, J., & Lüning, K. (1996). Sensitivity of intertidal and subtidal red algae to UVA and UVB radiation, as monitored by chlorophyll fluorescence measurements: Influence of collection depth and season, and length of irradiation. *European Journal of Phycology*, *31*(4), pp. 293–302.

Duerr, E. O., Molnar, A., & Sato, V. (1998). Cultured microalgae as aquaculture feeds. *Journal of Marine Biotechnology*, *6*(2), pp. 65–70.

Dufossé, L., Galaup, P., Yaron, A., Arad, S. M., Blanc, P., Chidambara Murthy, K. N., & Ravishankar, G. a. (2005). Microorganisms and microalgae as sources of pigments for food use: a scientific oddity or an industrial reality? *Trends in Food Science & Technology*, *16*(9), pp. 389–406.

Ebnet, E., Fischer, M., Deininger, W., & Hegemann, P. (1999). Volvoxrhodopsin, a light-regulated sensory photoreceptor of the spheroidal green alga *Volvox carteri*. *The Plant Cell*, *11*, pp. 1473–1484.

Environmental Protection Agency (2000). *Constructed Wetlands Treatment of Municipal Wastewaters (EPA/625/R-99/010)*. Cincinnati, OH.

Fachet, M., Hermsdorf, D., Rihko-Struckmann, L., & Sundmacher, K. (2016). Flow cytometry enables dynamic tracking of algal stress response: A case study using carotenogenesis in *Dunaliella salina*. *Algal Research*, *13*, pp. 227–234.

Farman, J. C., Gardiner, B. G., & Shanklin, J. D. (1985). Large losses of total ozone in Antarctica reveal seasonal ClOx/NOx interaction. *Nature*, *315*(6016), pp. 207–210.

Fernanda Pessoa, M. (2012). Harmful effects of UV radiation in algae and aquatic macrophytes – a review. *Emirates Journal of Food and Agriculture*, *24*(6), pp. 510–526.

Forján, E., Garbayo, I., & Henriques, M. (2011). UV-A mediated modulation of photosynthetic efficiency, xanthophyll cycle and fatty acid production of *Nannochloropsis*. *Marine Biotechnology*, *13*(3), pp. 366–375.

Gao, Q., & Garcia-Pichel, F. (2011). Microbial ultraviolet sunscreens. *Nature Reviews Microbiology*, *9*(11), pp. 791–802.

García-Gómez, C., Gordillo, F. J. L., Palma, A., Lorenzo, R. M., & Segovia, M. (2014). Elevated CO_2 alleviates high PAR and UV stress in the unicellular chlorophyte *Dunaliella tertiolecta*. *Photochemical & Photobiological Sciences*, *13*(9), pp. 1347–1358.

García-Gómez, C., Mata, T., van Breusegem, F., & Segovia, M. (2016). Low-steady-state metabolism induced by elevated CO_2 increases resilience to UV radiation in the unicellular green-algae *Dunaliella tertiolecta*. *Environmental and Experimental Botany*, *132*, pp. 163–174.

García-Gómez, C., Parages, M., Jiménez, C., Palma, A., Mata, T., & Segovia, M. (2012). Cell survival after UV radiation stress in the unicellular chlorophyte *Dunaliella tertiolecta* is mediated by DNA repair and MAPK phosphorylation. *Journal of Experimental Botany*, *63*(2), pp. 695–709.

Garcia-Pichel, F. (1994). A model for internal self-shading in planktonic organisms and its

implications for the usefulness of ultraviolet sunscreens. *Limnology and Oceanography*, *39*(7), pp. 1704–1717.

Ghetti, F., Checcucci, G., & Bornman, J. F. (Eds.). (2006). *Environmental UV radiation: Impact on ecosystems and human health and predictive models.* (Vol. 57). Dordrecht, Netherlands: Springer Netherlands.

Ghetti, F., Fuoco, S., & Checcucci, G. (1998). UV-B Monochromatic action spectrum for the inhibition of photosynthetic oxygen production in the green alga *Dunaliella salina*. *Photochemistry and Photobiology*, *68*(3), pp. 276–280.

Ghetti, F., Herrmann, H., Häder, D.-P., & Seidlitz, H. K. (1999). Spectral dependence of the inhibition of photosynthesis under simulated global radiation in the unicellular green alga *Dunaliella salina*. *Journal of Photochemistry and Photobiology B: Biology*, *48*(2–3), pp. 166–173.

Ginzburg, M., & Ginzburg, B. Z. (1985). Ion and glycerol concentrations in 12 isolates of *Dunaliella*. *Journal of Experimental Botany*, *36*(7), pp. 1064–1074.

Goiris, K., Muylaert, K., Voorspoels, S., Noten, B., De Paepe, D., E Baart, G. J., & De Cooman, L. (2014). Detection of flavonoids in microalgae from different evolutionary lineages. *Journal of Phycology*, *50*(3), pp. 483–492.

Grobbelaar, J. U. (2010). Microalgal biomass production: challenges and realities. *Photosynthesis Research*, *106*(1–2), pp. 135–144.

Grobbelaar, J. U. (2012). Microalgae mass culture: The constraints of scaling-up. *Journal of Applied Phycology*, *24*(3), pp. 315–318.

Häder, D.-P. (1997). Effects of solar UV-B radiation on aquatic ecosystems. In P. Lumsden (Ed.), *Plants and UV-B - Responses to environmental change* (pp. 171–194). Cambridge, United Kingdom: Cambridge University Press.

Hagen C., Braune, W., Birckner, E., & Nuske, J. (1993). Functional aspects of secondary carotenoids in *Haematococcus lacustris* (Girod) Rostafinski (Volvocales). I. The accumulation period as an active metabolic process. *New Phytologist*, *125*(3), pp. 625–633.

Hannach, G., & Sigleo, A. C. (1998). Photoinduction of UV-absorbing compounds in six species of marine phytoplankton. *Marine Ecology Progress Series*, *174*, pp. 207–222.

Harrison, P. J., & Berges, J. A. (2005). Marine culture media. In R. A. Andersen (Ed.), *Algal Culturing Techniques* (1st ed., pp. 21–35). Burlington, MA, USA: Elsevier Academic Press.

Havelková-Doušová, H., Prášil, O., & Behrenfeld, M. J. (2004). Photoacclimation of *Dunaliella tertiolecta* (Chlorophyceae) under fluctuating irradiance. *Photosynthetica*, *42*(2), pp. 273–281.

Hegemann, P. (2008). Algal sensory photoreceptors. *Annual Review of Plant Biology*, *59*(June), pp. 167–189.

Heraud, P., & Beardall, J. (2000). Changes in chlorophyll fluorescence during exposure of *Dunaliella tertiolecta* to UV radiation indicate a dynamic interaction between damage and repair processes. *Photosynthesis Research*, *63*(2), pp. 123–134.

Herrmann, H., Häder, D.-P., Köfferlein, M., Seidlitz, H. K., & Ghetti, F. (1996). Effects of UV radiation on photosynthesis of phytoplankton exposed to solar simulator light. *Journal of Photochemistry and Photobiology B: Biology*, *34*(1), pp. 21–28.

Herrmann, H., Häder, D. P., & Ghetti, F. (1997). Inhibition of photosynthesis by solar radiation in Dunaliella salina: relative efficiencies of UV-B, UV-A and PAR. *Plant, Cell & Environment*, *20*(3), pp. 359–365.

Hollósy, F. (2002). Effects of ultraviolet radiation on plant cells. *Micron*, *33*(2), pp. 179–197.

Holmes, M. (2006). Non-damaging and positive effects of UV radiation on higher plants. In F. Ghetti, G. Checcucci, & J. F. Bornman (Eds.), *Environmental UV Radiation: Impact on ecosystems and human health and predictive models* (Vol. 57, pp. 159–177). Dordrecht, Netherlands: Springer.

Holzinger, A., & Lütz, C. (2006). Algae and UV irradiation: effects on ultrastructure and related metabolic functions. *Micron*, *37*(3), pp. 190–207.

Hosseini Tafreshi, A., & Shariati, M. (2009). *Dunaliella* biotechnology: methods and applications. *Journal of Applied Microbiology*, *107*(1), pp. 14–35.

Im, C. S., Eberhard, S., Huang, K., Beck, C. F., & Grossman, A. R. (2006). Phototropin involvement in the expression of genes encoding chlorophyll and carotenoid biosynthesis enzymes and LHC apoproteins in *Chlamydomonas reinhardtii*. *Plant Journal*, *48*(1), pp. 1–16.

Jahnke, L. S. (1999). Massive carotenoid accumulation in *Dunaliella bardawil* induced by ultraviolet-A radiation. *Journal of Photochemistry and Photobiology B: Biology*, *48*(1), pp. 68–74.

Jahnke, L. S., White, A. L., & Sampath-Wiley, P. (2009). The effect of ultraviolet radiation on *Dunaliella*. In A. Ben-Amotz, J. E. Polle, & R. V. S. Rao (Eds.), *The alga* Dunaliella (1st ed., pp.

231–272). Enfield, CN: Taylor & Francis Inc.

Jenkins, G. I. (2009). Signal transduction in responses to UV-B radiation. *Annual Review of Plant Biology*, *60*, pp. 407–431.

Jiménez, C., Figueroa, F. L., Aguilera, J., Lebert, M., & Häder, D.-P. (1996). Phototaxis and gravitaxis in *Dunaliella bardawil*: Influence of UV radiation. *Acta Protozoologica*, *35*(4), pp. 287–295.

Karlicek, R. F. (2013). UV-LED's and curing applications: technology and market developments. *Radtech Report*, pp. 1–69.

Kianianmomeni, A., & Hallmann, A. (2014). Algal photoreceptors: in vivo functions and potential applications. *Planta*, *239*(1), pp. 1–26.

Kliebenstein, D. J., Lim, J. E., Landry, L. G., & Last, R. L. (2002). *Arabidopsis* UVR8 regulates ultraviolet-B signal transduction and tolerance and contains sequence similarity to human regulator of chromatin condensation. *Plant Physiology*, *130*(1), pp. 234–243.

Lamers, P. P., Janssen, M., De Vos, R. C., Bino, R. J., & Wijffels, R. H. (2008). Exploring and exploiting carotenoid accumulation in *Dunaliella salina* for cell-factory applications. *Trends in Biotechnology*, *26*(11), pp. 631–638.

Lemoine, Y., & Schoefs, B. (2010). Secondary ketocarotenoid astaxanthin biosynthesis in algae: a multifunctional response to stress. *Photosynthesis Research*, *106*(1–2), pp. 155–177.

Lerche, W. (1937). Untersuchungen über Entwicklung und Fortpflan- zung in der Gattung *Dunaliella*. *Archif Protistenkunde*, *88*, pp. 236–268.

Lesser, M. P. (2006). Oxidative stress in marine environments: Biochemistry and physiological ecology. *Annual Review of Physiology*, *68*(1), pp. 253–278.

Lesser, M. P., Cullen, J. J., & Neale, P. J. (1994). Carbon uptake in a marine diatom during acute exposure to ultraviolet B radiation: relative importance of damage and repair. *Journal of Phycology*. *30. pp. 183-192*

Lichtenthaler Hartmut K. (1987). Chlorophylls and carotenoids: pigments of photosynthetic biomembranes. In L. Packer & R. Douce (Eds.), *Methods in Enzymology* (148th ed., pp. 350–382). San Diego, CA: Academic Press.

Lichtenthaler Hartmut K. (2012). Biosynthesis, cocalization and concentration of carotenoids in plants and algae. In J. J. Eaton-Rye, B. C. Tripathy, & T. D. Sharkey (Eds.), *Photosynthesis: Plastid Biology, Energy Conversion and Carbon Assimilation* (34th ed., Vol. 34, pp. 95–112).

Dordrecht, Netherlands: Springer Netherlands.

Loeblich, L. A. (1982). Photosynthesis and pigments influenced by light intensity and salinity in the halophile *Dunaliella salina* (Chlorophyta). *Journal of the Marine Biological Association of the United Kingdom*, *62*(3), pp. 493–508.

Lorenz, M., Friedl, T., & Day, J. G. (2005). Perpetual Maintenance of actively metabolizing microalgal cultures. In R. A. Andersen (Ed.), *Algal Culturing Techniques* (1st ed., pp. 145–163). Burlington, MA: Elsevier Academic Press.

Luck, M., Mathes, T., Bruun, S., Fudim, R., Hagedorn, R., Tran Nguyen, T. M., … Hegemann, P. (2012). A photochromic histidine kinase rhodopsin (HKR1) that is bimodally switched by ultraviolet and blue light. *The Journal of Biological Chemistry*, *287*(47), pp. 40083–40090.

Lund, J. W. G., Kipling, C., & Cren, E. D. (1958). The inverted microscope method of estimating algal numbers and the statistical basis of estimations by counting. *Hydrobiologia*, *11*(2), pp. 143–170.

Macintyre, S. (1993). Vertical mixing in a shallow, eutrophic lake: Possible consequences for the light climate of phytoplankton. *Limnology and Oceanography*, *38*(4), pp. 798–817.

Madronich, S., McKenzie, R. L., Caldwell, M. M., & Björn, L. O. (1995). Changes in biologically-active ultraviolet radiation reaching the Earth's surface. *Ambio*, *24*(3), pp. 143–152.

Masi, A., & Melis, A. (1997). Morphological and molecular changes in the unicellular green alga *Dunaliella salina* grown under supplemental UV-B radiation: cell characteristics and Photosystem II damage and repair properties. *Biochimica et Biophysica Acta*, *1321*(2), pp. 183–193.

Masschelein, W. (2002). *Ultraviolet light in water and wastewater sanitation.* (R. G. Rice, Ed.) (1st ed.). Boca Raton, FL: CRC Press Taylor & Francis Group.

Massyuk, N. P. (1973). *Morphology, Taxonomy, Ecology and Geographic Distribution of the Genus* Dunaliella Teod*. and Prospects for Its Potential Utilization*. (N. P. Massyuk Eds). Kiev, Ukrain: Naukova Dumka.

Meghan Downes, C., & Hu, Q. (2013). First principles of techno-economic analysis of algal mass culture. In A. Richmond & Q. Hu (Eds.), *Handbook of Microalgal Culture: Applied Phycology and Biotechnology* (2nd ed., pp. 310–326). Oxford, United Kingdom: John Wiley & Sons Ltd.

Melis, A., Nemson, J. A., & Harrison, M. A. (1992). Damage to functional components and partial degradation of Photosystem II reaction center proteins upon chloroplast exposure to

ultraviolet-B radiation. *Biochimica et Biophysica Acta*, *1100*(3), pp. 312–320.

Metcalf, & Eddy. (2003). *Wastewater Engineering - Treatment and reuse*. (G. Tchobanoglous, F. L. Burton, & H. D. Stenself, Eds.) (4th ed.). Boston, MA: McGraw-Hill.

Mogedas, B., Casal, C., Forján, E., & Vílchez, C. (2009). β-carotene production enhancement by UV-A radiation in *Dunaliella bardawil* cultivated in laboratory reactors. *Journal of Bioscience and Bioengineering*, *108*(1), pp. 47–51.

Mogedas, B., Salguero, A., Casal, C., & Vílchez, C. (2007). UV-A promotes long-term carotenoid production of *Dunaliella* in photobioreactors with retention of cell viability. In A. Méndez-Vilas (Ed.), *Communicating current research and educational topics and trends in applied microbiology* (1st ed., pp. 348–355). Badajoz, Spain: Formatex.

Möglich, A., Yang, X., Ayers, R. A., & Moffat, K. (2010). Structure and function of plant photoreceptors. *Annual Review of Plant Biology*, *61*(June), pp. 21–47.

Molina Grima, E., Acien Fernandez, A. F. G., & Robles Medina, A. (2004). Downstream processing of cell-mass and products. In A. Richmond (Ed.), *Handbook of microalgal culture* (1st ed., pp. 215–251). Oxford, United Kingdom: Blackwell Science Ltd.

Molina Grima, E., Belarbi, E.-H., Acién Fernández, F. G., Robles Medina, A., & Chisti, Y. (2003). Recovery of microalgal biomass and metabolites: process options and economics. *Biotechnology Advances*, *20*(7–8), pp. 491–515.

Monte, J., Sá, M., Galinha, C. F., Costa, L., Hoekstra, H., Brazinha, C., & Crespo, J. G. (2018). Harvesting of *Dunaliella salina* by membrane filtration at pilot scale. *Separation and Purification Technology*, *190*(August 2017), pp. 252–260.

Montero, O., Klisch, M., Häder, D.-P., & Lubian, L. M. (2002). Comparative sensitivity of seven marine microalgae to cumulative exposure to ultraviolet-B radiation with daily increasing doses. *Botanica Marina*, *45*(4), pp. 305–315.

Moon, Y.-J., Kim, S. Il, & Chung, Y.-H. (2012). Sensing and Responding to UV-A in Cyanobacteria. *International Journal of Molecular Sciences*, *13*(12), pp. 16303–16332.

Moon, Y. J., Kim, S. Y., Jung, K. H., Choi, J. S., Park, Y. M., & Chung, Y. H. (2011). Cyanobacterial phytochrome Cph2 is a negative regulator in phototaxis toward UV-A. *FEBS Letters*, *585*(2), pp. 335–340.

Moulton, T. P., & Borowitzka, L. J. (1987a). The mass culture of *Dunaliella salina* for β-carotene: from pilot plant to production plant. *Hydrobiologia*, *151/152*, pp. 99–105.

Moulton, T. P., Sommer, T. R., Burford, M. A., & Borowitzka, L. J. (1987b). Competition between *Dunaliella* species at high salinity. *Hydrobiologia*, *151/152*, pp. 107–116.

Nagel, G. (2002). Channelrhodopsin-1: A light-gated proton channel in green algae. *Science*, *296*(5577), pp. 2395–2398.

Nagel, G., Szellas, T., Huhn, W., Kateriya, S., Adeishvili, N., Berthold, P., … Bamberg, E. (2003). Channelrhodopsin-2, a directly light-gated cation-selective membrane channel. *Proceedings of the National Academy of Sciences of the United States of America*, *100*(24), pp. 13940–13945.

Navarro, E., Muñiz, S., Korkaric, M., Wagner, B., De Cáceres, M., & Behra, R. (2014). Ultraviolet radiation dose calculation for algal suspensions using UV-A and UV-B extinction coefficients. *Journal of Photochemistry and Photobiology B: Biology*, *132*, pp. 94–101.

Neale, P. (2000). Spectral weighting functions for quantifying effects of UV radiation in marine ecosystems. In *The effects of UV Radiation in the marine environment* (pp. 72–100).

Neale, P. J., Helbling, W. E., Zagarese, H., Häder, D.-P., & Jori, G. (2003). Modulation of UVR exposure and effects by vertical mixing and advection. In E. W. Helbling & H. Zagarese (Eds.), *UV effects in aquatic organisms and ecosystems* (1st ed., pp. 107–134). Cambridge, United Kingdom: The Royal Society of Chemistry.

Niyogi, K. K., Björkman, O., & Grossman, A. R. (1997). The roles of specific xanthophylls in photoprotection. *Proceedings of the National Academy of Sciences of the United States of America*, *94*(25), pp. 14162–14167.

Oren, A. (2005). A hundred years of *Dunaliella* research: 1905-2005. *Saline Systems*, *1*:2.

Pfannschmidt, T. (2003). Chloroplast redox signals: How photosynthesis controls its own genes. *Trends in Plant Science*, *8*(1), pp. 33–41.

Plaza, M., Herrero, M., Cifuentes, A., & Ibáñez, E. (2009). Innovative natural functional ingredients from microalgae. *Journal of Agricultural and Food Chemistry*, *57*(16), pp. 7159–7170.

Portwich, A., & Garcia-Pichel, F. (2000). A novel prokaryotic UVB photoreceptor in the cyanobacterium Chlorogloeopsis PCC 6912. *Photochemistry and Photobiology*, *71*(4), pp. 493–498.

Prussi, M., Buffi, M., Casini, D., Chiaramonti, D., Martelli, F., Carnevale, M., … Rodolfi, L. (2014). Experimental and numerical investigations of mixing in raceway ponds for algae cultivation. *Biomass and Bioenergy*, *67*, pp. 390–400.

Pulz, O. (2001). Photobioreactors: production systems for phototrophic microorganisms. *Applied Microbiology and Biotechnology*, *57*(3), pp. 287–293.

Rastogi, R. P., Richa, Sinha, R. P., Singh, S. P., & Häder, D.-P. (2010). Photoprotective compounds from marine organisms. *Journal of Industrial Microbiology & Biotechnology*, *37*(6), pp. 537–558.

Richmond, A. (2004). *Handbook of microalgal culture*. (A. Richmond, Ed.) (1st ed.). Oxford, United Kingdom: Blackwell Science Ltd.

Richter, P. R., Häder, D.-P., Gonçalves, R. J., Marcoval, M. A., Villafañe, V. E., & Helbling, W. E. (2007). Vertical migration and motility responses in three marine phytoplankton species exposed to solar radiation. *Photochemistry and Photobiology*, *83*(4), pp. 810–817.

Rizzini, L., Favory, J.-J., Cloix, C., Faggionato, D., O'Hara, A., Kaiserli, E., … Ulm, R. (2011). Perception of UV-B by the *Arabidopsis* UVR8 protein. *Science*, *332*(6025), pp. 103–106.

Roy, S. (2000). Strategies for the minimisation of UV-induced damage. In P. G. . Campbell, R. M. Harrison, & S. J. de Mora (Eds.), *The effects of UV radiation in the marine environment* (1st ed., pp. 177–205). Cambridge, United Kingdom: Cambridge University.

Rozema, J., Björn, L. O., Bornman, J. F., Gaberscik, A., Häder, D.-P., Trost, T., … Meijkamp, B. B. (2002). The role of UV-B radiation in aquatic and terrestrial ecosystems--an experimental and functional analysis of the evolution of UV-absorbing compounds. *Journal of Photochemistry and Photobiology. B, Biology*, *66*(1), pp. 2–12.

Salguero, A., León, R., Mariotti, A., de la Morena, B., Vega, J. M., & Vílchez, C. (2005). UV-A mediated induction of carotenoid accumulation in *Dunaliella bardawil* with retention of cell viability. *Applied Microbiology and Biotechnology*, *66*(5), pp. 506–511.

Salinas, S., Brown, S. C., Mangel, M., & Munch, S. B. (2013). Non-genetic inheritance and changing environments. *Non-Genetic Inheritance*, *1*, pp. 38–50.

Segovia, M., Mata, T., Palma, A., García-Gómez, C., Lorenzo, R., Rivera, A., & Figueroa, F. L. (2015). *Dunaliella tertiolecta* (Chlorophyta) avoids cell death under ultraviolet radiation by triggering alternative photoprotective mechanisms. *Photochemistry and Photobiology*, *91*(6), pp. 1389–1402.

Shaish, A., Avron, M., Pick, U., & Ben-Amotz, A. (1993). Are active oxygen species involved in induction of β-carotene in *Duniella bardawil*? *Planta*, *190*(3), pp. 363–368.

Shelly, K., Heraud, P., & Beardall, J. (2002). Nitrogen limitation in *Dunaliella tertiolecta*

(Chlorophyceae) leads to increased susceptibility to damage by ultraviolet-B radiation but also increased repair capacity. *Journal of Phycology*, *38*(4), pp. 713–720.

Sinha, R. P., & Häder, D.-P. (2002). UV-induced DNA damage and repair: a review. *Photochemical & Photobiological Sciences*, *1*(4), pp. 225–236.

Sinha, R. P., Klisch, M., Gröniger, A., & Häder, D.-P. (2001). Responses of aquatic algae and cyanobacteria to solar UV-B. *Plant Ecology*, *154*(1), pp. 221–236.

Smith, B. M., Morrissey, P. J., Guenther, J. E., Nemson, J. . A., Harrison, M. A., Allen, J. F., & Melis, A. (1990). Response of the photosynthetic apparatus in *Dunaliella salina* (green algae) to irradiance stress. *Plant Physiology*, *93*(4), pp. 1433–1440.

Song, J.-Y., Cho, H. S., Cho, J.-I., Jeon, J.-S., Lagarias, J. C., & Park, Y.-I. (2011). Near-UV cyanobacteriochrome signaling system elicits negative phototaxis in the cyanobacterium *Synechocystis sp.* PCC 6803. *Proceedings of the National Academy of Sciences of the United States of America*, *108*(26), pp. 10780–10785.

Spolaore, P., Joannis-Cassan, C., Duran, E., & Isambert, A. (2006). Commercial applications of microalgae. *Journal of Bioscience and Bioengineering*, *101*(2), pp. 87–96.

Srinivas, R., & Ochs, C. (2012). Effect of UV-A irradiance on lipid accumulation in *Nannochloropsis oculata*. *Photochemistry and Photobiology*, *88*(3), pp. 684–689.

Steinbrenner, J., & Linden, H. (2003). Light induction of carotenoid biosynthesis genes in the green alga *Haematococcus pluvialis*: Regulation by photosynthetic redox control. *Plant Molecular Biology*, *52*(2), pp. 343–356.

Takahashi, F., Yamagata, D., Ishikawa, M., Fukamatsu, Y., Ogura, Y., Kasahara, M., … Kataoka, H. (2007). Aureochrome, a photoreceptor required for photomorphogenesis in stramenopiles. *Proceedings of the National Academy of Sciences of the United States of America*, *104*(49), pp. 19625–19630.

Tian, J., & Yu, J. (2009). Changes in ultrastructure and responses of antioxidant systems of algae (*Dunaliella salina*) during acclimation to enhanced ultraviolet-B radiation. *Journal of Photochemistry and Photobiology. B, Biology*, *97*(3), pp. 152–160.

Tilbrook, K., Arongaus, A. B., Binkert, M., Heijde, M., Yin, R., & Ulm, R. (2013). The UVR8 UV-B photoreceptor: Perception, signaling and response. *The Arabidopsis Book*, *11*, pp. e0164.

Tilbrook, K., Dubois, M., Crocco, C. D., Yin, R., Chappuis, R., Allorent, G., … Ulm, R. (2016). UV-B perception and acclimation in *Chlamydomonas reinhardtii*. *The Plant Cell*, *28*, pp. 966–983.

Tredici, M. R. (2004). Mass Production of Microalgae: Photobioreactors. In A. Richmond (Ed.), *Handbook of Microalgal Culture: Applied Phycology and Biotechnology* (pp. 178–214). Oxford, United Kingdom: Blackwell Science Ltd.

Tredici, M. R. (2010). Photobiology of microalgae mass cultures: understanding the tools for the next green revolution. *Biofuels*, *1*(1), pp. 143–162.

Tripathy, B. C., & Oelmüller, R. (2012). Reactive oxygen species generation and signaling in plants. *Plant Signaling & Behavior*, *7*(12), pp. 1621–1633.

Trippens, J., Greiner, A., Schellwat, J., Neukam, M., Rottmann, T., Lu, Y., … Kreimer, G. (2012). Phototropin influence on eyespot development and regulation of phototactic behavior in *Chlamydomonas reinhardtii*. *The Plant Cell*, *24*(11), pp. 4687–702.

Uriarte, I., Farias, A., Hawkins, A. J. S., & Bayne, B. L. (1993). Cell characteristics and biochemical composition of *Dunaliella primolecta* Butcher conditioned at different concentrations of dissolved nitrogen. *Journal of Applied Phycology*, *5*(4), pp. 447–453.

van de Poll, W. H., Buma, A. G. J., Visser, R. J. W., Janknegt, P. J., Villafañe, V. E., & Helbling, E. W. (2010). Xanthophyll cycle activity and photosynthesis of *Dunaliella tertiolecta* (Chlorophyceae) and *Thalassiosira weissflogii* (Bacillariophyceae) during fluctuating solar radiation. *Phycologia*, *49*(3), pp. 249–259.

Vass, I., Turcsányi, E., Touloupakis, E., Ghanotakis, D., & Petrouleas, V. (2002). The mechanism of UV-A radiation-induced inhibition of photosystem II electron transport studied by EPR and chlorophyll fluorescence. *Biochemistry*, *41*(32), pp. 10200–10208.

Verdaguer, D., Jansen, M. A. K., Llorens, L., Morales, L. O., & Neugart, S. (2016). UV-A radiation effects on higher plants: exploring the known unknown. *Plant Science*, *255*, pp. 72–81.

Wang, S.-B., Chen, F., Sommerfeld, M., & Hu, Q. (2004). Proteomic analysis of molecular response to oxidative stress by the green alga *Haematococcus pluvialis* (Chlorophyceae). *Planta*, *220*, pp. 17–29.

Wargent, & Jordan, B. (2013). From ozone depletion to agriculture: understanding the role of UV radiation in sustainable crop production. *New Phytologist*, *197*(4), pp. 1058–1076.

White, A. L., & Jahnke, L. S. (2002). Contrasting effects of UV-A and UV-B on photosynthesis and photoprotection of β-carotene in two *Dunaliella* spp. *Plant & Cell Physiology*, *43*(8), pp. 877–84.

White, A. L., & Jahnke, L. S. (2004). Removing UV-A and UV-C radiation from UV-B fluorescent lamp

emissions. Differences in the inhibition of photosynthesis in the marine alga *Dunaliella tertiolecta* using chromate versus cellulose acetate-polyester filters. *Photochemistry and Photobiology*, *80*(2), pp. 340–5.

Winkel, B. S. J. (2006). The biosynthesis of flavonoids. In E. Grotewold (Ed.), *The science of flavonoids* (1st ed., pp. 71–95). New York, NY: Springer-Verlag New York.

Wright, S. W., Jeffrey, S. W., Mantoura, R. F. C., Llewellyn, C. A., Bjornland, T., Repeta, D., & Welschmeyer, N. (1991). Improved HPLC method for the analysis of chlorophylls and carotenoids from marine phytoplankton. *Marine Ecology Progress Series*, *77*(2), pp. 183–196.

Wu, Z., Chen, G., Chong, S., Mak, N.-K., Chen, F., & Jiang, Y. (2010). Ultraviolet-B radiation improves astaxanthin accumulation in green microalga *Haematococcus pluvialis*. *Biotechnology Letters*, *32*(12), pp. 1911–1914.

Xiong, F., & Komenda, J. (1997). Strategies of ultraviolet-B protection in microscopic algae. *Physiologia Plantarum*, *100*(2), pp. 378–388.

Xue, L., Zhang, Y., Zhang, T., An, L., & Wang, X. (2005). Effects of enhanced ultraviolet-B radiation on algae and cyanobacteria. *Critical Reviews in Microbiology*, *31*(2), pp. 79–89.

Ye, Z.-W., Jiang, J.-G., & Wu, G.-H. (2008). Biosynthesis and regulation of carotenoids in *Dunaliella*: progresses and prospects. *Biotechnology Advances*, *26*(4), pp. 352–360.

Yu, X., Liu, H., Klejnot, J., & Lin, C. (2010). The cryptochrome blue light receptors. *The Arabidopsis Book*, *8*, pp. e0135.

Zhang, X., Tang, X., Zhou, B., Hu, S., & Wang, Y. (2015). Effect of enhanced UV-B radiation on photosynthetic characteristics of marine microalgae *Dunaliella salina* (Chlorophyta, Chlorophyceae). *Journal of Experimental Marine Biology and Ecology*, *469*, pp. 27–35.

Zhu, C., & Lee, Y. (1997). Determination of biomass dry weight of marine microalgae. *Journal of Applied Phycology*, *9*(2), pp. 189–194.

Ziegler, T., & Möglich, A. (2015). Photoreceptor engineering. *Frontiers in Molecular Biosciences*, *2*, pp. Article 30.

9 Appendices

9.1 Appendix – Industrially relevant cultivated microalgae species and their products

Table 9-1 Industrially relevant cultivated microalgae species and their products

Product class	Microalgae species	Primary high-value product	Annual production	Known secondary products	Application
Health Food	*A. platensis (Spirulina)* [19, 25]	Health food	5000 t dry weight	Phycobiliprotein (allophycocyanin, c-phycocyanin), antimicrobial compounds, DHA	Aquaculture, health food, animal feed
	C. vulgaris[20, 25]	Health food	2000 t dry weight	Lutein, canthaxanthin, astaxanthin, bioactive substances with medical properties	Aquaculture, health food, animal feed

Product class	Microalgae species	Primary high-value product	Annual production	Secondary products	Application
Carotenoids	*D.salina/ D.bardawil*[24]	β-carotene	1200 t dry weight	Zeaxanthin (from mutants)	Pigmenter (Food), pro-vitamin A, antioxidant
	H.pluvialis[24]	Astaxanthin	300 t dry weight		Pigmenter (aquaculture), anti-oxidant
	Botryococcus braunii[21]	Echinenone	No data found	Neoxanthin, loroxanthin, violaxanthin, lutein, and β-carotene	Extracellular lipids
	Chlorella ellipsoidea[25]	Zeaxanthin	No data found		
	Auxochlorella (Chlorella) protothecoides[25]	Lutein	No data found -		
	Chlorella zofingiensis[25]	Astaxanthin	No data found	Canthaxanthin and lutein	
	Scenedesmus almeriensis[25]	Lutein	No data found		

Product class	Microalgae species	Primary high-value product	Annual production	Secondary products	Application

[19] Source: Borowitzka (2013b)

[20] Source: Spolaore et al. (2006)

[21] Source: Plaza et al. (2009)

Lipids	*Nannochloropsis oculata*[24, 22]	Lipids	No data found	EPA, DHA, Feed aquaculture	
	Scenedesmus obliquus[24,25, 26]	Lipids	No data found -	EPA, DHA, Feed aquaculture	
	Phaeodactylum tricornutum[24, 26]	EPA	No data found	Fucoxanthin, Feed aquaculture	
	Porphyridium purpureum[25]	Phycoerythrin (phycobiliprotein)	No data found	Phycobiliproteins, sulphated polysaccharides, EPA, AA	

Product class	Microalgae species	Primary products	Annual production	Secondary products	Application
Sunscreens	*Nostoc punctiforme*[23]	Scytonemin	No data found		Microbial sunscreen
	Nostoc commune[27]	Mycosporine-like amino acids	No data found		Microbial sunscreen

[22] Source: Duerr et al. (1998)

[23] Source: Gao & Garcia-Pichel (2011)

9.2 Appendix – Proof of Principle Results

The current appendix offers a brief summary of the most important proof-of-principle results. An overview of all experiments is shown in Table 9-2. Proof-of-principle experiments also served to develop experimental methods and so not all experiments carried out have a significant result.

9.2.1 Proof-of-principle - Materials and methods

During the proof-of-principle stage of the project four microalgae species were tested to determine presence of a commercially beneficial UV responses, namely: *A. platensis, C. vulgaris, D. salina and H. pluvialis*. An overview of the experiments carried out is shown in Table 9-2.

Experiments were carried out using two different setups. Experiments were conducted using:

- The experimental setup described in Chapter 3 using fluorescent tubes as PAR and UV source ('unbranded UV tubes' as show in Figure 3-2).
- Custom setup using prototype LED panels provided by BioLumic as PAR and UV Source (Figure 9 1).

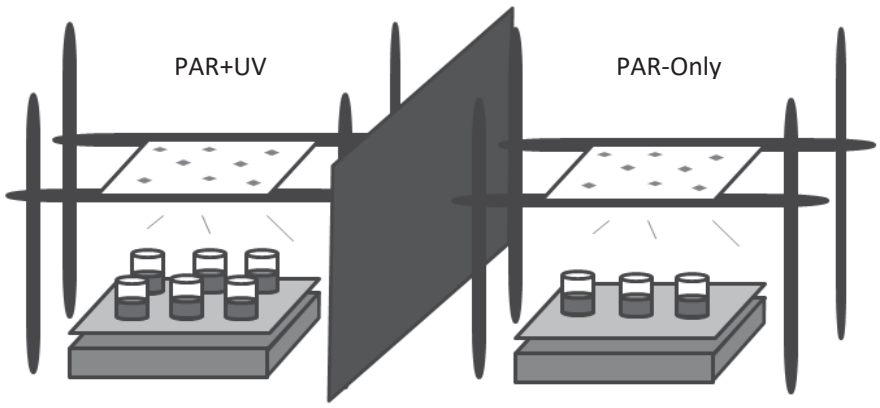

Figure 9-1 Schematic representation of experimental setup used during experiments carried out with BioLumic LED boards. Beakers covered with Petri-dish lids were placed on a shaker and illuminated from above with PAR or PAR+UV LED light.

Briefly: the custom setup experiments using the prototype LED panels were conducted in 250 mL beakers filled with 125 mL culture and covered with high clarity polystyrene Petri dish lids (Nest Biotechnology, China) (Figure 9-1). Cultures were placed on an orbital shaker (150 rpm) and illuminated with either PAR LEDs only or PAR and UV LEDs ("PAR+UV"). The setup was surrounded by large cardboard panels to prevent interference from outside light and protect the user from UV radiation. All UV experiments were carried out on the bench top without temperature,

humidity or CO_2 control. Temperature was recorded during the entire experiments using Thermochron iButton temperature data loggers (Maxim Integrated, San Jose, CA).

PAR and UV levels on the UV LED panels were controlled by setting the current on the panels and measuring the output PAR light meter and spectroradiometer, respectively. Prototype LED boards contained either PAR-Only LEDs (blue and red PAR LEDs at λ_{max} = 460 nm or λ_{max} = 665 nm) or PAR+UV LEDs (either λ_{max} = 336 nm or λ_{max} = 353 nm, Figure 9-2). Panels were named UV336 and UV353. The blue/red PAR LEDs were set to 30 µmol m^{-2} s^{-1} for each experiment. UV output was set to maximum on the PAR+UV resulting in UV irradiances 0.35-0.51 W·m^{-2}.

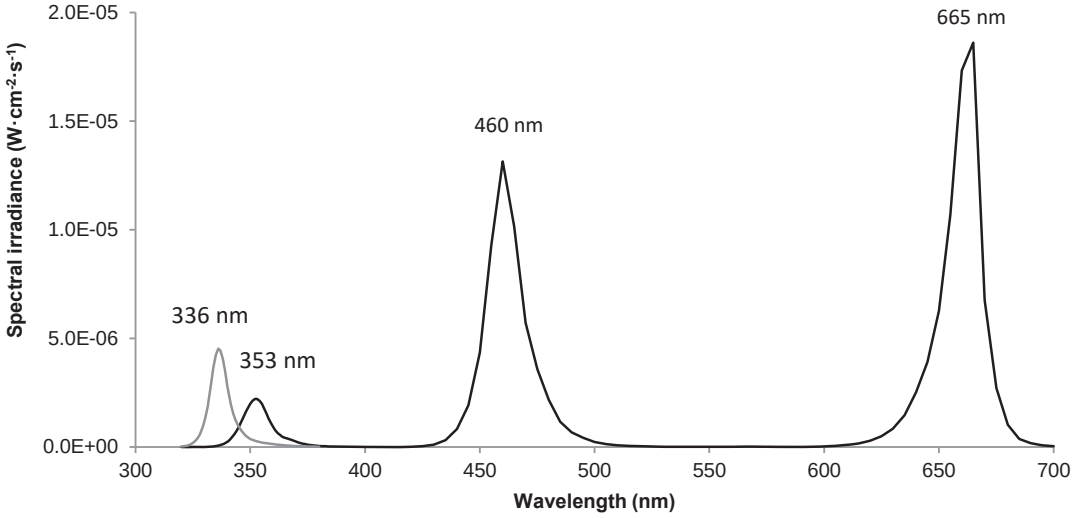

Figure 9-2 PAR and UV irradiance of panels PAR-Only, PAR+UV336 (λ_{max} = 336 nm) and PAR+UV353 (λ_{max} = 353 nm). UV spectral irradiance levels have been normalized to PAR spectral irradiance peaks (λ_{max} = 460 nm and λ_{max} = 665 nm)

Table 9-2 Overview of proof-of-principle experiments.

Strain	Media	Board/tubes	UV irradiance (W/m^2)	UV Exposure Duration ($h \cdot d^{-1}$)	PAR PFD ($\mu mol\ m^{-2}\ s^{-1}$)	PAR Exposure duration ($h \cdot d^{-1}$)	Experiment Duration (d)	Most significant change recorded
C. vulgaris UTEX 259	BG-11	LED UV353	0.35	3 or 6 hr total	PAR LED: 20 ± 2	24	6	No significant change
	BG-11	LED UV353	0.35	6 and 12	PAR LED: 30 ± 2	24	10	No significant change
	BG-11	LED UV336	0.38	6 or 12	PAR LED: 30 ± 2	24	8	No significant change
	BG-11	LED UV336	0.38	12:12 $h \cdot d^{-1}$ PAR:dark+UV	PAR LED: 30 ± 2	12 :12 $h \cdot d^{-1}$ light:dark	10	Decreased growth
	BG-11	LED UV336	0.38	12:12 $h \cdot d^{-1}$ PAR+UV:dark	PAR LED: 140 ± 10	12 :12 $h \cdot d^{-1}$ light: dark	7	No significant change
	BG-11	Fluorescent UV-A tubes	9.3	5 $h \cdot d^{-1}$ instead of PAR	Fluorescent tubes: 68 ± 5	16:8 $h \cdot d^{-1}$ light: dark	16	No significant change
D. salina UTEX LB 1644	MJM '3:1'	LED UV336	0.38	12	PAR LED: 29 ± 2	24	5	Decreased Car:Chl, decreased growth
	MJM '3:1'	LED UV336	0.38	12	PAR LED: 29 ± 2	24	4	Decreased Car:Chl, decreased growth
	MJM Tris 50 mM	LED UV353	0.35	12	PAR LED: 30 ± 1	24	12	Increased Chl
	MJM Tris 50 mM	Fluorescent UV-A tubes	10.7	24	Fluorescent tubes: 95 ± 5	24	18 (2x repeat)	Increase Car:Chl
	MJM Tris 50 mM	Fluorescent UV-A tubes	18.4	24	Fluorescent tubes: 62 ± 5	24	9	Increase Car:Chl
A. platensis UTEX LB 1926	Zarrouk	LED UV336	0.38	12	PAR LED: 29 ± 2	24	10 (2x repeat)	Increased pigment content (PC, Chl, Car)
H.pluvialis UTEX 2505	3N BBM	Fluorescent UV-A tubes	4.75	12	Fluorescent tubes: 32 ± 5	24	8	Increased reddening of cells

9.2.2 Proof-of-principle - Results

9.2.2.1 *D. salina* – '24 h·d^{-1} PAR and 24 h·d^{-1} UV' under fluorescent UV-A tubes

PAR: 95 µmol m^{-2} s^{-1} for 24 h·d^{-1} for the duration of the experiment from fluorescent tubes

UV: Broad wavelength UV-A was used for UV-A exposure (λ = 320 – 400 nm, 10.7 W·m^{-2}, 24 h·d^{-1})

Cultures were acclimatized for 4 days (PAR-Only, no UV).

At the start of culture day 5 UV was turned on (UV exposure = 0 h)

At the start of culture day 12 UV was turned off (UV exposure = 168 h)

The experiment below was the first clear proof-of-principle that a desired trait could be induced using UV radiation. Optical density, pigment extraction and cell counting were used as analytical tools. Results of a repeat experiment are shown in Figure 9-3 (initial experiment didn't record all relevant data). The increase in Car:Chl at the peak (culture day 8, UV day 4) is 52% while the difference at the end (culture day 12, UV day 8) increases to 115%.

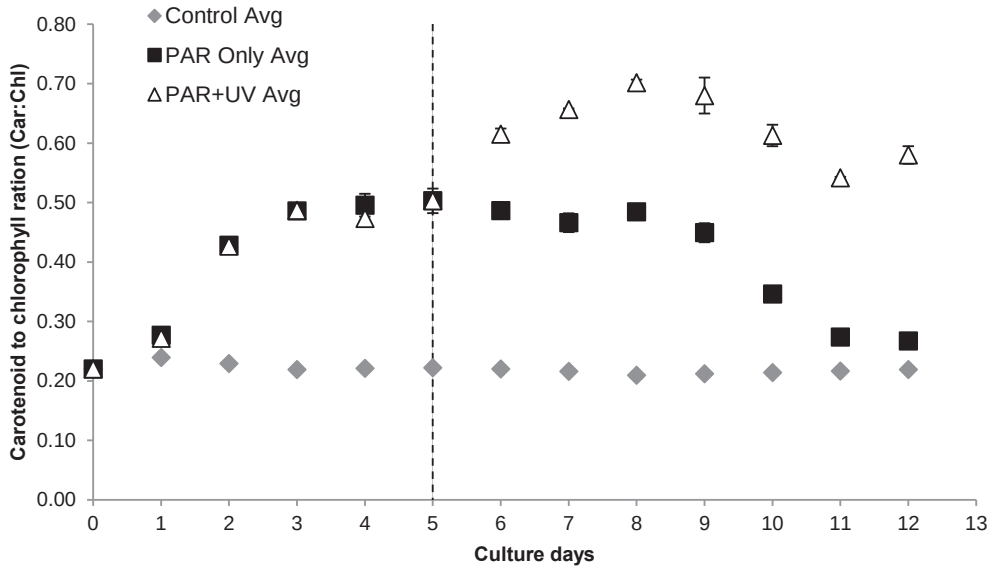

Figure 9-3 Carotenoid to chlorophyll (a+b) ratio changes during UV-A irradiance. The dotted line indicates the day that the UV lights were turned on. Besides the PAR Only control a culture, kept under normal culture conditions in the incubator, was also included in this experiment for comparison ('Control' in figure is a culture kept under standard incubator conditions). Error bars show range (n = 2).

The Car:Chl rises steadily for both experimental cultures, likely as a response of cultures being moved from maintenance conditions (24 $h \cdot d^{-1}$, 30 $\mu mol \cdot m^{-2} \cdot s^{-1}$ PAR at 2% CO_2-air content with temperature control) to the bench tope experimental setup changing culture conditions (24 $h \cdot d^{-1}$, 95 $\mu mol \cdot m^{-2} \cdot s^{-1}$ PAR at ambient CO_2-air content and no temperature control). The decrease in the Car:Chl of the PAR Only cultures is caused by a relative increase in cellular chlorophyll *(a+b)* content thought to be facilitated by increased by self-shading at higher cell density (relieved by self-shading (chloroplyll*(a+b)* data not shown, carotenoid data shown in Figure 9-4).

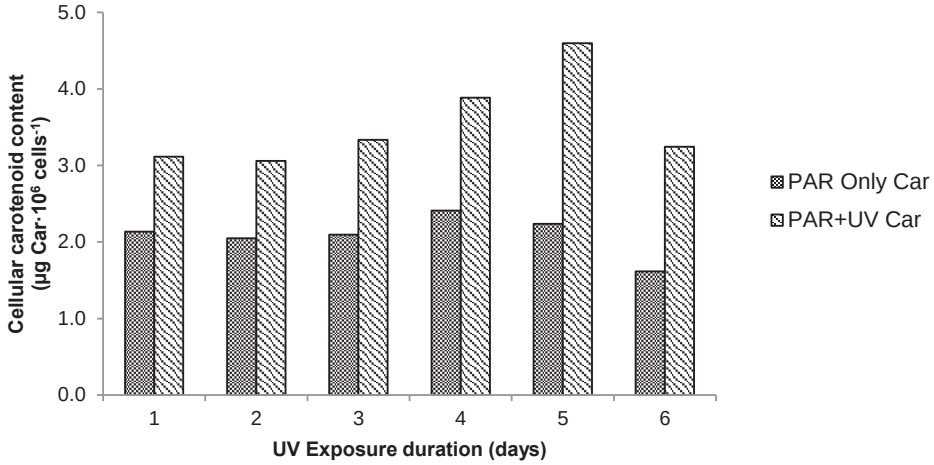

Figure 9-4 Changes in cellular carotenoid content during from continuous (24 $h \cdot d^{-1}$) UV-A exposure. Only one culture per experiment was counted so no range can be shown (n = 1).

The increase in Car:Chl ratio as a result of UV exposure can be shown to be a result of increasing carotenoid content as shown in Figure 9-4. Chlorophyll *(a+b)* levels stay similar while cellular carotenoid contents increase (µg $Car \cdot 10^6$ $cells^{-1}$). Cell numbers were similar in both PAR-Only and PAR+UV cultures indicating no large decrease of cell growth (data not shown).

9.2.2.2 *C. vulgaris* - '12 h·d^{-1} PAR only/12 h·d^{-1} UV only' under UV336 board

The experiment described below describes the UV response of *C. vulgaris* exposed to UV-A LEDs in the UV exposure regime shown below:

PAR 30 µmol m^{-2} s^{-1} from PAR LEDs – see exposure regime below

UV UV336 LED board was used for UV-A exposure (λ = 320 – 350 nm, 0.38 W·m^{-2}) – see exposure regime below

Cultures were acclimatized for 3 days (PAR-Only, no UV).

At the start of culture day, 4 UV was turned on

At the start of culture day, 10 UV was turned off

Exposure schedule:	0-12h	12-24 h
Control	PAR + UV	Dark
Treatment	PAR-Only	UV-Only

Growth was limited as a result of UV exposure as evidenced by OD measurements (Figure 9-5). Pigment levels per gram of DW remain similar in both cultures (data not shown). Experiments carried out with the UV blacklight tubes (8W·m^{-2}) on the same strain shows no decrease in growth when the culture was exposed to 5 hours of UV-A only indicating both exposure duration and wavelength may play an important role (data not shown).

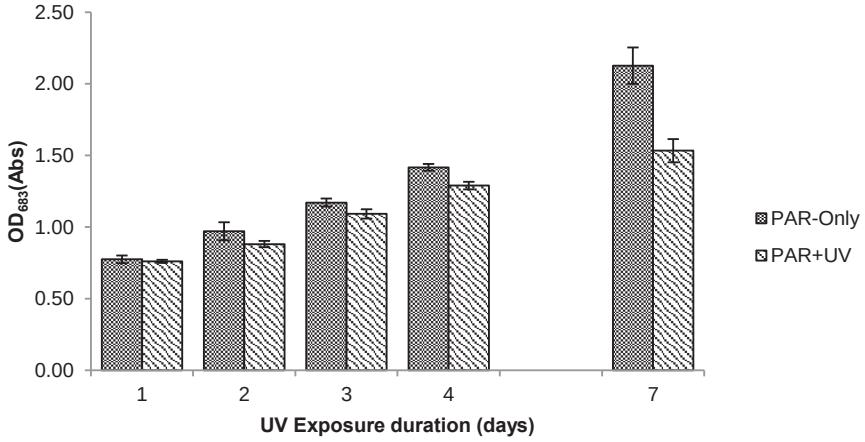

Figure 9-5 Optical density measurements of C. vulgaris under UV325 UV-A exposure. Error bars represent range (n = 3).

There was a clear difference between the three samples on UV exposure day 7, with one sample behaving like the control and the other two clearly affected by the UV. Unfortunately, UV LEDs over one of the three positions were broken (unknown at the time). Upon rotation of the beakers to randomise samples, one of three samples would not receive (direct) UV-A, only PAR. This experimental error did suggest that the effect of UV cell growth could potentially be reversed trough removal of the UV-A signal. This was not confirmed with further experiments.

9.2.2.3 *A. platensis* – '12 h·d^{-1} UV, 24 h·d^{-1} PAR' – under UV336 board

PAR — 30 µmol m^{-2} s^{-1} from PAR LEDs for 24 h·d^{-1} for the duration of the experiment

UV — UV336 LED board was used for UV-A exposure (λ = 320 – 350 nm, 0.38 W·m^{-2}, 12 h·d^{-1})

Cultures were acclimatized for 3 days (PAR-Only, no UV).

At the start of culture day 4, UV was turned on

At the start of culture day 10, UV was turned off

Figure 9-6 and Figure 9-7 below show changes in pigment levels in *A. platensis* exposed to UV-A (UV336 board) in a 24 h·d^{-1} PAR environment supplemented with UV 12 h·d^{-1}. The position was not changed to prevent a repeat of the situation described above. Duplicate samples and no position change means statistics for this experiment are weak.

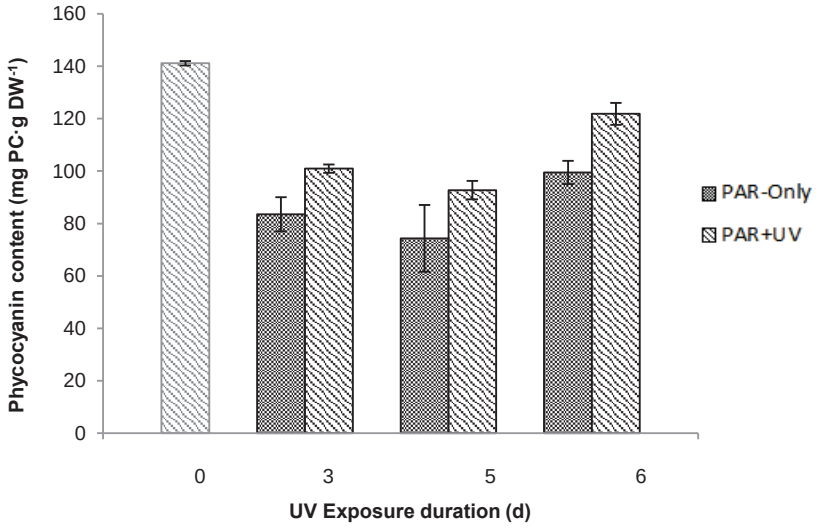

Figure 9-6 Phycocyanin levels as measured in A. platensis *during to UV exposure under UV336 board. Error bars show range (n = 2).*

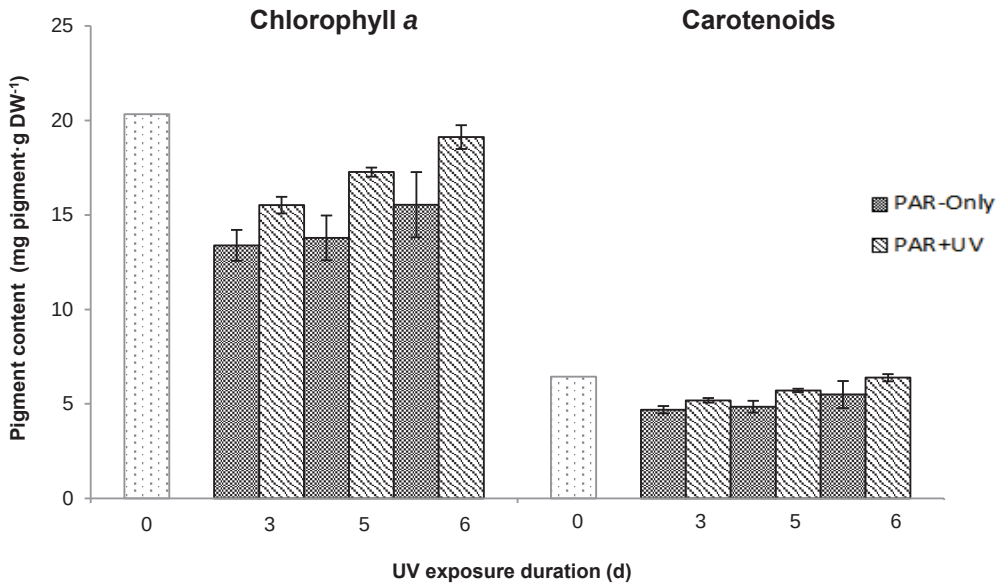

Figure 9-7 Chlorophyll a *and carotenoid levels as measured in A. platensis exposed to UV under UV336 board for 6 days. Chlorophyll* b *levels were found to be negligible in A. platensis. Error bars show range (n = 2).*

There were indications that levels of phycocyanin and chlorophyll a may be increased upon UV exposure. Any differences in carotenoid levels were unclear. Pigment levels never reached those of stock cultures grown in the incubator shaker, likely due to the change in culture environment from the incubator shaker to the bench top (as the effect is observed in both UV exposed and PAR culture). It also shows that the pigment levels in *A. platensis* are highly variable and can change and adapt reasonably quickly. Interestingly we found extremely low levels of chlorophyll b in all *A. platensis* samples. Repeat of the same experiment to confirm the results was cut short due to contamination but trends looked similar. Because only duplicates were used, a lack of adequate statistical analysis combined with inherent problems of the experimental setup make it difficult to draw any conclusions from these experiments. None the less this experiment indicates a possible 'proof-of-principle' for the strain.

9.2.2.4 *H.pluvialis* – '24 h·d^{-1} PAR and 24 h·d^{-1} UV' under fluorescent UV-A tubes

Cultures were of *H. pluvialis* were exposed to UV-A from fluorescent UV-A tube for 3 days (24 h·d^{-1}, 30 µmol m^{-2} s^{-1} PAR and 12 W·m^{-2} UV-A). Due to the exploratory nature of the experiments and the failure to develop an adequate pigment extraction protocol, only microscopic analysis were carried out. The most notable observation is shown in Figure 9-8. Cells exposed to UV-A suffered a dramatic loss in cell numbers (data not shown) but those that survived presented as deep red haematocysts (Lemoine et al., 2010) (right Figure 9-8). Formation of haematocysts was also observed in the PAR-Only cultures but these were almost exclusively green (left, Figure 9-8). As no protocols were developed for further investigation into the response, no comment can be made about the pigment contents or the pigment composition. No reports of UV-A induced carotenoid accumulation in *H.pluvialis* have been found in literature.

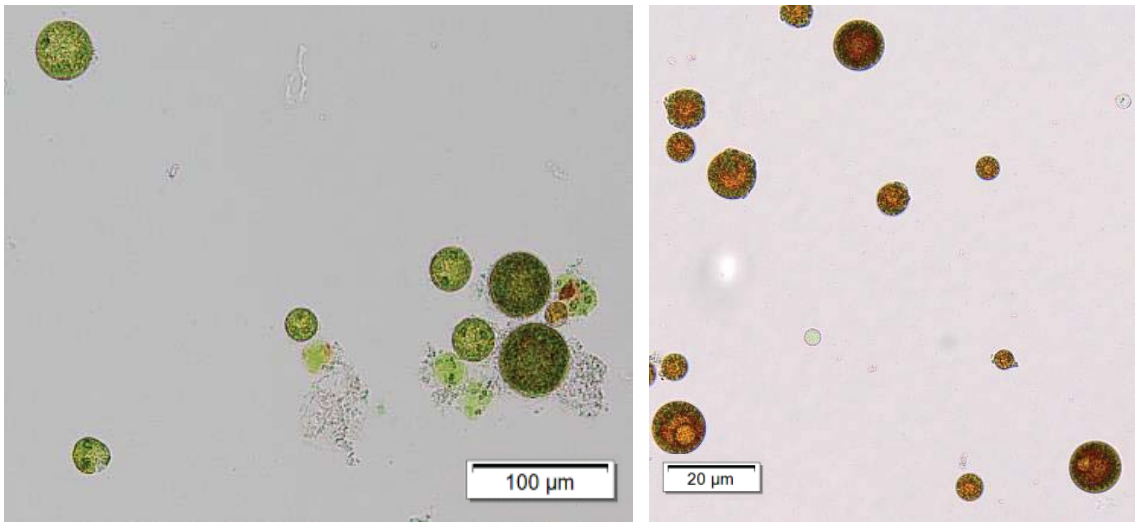

Figure 9-8 Comparison between cells of H. pluvialis *exposed to PAR-Only (left) and those exposed to PAR and UV-A. UV-A exposure of* H. pluvialis *leads to the formation of large red haematocysts. Please be aware of the difference in scale bar difference between left (100 µm) and right (20 µm). Images captured using an Olympus BX53 microscope at 100x and 400x magnification.*

9.3 Appendix – Growth experiments

A number of options were investigated to assess the effect of different parameters on the growth in the experimental setup. The experiment was set up as follows:

- Control (normal experimental conditions = 30 µmol·m^{-2}·s^{-1} PAR)
- Addition of $NaHCO_3$ up to 1 gr·L^{-1}, simulating higher CO_2 conditions
- Increased PAR up to 45 µmol·m^{-2}·s^{-1} PAR
- Increased PAR + added HCO_3 up to 45 µmol·m^{-2}·s^{-1} PAR and 1 gr·L^{-1} respectively

The increased $NaHCO_3$ content was based off White (2013). It is assumed that addition of 1 gr·L^{-1} $NaHCO_3$ saturated the media but this was not confirmed. No significant change in pH was observed as a result of adding $NaHCO_3$.

Increases of (simulated) CO_2 levels and PAR intensity separate from one another yielded increased cell growth over the control in both instances (Figure 9-9). This indicates that both separate factors are limiting. Combined increase of both CO_2 and PAR shows a large increase (close to doubling) of cell numbers after 4 days of culture.

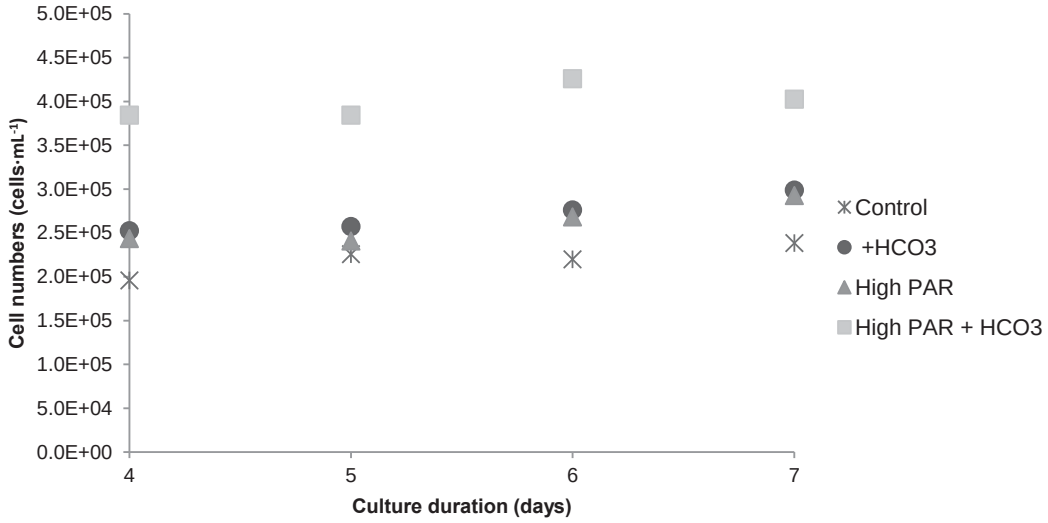

Figure 9-9 Impact of increased PAR (45 µmol·m^{-2}·s^{-1}), added $NaHCO_3$ and increased PAR + added $NaHCO_3$ on D. salina *(strain UTEX 1644) cell proliferation (n=1).*

9.4 Appendix - UV transmission of culture flasks

PAR and UV transmission through the vessel wall was confirmed by both spectrophotometer readings (UV-1800, Shimadzu, Kyoto, Japan) as well as spectroradiometer readings (OL-756, Gooch and Housego, Ilminster, UK). A flask identical to those used in the experiments was cut and placed in a spectrophotometer to measure transmission (Figure 9-10, left). The resulting reduction in spectral irradiance in the flask was measured by placing a flask in front of the integration sphere of the spectroradiometer (i.e. UV light passes through 2 flask walls) (Figure 9-10, right). Reduction in spectral irradiance in the UV-A region was shown to be minimal.

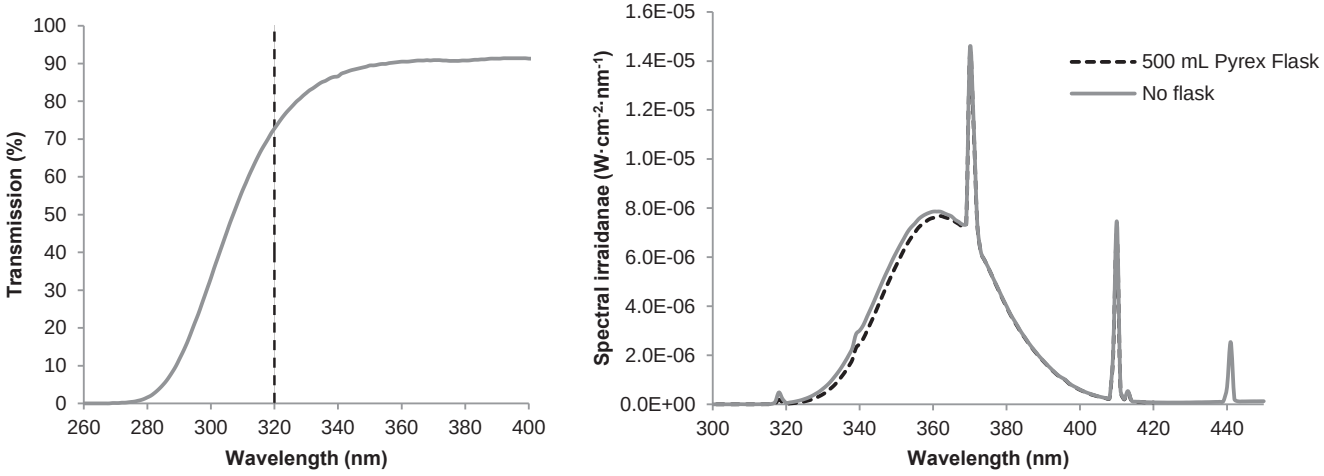

Figure 9-10 UV transmission of borosilicate flasks used during experiments. (Left) Transmission measured using cut flask in spectrophotometer. (Right) Spectral irradiance measured through flask, measured using spectroradiometer.

9.5 Appendix – UV filter

Various short wavelength UV-A wavebands were created using Q-panel UV-A-340 fluorescent tubes (Q-Lab) and a combination of a 350 nm shortpass filter (custom sized Filter ZHS0350, Asahi Spectra USA Inc.) and UV-B screening mylar plastic film (130 clear, LEE Filters). The decreased irradiance using the Asahi filters results from (unexpectedly) poor UV transmission in the shortpass region.

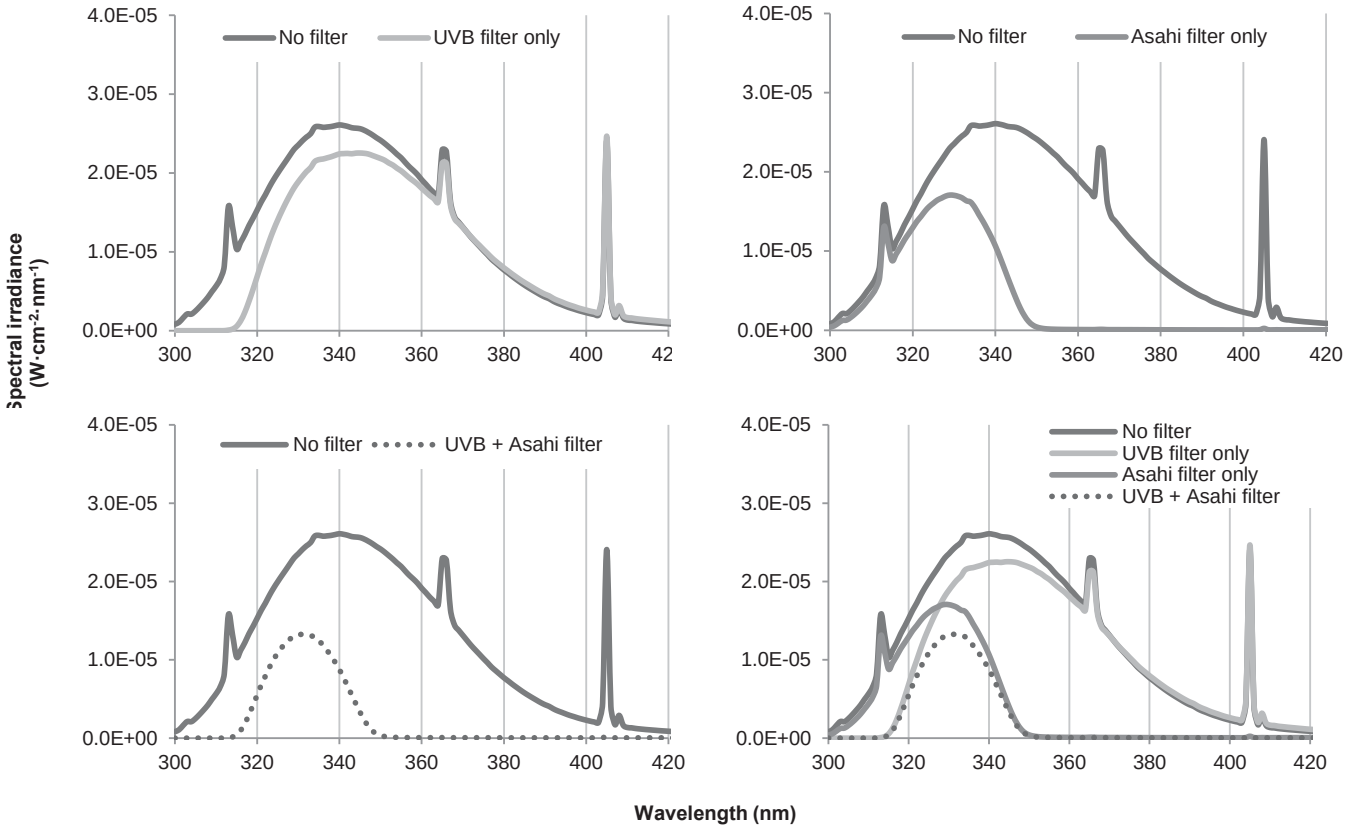

Figure 9-11 Emission spectra of Q-panel UVA-340 fluorescent tube filtered by: Top left - mylar film (UVB filter), Top right - 350 nm shortpass filter (Asahi filter), Bottom left - a combination of both filters. Bottom right graph shows all data in one graph.

9.6 Appendix – Algae counting methodology

9.6.1 Protocol – Automated microalgae cell counting using haemocytometer and

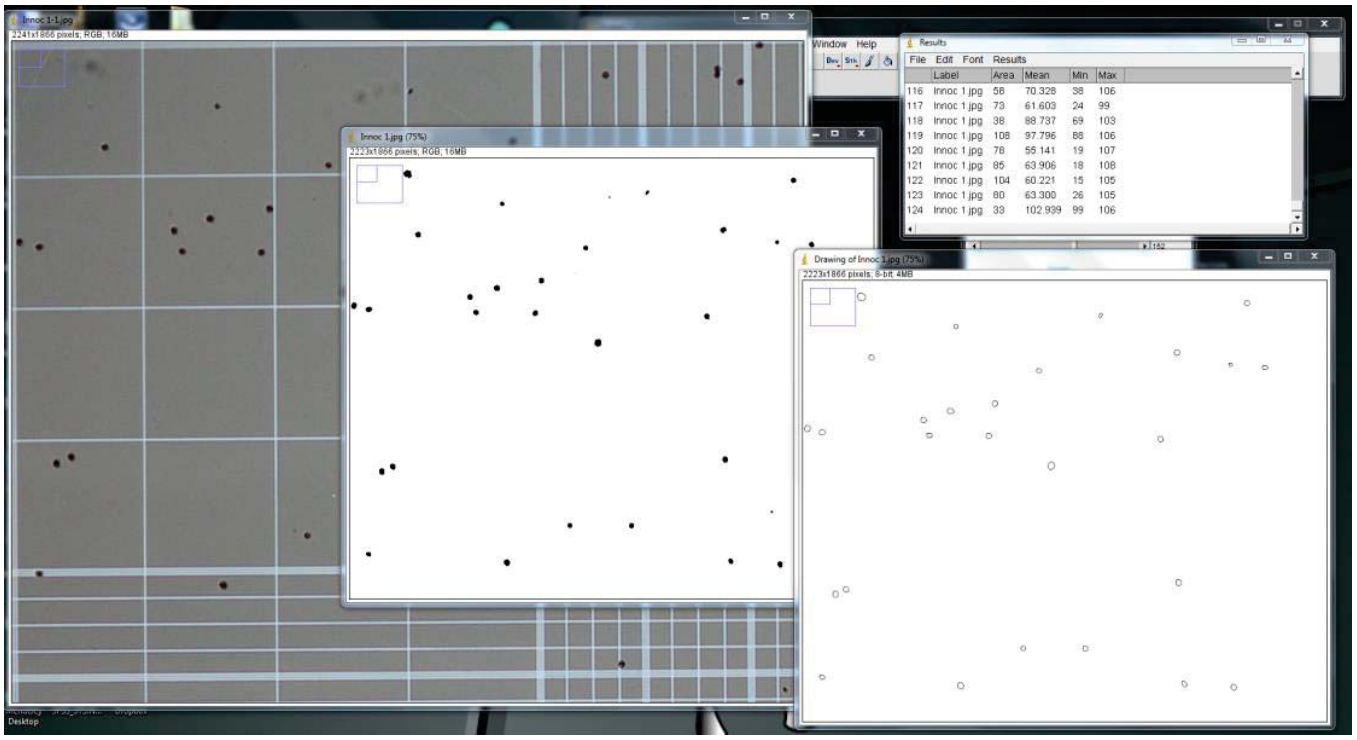

Figure 9-12 Example image of workspace and output resulting from automated cell counting using ImageJ

ImageJ[24]

1. ImageJ Version 1.47v using the basic installation (no additional packages used)
2. Crop image slightly wider than hemocytometer outline – Select area -> Ctrl+Shift+X
3. Go to 'Image>Type>8-bit' to convert the image to 8-bit format. This creates a single channel black-and-white image which is easiest to process.
4. Go to 'Image>Adjust>Threshold' and press 'Apply'. Adjust so that none of the background in the image is visible if necessary. Normally the standard settings work well however.
5. The clumped cells in the image need to be separated so as not to be counted as one. To do this 'Process>Binary>Watershed' which uses an algorithm to separate objectsc. To

[24] Schneider, C. A.; Rasband, W. S. & Eliceiri, K. W. (2012), "NIH Image to ImageJ: 25 years of image analysis", *Nature methods 9*(7): 671-675

remove the empty spaces in some cells also apply ‘Process>Binary>Fill holes’ on the 8-bit file.

6. Go to Analyze>Analyze Particles and use the following settings (right). A window will appear with the count and the objects that the count has actually identified. Changing the ‘Size’ may be required to include/exclude certain objects.

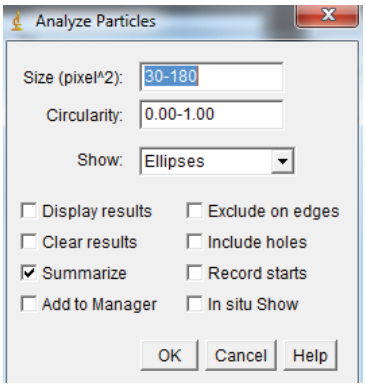

Steps 2-4 were rolled up into an ImageJ macro using Macro Recorder and carrying out steps 2-4 and then saving. The macro contains the following algorithm:

Macro: Roland – Image Processing + Counting

```
run("8-bit");
setAutoThreshold("Default");
//run("Threshold...");
setOption("BlackBackground", false);
run("Convert to Mask");
run("Fill Holes");
run("Watershed");
run("Analyze Particles...", "size=30-150 circularity=0.00-1.00 show=Ellipses summarize");
```

9.6.2 Automated vs Manual count accuracy

Counting performed on exactly the same (cropped) image. Cells on left and top borders were included in the manual count while the right and bottom border are excluded (cropped to exclude bottom/right border). Automated counts are corrected for any errors occurring from anomalous objects (flocks/strands) being counted as objects by subtracting the number generated by the object.

Table 9-3 Comparing automated counting algorithm to manual counting.

Sample	Manual count (cells)	Automated count (cells)	Difference (cells)	% Difference	Automated count using different cropping
PAR 1 -1	282	284	2	0.7	284
PAR 1 -2	307	315	7	2.3	312
PAR 1 -3	250	253	3	1.2	260
PAR 2 -1	313	317	4	1.3	314
PAR 2 -2	265	265	0	0	266
PAR 2 -3	269	265	-4	1.5	269
UV 1.1 – 1	284	281	-3	1.1	285
UV 1.1 – 2	296	299	3	1.0	301
UV 1.1 – 3	262	268	6	2.3	272
UV 1.2 – 1	264	264	0	0	271
UV 1.2 – 2	305	306	1	0.3	308
UV 1.2 – 3	256	257	1	0.4	255
UV 2.1 – 1	305	302	-3	1.0	302
Total	3658	3676	18	0.5%	

Counts are overestimated by 0.5%. This is likely because the images used are at a slight angle, meaning the square drawn for cropping does not overlap with the grid in the image (which is at an angle). This means that sometimes cells outside the grid in the image are included in the crop and counted by the software. The manual cropping was shown to have a minimal effect on the automated cell counts (far right column Table 9-3).

9.7 Appendix – UV-B inclusion results

Very similar results were observed in cellular pigments content changes (Figure 9-13 and Figure 9-14) and cell numbers (Figure 9-15) resulting from the inclusion or removal of UV-B (λ = 300-320 nm, 1.1 $W \cdot m^{-2}$) from the UV-A spectrum as tested during the experimental procedure. Experiment was only carried out once.

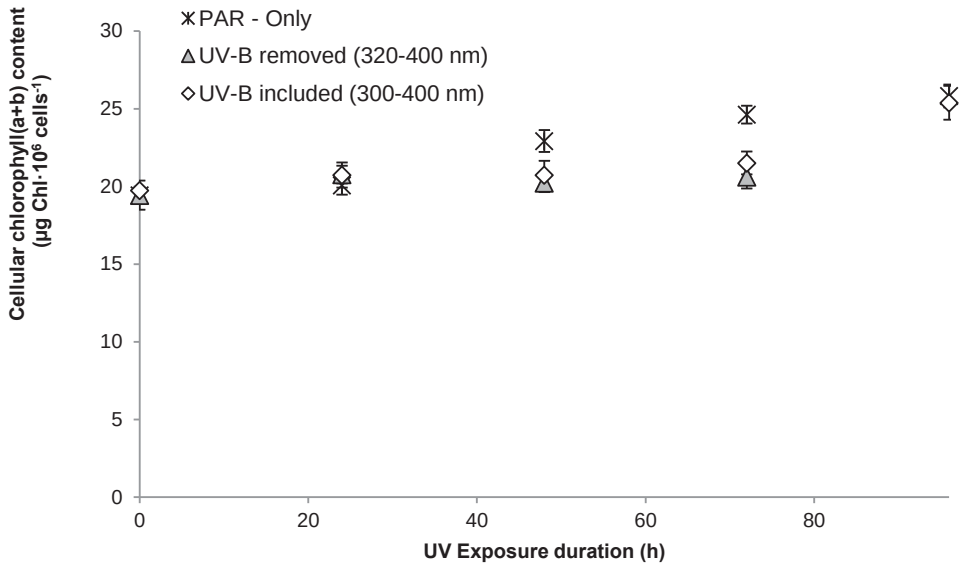

Figure 9-13 Cellular chlorophyll (a+b) content changes resulting from the inclusion or removal of UV-B in the UV-A spectrum. Error bars represent the range (n = 2).

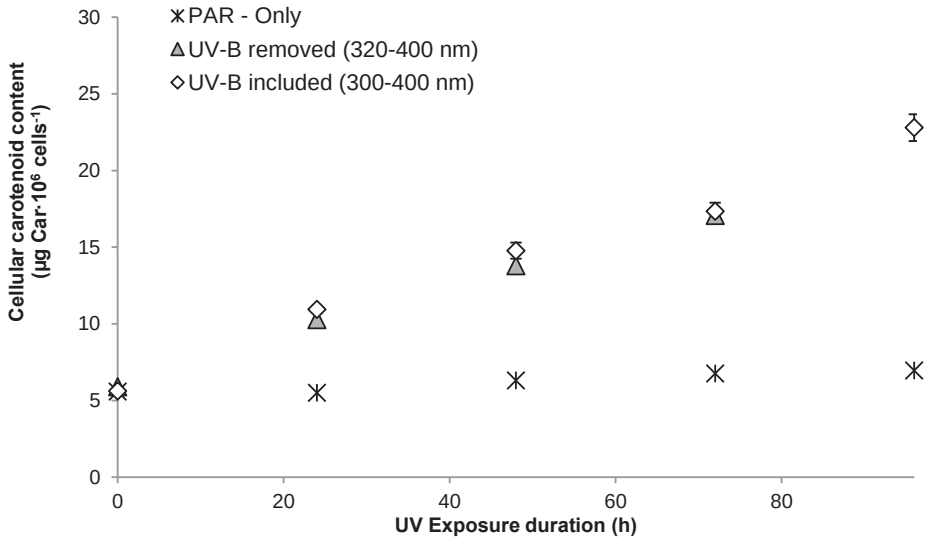

Figure 9-14 Cellular carotenoid content changes resulting from the inclusion or removal of UV-B in the UV-A spectrum. Error bars represent the range (n = 2).

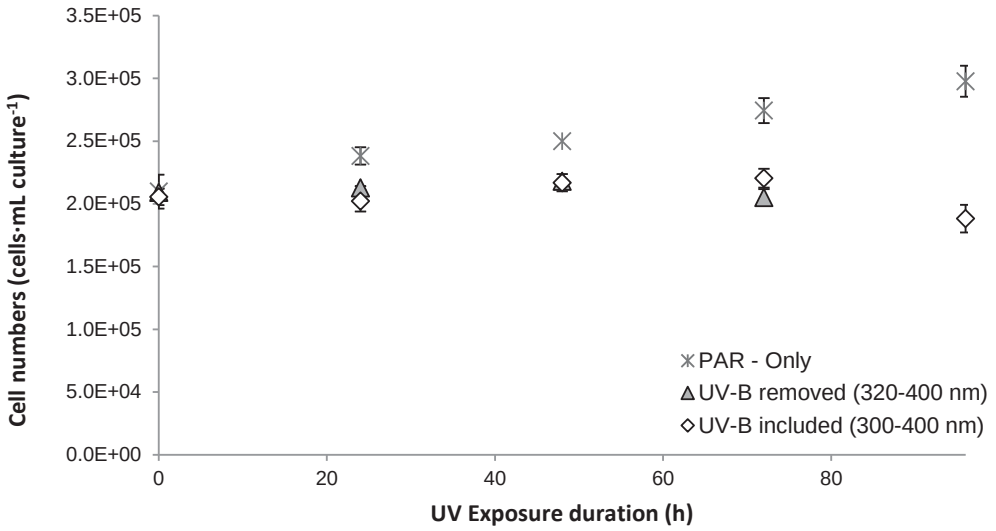

Figure 9-15 Cell number changes resulting from the inclusion or removal of UV-B in the UV-A spectrum. Error bars represent the range (n = 2).

9.8 Appendix – UV-A Irradiance

Figure 9-16 and Figure 9-17 illustrate the trend described in Ch. 5.1.2, where similar cumulative UV doses ($MJ \cdot m^{-2}$) generated by different irradiance levels did not generate the same carotenoid accumulation, also occur in the other wavebands tested.

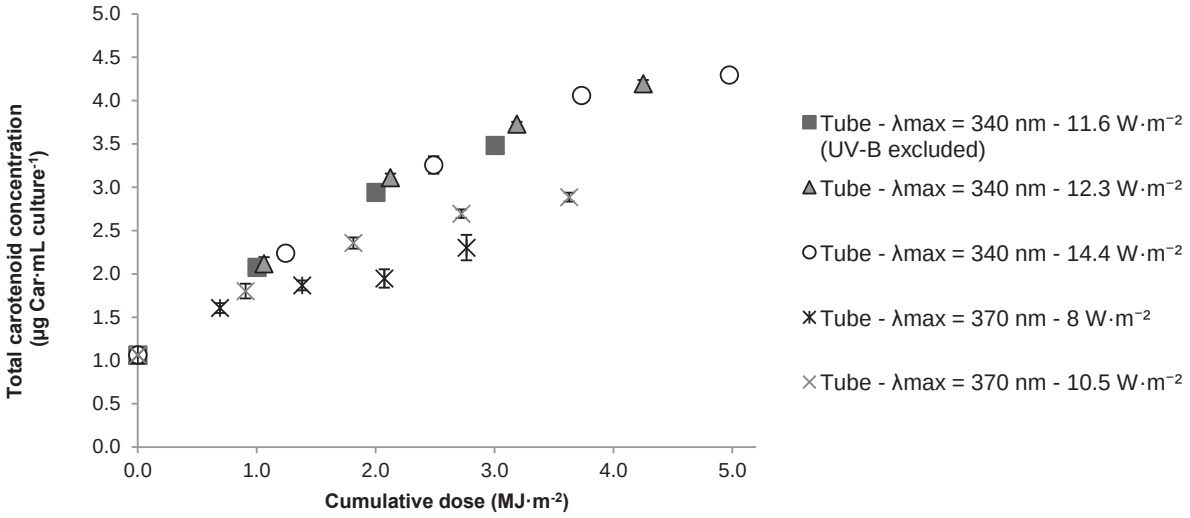

Figure 9-16 Total carotenoid increases under different irradiances in the broad wavelength UV-A (λ = 320-400 nm) regimes. Two different fluorescent tubes in the broad wavelength UV-A region were tested, namely Unbranded and QLab UVA-340, differentiated in the legend by the λ_{max}. Error bars represent standard error for λ_{max} = 370 nm at 8 and 10.5 $W \cdot m^{-2}$ (n=8) and λ_{max} = 340 nm at 11.6 $W \cdot m^{-2}$ (n=4) and range for λ_{max} = 340 nm for 12.3 and 14.4 $W \cdot m^{-2}$ (n=2).

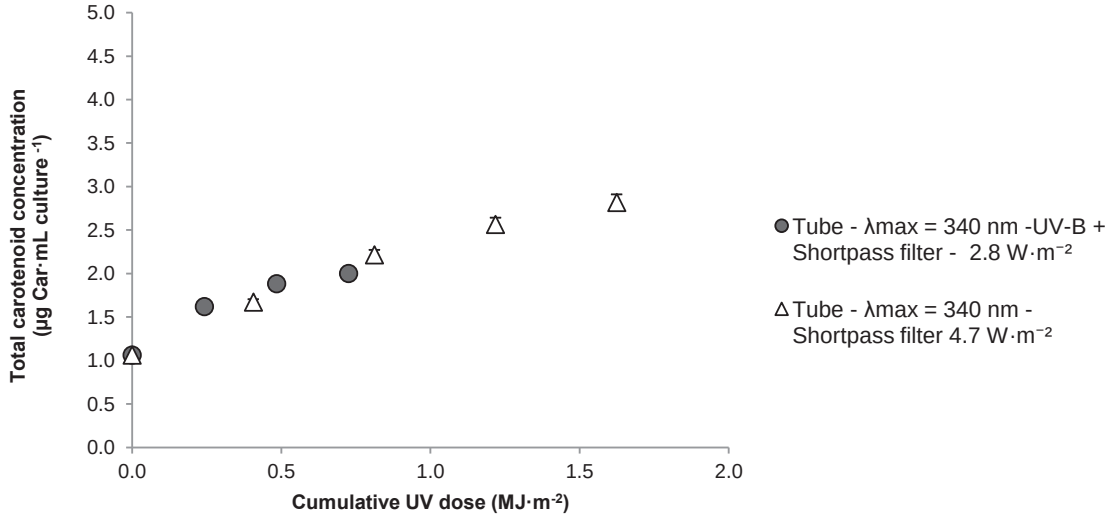

Figure 9-17 Total carotenoid increases during different irradiances in the short wavelength UV-A (λ = 300-350 nm) regimes. Two different filters were used, namely 350 nm Shortpass filter and mylar UV-B filter. Where visible error bars represent standard error (n=4).

The UV-A induced carotenoid accumulation led to increased total carotenoid content compared to PAR-Only under the influence of all UV-A wavebands (Figure 9-19).

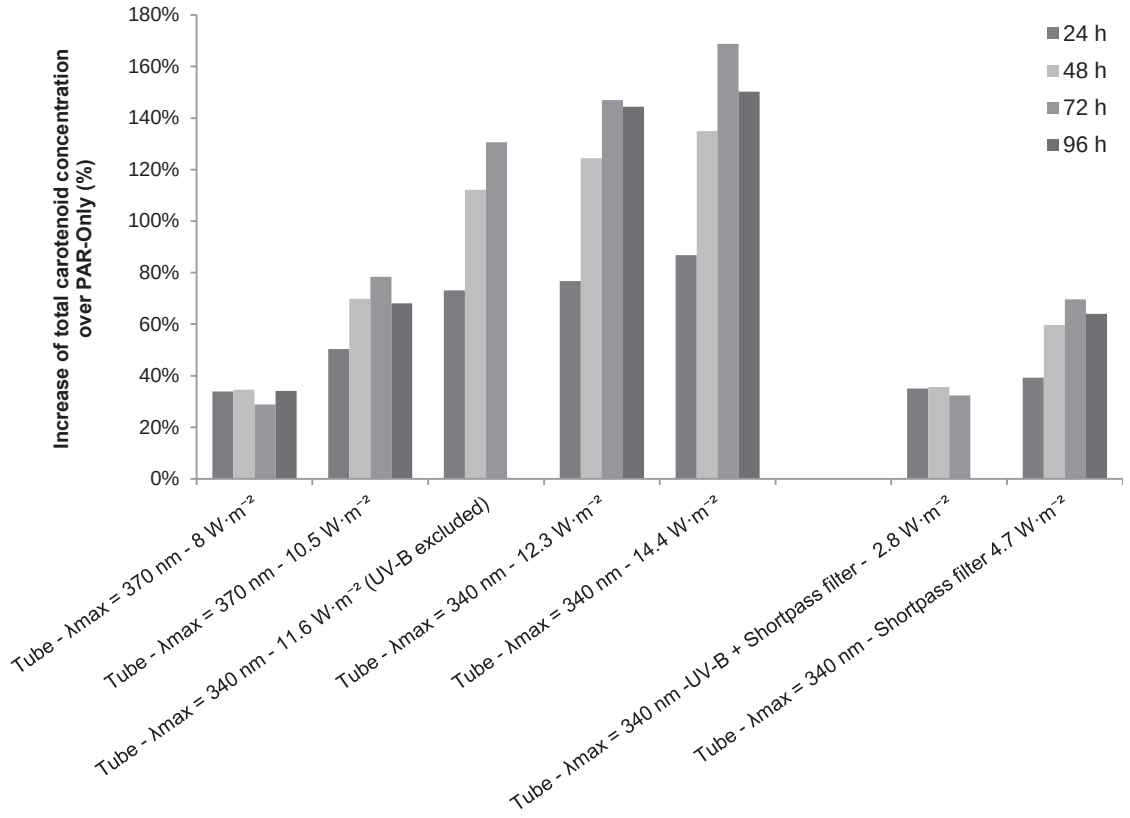

Figure 9-18 Time course of total carotenoid concentration over the PAR-Only control (%) as a function of UV irradiance. Values represent total carotenoid increase in hours after experiment was started (h, see legend) over cultures exposed to PAR only, no UV (%). Cultures were exposed to PAR (30 µmol m^{-2} $s^{-1,}$ 24 hr·d^{-1}) or PAR + UV-A at the specified irradiance (24 hr·d^{-1}). Data points for UV exposure = 96 h were not collected for 11.6 W·m^{-2} and 2.8 W·m^{-2}.

Figure 9-20 and Figure 9-19 illustrate the trend described in Ch. 5.1.2, where total carotenoid accumulation rate (µg carotenoid·mL culture^{-1}·day^{-1}) is most rapid at increased irradiance levels during initial delivery, are also found to occur in the other wavebands tested.

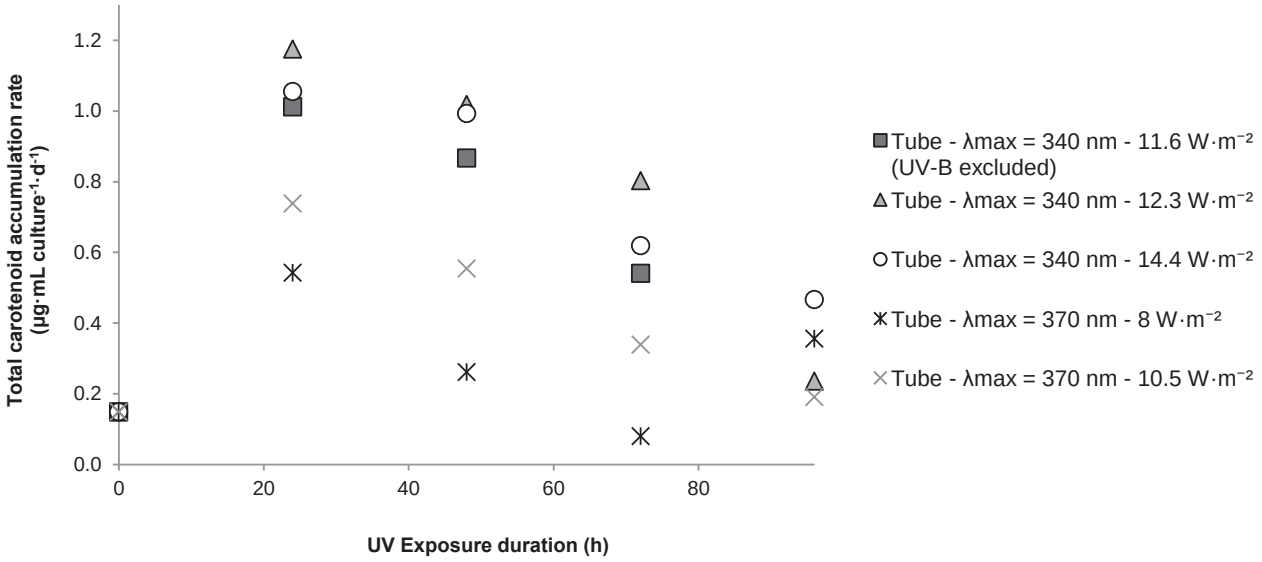

Figure 9-20 Total carotenoid accumulation changes during different irradiances in the broad wavelength (λ = 320-400 nm) regimes. Two different fluorescent tubes in the broadband wavelength region were tested, namely Unbranded and QLab UVA-340, differentiated in the legend by the λ_{max}.

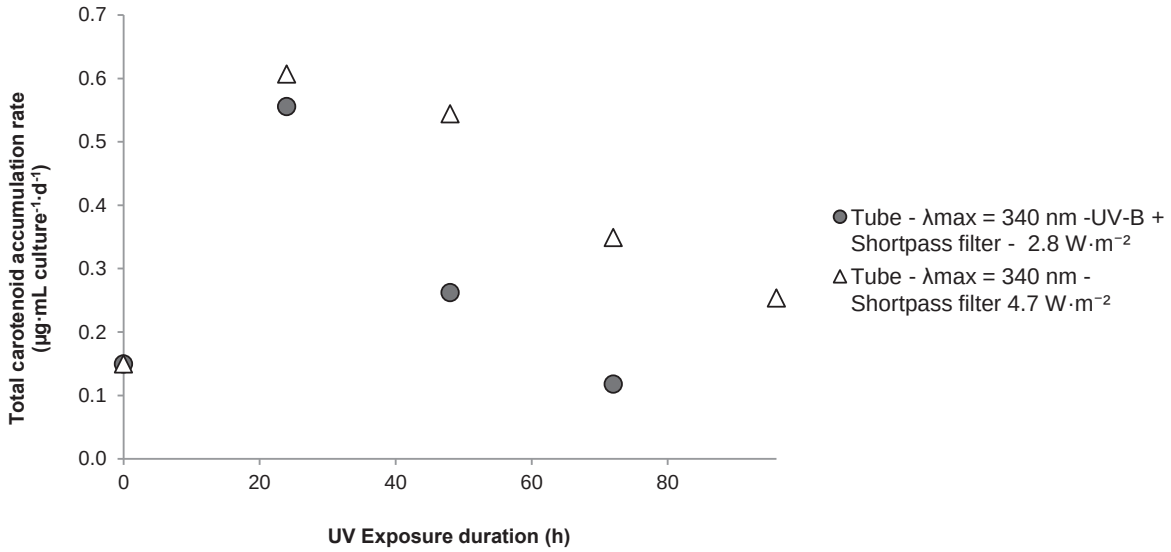

Figure 9-19 Total carotenoid accumulation changes during different irradiances in the short wavelength UV-A (λ = 300-350 nm) regimes. Two different filters were used, namely 350 nm Shortpass filter and mylar UV-B filter.

Figure 9-21 illustrates the trend described in Ch. 5.1.2, where increased total carotenoid accumulation as a result of increased UV irradiance levels leads to a decrease or cessation of cell proliferation, are also found to occur in the other wavebands tested.

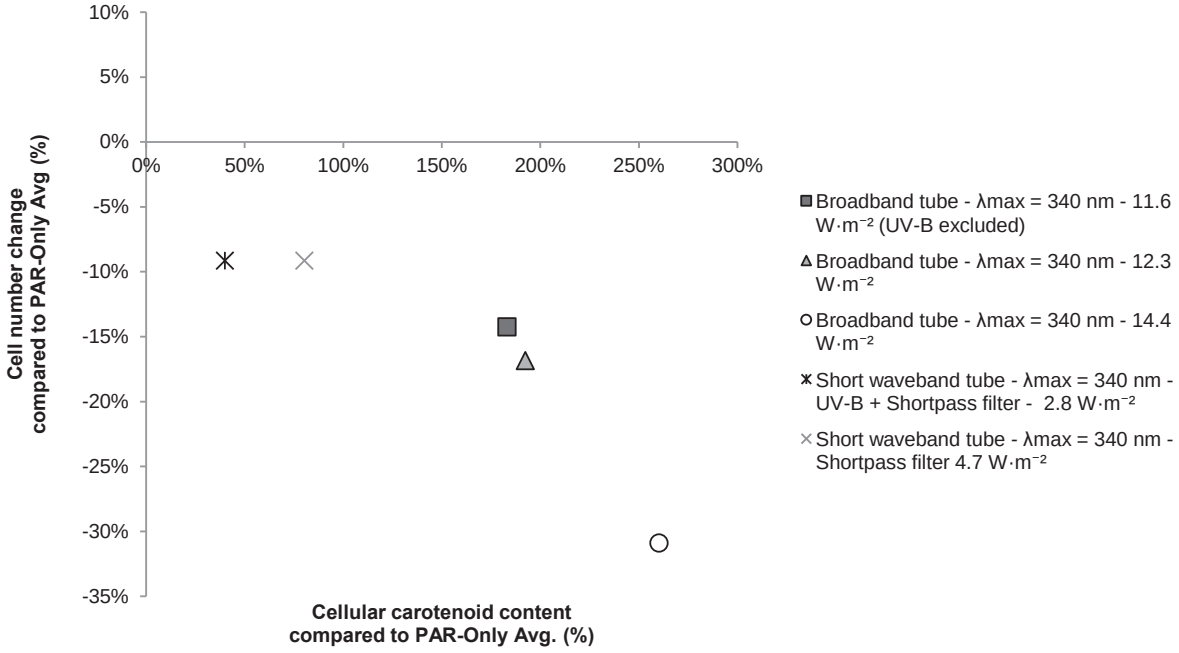

Figure 9-21 Impact of the magnitude of the UV-A induced carotenoid accumulation (x-axis) on cell proliferation (y-axis) under different UV-A irradiance exposure regimes. Cultures were exposed UV-A at the specified irradiance (24 hr·d^{-1}) for UV treatment = 72 h. Two different filters were used, namely 350 nm Shortpass filter and mylar UV-B filter.

9.9 Appendix – UV exposure duration

The general experimental procedure used is described in the Material and Methods sub-section. In summary:

PAR 30 µmol m^{-2} s^{-1} for 24 $h \cdot d^{-1}$ for the duration of the experiment

UV Broad wavelength UV-A (λ = 320 – 400 nm, unbranded tubes, 8 $W \cdot m^{-2}$) during or 6, 12 and 24 $h \cdot d^{-1}$ UV-A exposure (please see legend)

Cultures were acclimatized for 2 days at 30 µmol m^{-2} s^{-1} PAR, no UV.

At the start of culture day 3, UV was turned on (UV day = 0)

At the start of culture day 7, UV was turned off (UV day = 4)

Carotenoid accumulation was increased under all UV-A exposure durations (6, 12 and 24 $h \cdot d^{-1}$) (Figure 9-22, Figure 9-23)[25]. The increase observed towards the end of the 6 $h \cdot d^{-1}$ exposure is thought to be due to an artefact in the experiment.

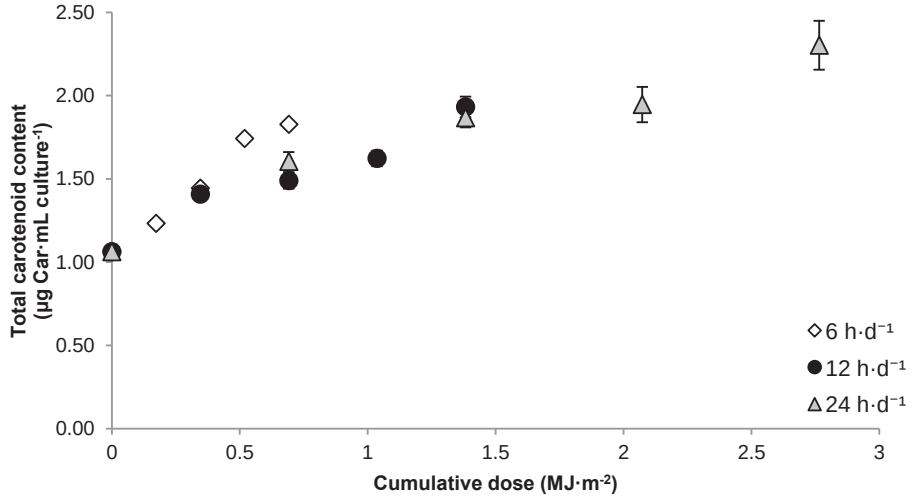

Figure 9-22 Total carotenoid accumulation during semi-continuous and continuous UV-A exposure (6, 12 and 24 $h \cdot d^{-1}$) regimes. Cultures were exposed to broad wavelength UV-A (λ = 320-400 nm, 8 $W \cdot m^{-2}$). Error bars represent standard error (n = 4 for 6 $h \cdot d^{-1}$, n = 8 for 12 and 24 $h \cdot d^{-1}$).

[25] During data collection for Figure 9-22, sampling was carried out immediately after UV exposure, meaning sampling was done at the high point of an 'increased accumulation'-state shown in Figure 9-22.

UV dose efficiency was found to differ substantially from values reported in Ch. 5.2.2.2, likely due to the use of different UV-A light source and different irradiance (Figure 9-24).

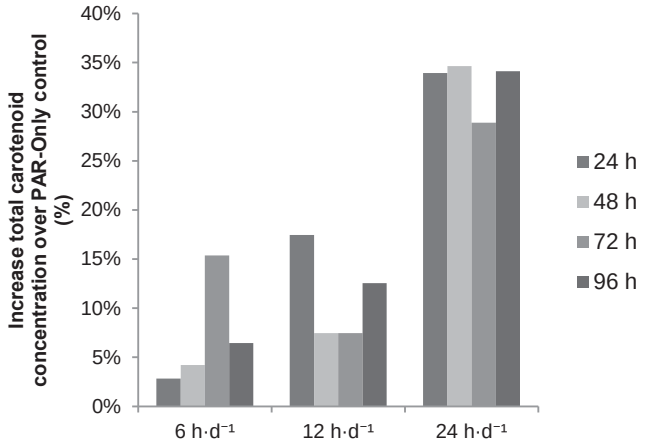

Figure 9-23 Time course of total carotenoid concentration over the PAR-Only control (%) as a function of UV exposure duration. Values represent total carotenoid increase in hours after experiment was started (h, see legend) over cultures exposed to PAR only, no UV (%).

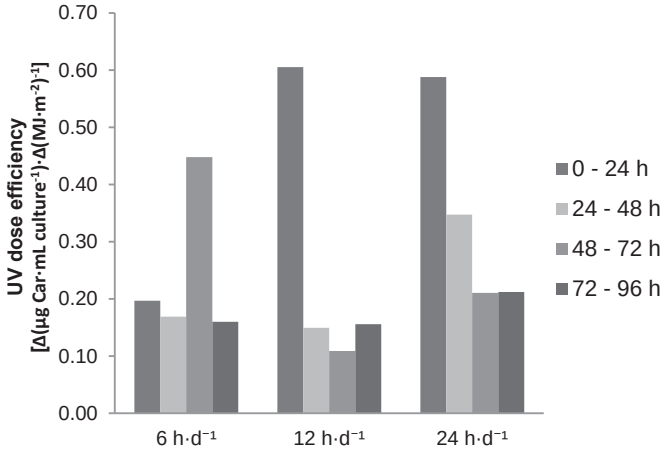

Figure 9-24 Dose efficiency of UV-A induced carotenoid accumulation during semi-continuous and continuous UV-A exposure. Series represents dose efficiency per UV-A irradiance between successive data points (separated by 24 h UV exposure) in Figure 9-22

No significant change in cell proliferation was found resulting from 6, 12 or 24 h·d^{-1} UV exposure duration (Figure 9-25).

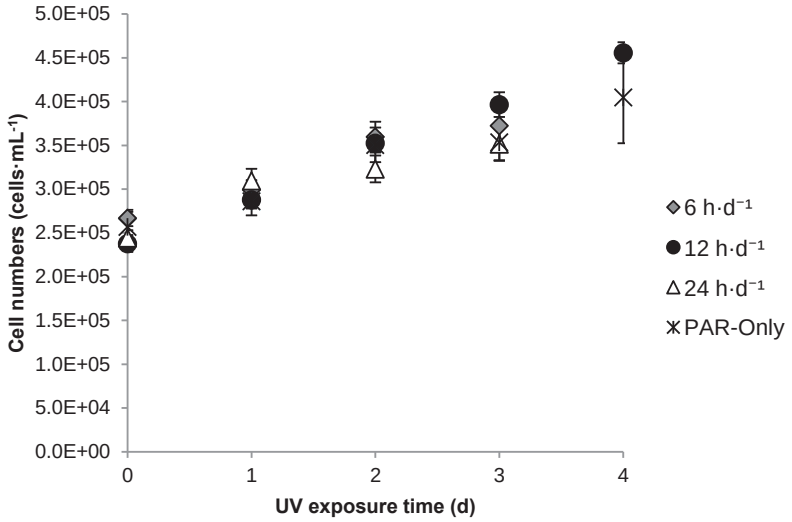

Figure 9-25 Cell proliferation under the influence of 6, 12 or 24 h·d^{-1} UV exposure. Cell counts were carried out every 24 h, just after UV exposure. Each data point therefore represents the cumulative effect of the UV exposure duration (6, 12 or 24 h) and the remaining PAR exposure (18, 12 or 0 h). Error bars represent standard error (n = 48 PAR-Only, n = 4 for 6 h·d^{-1}, n = 8 for 12 and 24 h·d^{-1})

9.10 Appendix – UV exposure duration (II)

The results in Figure 5-10 indicate that carotenoid accumulation during semi-continuous is efficient despite the total carotenoid accumulation. It is thought that the effectiveness stems from the fact that the semi-continuous exposure does not interfere with cell proliferation while continuous exposure does albeit not convincingly (Figure 9-26).

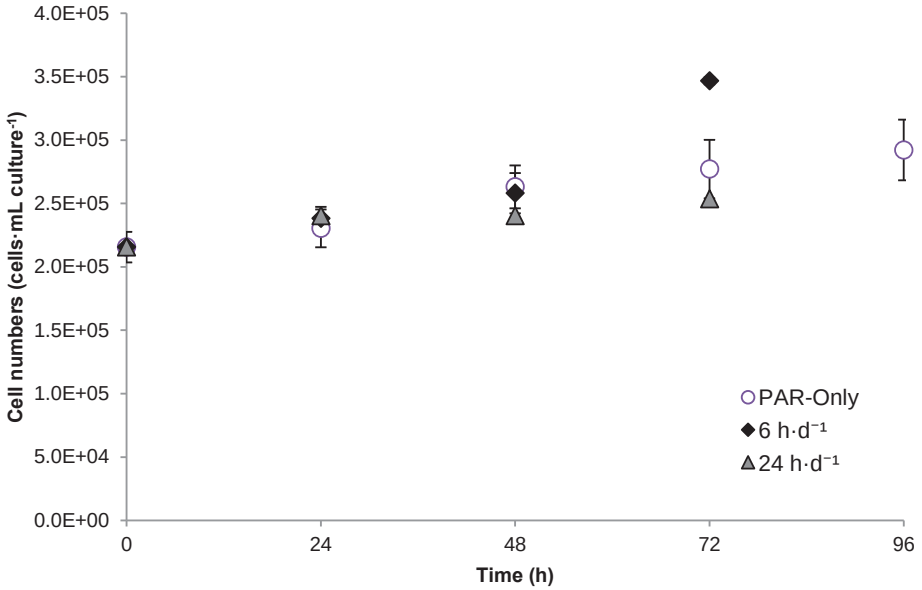

Figure 9-26 Cell proliferation during semi-continuous (6 h·d^{-1}) and continuous UV exposure regimes. Cell counts were carried out every 24 h, just after UV exposure. Each data point therefore represents the cumulative effect of the UV exposure duration (6 or 24 h) and the remaining PAR exposure (18 or 0 h). Error bars represent standard error (n = 48 PAR-Only, n = 8 for 6 h·d^{-1}, n = 4 for 24 h·d^{-1})

9.11 Appendix – UV-A transmittance

UV transmittance ($T = I_z \cdot I_0^{-1}$, with z = 0.01 m) was found to decrease rapidly at increasing cell density (as OD_{687}). A UV transmittance curve was constructed by applying $I_z = I_0 \cdot T^z$ for each optical pathlength z (i.e. z = 1 – 10 cm).

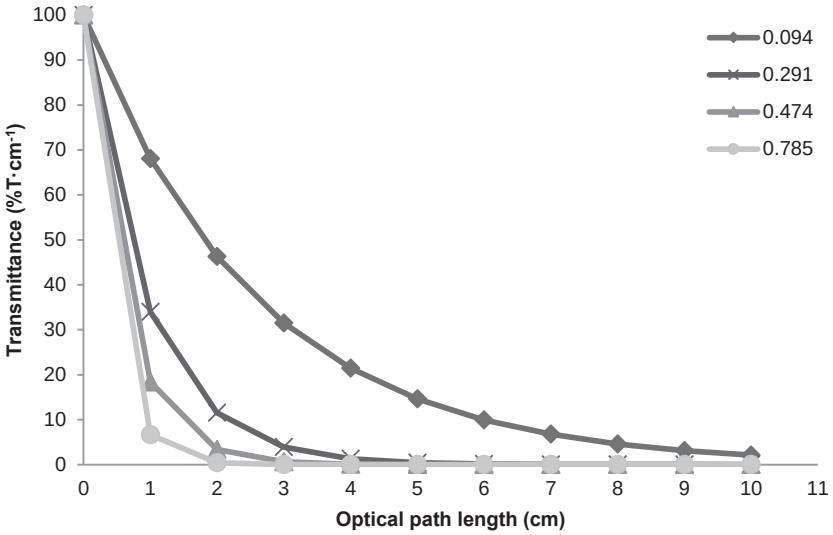

Figure 9-27 UV transmittance as a function of optical path length for a range of cell densities. OD_{687} values are shown in the graph legend.

9.12 Appendix – UV-A treatment: Cultivation stage 'Intermittent exposure' - Lamp warmup

Fluorescent UV-A tubes (Philips TLD-18W BLB) were tested prior to the intermittent exposure experiments to ensure compatibility with the intended experiments. The goal of the experiment is to assess the impact of small UV-A exposure duration (minutes) on the UV carotenoid accumulation response. The current appendix describes how fluorescent UV tube warm-up defines the limits of the experiment.

The spectroradiometer was used at a fixed wavelength of 370 nm (peak emission of the tubes) and irradiance was monitored over time. Tubes were left at ambient temperature for 1 hour before measurements were taken. Within 15 seconds after being turned on the output of the fluorescent tube is at 68%, with the 100% output achieved in 3:00 minutes (100% output being defined as the stable value obtained for at least 10 consecutive minutes without change). Interestingly, the tube is not fully 'warmed up' in terms of temperature after 3 minutes. The fluorescent tube was shown to achieve a stable temperature after 14 minutes (measured using taping an iButton to a room temperature tube, data not shown).

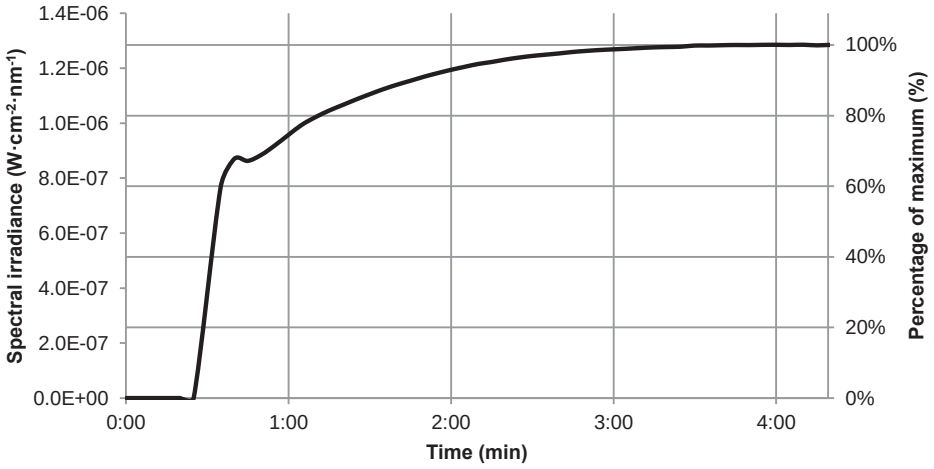

Figure 9-28 Fluorescent UV tube warmup as a function of time. Irradiance measured at 370 nm as a function of time using tubes at room temperature. Left axis shows absolute irradiance measured. Right axis shows the percentage of the stable maximum output measured over a period 15 minutes. An arbitrary distance/position of the integration sphere from the tubes was used.

9.13 Appendix – Intermittent exposure

Under the influence of the intermittent UV exposure regimes cells were observed to undergo morphological changes ordinarily only observed during continuous UV-A exposure (24 $h \cdot d^{-1}$) (Figure 9-29). Similar morphological changes have only been observed during continuous irradiance and not semi-continuous UV-A exposure regimes (i.e. 6 and 12 $h \cdot d^{-1}$). Cells exhibit what appears to be compartmentalisation of the thylakoid membrane without concomitant yellowing (as shown in Figure 4-6).

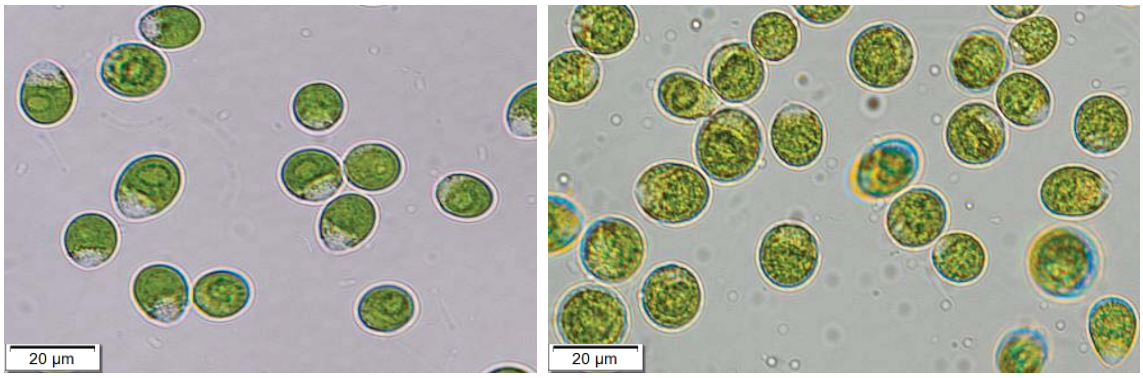

Figure 9-29 Images of cells from PAR-Only (left) and intermittent UV-A exposed '15 min on/15 min off' (right) cultures. Imaged after UV exposure = 96 h. Images are representative of what is observed in Intermittent '5 min on/25 min off'. Images were taken of live cells using an Olympu BX53 at 400x magnification.

Cells are on average larger and rounder than then cultures exposed to PAR-Only (Table 9-4). As a result of intermittent UV-A exposure cell area is increased but roundness was not found to be significantly different.

Table 9-4 Cell area and roundness with standard deviations as calculated from microscopy images and analysis using ImageJ. Values based on a digital images taken at 400x magnification with a minimum of 225 counts per culture.

Cultures	Cell area (μm^2)	Roundness*
PAR-Only	116 ± 32	0.81 ± 0.15
Intermittent UV	147 ± 40	0.87 ± 0.11

*Roundness in ImageJ is defined as $R = 4 \times \frac{[Area]}{\pi \times [Major\ axis]^2}$. This compares the area of an ellips to that of a circle based on the length of the major axis, where Roundness = 1 donates a perfect circle.

Total carotenoid accumulation for continuous (24 h·d^{-1}) increased much more than those of intermittent exposure cultures (left, Figure 9-30). Total chlorophyll *(a+b)* content appeared unaffected by UV exposure in '5 min ON – 25 min Off' cultures, whereas '15 min on – 15 min off' showed a slowed and subsequently decreased total chlorophyll *(a+b)* content, leading to similar levels as the continuous cultures (24 h·d^{-1}). So while Total chlorophyll *(a+b)* content changes during UV exposure were comparable in '15 min on – 15 min off' and continuous cultures, the carotenoid accumulation was not.

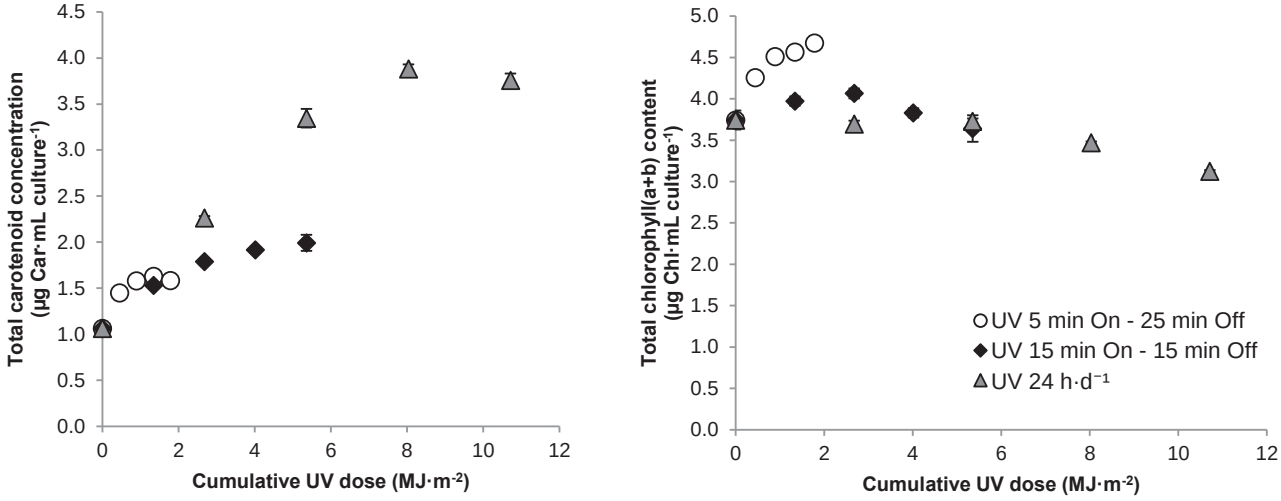

*Figure 9-30 Total carotenoid content (left) and cellular chlorophyll(*a+b*) content (right) during from intermittent UV exposure regimes. Where larger than icons, error bars represent standard error (n = 8).*

Interestingly the trend was reversed for cell numbers, with '15 min on – 15 min off' appearing unaffected whereas '5 min ON – 25 min Off' showed a trend comparable to continuous exposure (Figure 9-31).

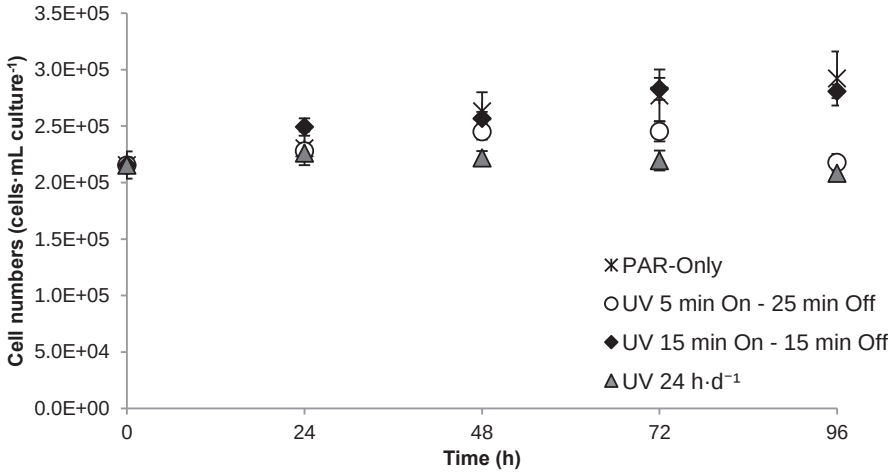

Figure 9-31 Cell number changes during intermittent UV exposure regimes. Where larger than icons, error bars represent standard error (n = 48 PAR-Only, n = 8 UV exposed)

9.14 Appendix – TEA model assumptions

Throughout the Appendix the variables used in the model will be highlighted in **bold**.

9.14.1 Background

The TEA model considers two cultivation systems currently used for commercial *D. salina* cultivation, namely extensive cultivation (unmixed open ponds) and intensive cultivation (mixed raceway ponds). The development, economics and operation of extensive cultivation for *Dunaliella* are described in detail in research by Michael Borowitzka (Borowitzka et al., 1984, 1989a, 1990, 1990c; Moulton et al., 1987a; Borowitzka, 1990, 2013a). The development and operation of intensive cultivation is described in detail in research by Ami Ben-Amotz (Ben-Amotz et al., 1989a; Ben-Amotz, 1995, 2004). Both cultivation approaches have been shown to be economically viable and are currently employed by Cognis (Hutt, Lagoon, Western Australia) and NBT Ltd. (Eilat, Isreal) respectively. The two cultivation systems used in the current TEA analysis are modelled on the available literature for each and uses data from the cited literature where possible.

The TEA case-study assumes a small-scale production facility producing 1000 kg of pure β-carotene (i.e. formulation of a final product is not considered in this TEA) from *D. salina*, representing 2% of the estimated annual *D. salina* biomass production (Spolaore et al., 2006). The TEA uses cultivation parameters described in literature as inputs. Due to their modes of operation, extensive and intensive cultures differ significantly in biomass- and β-carotene productivities but both have been shown to be commercially viable.

In particular the extensive cultivation system has a number of pre-requisites for low-cost production of *Dunaliella* biomass. The extensive culture systems used in Australia are economically viable due to naturally high salinity and high PAR irradiances combined with low land cost and optimum climate allowing production of the microalgae throughout the whole year (Borowitzka, 2013a). Extensive cultivation is not possible areas with limited availability and high value of the land or unsuitable weather conditions for part of the year (i.e. high rainfall or very cold winters) (Borowitzka, 2013a). The intensive cultivation system used in Israel is on high value land but is feasible for *Dunaliella* cultivation due to favourable climate conditions.

An overview of key cultivation parameters for both systems is shown in Table 6-4 in the thesis (copied below in Table 9-5).

Table 9-5 Key cultivation parameters as found in literature describing commercial D. salina cultivation. Literature sources are given below table.

	Unit	Extensive	Intensive
Cellular β-carotene content	% w/w algal DW	5%[d]	5%[a]
β-carotene conc.	g β-carotene·m^{-3}	0.1[b,e]	5-15[b,e]
$P_{\beta\text{-carotene}}$	g β-carotene·m^{-2}·d^{-1}	0.01[e]	0.2-0.25[a,b]
Cell numbers	cells·mL culture $^{-1}$	$0.5 – 5 \cdot 10^{6}$[, c]	$3 – 10 \cdot 10^{5}$[, a]
Biomass conc.	g algal DW·L^{-1}	0.1[c,d]	0.5[a]
$P_{Biomass}$	g algal DW·m^{-2}·d^{-1}	0.05 – 0.1[e]	5[a]
Surface area pond	m^2	6,000 - 2,000,000[f]	3,000-4,000[b]
Pond depth	m	0.3[d]	0.2-0.3[d]
Active mixing	N/A	No[b,d]	Yes[b,d]

Sources:

[a] (Ben-Amotz et al., 1989a), [b] (Ben-Amotz, 2004), [c] (Borowitzka et al., 1990), [d] (Borowitzka, 2013a) [e] (Hosseini Tafreshi et al., 2009), [f] (Moulton et al., 1987a)

For the purpose of the TEA all values were averaged from literature and assumed constant throughout the cultivation process. Cultivation data represented in Table 9-5 was used to construct a base-case scenario. The base-case emulates current commercial *D. salina* β-carotene production practices and assumes a process excluding a post-cultivation stage (highlighted in Figure 6-9 in the thesis). The TEA UV treatment scenario will include the base-case with the addition of dedicated UV treatment post-cultivation.

9.14.2 Cultivation system

The size of both cultivation systems was determined based on the **Avg. aerial biomass productivity (g algal DW·m^{-2}·d^{-1})** assuming constant **cellular carotenoid content** (**% w/w algal DW**) (Eq. 6):

$$Required\ biomass\ production\ (kg \cdot d^{-1}) = \frac{\left(\frac{Annual\ production\ of\ pure\ \beta - carotene\ (kg \cdot y^{-1})}{Operational\ days\ (d \cdot y^{-1})}\right)}{Cellular\ carotenoid\ content\ (\%\, w/w\ DW)}$$

(Eq. 6)

Assumptions:

- **Operational days per year** ($d \cdot y^{-1}$) is assumed to be 300. Downtime is assumed to result from cultivation system start-up, shut-down, cleaning and maintenance. The model assumes no interruptions to cultivation due to e.g. culture collapse and reactor restart. Reactor start-up after interruptions is reported as 6-8 weeks for intensive cultivation systems (Pulz, 2001)

Based on the **required biomass production ($kg \cdot d^{-1}$)** to achieve an annual production of 1000 kg of pure β-carotene, the cultivation system was sized based on the **Avg. aerial biomass productivity (g algal DW·m^{-2}·d^{-1})**. The **aerial β-carotene productivity (g β-carotene·m^{-2}·d^{-1})** could also have been used. However, in literature the aerial β-carotene productivity is calculated from the **Avg. aerial biomass productivity (g algal DW·m^{-2}·d^{-1})** and the **cellular carotenoid content (% w/w DW)** and yields the same numbers (Ben-Amotz et al., 1989a) (Eq. 7).

$$Cultivation\ area\ (m^2) = \left(\frac{Required\ biomass\ production\ (kg \cdot d^{-1}) * 1000}{Aerial\ productivity\ (g\ algal\ DW \cdot m^{-2} \cdot d^{-1}}\right) \quad \text{(Eq. 7)}$$

Assumption:

- The **cultivation area (m^2)** is sized such that the harvested biomass is replenished on a daily basis (assuming constant climatic conditions).

The **theoretical hydraulic retention time (HRT, d)** for each cultivation system is then calculated as follows (Eq. 8):

$$\frac{Total\ cultivation\ volume\ (m^3)}{Required\ biomass\ harvest\ volume\ (m^3 \cdot d^{-1})} = \frac{(Cultivation\ area\ (m^2) \cdot Pond\ depth\ (m))}{\left(\frac{\left(\frac{Biomass\ production\ (kg \cdot d^{-1}) * 1000}{Efficiency\ biomass\ harvest\ (\%)}\right)}{Biomass\ conc.\ (g\ DW \cdot L^{-1})}\right)} \quad \text{(Eq. 8)}$$

Assumptions:

- **Pond depth (m)** is set at 0.3 m (Borowitzka, 2013b). While shallower ponds are seen as preferable (due to shorter optical path length), a pond depth of 0.2 – 0.3 m is the

shallowest that is practical to construct and operate during large scale *D. salina* cultivation (Ben-Amotz et al., 1989a).

- **Efficiency biomass harvest (%)** is assumed 80% (Borowitzka, 1992). Losses are assumed due to spillage, losses in equipment (e.g. filters/centrifuge) and cell death.
- **Biomass conc**. **(g DW·L^{-1})** is assumed constant throughout the year for the purpose of the TEA. This is based on data from *D. salina* cultivation in areas with stable climate throughout the year (i.e. Western Australia & Israel).
- **Required HRT(d)** was used to size the additional ponds following the main cultivation reactors such as the post-cultivation stage discussed in the thesis as well as a waste water treatment pond (waste media treatment after harvest) where applicable.

9.14.3 Cultivation CAPEX

Due to the pre-requisites for both cultivation systems cultivation of *Dunaliella* in New Zealand would not be an option due to high land prices of level land (i.e. competition with dairy industry) and unsuitable weather conditions. Due to a lack of data on the CAPEX of the extensive and intensive systems in their respective locations, the TEA model has had to model a cultivation system in a 'fictional location suitable for the type of cultivation process'. CAPEX costing was done using New Zealand based prices where possible supplemented with values from literature. Inputs for the base-case CAPEX calculations and outcomes (based on calculations above) are shown in Table 9-6.

Table 9-6 Base-case calculation inputs and outcomes.

Base-case inputs	**Extensive**	**Intensive**
Process life span (y)	20	20
Targeted annual production (kg pure β-carotene)	1,000	1,000
Target sale price ($·kg pure β-carotene^{-1})	2,400	2,400
Assumed biomass productivity (g algal DW·m^{-2}·d^{-1})	0.1	5
Assumed β-carotene content (% algal DW)	5	5

Outcomes	**Extensive**	**Intensive**
Required biomass production (kg algal DW)	25,000	25,000
Daily harvest volume (m^3·d^{-1})	833	167
Size of cultivation reactor (m^2)	833,333	16,667
Cultivation reactor HRT (d)	300	30

For construction cost and process control purposes cultivation area was divided into separate ponds of 50,000 m^2 and 3000 m^2 ponds for extensive and intensive cultivation respectively (Ben-

Amotz, 2004). CAPEX items were chosen based on Table 15.4 in Meghan Downes (2013). The CAPEX items were intentionally kept very general to avoid incorporating unnecessary complexity into the TEA – i.e. less emphasis was given to the costing of the production system in order to focus instead on the added value of the UV treatment regime and technology. Individual CAPEX items were cost as shown in Table 9-7. All prices are converted to New Zealand dollars (NZD)[26] and adjusted for inflation[27].

[26] Assuming NZD to USD conversion rate of 1 USD = 1.38 NZD (13/01/2018)

[27] Using inflation calculator Reserve Bank of New Zealand (https://www.rbnz.govt.nz/monetary-policy/inflation-calculator)

Table 9-7 CAPEX cost assumptions

Cost	Unit	Extensive cultivation	Intensive cultivation	Source/assumption
Land	$\$\cdot ha^{-1}$	5,000	27,000	- Extensive cultivation systems are only economically viable if land and site preparation cost are low. Therefore, low value land for production was assumed (i.e. forestry land, median sale price in 2017 obtained from www.interest.co.nz - based on numbers from Real Estate Institute of New Zealand REINZ). Value in $NZD from 2017. Sensitivity analysis - Intensive cultivation was assumed to be viable on prime land. The median cost of farm land in NZ was used (median sale price in 2017 obtained from www.interest.co.nz - based on numbers from Real Estate Institute of New Zealand REINZ).
Pond construction	$\$\cdot m^{-2}$	4.00	41.00	- No pond liner is used during large scale cultivation in open ponds (Borowitzka et al., 1990). Cost for extensive cultivation is assumed similar to site preparation cost only (based on Borowitzka, 1992, and pers. comm. Prof. Benoit Guieysse). Cost includes clearing, grubbing and earthworks assuming relatively level land like that found at the large-scale culturing facilities in Western Australia (based on EPA report EPA/625/R-99/010, 2000), p. 133). Cost would be significantly higher if ground was not level. - Intensive cultivation pond cost Meghan-Downes (2013), price based on 0.5 ha raceway pond and includes land preparation.

Site infrastructure	$, one time cost (buildings, roads)	434,453	434,453	Source: Meghan-Downes (2013) based on a 7 ha intensive cultivation system
Laboratory	$, one time cost	217,226	217,226	Source: Meghan-Downes (2013) based on a 7 ha intensive cultivation system
Pumps	$ per "$m^3 \cdot h^{-1}$"	100	100	Estimated cost based on pers. comm. Prof. Benoit Guieysse, based on costing of $500 for pump with capacity 5 $m^3 \cdot h^{-1}$. The unit "$m^3 \cdot h^{-1}$" denotes the pump capacity.
Mixing and material handling equipment	$\cdot pond^{-1}$	1,737	8,689	Source: Meghan-Downes (2013) based on a 0.5 ha raceway pond. This includes paddle wheels and pumps (in the case of extensive cultivation).
Pre-culture (inoculation)	"Total culture area" units	0.1	0.1	Source: Meghan-Downes (2013)
	$\cdot pond^{-1}$ (3000 m^2)	123,000	123,000	Source: Meghan-Downes (2013)
Engineering fees	% of total CAPEX	15%	15%	Based on Borowitzka (1992) and Molina Grima (2013)
Contingency	% of total CAPEX	5%	5%	Based on Borowitzka (1992) and Molina Grima (2013)
Post-harvest media waste water treatment	$\cdot m^{-3}$ treated	1.10	1.10	Source: Molina Grima (2003)

Media recycling (filtration)	$ per "$m^3 \cdot h^{-1}$"	1,118	5,593	Based on Molina Grima (2003) – pricing of media filter unit. Media filtration for extensive cultivation assumed cheaper due to lower load of media (i.e. in terms of biomass and excreted products, see 'Harvest' sub-section)

Borowitzka (2013) says: “Cost-effective and efficient harvesting and dewatering of the algae and extracting the β-carotene are major challenges for the commercial process, and the exact details of the processes used by the various producers are therefore closely guarded by the commercial producers.”. Based on what is described in the literature harvesting of *D. salina* is assumed to occur via:

Extensive cultivation:	Membrane filtration
CAPEX cost:	19,000 $\$\cdot(m^3 \text{ harvest volume})^{-1}\cdot h^{-1}$
Source:	Cost estimation based on *D. salina* specific membrane filtration system as described by Monte et al. (2018).
Intensive cultivation:	Continuous flow centrifuge with automatic discharge (Hosseini Tafreshi et al., 2009)
CAPEX cost:	41,667 $\$\cdot(m^3 \text{ harvest volume})^{-1}\cdot h^{-1}$
Source:	Cost adapted from Molina Grima (2003)

It should be noted that the harvesting system employed at the extensive cultivation system operated by Cognis has been described as Salinity dependent hydrophobic binding (Hosseini Tafreshi et al., 2009). No information could be found for the costing of such a sytem. Post-harvest media waste water treatment and media recycling are included in the calculation. The waste water treatment for recycling or discharge is a challenge faced by both systems due to large volumes, high ion concentrations and organic matter content (mainly glycerol) and thought to play an important role in cost for the *D. salina* cultivation process (Hosseini Tafreshi et al., 2009).

9.14.4 Cultivation OPEX

The OPEX items were chosen based on Table 15.4 in Meghan-Downes (2013). Individual OPEX items were costed as follows (in the Table 9-8 below):

Table 9-8 OPEX cost assumptions

Cost	Unit	Extensive cultivation	Intensive cultivation	Source/assumption
Labor	$\$\cdot h^{-1}$	15	15	Estimate. New Zealand minimum wage used as reference.
Number of staff	$Staff\cdot ha^{-1}$	0.1	2	Ben-Amotz (2011) states 20 staff operate the 10 ha intensive cultivation facility in Eilat, Israel – i.e. 2 $staff\cdot ha^{-1}$. Extensive cultivation is assumed to less staff due to lower man power input requirement for operation of the extensive cultivation process and is adjusted accordingly.
Pump power consumption	$kWh\cdot m^{-3}$	0.4	0.4	Source: Tipperary Energy Agency (www.tea.ie)
Paddlewheel mixing[28]	$kWh\cdot d^{-1}\cdot pond^{-1}$	N/A	3.3	Calculated based on Borowitzka (1989). Calculated using $P = \frac{9810AV^3n^2}{d^{0.3}e}$ where A is area, V is mixing speed, n is the Manning's number (assumed 0.012), d is depth and e is paddlewheel efficiency (assumed 40%).
Electricity	$\$\cdot kWh^{-1}$	0.16	0.16	Source: Ministry of Primary Industries (MBIE), New Zealand 2017 residential electricity prices. Assumes 'Energy Only' cost (removing 'Lines' component of residential electricity cost).

Pump maintenance	$· "$m^3 \cdot h^{-1}$"·$y^{-1}$	0.1	0.1	Unit represents "cost per unit pump capacity per year". Estimate, no source – Due to highly saline water, maintenance is likely higher than when fresh water is used.
Pond maintenance	% of pond CAPEX	0.1	0.1	Estimate, no source.
Consumables	$·kg algal DW $^{-1}$	1	1	Based on Meghan-Downes (2013)
Harvesting power consumption	$kWh \cdot m^{-3}$	1.46	15	Source: Molina Grima et al. (2004) and Monte et al. (2018),
Harvesting Consumables and Maintenance	$\$ \cdot m^{-3}$	0.22	0.46	Based on Monte et al. (2018). Authors estimate maintenance to account for saline conditions which tend to result in higher maintenance cost.
Chemicals (nutrients, CO_2, disinfection etc.)	$·'kg algal DW produced'$^{-1}$	2.5	2.5	Based on Meghan-Downes (2013), added additional amount to account for salt water
Seawater (pump operation + filtration)	$\$ \cdot m^{-3}$	0.25	0.25	Source: Ben-amotz (2011). Water evaporation is assumed to occur at 0.03 $m \cdot d^{-1}$ (Borowitzka, 1992).

9.14.5 CAPEX and OPEX biomass production – Overall

Results of calculations are shown in Table 6-5. A sensitivity analysis was carried out on all costing for the CAPEX and OPEX components used in the biomass production model cultivation system. Sensitivity analysis results are shown in Figure 9-32 and Figure 9-33.

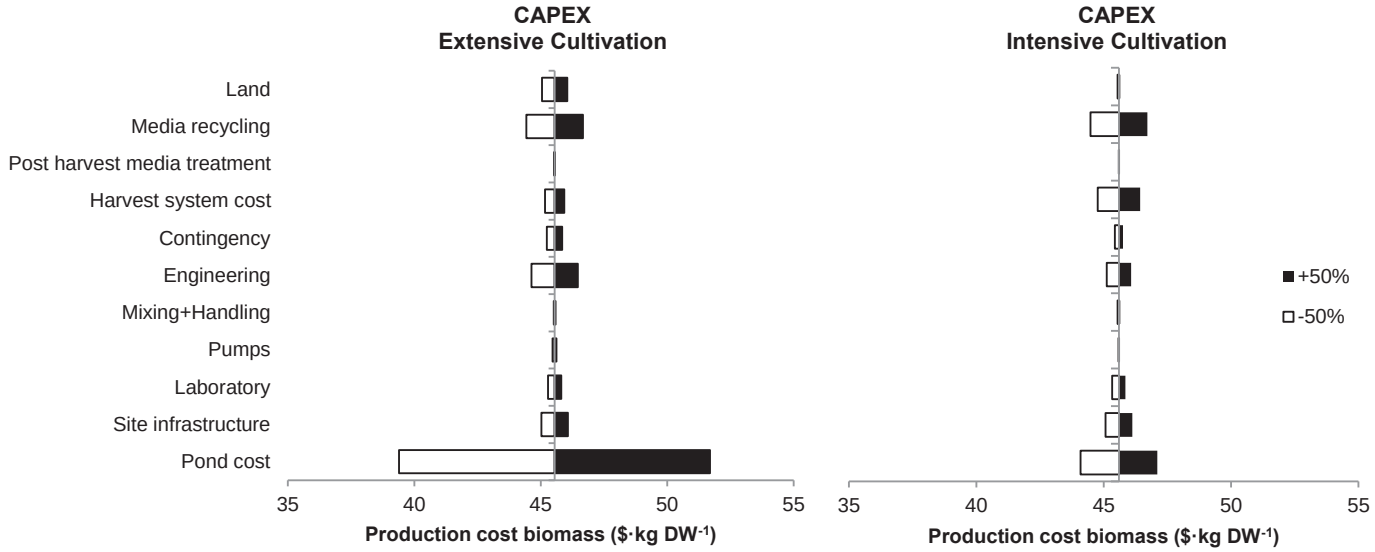

Figure 9-32 Sensitivity analysis of CAPEX item cost. Bars represent the impact of an increase or decrease in the price of the component on the production cost of biomass.

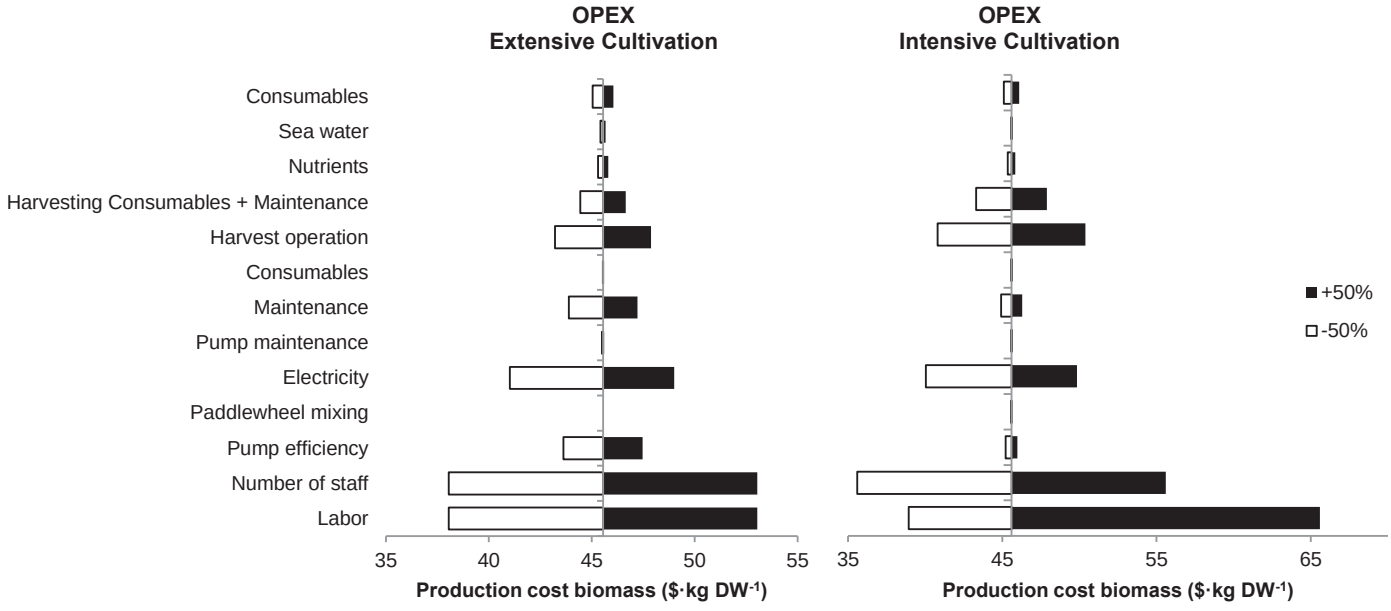

Figure 9-33 Sensitivity analysis of OPEX item cost. Bars represent the impact of an increase or decrease in the price of the component on the production cost of biomass.

9.14.6 UV treatment system

UV treatment options were considered based on the research in the thesis – i.e. focus being on UV waveband, UV irradiance and UV exposure duration. UV LED's light sources were included as these 1) provide greater UV waveband control than UV fluorescent tubes and 2) UV LED technology is employed by BioLumic. UV light source choices are presented in Table 6-5 in the thesis (repeated in Table 9-9).

Table 9-9 Input parameters for TEA UV treatment system. Where possible, values are based on supplier information. As not all suppliers readily provide values for all parameters values are based on the sources provided below the table.

		Waveband		
UV Source		Short waveband (λ = 320-350 nm)	Broad waveband (λ = 320-400 nm)	Long waveband (λ = 360-400 nm)
Post-cultivation UV treatment pond		UV treatment pond is sized for 72 h HRT. Time is based on experimental observations (Ch. 5.1), in which UV-A induced carotenoid accumulation achieves steady-state after 72 h.		
UV LED	Name	SETi UVTOP335	Nichia NCSU275-T U365	Nichia NCSU275-T U385
	Peak emission λ_{max}	335 nm	365 nm	385 nm
	Maximum optical power per LED	0.0004 W	0.148 W	0.35 W
	Lifetime	10,000 h[a]	50,000 h[b]	50,000 h[b]
	Electrical conversion efficiency*	40%[b]	40%[b]	40%[b]
	Optical efficiency**	50%	50%	50%
Fluorescent UV tube	Name	No products found. Would require use of expensive shortpass filters to achieve	QPanel UVA-340	Philips TLD BLB
	Peak emission λ_{max}		340 nm	370 nm
	Maximum optical power per tube		40 W	36 W
	Lifetime		5,000 h[d]	9,000 h[c]
	Electrical conversion efficiency*		25%[c]	25%[c]
	Optical efficiency**		50%	50%

* Electrical conversion efficiency is defined as conversion efficiency of electricity energy to the theoretical UV source optical power (W electricity·W UV optical power^{-1})

** Optical efficiency is defined as the UV irradiance loss between the UV source and culture surface as a function of distance

Sources: [a] SETi (www.s-et.com), [b] Phoseon Technology (www.phoseon.com), [c] Philips Lighting (www.philips.com), [d] Pers. Comm. Dr. Jason Wargent.

The thesis research was used as an input for the TEA to design the UV treatment system requirements as discussed below. In the case of UV treatment during a dedicated post-cultivation stage (as outlined in sub-chapter 6.4.3) both CAPEX and OPEX also include the cost of pond construction and operation (sized based on HRT).

9.14.7 UV treatment CAPEX

The number of UV lights required to achieve the **desired irradiance at culture surface (W·m^{-2})** aimed to take into account electrical and optical efficiency of the UV light source and was calculated as (Eq. 9):

$$No.\,of\ UV\ light\ sources\ (unit \cdot m^{-2}) = \frac{Desired\ irradiance\ at\ culture\ surface\ (W \cdot m^{-2})}{(Maximum\ optical\ power\ (W \cdot light\ source^{-1}) \cdot Electrical\ efficiency\ (\%) \cdot Optical\ efficiency\ (\%))} \quad \text{(Eq. 9)}$$

Assumptions:

- **Desired irradiance at culture surface (W·m^{-2})** is assumed to be correspond to the UV irradiance values used during experiments (i.e. those measured at flask surface)
- **Maximum optical power (W·light source^{-1})** is assumed to be the value provided by manufacturer.
- **Electrical conversion efficiency (%)** is defined as conversion efficiency of electricity energy to the theoretical UV source optical power (W electricity·W UV optical power^{-1}).
- **Optical efficiency (%)** is defined as the UV irradiance loss between the UV source and culture surface as a function of distance. The TEA assumes a distance of the light to the culture surface the same as that used during experiments and uses radiospectrometer readings of irradiance drop-off as a function of distance as input.

CAPEX is calculated using the following equation (Eq. 10) and inputs shown in Table 9-10 below.

$$CAPEX\ UV\ treament\ system\ (\$) = Cultivation\ area\ (m^2) \cdot [(No.\,of\ light\ sources(unit \cdot m^{-2}) \cdot Price\ per\ light\ source\ (\$ \cdot light\ source^{-1}) + (Mounting\ infrastructure\ cost\ (\$ \cdot m^{-2})] \quad \text{(Eq. 10)}$$

Assumptions:

- Based on UV light source mounting infrastructure specifications and physical light source size there is a restriction on the **maximum number of light sources (m^{-2})**.
- The UV treatment CAPEX assumes purchase price for consumer is same as of raw material purchase cost.
- Installation cost is not considered in the TEA.

9.14.8 UV treatment OPEX

OPEX cost is assumed to consist of 2 elements, namely: running cost (power consumption) and UV light source replacement cost at the end of lifetime (Eq. 11 and Eq. 12):

$$OPEX\ running\ cost\ (\$ \cdot y^{-1}) = \ Cultivation\ area\ (m^2) \cdot \left[\left(\frac{(\ Desired\ irradiance\ at\ culture\ surface\ (W \cdot m^{-2})}{Electrical\ efficiency\ (\%) \cdot Optical\ efficiency\ (\%)}\right) \cdot Running\ time\ (h \cdot y^{-1}) \cdot Electricity\ cost\ (\$ \cdot kWh^{-1})\right] \quad \text{(Eq. 11)}$$

$$OPEX\ UV\ light\ source\ replacement\ cost\ (\$ \cdot y^{-1}) = \ Cultivation\ area\ (m^2) \cdot \left[(No.of\ light\ sources(unit \cdot m^{-2}) \cdot\ Price\ per\ light\ source\ (\$ \cdot light\ source^{-1}) \cdot \left(\frac{Running\ time\ (h \cdot y^{-1})}{UV\ light\ source\ lifetime\ (h)}\right)\right] \quad \text{(Eq. 12)}$$

Assumptions:

- For **running time (h·y^{-1})** lights are assumed to run continuously (i.e. 24 h·d^{-1})
- **UV light source lifetimes (h)** are based on literature. Light sources are assumed to require replacement at the end of lifetime to ensure maximum irradiance output.

Table 9-10 Inputs CAPEX and OPEX calculations UV treatment system.

	UV LED			UV fluorescent tube			
Brand	**SETi**	**Nichia**	**Nichia**	**Q-Lab**	**Unbranded**	**Philips**	**Source/assumptions**
Name	UVTOP335	NCSU275T- U365	NCSU275T-U385	UVA340	N/A	TLD-Blacklight	UV LEDs were chosen based on pers. comm. BioLumic, UV fluorescent tubes were chosen based on own research.
Emission peak	335 nm	365 nm	385 nm	340	360	370	Half-peak emission per light source is not reported here.
Maximum optical power (supplier dependent) (W)	0.0004	0.148	0.35	40	40	40	Source: Manufacture technical specifications
Optical efficiency (function of distance)	50%	50%	50%	50%	50%	50%	Based on radiospectrometer readings on UV fluorescent tubes during experiments. UV LED values are assumed similar (i.e. physical properties of radiation assumed the same)
Electrical efficiency (power to light)	40%	40%	40%	25%	25%	25%	UV LEDs: Phoseon Technology (www.phoseon.com), based on long wavelength UV-A curing UV fluorescent tubes: Philips Lighting (www.philips.com)
Price per light source ($)	10	7.5	5	17.5	8.75	8.75	UV LED price from pers. comm. BioLumic, UV fluorescent tubes based on bulk trade price.

Mounting infrastructure cost (m^{-2})	1,000	1,000	1,000	200	200	200	Based on pers. comm. BioLumic.
Lifetime (h)	10,000	50,000	50,000	5,000	5,000	9,000	UV LEDs: Phoseon Technology (www.phoseon.com), and pers. comm. BioLumic UV fluorescent tubes: Philips Lighting (www.philips.com)
Light source size	not reported	3.5x3.5 mm	3.5x3.5 mm	1200x30mm	1200x30mm	1200x30mm	Source: Manufacturer technical specifications. Size of mounting infrastructure adds to the dimensions that cause PAR occlusion.
Max no. light sources (m^{-2})	8163	8163	8163	27.8	27.8	27.8	
Running time lights ($h \cdot y^{-1}$)	7,200	7,200	7,200	7,200	7,200	7,200	Assuming 300 $d \cdot y^{-1}$ operational time.

Note: Specifications of BioLumic technology regarding the UV LED treatment systems has been intentionally left out of this table (e.g. mounting infrastructure design and size).

9.14.9 Final CAPEX and OPEX calculations

Assumptions made based on thesis research:

- Short- and broad wavelength UV-A (λ = 320 – 350 and λ = 320 - 400 respectively) are most efficient at inducing carotenoid accumulation in *D. salina*.
- The highest long wavelength UV-A induced carotenoid accumulation rates and total carotenoid concentrations are achieved at the highest UV-A irradiance tested (30 $W \cdot m^{-2}$).
- The highest UV-A induced carotenoid accumulation rates and total carotenoid concentrations are achieved under continuous UV exposure (24 $h \cdot d^{-1}$).
- The UV-A induced carotenoid accumulation response is induced within 6 hours and is largely complete in 96 hours (24 $hr \cdot d^{-1}$ UV exposure).

In order to calculate the increase β-carotene attained from UV treatment, the annual β-carotene production of the base-case (i.e. 1,000 kg β-carotene$\cdot y^{-1}$) was increased by "**Increase of carotenoid content over PAR-Only (%)"** values obtained from the thesis research (see e.g. Figure 5-5, Figure 5-17 and Figure 6-8). The %-increase was applied to the annual β-carotene production to yield an increased annual β-carotene production. The value **162% increase of carotenoid content** over PAR-Only was used for calculations and is based on observations for during 30 $W \cdot m^{-2}$ long wavelength UV-A exposure @24 $h \cdot d^{-1}$ after 3 days- See Figure 5-2 in thesis (day 3). The analytical methods used in the thesis provide the **total carotenoid concentration (µg·mL culture^{-1})** rather than total β-carotene concentration and thus had to be converted. A conversion factor of 65% (w/w) was used to convert "Increase of carotenoid content over PAR-Only (%)" to "Increase of β-carotene content over PAR-Only (%)" based on (Borowitzka et al., 1989a).

Occlusion of PAR light resulting from coverage of the cultivation area with a UV treatment system was introduced. Exerpt from thesis:

- The TEA model assumes outdoor cultivation under solar radiation. A top-down UV treatment system with solar radiation is likely to interfere with non-UV induced carotenogenesis in *D. salina*. Non-UV-A induced carotenoid accumulation has been shown to decrease linearly with decreasing PAR intensity (Loeblich, 1982). Furthermore, interference with solar PAR supply is assumed to interfere with photosynthetic processes required for carotenoid accumulation (e.g. carbon fixation). Therefore, in the TEA model a 'solar radiation occlusion penalty' is imposed on total accumulated β-carotene proportional to the size of the mounting infrastructure of the UV light sources. The impact on biomass productivity resulting from solar

radiation occlusion is not considered in the TEA calculations as this is not a priority of the post-cultivation stage.

This was implemented as follows (Eq.13):

$$\begin{aligned} &Solar\ occlusion\ penalty \\ &\quad = (Increased\ carotenoid\ content\ as\ a\ result\ of\ UV\ treatment(kg \cdot y^{-1}) \\ &\quad - [(Increased\ caroten\text{oid content as a result of UV treatment}(\text{kg} \cdot \text{y}^{-1}) \\ &\quad \cdot ((\text{No. of light sources}(\text{m}^{-2}) \cdot (\text{Light source size}(\text{m}^2) \\ &\quad + \text{mounting infrastructure}(\text{m}^2))\ ] \end{aligned} \qquad \text{(Eq. 13)}$$

Further assumptions:

- CAPEX was annualized over a period of 20 years for biomass production and UV treatment system.
- Interest rate on loans and inflation over this period was not taken into consideration for this period.

9.15 Appendix - TEA UV treatment scenarios

The use of semi-continuous UV exposure to reduce operational expense (<24 h·d^{-1}, Ch. 5.2) or partial coverage of the cultivation area (intermittent exposure, Ch. 6.3) to reduce capital expense were shown to reduce carotenoid accumulation compared to continuous (24 h·d^{-1}) UV treatment and full coverage. The carotenoid accumulation reduction is disproportionate to the reduction in UV exposure duration or UV treatment system reactor coverage. Results of a TEA fast-pass analysis of varying UV treatment parameters - UV irradiance, semi-continuous UV exposure and partial coverage (intermittent exposure) - during post-cultivation are shown in Figure 9-34. The largest profit is found with UV parameters at 30 W·m^{-2} U V-A irradiance, continuous 24 h·d^{-1} exposure and full UV treatment coverage of the post-cultivation reactor.

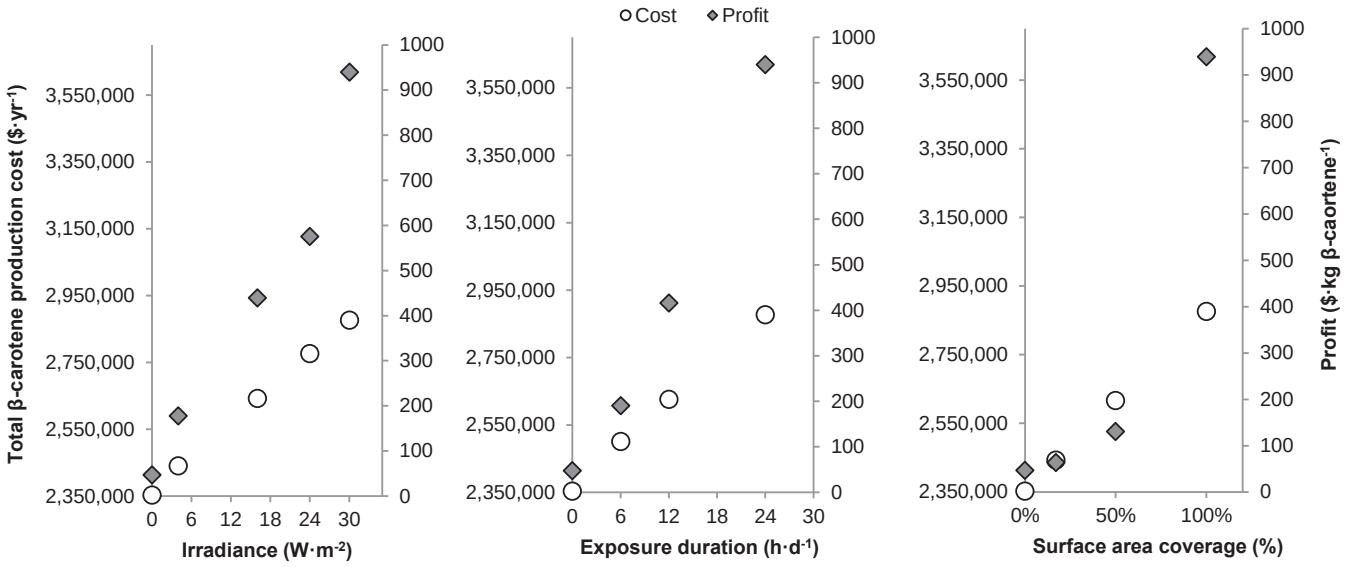

Figure 9-34 Total production β-carotene cost ($·year^{-1}) and profit ($·kg β-carotene^{-1}) under varying UV treatment parameters. Analysis is based on the 'Intensive Post-cultivation stage' scenario assuming the use of long waveband UV-A (λ = 360 – 400 nm) fluorescent tubes as UV radiation source.

As exemplified by Figure 9-34, no further growth potential in the exposure duration and surface area coverage metrics (i.e. exposure longer than 24 h·d^{-1} and coverage of more than 100% is not possible). The only way to improve profitability based on these UV treatment parameters is by increasing UV-A irradiance. The non-linear nature of UV irradiance and UV-A induced carotenoid accumulation indicates further increases in UV irradiance may yield increasing profitability gains. While the limit for UV-A induced carotenoid accumulation resulting from increasing UV-A

irradiance was not identified, it follows that there is likely limit above which carotenoid content may not increase further or eventually decrease.

JOHN WILEY AND SONS LICENSE TERMS AND CONDITIONS

Feb 19, 2018

This Agreement between Massey University -- Roland Schaap ("You") and John Wiley and Sons ("John Wiley and Sons") consists of your license details and the terms and conditions provided by John Wiley and Sons and Copyright Clearance Center.

License Number	4125721502519
License date	Jun 11, 2017
Licensed Content Publisher	John Wiley and Sons
Licensed Content Publication	Wiley oBooks
Licensed Content Title	Dunaliella: Biology, Production, and Markets
Licensed Content Author	Michael A. Borowitzka
Licensed Content Date	Apr 12, 2013
Licensed Content Pages	10
Type of use	Dissertation/Thesis
Requestor type	University/Academic
Format	Print and electronic
Portion	Figure/table
Number of figures/tables	2
Original Wiley figure/table number(s)	Figure 18.1 Figure 18.2
Will you be translating?	No
Title of your thesis / dissertation	UV radiation as a new tool to control microalgal bio-product yield and quality
Expected completion date	Jun 2017
Expected size (number of pages)	200
Requestor Location	Massey University Tennent Drive Palmerston North, Manawatu 4474 New Zealand Attn: SEAT
Publisher Tax ID	EU826007151
Billing Type	Invoice
Billing Address	Massey University Tennent Drive Palmerston North, New Zealand 4474 Attn: SEAT
Total	0.00 USD

Terms and Conditions

TERMS AND CONDITIONS

This copyrighted material is owned by or exclusively licensed to John Wiley & Sons, Inc. or one of its group companies (each a"Wiley Company") or handled on behalf of a society with which a Wiley Company has exclusive publishing rights in relation to a particular work (collectively "WILEY"). By clicking "accept" in connection with completing this licensing transaction, you agree that the following terms and conditions apply to this transaction (along with the billing and payment terms and conditions established by the Copyright Clearance Center Inc., ("CCC's Billing and Payment terms and conditions"), at the time that you opened your RightsLink account (these are available at any time at http://myaccount.copyright.com).

Terms and Conditions

- The materials you have requested permission to reproduce or reuse (the "Wiley Materials") are protected by copyright.

- You are hereby granted a personal, non-exclusive, non-sub licensable (on a stand-alone basis), non-transferable, worldwide, limited license to reproduce the Wiley Materials for the purpose specified in the licensing process. This license, **and any CONTENT (PDF or image file) purchased as part of your order,** is for a one-time use only and limited to any maximum distribution number specified in the license. The first instance of republication or reuse granted by this license must be completed within two years of the date of the grant of this license (although copies prepared before the end date may be distributed thereafter). The Wiley Materials shall not be used in any other manner or for any other purpose, beyond what is granted in the license. Permission is granted subject to an appropriate acknowledgement given to the author, title of the material/book/journal and the publisher. You shall also duplicate the copyright notice that appears in the Wiley publication in your use of the Wiley Material. Permission is also granted on the understanding that nowhere in the text is a previously published source acknowledged for all or part of this Wiley Material. Any third party content is expressly excluded from this permission.

- With respect to the Wiley Materials, all rights are reserved. Except as expressly granted by the terms of the license, no part of the Wiley Materials may be copied, modified, adapted (except for minor reformatting required by the new Publication), translated, reproduced, transferred or distributed, in any form or by any means, and no derivative works may be made based on the Wiley Materials without the prior permission of the respective copyright owner.**For STM Signatory Publishers clearing permission under the terms of the STM Permissions Guidelines only, the terms of the license are extended to include subsequent editions and for editions in other languages, provided such editions are for the work as a whole in situ and does not involve the separate exploitation of the permitted figures or extracts,** You may not alter, remove or suppress in any manner any copyright, trademark or other notices displayed by the Wiley Materials. You may not license, rent, sell, loan, lease, pledge, offer as security, transfer or assign the Wiley Materials on a stand-alone basis, or any of the rights granted to you hereunder to any other person.

- The Wiley Materials and all of the intellectual property rights therein shall at all times remain the exclusive property of John Wiley & Sons Inc, the Wiley Companies, or their respective licensors, and your interest therein is only that of having possession of

and the right to reproduce the Wiley Materials pursuant to Section 2 herein during the continuance of this Agreement. You agree that you own no right, title or interest in or to the Wiley Materials or any of the intellectual property rights therein. You shall have no rights hereunder other than the license as provided for above in Section 2. No right, license or interest to any trademark, trade name, service mark or other branding ("Marks") of WILEY or its licensors is granted hereunder, and you agree that you shall not assert any such right, license or interest with respect thereto

- NEITHER WILEY NOR ITS LICENSORS MAKES ANY WARRANTY OR REPRESENTATION OF ANY KIND TO YOU OR ANY THIRD PARTY, EXPRESS, IMPLIED OR STATUTORY, WITH RESPECT TO THE MATERIALS OR THE ACCURACY OF ANY INFORMATION CONTAINED IN THE MATERIALS, INCLUDING, WITHOUT LIMITATION, ANY IMPLIED WARRANTY OF MERCHANTABILITY, ACCURACY, SATISFACTORY QUALITY, FITNESS FOR A PARTICULAR PURPOSE, USABILITY, INTEGRATION OR NON-INFRINGEMENT AND ALL SUCH WARRANTIES ARE HEREBY EXCLUDED BY WILEY AND ITS LICENSORS AND WAIVED BY YOU.

- WILEY shall have the right to terminate this Agreement immediately upon breach of this Agreement by you.

- You shall indemnify, defend and hold harmless WILEY, its Licensors and their respective directors, officers, agents and employees, from and against any actual or threatened claims, demands, causes of action or proceedings arising from any breach of this Agreement by you.

- IN NO EVENT SHALL WILEY OR ITS LICENSORS BE LIABLE TO YOU OR ANY OTHER PARTY OR ANY OTHER PERSON OR ENTITY FOR ANY SPECIAL, CONSEQUENTIAL, INCIDENTAL, INDIRECT, EXEMPLARY OR PUNITIVE DAMAGES, HOWEVER CAUSED, ARISING OUT OF OR IN CONNECTION WITH THE DOWNLOADING, PROVISIONING, VIEWING OR USE OF THE MATERIALS REGARDLESS OF THE FORM OF ACTION, WHETHER FOR BREACH OF CONTRACT, BREACH OF WARRANTY, TORT, NEGLIGENCE, INFRINGEMENT OR OTHERWISE (INCLUDING, WITHOUT LIMITATION, DAMAGES BASED ON LOSS OF PROFITS, DATA, FILES, USE, BUSINESS OPPORTUNITY OR CLAIMS OF THIRD PARTIES), AND WHETHER OR NOT THE PARTY HAS BEEN ADVISED OF THE POSSIBILITY OF SUCH DAMAGES. THIS LIMITATION SHALL APPLY NOTWITHSTANDING ANY FAILURE OF ESSENTIAL PURPOSE OF ANY LIMITED REMEDY PROVIDED HEREIN.

- Should any provision of this Agreement be held by a court of competent jurisdiction to be illegal, invalid, or unenforceable, that provision shall be deemed amended to achieve as nearly as possible the same economic effect as the original provision, and the legality, validity and enforceability of the remaining provisions of this Agreement shall not be affected or impaired thereby.

- The failure of either party to enforce any term or condition of this Agreement shall not constitute a waiver of either party's right to enforce each and every term and condition of this Agreement. No breach under this agreement shall be deemed waived or excused by either party unless such waiver or consent is in writing signed by the party

granting such waiver or consent. The waiver by or consent of a party to a breach of any provision of this Agreement shall not operate or be construed as a waiver of or consent to any other or subsequent breach by such other party.

- This Agreement may not be assigned (including by operation of law or otherwise) by you without WILEY's prior written consent.
- Any fee required for this permission shall be non-refundable after thirty (30) days from receipt by the CCC.
- These terms and conditions together with CCC's Billing and Payment terms and conditions (which are incorporated herein) form the entire agreement between you and WILEY concerning this licensing transaction and (in the absence of fraud) supersedes all prior agreements and representations of the parties, oral or written. This Agreement may not be amended except in writing signed by both parties. This Agreement shall be binding upon and inure to the benefit of the parties' successors, legal representatives, and authorized assigns.
- In the event of any conflict between your obligations established by these terms and conditions and those established by CCC's Billing and Payment terms and conditions, these terms and conditions shall prevail.
- WILEY expressly reserves all rights not specifically granted in the combination of (i) the license details provided by you and accepted in the course of this licensing transaction, (ii) these terms and conditions and (iii) CCC's Billing and Payment terms and conditions.
- This Agreement will be void if the Type of Use, Format, Circulation, or Requestor Type was misrepresented during the licensing process.
- This Agreement shall be governed by and construed in accordance with the laws of the State of New York, USA, without regards to such state's conflict of law rules. Any legal action, suit or proceeding arising out of or relating to these Terms and Conditions or the breach thereof shall be instituted in a court of competent jurisdiction in New York County in the State of New York in the United States of America and each party hereby consents and submits to the personal jurisdiction of such court, waives any objection to venue in such court and consents to service of process by registered or certified mail, return receipt requested, at the last known address of such party.

WILEY OPEN ACCESS TERMS AND CONDITIONS

Wiley Publishes Open Access Articles in fully Open Access Journals and in Subscription journals offering Online Open. Although most of the fully Open Access journals publish open access articles under the terms of the Creative Commons Attribution (CC BY) License only, the subscription journals and a few of the Open Access Journals offer a choice of Creative Commons Licenses. The license type is clearly identified on the article.

The Creative Commons Attribution License

The Creative Commons Attribution License (CC-BY) allows users to copy, distribute and transmit an article, adapt the article and make commercial use of the article. The CC-BY license permits commercial and non-

Creative Commons Attribution Non-Commercial License

The Creative Commons Attribution Non-Commercial (CC-BY-NC)License permits use, distribution and reproduction in any medium, provided the original work is properly cited and is not used for commercial purposes.(see below)

Creative Commons Attribution-Non-Commercial-NoDerivs License
The Creative Commons Attribution Non-Commercial-NoDerivs License (CC-BY-NC-ND) permits use, distribution and reproduction in any medium, provided the original work is properly cited, is not used for commercial purposes and no modifications or adaptations are made. (see below)
Use by commercial "for-profit" organizations
Use of Wiley Open Access articles for commercial, promotional, or marketing purposes requires further explicit permission from Wiley and will be subject to a fee.
Further details can be found on Wiley Online Library
http://olabout.wiley.com/WileyCDA/Section/id-410895.html

Other Terms and Conditions:

v1.10 Last updated September 2015

Questions? customercare@copyright.com or +1-855-239-3415 (toll free in the US) or +1-978-646-2777.

RE: Image permission request

Ami Ben-Amotz <amiba@bezeqint.net>

Sun 11/06/2017 22:01

To: Schaap, Roland <R.Schaap@massey.ac.nz>;

1 attachments (425 KB)

NBT areal photo (2015_06_28 06_24_20 UTC).jpg;

Dear Ronald Schaap,
Thank you for the kind mail and the request for NBT Plant Image as already published.
You have my consent to use the photo you have or the one attached.
Please note that the species NBT cultivates in Eilat ponds is ***Dunaliella bardawil*** a variant *of D. salina*, close but not the same genetically. The new genetics of these two species and others of *Dunaliella* will be presented at the coming ISAP 2017: https://isap2017.sciencesconf.org/resource/page/id/18 by Dr. Declan Schroeder of MBA, UK.
I will be glad to follow your work and get copy of your dissertation.

Regards,
Ami

Prof. Emeritus, Ami Ben-Amotz
Marine Biology
The National Institute of Oceanography
Israel

From: Schaap, Roland [mailto:R.Schaap@massey.ac.nz]
Sent: Sunday, June 11, 2017 8:19 AM
To: ami@benamotz.com
Subject: Image permission request

Dear Mr. Ben-Amotz,

I am a PhD student at Massey University (New Zealand) currently carrying out research into the UV carotenoid accumulation in Dunaliella salina. In my dissertation literature review I discuss commercial D. salina cultivation processes. I would like to request permission to reproduce the image of the NBT plant (Eilat, Isreal) from your 2011 ISES Annual Meeting presentation (Tel-Aviv, 5th October 2011, image on sheet 6). The dissertation will be made available in an open access institutional repository upon completion. The image will be cited correctly in my work.

Kind regards,

Roland Schaap

RightsLink®

Home | Account Info | Help

Title:	Wavelength-dependent xanthophyll cycle activity in marine microalgae exposed to natural ultraviolet radiation
Author:	Anita G. J. Buma, Ronald J. W. Visser, Willem H. Van De Poll, et al
Publication:	European Journal of Phycology
Publisher:	Taylor & Francis
Date:	Nov 1, 2009

Rights managed by Taylor & Francis

Logged in as:
Roland Schaap
Massey University
Account #: 3001161374
LOGOUT

Thesis / Dissertation Reuse Request

Taylor & Francis is pleased to offer reuses of its content for a thesis or dissertation free of charge contingent on resubmission of permission request if work is published.

BACK | CLOSE WINDOW